

SLAC-210  
UC-32  
June 1978  
(I)

THE EGS CODE SYSTEM:  
COMPUTER PROGRAMS FOR THE MONTE CARLO  
SIMULATION OF ELECTROMAGNETIC CASCADE SHOWERS  
(VERSION 3)

RICHARD L. FORD \*  
SCIENCE APPLICATIONS, INC.  
La Jolla, California 92037

AND

WALTER R. NELSON  
STANFORD LINEAR ACCELERATOR CENTER  
Stanford, California 94305

PREPARED FOR THE DEPARTMENT OF ENERGY  
UNDER CONTRACT NO. EY-76-C-03-0515

June 1978

Printed in the United States of America. Available from National  
Technical Information Service, U.S. Department of Commerce, 5285 Port  
Royal Road, Springfield, VA 22161. Price: Printed copy \$11.75;  
Microfiche \$3.00.

---

\* Present address: Sanders Associates, Inc.  
95 Canal Street  
Nashua, New Hampshire 03061

THE  
STATE-OF-THE-ART  
TWENTY-FIVE YEARS AGO

"The procedure used was a simple graphical and mechanical one. The distance into lead was broken into intervals of one-fifth of a radiation length (about one mm). The electrons or photons were followed through successive intervals and their fate in passing through a given interval was decided by spinning a wheel of chance; the fate being read from one of a family of curves drawn on a cylinder. . . . .

A word about the wheel of chance: The cylinder, 4 in. outside diameter by 12 in. long, is driven by a high speed motor geared down by a ratio of 20 to 1. The motor armature is heavier than the cylinder and determines where the cylinder stops. The motor was observed to stop at random and, in so far as the cylinder is concerned, its randomness is multiplied by the gear ratio . . . . ."

\*R. R. Wilson, "Monte Carlo Study of Shower Production", Phys. Rev. 86, 261 (1952).

## PREFACE

Over a decade has passed since H. H. Nagel visited SLAC and "planted the seed" to what is now called EGS---or more appropriately, the EGS Code System. Nagel's original program was one of three during the early 1960's aimed at solving the electromagnetic shower problem by Monte Carlo simulation. As a matter of fact, the ORNL shower code by Zerby and Moran was motivated by Dr. W. K. H. Panofsky at SLAC, who recognized that a large number of engineering and physics problems associated with the design of the two-mile accelerator might best be solved using this technique, and calculations that were being done for SLAC by Oak Ridge were greatly appreciated at the time. Unfortunately, neither the ORNL code, nor a comparable version by Messel and coworkers in Australia, were available to users in the outside scientific community, and the Nagel program was quickly accepted and put to immediate use both at SLAC and at DESY in Hamburg.

It became quite clear to one of us (WRN) at the very beginning that the Nagel code had rather limited use as it stood. In fact, most of the problems that could be solved by any of the three codes mentioned above, had been solved and published. Many interesting problems still remained to be solved, but Nagel's code, because of the way it was structured, was too limited to be of real use without considerable effort on the part of the user. So a program was initiated (by WRN) to develop the Nagel code into a general, multi-media, modularized, and versatile form. Although considerable progress had been made in this direction, the most significant achievements in the EGS code were made (by RLF) just prior to and after the conversion to the MORTRAN language (the reader may refer to the introductory sections of this report for chronological details of the

PREFACE  
(continued)

development of EGS/PEGS/TESTSR). Very slowly and deliberately, then, the EGS Code System has evolved into the Version 3 form that we have today.

With the presentation of this document, we feel that we now have a means of simulating almost any electron-photon transport problem conceivable. That is to say, the structure of the EGS Code System, with its global features, modular form, and structured programming, is readily adaptable to virtually any interfacing scheme that is desired on the part of the user.

Because of its versatility, and because we spent a lot of time working with our colleagues on problems that were "more important at the time than documentation," this report has been long in coming. As a result of a sudden popularity of the code, we have also been under considerable pressure of late to get the job of documentation finished. In view of the vast number of pages that make up the total report, a certain amount of editorial license had to be taken, and we ask for your indulgence.

The sudden popularity that we speak of is due to the continually mounting interest in the high energy physics that is being done at electron-positron storage ring facilities---particularly since the psi-particle discoveries. EGS has proven to be invaluable in the design of shower counters, liquid argon chambers, calorimeters, sodium iodide arrays, and the like. So it is, indeed, a pleasure to be able to present this work just when it is probably the most needed.

As we have stated above, and which comes as no shock to the reader,



## PREFACE

(continued)

this report is extremely bulky. We would, therefore, like to present a guide as to the best (or at least most efficient) way to use it. This is especially important to the new user of EGS. The most significant chapters are 4 and 5---the EGS and PEGS User Manuals, respectively. They are really indispensable and, as a result, will be maintained separately from this report. In fact, they were created by means of the text editing features of the WYLBUR system at SLAC, and are expected to be kept updated. Copies of Chapters 4 and 5 can be obtained through WYLBUR and used as "working manuals."

To those who are already "EGS Users," we recommend that you read Chapter 1. As can be expected, there are a number of versions of EGS, both in MORTRAN and in FORTRAN, and you should be aware of "your" version.

Chapter 3 should eventually be read by all users. It is an applications-chapter and provides the reader with a fair number of experimental (and other) verifications of the system. The EGS User is required to interface with EGS by means of User Codes. Appendix UC, which goes hand-in-hand with Chapter 3, provides the EGS User with a number of ideas as to how to attack a particular problem.

Chapters 2 and 6 are not truly important in terms of using EGS to solve problems. They could be ignored completely if the reader prefers to save time. Chapter 6 is a description and listing of the TESTSR User Code, which was important to the authors during the development of the EGS Code System itself. Conceivably it could be of further use

PREFACE  
(continued)

should new routines be developed or should (for example) other random number generators need to be checked out. Chapter 2, on the other hand, presents the physics that EGS and PEGS are based on, and it gives the various mathematical and statistical methods that are employed. A graduate student, for example, might be well-advised to study Chapter 2 in order to truly understand what he is doing when he uses EGS to design the apparatus for his experiment. We have been approached many times with questions directed at the physics that has been employed in the codes, and Chapter 2 is useful to those readers with such questions. There are a number of "tricks" that one can play in Monte Carlo sampling, and we use some of them in EGS/PEGS. The reference list at the end of the report is deliberately lengthy in order to provide the serious reader with a good source, should he be interested in creating his own "experimental mathematics."

This subject is far from complete. We expect to see a number of improvements to the EGS Code System as a result of the problems that we see being attacked by the most recent users. Two that immediately come to mind are i.) the transport of charged particles in magnetic fields, and ii.) the transport of fluorescent photons from K, L, ..... absorption. The latter is expected to be important in the design of "masks" for counters that intercept the synchrotron radiation fields that are associated with electron-positron storage rings. A number of other improvements are left for the future. Without further explanation at this time (the reader can find additional mention of them throughout the

## PREFACE

(continued)

text), they include:

1. Shower development in very low-Z elements---a better treatment of bremsstrahlung and pair production (might refer to the work by Tsai(1974));
2. A more rigorous treatment of bremsstrahlung near the high frequency limit;
3. Including the Migdal suppression effect---a very high energy phenomenon;
4. An option to sample from the Landau distribution;
5. Using a Combinatorial Geometry package as is done in the ORNL code called MORSE-CG;
6. Implementation of Sternheimer's general scheme for determining the density effect correction;
7. A more careful treatment of charged particle interactions below a kinematic energy of 1 MeV.

Getting the EGS Code System to the stage that it is today has been a monumental task, to say the least! The majority of this manuscript was created at SLAC by the two of us, although significant portions have been re-done by telephone or by mail. In order to bring one of us (RLF) to SLAC during a critical period of writing last summer, we required some funding from a number of groups. We wish to thank those Group Leaders at SLAC (J. Rees, D. Leith, B. Richter, R. Taylor, R. McCall) and especially H. DeStaebler who arranged the whole thing for us. The support of R. Hofstadter and E. B. Hughes at HEPL is appreciated, especially by

PREFACE

(continued)

RLF who was a graduate student of theirs during most of the developmental stages of EGS/PEGS. WRN wishes to express his gratitude to his Group Leader in the Radiation Physics Group, R. C. McCall, who has been most patient for a number of years now! We both wish to acknowledge the work of those people who contributed to the design of the code as it now stands; namely, D. Nicoli, V. Whitis, J. Ryder, B. Talwar, E. Miller, A. Clark, and T. McPharlin. H. Israel of LASL was most helpful in that he provided us with the Storm and Israel data-tape, thus ensuring us the ability to be able to create showers in "100 different elements." A number of people have assisted us in the preparation of this document, and we would like to acknowledge our gratitude to R. Parker, T. Johnson, D. Mark, V. Bennett, L. Santiago, R. Millers, C. Washington, and to T. Hunter and her entire crew in the SLAC Publications Office.

Much of the work was done while RLF was employed at Science Applications, Inc. in La Jolla, California. We would like to thank, in particular, W. Woolson and W. Coleman of that organization for their encouragement and support.

It goes without saying that we probably would never have ventured as far as we have into this field, much to everyone's loss, had we not had a copy of H. H. Nagel's program. We have never met the gentleman, but we would like to thank him for the beginning of things.

PREFACE  
(continued)

Finally, it should be noted by the readers that RLF no longer works in the radiation transport field, having gone on to other areas of interest. All inquiries would best be directed to WRN, including any errors and/or improvements to the codes and manuscript. Copies of the EGS Code System can be obtained from him by simply sending a 9-track tape and writing a letter.

The genius of the methods that we use truly belongs to RLF; the administration of the system and the idea of doing this in the first place were due to WRN. We both contributed to the physics. During the last two years WRN has often wondered why he kept at it, and the answer lies in the fact that he is continuously in contact with high energy physicists who appreciate the effort and tell him so by sharing with him the results of their work using EGS. We are truly grateful for this form of encouragement.

June, 1978

Walter R. Nelson

and

Richard L. Ford

## TABLE OF CONTENTS

	<u>Page</u>
THE STATE-OF-THE-ART TWENTY-FIVE YEARS AGO	ii
PREFACE	iii
1. INTRODUCTION	1.1-1
1.1 History	1.1-1
1.2 Description of the Shower Generation Process	1.2-1
1.3 Outline of the Remainder of this Paper	1.3-1
2. SHOWER PHYSICS AND SAMPLING DETAILS	2.1-1
2.1 Probability Theory	2.1-1
2.2 Sampling Theory	2.2-1
2.3 Simulating the Physical Processes---An Overview	2.3-1
2.4 Particle Transport	2.4-1
2.5 Particle Interactions	2.5-1
2.6 General Implementation Notes	2.6-1
2.7 Bremsstrahlung and Electron-Positron Pair Production	2.7-1
2.8 Interactions With Atomic Electrons---General Discussion	2.8-1
2.9 Compton Scattering	2.9-1
2.10 Møller Scattering	2.10-1
2.11 Bhabha Scattering	2.11-1
2.12 Two Photon Positron-Electron Annihilation	2.12-1
2.13 Continuous Electron Energy Loss	2.13-1
2.14 Multiple Scattering	2.14-1
2.15 Photoelectric Effect	2.15-1

TABLE OF CONTENTS

(continued)

	<u>Page</u>
3. COMPARISON BETWEEN EGS CALCULATIONS AND VARIOUS EXPERIMENTS AND OTHER MONTE CARLO RESULTS	3.1-1
3.1 Conversion Efficiency of Lead For 30-200 MeV Photons	3.1-1
3.2 The Charged Component of 1 GeV Electron Showers	3.2-1
3.3 Low Energy Bremsstrahlung from High-Z Targets	3.3-1
3.3.1 Comparison of EGS with ETRAN	3.3-1
3.3.2 Comparison of EGS with Experimental Results	3.3-4
3.4 Comparison of EGS with Large, Modularized NaI(Tl) Detector Experiment	3.4-1
3.5 Comparison of EGS with Longitudinal and Radial Shower Experiment at 1 GeV in Water and Aluminum	3.5-1
3.6 Track Length Calculations	3.6-1
3.6.1 Differential Photon Track Length	3.6-2
3.6.2 Differential Electron Track Length	3.6-2
3.7 Multiple Scattering of 15.7 MeV Electrons in Thin Foils	3.7-1
3.8 Concluding Remarks	3.8-1
4. USER MANUAL FOR EGS	4.1-1
4.1 Introduction	4.1-1
4.2 General Description of Implementation	4.2-1
4.3 The COMMON Blocks	4.3-1
4.4 The Sequence of Operations	4.4-1
4.4.1 User-Over-Ride-Of-EGS-Macros (Step 1)	4.4-2
4.4.2 Pre-HATCH-Call-Initialization (Step 2)	4.4-5
4.4.3 HATCH-Call (Step 3)	4.4-8

TABLE OF CONTENTS

(continued)

	<u>Page</u>
4.4.4 Initialization-For-HOWFAR (Step 4)	4.4-8
4.4.5 Initialization-For-AUSGAB (Step 5)	4.4-8
4.4.6 Determination-Of-Incident-Particle-Parameters (Step 6)	4.4-9
4.4.7 SHOWER-Call (Step 7)	4.5-1
4.4.8 Output-Of-Results (Step 8)	4.5-1
4.5 Specifications for HOWFAR	4.5-1
4.6 Specifications for AUSGAB	4.6-1
4.7 UCSAMPLE --- An Example of a "Complete" User Code	4.7-1
5. USER MANUAL FOR PEGS	5.1-1
5.1 Introduction	5.1-1
5.2 Structural Organization of PEGS	5.2-1
5.3 PEGS Options and Input Specifications	5.3-1
5.3.1 Interrelations Between Options	5.3-1
5.3.2 The ELEM, MIXT, COMP Options	5.3-1
5.3.3 The ENER Option	5.3-13
5.3.4 The PWLF Option	5.3-13
5.3.5 The DECK Option	5.3-16
5.3.6 The MIMS Option and the CMS Code	5.3-17
5.3.7 The TEST Option	5.3-17
5.3.8 The CALL Option	5.3-18
5.3.9 The PLTI and PLTN Options	5.3-18
5.3-10 The HPLT Option	5.3-19
5.4 Concluding Remarks	5.4-1



TABLE OF CONTENTS

(continued)

	<u>Page</u>
6. TESTSR---A USER CODE TO TEST THE SAMPLING ROUTINES	6.1-1
6.1 Introduction	6.1-1
6.2 TESTSR Code Listing	6.2-1
6.3 Output from TESTSR	6.3-1
6.4 Using the TESTSR Card Output with the HPLT Option of PEGS	6.4-1
 APPENDIX UC	 UC-1
 REFERENCES	 R-1

## CHAPTER 1

### 1. INTRODUCTION

#### 1.1 History

The EGS\* Code System (Version 3) is a package of computer programs that simulate the development of electromagnetic cascade showers in various media using the Monte Carlo method. A number of shower codes have been written during the last 10 to 15 years and a short summary of these codes, as well as the historical development of EGS, is presented in the following paragraphs.

The Monte Carlo method was originally suggested by Ulam and von Neumann (1947), and was first used by Goldberger (1948) in order to study nuclear disintegrations produced by high-energy particles. The first application of the Monte Carlo technique to study shower production was done by Wilson (1952). Wilson's approach was a simple graphical-mechanical one that was apparently quite tedious, but was still an improvement over analytical methods available at the time--- particularly in studying the average behavior of showers and fluctuations about the average (Rossi 1952).

The first use of an electronic digital computer in simulating high-energy cascades by Monte Carlo methods was reported by Butcher and Messel (1958, 1960), and independently by Varfolomeev and Svetloolobov (1959). These two groups collaborated in a much publicized work (Messel et al 1962) that eventually led to an extensive set of tables describing the shower distribution functions (Messel and Crawford 1970)---the so-called "shower book."

For various reasons two completely different codes were written in

---

\*Electron-Gamma Shower

## CHAPTER 1

the early-to-mid-1960's. The first was written by Zerby and Moran (1962a, b, 1963) at the Oak Ridge National Laboratory and was motivated by the construction of the Stanford Linear Accelerator Center and by the many physics and engineering problems that were anticipated as a result of high-energy electron beams showering in various devices and structures at that facility. This code has been used by Alsmiller and others (1966, 1968, 1969a,b, 1974a,b) for a number of studies since its development.

The second code was developed by Nagel (1963, 1964, 1965) and several versions have appeared since then (Völkel 1965, Nicoli 1966, Burfeindt 1967), including the one that is being reported here. The original Nagel version, which we shall call SHOWER1, was a FORTRAN code written for high-energy electrons (1000 MeV or less) incident upon lead in cylindrical geometry. Six significant electron and photon interactions (bremsstrahlung, electron-electron scattering, ionization-loss, pair-production, Compton scattering, and the photoelectric effect) plus multiple Coulomb scattering were accounted for. Except for annihilation, positrons and electrons were treated alike and were followed until they reached a cutoff energy of 1.5 MeV (total energy). Photons were followed down to 0.25 MeV. The cutoff energies were as low as or lower than those used by either Messel and Crawford or by Zerby and Moran.

The availability of Nagel's dissertation (Nagel 1964) and a copy of his original shower program provided the incentive for Nicoli (1966) to extend the dynamic energy range and flexibility of the code in order for it to be made available as a practical tool for the experimental physicist. Nicoli's modifications of SHOWER1 fell into three categories:

1. High-energy extensions to the least squares fits for total interaction probabilities and branching ratios.

## CHAPTER 1

2. Provisions for including boundary condition interrogation in the transport cycle, allowing for particle marking and/or discarding and the use of generalized energy cutoffs for electrons and photons.
3. The handling of input/output requirements.

In August, 1966 the Nicoli version (SHOWER2) was brought to SLAC by Nagel, who had been working at MIT and had consulted with Nicoli on the changes and extensions above. The SLAC Computation Group undertook the task of getting the code running on the IBM-360 system and generalizing the program to run in elemental media other than just lead. The latter was facilitated by a set of notes---brought to SLAC by Nagel (1966) ---on the best way to accomplish this and V. Whitis was assigned this job. Whitis left SLAC in the summer of 1967 and his work, which consisted mainly of a series of fitting-programs written in the ALGOL language, was passed on to one of us (WRN). Under Nelson's direction, a programmer (J. Ryder) constructed SHOWER3 in modular form and wrote a pre-processing code called PREPRO that computed fit-coefficients for the cross section and branching ratio data needed by SHOWER3. The values of these constants depended on the material in which the shower was to be simulated. During the summer of 1972 the Ryder version of SHOWER3/PREPRO was successfully tested for several different elements by B. Talwar under the direction of Nelson, thus bringing SHOWER3/PREPRO into an operational status.

Meanwhile, interest in a computer code capable of simulating electromagnetic cascade showers had been developing for several years at the High Energy Physics Laboratory (HEPL) at Stanford University, where a

## CHAPTER 1

group led by R. Hofstadter and E. Hughes was continuing their development of large NaI(Tl) Total Absorption Shower Counters (TASC's). A method of accurately predicting shower behavior in these counters was needed. A version of Nagel's code (SHOWER2) was obtained from Nelson in the fall of 1970; however, efforts to scale from lead to NaI were uncertain and led to a growing conviction that a generalized code was necessary. Thus it was that one of the authors of this report (RLF) undertook the task of generalizing SHOWER2 to run in any element, mixture, or compound in September 1971---an effort similar to the one already underway by Ryder, Talwar, and Nelson that resulted in the final version of SHOWER3/PREPRO.

Ford obtained a copy of a Ryder version of SHOWER3/PREPRO and Nagel's notes from Nelson. In addition to the references mentioned in Nagel's notes, the "shower book" (Messel and Crawford 1970), as well as the review by Scott (1963) on multiple scattering, were found to be very useful sources of information. The essential physics was formulated and the coding was completed by February, 1972. At that time the HEPL version was called SHOWER (from now on it will be referred to as SHOWER4) and the corresponding preprocessor was completely new and was called SHINP (for SHOWER Input). Both codes were in FORTRAN and were made operational on the IBM-7700 machine at HEPL---a second generation experimental data acquisition computer. A number of interesting studies were subsequently performed, including calculations of detector resolutions and expected self-vetoes in gamma detectors due to backscattered photons from shower detectors downstream.

In January 1974, it began to appear likely that HEPL's computer would be sold. In addition, the Hofstadter group was involved in an

## CHAPTER 1

experiment at SLAC that required shower simulations and the SHOWER4/SHINP codes were therefore made operational on the considerably faster and more efficient IBM-360/91 at SLAC. During the calculations that had been performed at HEPL, a couple of errors were found in the sampling routines that would have been detected earlier if it had been possible to test them in a more systematic way. Therefore, it was desired to incorporate into the new version being brought to SLAC test facilities to insure the correctness of these sampling routines. In order to facilitate comparison between the sampled secondary spectra and the theoretical distributions, the preprocessing code was split up and modularized into subprograms

About this time Nelson became interested in being able to use Ford's version of the code and offered to help support its further development. One of Ford's objectives was to make the preprocessor code produce data for the shower code in a form that was directly useable by the shower code with a minimum of input required by the user. In SHOWER3/PREPRO and in SHOWER4/SHINP, whenever it was desired to create showers in a new medium, it was necessary to look-up the photon cross sections in the literature and keypunch them for the preprocessing code to use. Subsequent to this it was necessary to select from several fits produced by the preprocessing code and to include this new information, consisting of many data cards, with other data used by the shower program. Ford rewrote the preprocessor to automatically produce all of the data needed by the shower code in a readily acceptable form and, with the assistance of Nelson, obtained photon cross sections for elements 1 to 100 (Storm and Israel 1970) on magnetic tape. Ford also separated the shower code's material-input from its control-input. For flexibility and ease of use,

## CHAPTER 1

the NAMELIST facility of FORTRAN-IV was utilized for reading-in control data in both the preprocessor and the shower codes. The resultant shower code was re-named EGS (Electron-Gamma Shower) and its companion code was called PEGS (Processor for EGS). This version, written completely in the FORTRAN language, is referred to as Version 1 of the EGS Code System (or more simply EGS1 and PEGS1).

The EGS1 sampling routines were tested using its internal test procedure facility and, with the exception of the bremsstrahlung process, were found to be operating very nicely. In the bremsstrahlung case a ripple, amounting to only 5% but still noticeable, was observed when the sampled data was compared with the theoretical secondary distribution. This effect went away upon selection of another random number generator, and it was concluded that correlations in the original number generator were the cause. EGS1 was then tested against various experiments in the literature and with other Monte Carlo results that were then available and the authors found reasonably good agreement in all cases.

By the Fall of 1974 the Hofstadter group had obtained some hexagonal modular NaI detectors and the discovery of the psi particle in November 1974 opened up an exciting area of high energy gamma-ray spectroscopy for which the modularized NaI detectors were ideally suited. EGS1, however, could not be readily used to simulate showers in complex geometries such as those presented by modular stacks of NaI. A good example of this was the Crystal Ball detector for which EGS1, under the direction of E. Bloom at SLAC, was modified to handle the particular geometry in question. Furthermore, Nelson had received a large number of requests from the growing list of EGS users, both at SLAC and elsewhere in the high-energy physics community, to further improve EGS1 so that complex geometries

## CHAPTER 1

could be realized in the near future. Thus it was decided that EGS1, which was a one-region, one-medium code, should be generalized in order to handle many-region, many-media, complex, three-dimensional geometries.

It soon became clear that, in the time available at least, it would not be possible to construct a self-contained code that would have all of the control, scoring, and output options that might ever be wanted, as well as a geometry package that would automatically handle arbitrary complex geometries. Therefore, Ford decided to put in only the necessary multi-region structures, to replace all scoring and output code in EGS1 with a user interface, and to dispense with the EGS1 main control program completely. Thus EGS1 became a subprogram in itself with two user-callable subroutines (HATCH and SHOWER) that require two user-written subroutines (HOWFAR and AUSGAB) in order to define the geometry and do the scoring, respectively.

For added flexibility and portability, EGS1 and PEGS1 were rewritten in an extended FORTRAN language which is translated by the MORTRAN2 Macro Processor into standard FORTRAN. The part of EGS1 that was used to test the sampling routines was reconfigured into a separate main program called the TESTSR code, also in MORTRAN. These revisions were completed by the end of 1975 and the new versions of EGS, PEGS, and TESTSR comprise what is called Version 2 of the EGS Code System---or more simply EGS2, PEGS2, and TESTSR2.

One part of EGS2 which seemed aesthetically displeasing was the complex control logic needed in the electron transport routine (ELECTR) in order to transport electrons by the variable distances to interaction points or boundaries using only step lengths taken from a set of 16 discrete step lengths. This procedure had been necessary in order to implement



## CHAPTER 1

Nagel's discrete reduced angle multiple scattering scheme (Nagle 1963-1966) in a general multi-region environment. In addition, comparisons of backscattered photon fluence as computed by EGS2 versus unpublished HEPL data, as well as bremsstrahlung angular distribution calculations comparing EGS2 results with those using ETRAN (Berger and Seltzer 1970), suggested that EGS2 might be predicting values in the backward direction that were low by up to a factor of two. For these reasons, and in order to achieve greater universality of application (e.g., so that a monochromatic beam of electrons impinging on a very thin slab would have a continuous angular distribution on exit), Ford decided in the summer of 1976 to try to implement a multiple scattering scheme that would correctly sample the continuous multiple scattering distribution for arbitrary step lengths. After some thought, an extension of the method used by Messel and Crawford (1970) was devised. Most of the code for this addition was written by Ford at Science Applications, Inc., and was brought up to SLAC in August 1977 where it was debugged and tested by Nelson and Ford. The implementation of this system required some once only calculations which were made using the stand-alone code CMS (Continuous Multiple Scattering)\*. It should be mentioned that the version of PEGS brought up to SLAC at this time had the same physics in it as Version 2, but had been partly rewritten in order to be more machine independent (e.g., IBM versus CDC), its main remaining machine dependency being its use of NAMELIST. Another option was added to the TESTSR code to allow testing of the new EGS multiple scattering sampling routine, MSCAT.

---

\*Logically, the CMS code should be put in as a part (option?) of PEGS, but this has not been done as of this writing.

## CHAPTER 1

These versions of EGS, PEGS, and TESTSR comprise what we call Version 3 of the EGS code system, and they will carry the numeral three; namely, EGS3, PEGS3, and TESTSR3.

Subsequent comparisons of EGS3 calculations against experiments and other Monte Carlo results have been made by the authors (see Chapter 3) and others and the agreements have again verified the validity of the EGS Code System.

The EGS Code System (Version 3)\* can be distinguished from Nagel's original code (SHOWER1) in a number of ways, the most noteworthy being:

1. Showers can be simulated in any element, compound, or mixture. That is, PEGS creates data, to be used by EGS, using a cross section table for elements 1 through 100.
2. Photons and charged particles are transported in random rather than in discrete steps, resulting in a much faster running code.
3. Positrons may annihilate either in-flight or at rest, and their annihilation quanta are followed to completion.
4. Electrons and positrons are treated separately and the appropriate formulae are used (e.g., Møller and Bhabha, respectively). Exact rather than asymptotic formulae are used.
5. Sampling schemes have been made more efficient.

---

\* Except when otherwise necessary, we will generally refer to the codes as EGS or PEGS rather than EGS3 or PEGS3 throughout the remainder of this paper.

## CHAPTER 1

6. The dynamic range of charged particles has been extended so that showers can be initiated and followed in the energy range of 1.5 MeV to 100 GeV (total energy).
7. The dynamic range of photons has been extended and lies between 1 keV and 100 GeV.
8. The output data from the preprocessing code (PEGS) is in convenient form for direct use by EGS.
9. PEGS control input uses the NAMELIST read facility. In addition to the options needed to produce data for EGS, PEGS contains options to plot any of the physical quantities used by EGS, as well as to compare sampled distributions produced by the TESTSR code with theoretical spectra.
10. PEGS constructs piecewise-linear fits over a large number of energy intervals of the cross section and branching ratio data; whereas, PREPRO and SHINP both made high-order polynomial fits over a small number of intervals. SHOWER1 and SHOWER2 worked in this manner also.
11. EGS is a subroutine package with user interface. This allows the user great flexibility in the way he uses EGS without requiring him to be familiar with the internal details of the code. This also reduces the likelihood that user edits will introduce bugs into the code.
12. A main program and user routines, which simulate the options used in Version 1, are available.

## CHAPTER 1

13. The geometry is specified by a user-written subprogram. Routines are available from the authors for some commonly used geometries (e.g., planes, cylinders, cones, boxes). Some of these are given in the code listings for the examples that are in Chapter 3.

### In particular, for Version 3 versus Version 2:

14. The control logic in the charged particle transport subroutine, ELECTR, has been greatly simplified.
15. The control logic in both the charged particle and photon transport subroutines (ELECTR and PHOTON, respectively) has been modified in order to make interaction at a boundary impossible.
16. As a result of 14. and 15. above, it should now be possible to implement importance sampling\* into EGS without any further "internal" changes to the system itself. Examples that come to mind include the production of secondary electron beams at large angles, photon energy deposition in relatively small (low Z) absorbers, and deep penetration (radial and longitudinal) calculations associated with shower counter devices.
17. Provision has been made for allowing the density to vary continuously in a region.

---

\* For those who may be unfamiliar with the term, importance sampling refers to sampling the most important regions of a problem and correcting for this bias by means of weight factors (see, for example, Carter and Cashwell 1975).

## CHAPTER 1

18. The multiple scattering reduced angle is now sampled from a continuous rather than discrete distribution. This is done for arbitrary step sizes provided that they are not too large to invalidate the theory. An immediate application of this is the simplification mentioned in 14. above.
19. A new subroutine (PHOTO) has been added in order to deal with the photoelectric effect in a manner comparable to the other interaction processes. This should facilitate in developing more general photoelectric routines. For example, rather than simply depositing the energy of fluorescent photons, as is the case in the versions of EGS up to now, these photons, can be followed as well. A practical use for this is envisioned in the design of shields for detectors that are placed in the synchrotron radiation associated with electron-positron storage rings, as well as various engineering applications and solutions to problems arising because of this synchrotron radiation.
20. Additional calls to AUSGAB, bringing the total from 5 to 23, have been made possible in order to allow for the extraction of additional information without requiring the user to edit the EGS code proper. For example, the user can now determine the number of various collision types (Compton, Møller, etc.) by means of the user-written codes.

## CHAPTER 1

We feel that the EGS Code System (Version 3) is much more generally useful than the original Nagel program (SHOWER1) or the codes published by either Messel et al or by Zerby and Moran. Another code does exist, and we should mention it at this point since it has received a fair amount of attention in the last few years. We refer to the ETRAN Monte Carlo shower code written by Berger and Seltzer (1970). A later version of this program, which contains a fairly general geometry package, is known as SANDYL (Colbert 1973). ETRAN is complementary to the other ones in the literature in that it treats the low energy processes (down to 1 keV) in greater detail. Instead of using the Moliere (1947, 1948) multiple scattering formulation, they use the Goudsmit-Saunderson (1940a, b) approach which avoids the small angle approximations. They also treat fluorescence, the effect of atomic binding on the atomic electrons, and energy-loss straggling. Because of the greater detail taken at low energies, the ETRAN code might run significantly slower than EGS, but this remains to be verified. The code was initially written for incident energies less than 100 MeV, although recent changes have apparently been made in the program to allow for shower simulation at somewhat higher energies (Berger 1976). Nevertheless, the Berger and Seltzer code appears to be accurate and available, and we will make a number of comparisons with it in Chapter 3.

### 1.2 Description of the Shower Generation Process

Electrons<sup>\*</sup>, as they traverse matter, loss energy by two basic processes: collision and radiation. The collision process is one

---

\* In this report, we will often refer to both positrons and electrons as simply "electrons," and distinguishing features will be brought out in the context.

## CHAPTER 1

whereby either the atom is left in an excited state or it is ionized. Most of the time the ejected electron, in the case of ionization, has small energy that is locally deposited. On occasion, however, an orbital electron is given a significant amount of kinetic energy such that it is regarded as a secondary particle called a delta ray.

Energy-loss by radiation (bremsstrahlung) is fairly uniformly distributed among secondary photons of all energies from zero up to the energy of the primary particle itself. At low-energies the collision-loss mechanism dominates and at high-energies the bremsstrahlung process is the most important. At some electron energy the two losses are equal and this energy coincides approximately with the critical energy of the material, a parameter that is used in shower theory for scaling purposes (Rossi 1952). Therefore, at high-energies a large fraction of the electron energy is spent in the production of high-energy photons that, in turn, may interact in the medium. Three photoprocesses dominate, depending on the energy of the photon and the nature of the medium. At high-energies materialization into an electron-positron pair dominates over Compton scattering and at some lower energy the reverse is true. The two processes provide a return of energy to the system in the form of electrons which, with repetition of the bremsstrahlung process, results in a multiplicative process known as an electromagnetic cascade shower. The third photon process, the photoelectric effect, as well as multiple Coulomb scattering of the electrons by atoms, perturbs the shower to some degree. The latter, coupled with the Compton process, gives rise to a lateral spread. The net effect in the forward (longitudinal) direction is an increase in the number of

## CHAPTER 1

particles and a decrease in their average energy at each step in the process.

Eventually, radiation losses can no longer compete with collision losses, and the energy of the primary electron is dissipated in excitation and ionization of the atoms. The so-called tail of the shower consists mainly of photons having energies near the minimum in the mass absorption coefficient for the medium since it is the Compton scattered photons that predominate at large shower depths.

Analytical treatments generally begin with a set of coupled integro-differential equations that are prohibitively difficult to solve except under severe approximation. One such approximation (Approximation A), for example, uses asymptotic formulae to describe pair production and bremsstrahlung, and all other processes are ignored. The mathematics in this case is still rather tedious (Rossi 1952), and the results only apply in the longitudinal direction and for certain energy restrictions. Three dimensional shower theory is exceedingly more difficult, even with modern computer techniques.

The Monte Carlo technique obviously provides a much better way for solving the shower generation problem, not only because all of the fundamental processes can be included, but because arbitrary geometries can be treated. In addition, other minor processes, such as photoneutron production, can be added as a further generalization.

Another fundamental reason for using the Monte Carlo method to simulate showers is their intrinsic random nature. Since showers develop randomly according to the quantum laws of probability each shower is different. For applications when only averages over many



## CHAPTER 1

showers are of interest, an analytic solution of the average shower behavior, if it were available, would be sufficient. However, for many situations of interest (such as in the use of large NaI crystals to measure the energy of single high-energy electrons and gamma-rays), the shower-by-shower fluctuations are important. Analytic solutions for applications such as these would require not just computation of mean values, but such quantities as the probability that a certain amount of energy is contained in a given volume of material. Such calculations are much more difficult than merely computing mean shower behavior and are beyond our present computational ability. Thus we again are led to the Monte Carlo method.

### 1.3 Outline of the Remainder of this Paper

Chapter 2 will present the detailed physics of the shower processes and the methods that have been used to simulate them. The first two sections establish the ideas and notations of probability and sampling theory. An overview of the physical processes, a discussion of particle transport techniques, as well as particle interactions in general, are followed by a section on implementation. Cross section, sampling, and programming details for each of the physical processes involved is then given. An attempt has been made to bring all of the information about a given process together in one spot.

Chapter 3 presents comparisons between EGS calculations and various experiments and other Monte Carlo results. The User Code (i.e., MAIN/ HOWFAR/AUSGAB) and input data necessary to do some of these calculations are included (in Appendix UC) in order to illustrate the use of the EGS code.

## CHAPTER 1

Chapter 4 is a User Manual for the EGS code itself. The detailed specifications of the user-callable and user-written routines are presented here along with general implementation rules and suggestions. An example of a complete User Code is given in this chapter along with corresponding output results.

The User Manual for PEGS is given in Chapter 5 where the various options are discussed in conjunction with input specifications. Flow diagrams are used to show the structural organization of PEGS as well as the interrelations between options.

Chapter 6 describes and demonstrates the TESTSR User Code.

## CHAPTER 2

### 2. SHOWER PHYSICS AND SAMPLING DETAILS

#### 2.1 Probability Theory

There are many good references on probability theory and Monte Carlo methods (viz. Halmos 1950, Hammersley and Handscomb 1964, Kingman and Taylor 1966, Loeve 1950, Parzen 1960, Shreider 1966, Spanier and Gelbard 1969, and Carter and Cashwell 1975) and we shall not try to duplicate their effort here. Rather, we shall mention only enough to establish our own notation and make the assumption that the reader is already acquainted with the elements of probability theory.

The primary entities of interest will be random variables which take values in certain subsets of their range with specified probabilities. We shall denote random variables by putting a  $\hat{\phantom{x}}$  above them (e.g.,  $\hat{x}$ ). If  $E$  is a logical expression involving some random variables, then we shall write  $\text{Pr}\{E\}$  for the probability that  $E$  is true. We will call  $F$  the distribution function (or cumulative distribution function) of  $\hat{x}$  if

$$F(x) = \text{Pr}\{\hat{x} < x\} \quad . \quad 2.1.1$$

When  $F(x)$  is differentiable, then

$$f(x) = F'(x) \quad 2.1.2$$

is the density function (or probability density function) of  $\hat{x}$  and

$$\text{Pr}\{a < \hat{x} < b\} = \int_a^b f(x) dx \quad . \quad 2.1.3$$

In this case  $\hat{x}$  is called a continuous random variable.

In the other case that is commonly of interest,  $\hat{x}$  takes on discrete

CHAPTER 2

values  $x_i$  with probabilities  $p_i$  and

$$F(x) = \sum_{x_i \leq x} p_i \quad . \quad 2.1.4$$

We call  $P$  the probability function of  $\hat{x}$  if

$$\begin{aligned} P(x) &= p_i && \text{if } x = x_i \\ &= 0 && \text{if } x \text{ equals none of the } x_i \quad . \end{aligned} \quad 2.1.5$$

Such a random variable is called a discrete random variable.

When we have several random variables  $x_i$  ( $i=1, n$ ), we define a joint distribution function  $F$  by

$$F(x_1, \dots, x_n) = \Pr\{\hat{x}_1 \leq x_1 \& \dots \& \hat{x}_n \leq x_n\} \quad . \quad 2.1.6$$

The set of random variables is called independent if

$$\Pr\{\hat{x}_1 \leq x_1 \& \dots \& \hat{x}_n \leq x_n\} = \prod_{i=1}^n \Pr\{\hat{x}_i \leq x_i\} \quad . \quad 2.1.7$$

If  $F$  is differentiable in each variable, then we have a joint density function given by

$$f(x_1, \dots, x_n) = \partial^n F(x_1, \dots, x_n) / \partial x_1 \dots \partial x_n \quad . \quad 2.1.8$$

Then, if  $A$  is some subset of  $R^n$  ( $n$ -dimensional Euclidian Space),

$$\Pr\{\hat{x} \in A\} = \int_A f(x) d^n x \quad . \quad 2.1.9$$

If  $E_1$  and  $E_2$  are expressions involving random variables and  $\Pr\{E_2\} \neq 0$ .

we define the conditional probability of  $E_1$  given  $E_2$  by \*

$$\Pr\{E_1|E_2\} = \Pr\{E_1 \& E_2\} / \Pr\{E_2\}. \quad 2.1.10$$

Thus, we can define conditional distributional functions

$$F_3(x_1, \dots, x_j | x_{j+1}, \dots, x_n) = F_1(x_1, \dots, x_n) / F_2(x_{j+1}, \dots, x_n) \quad 2.1.11$$

For continuous random variables, we define conditional density functions by

$$f_3(x_1, \dots, x_j | x_{j+1}, \dots, x_n) = f_1(x_1, \dots, x_n) / f_2(x_{j+1}, \dots, x_n) \quad 2.1.12$$

With this preliminary introduction we move now to sampling methods.

## 2.2 Sampling Theory

In practice almost all sampling is based on the possibility of generating (using computers) sequences of numbers which behave in many ways like sequences of random variables that are uniformly distributed between 0 and 1. We shall denote uniformly distributed random variables by  $\hat{\zeta}_i$ , and values sampled from the uniform distribution by  $\zeta_i$ . Clearly, if  $F$  and  $f$  are distribution and density functions, respectively, of  $\hat{\zeta}$ , then they are given by

$$\begin{aligned} F(\zeta) &= 0, & \text{if } \zeta < 0, \\ &= \zeta, & \text{if } 0 \leq \zeta < 1, \\ &= 1, & \text{if } 1 \leq \zeta; \end{aligned} \quad 2.2.1$$

---

\* The notation  $\Pr\{E_1|E_2\}$  reads "the probability of  $E_1$  given  $E_2$ ."

CHAPTER 2

$$f(\zeta) = 1, \quad \text{if } \zeta \in (0,1), \\ = 0, \quad \text{otherwise.}$$

We assume, in what follows, that we have an unlimited number of uniform random variables available.

Now, suppose that  $\hat{x}$  and  $\hat{y}$  are related by  $\hat{y} = h(\hat{x})$  (with  $h$  monotonically increasing), and that  $\hat{x}$  and  $\hat{y}$  have distribution functions  $F$  and  $G$ ; then,

$$F(x) = \Pr\{\hat{x} < x\} = \Pr\{h^{-1}(\hat{y}) < x\} \quad 2.2.2 \\ = \Pr\{\hat{y} < h(x)\} \\ = G(h(x)).$$

Thus, we can find  $F$  given  $G$  and  $h$ . In particular, if we define  $\hat{x}$  by

$$\hat{x} = F^{-1}(\hat{\zeta}), \quad 2.2.3$$

then

$$G(y) = y$$

and

$$h(x) = F(x),$$

so that

$$\Pr\{\hat{x} < x\} = G(h(x)) = F(x).$$

This is the basis of the so called direct method of sampling  $\hat{x}$  in which we set

$$F(x) = \zeta$$

and solve for  $x$ . The  $x$ -values so chosen will have the distribution  $F$ .

Another method involves evaluating a function of several variables using uniform random variables for arguments. Thus we let

$$\hat{x} = h(\hat{\zeta}_1, \dots, \hat{\zeta}_n), \quad 2.2.4$$

then

$$\Pr\{\hat{x} < x\} = \int_{h(\vec{\zeta}) < x} d^n \zeta \quad 2.2.5$$

This method has been used to find simple schemes for sampling many distributions. For example, suppose we pick  $n+m+1$  values of  $\zeta$  and number them such that

$$\zeta_1 < \zeta_2 \cdots < \zeta_n \leq \zeta_{n+1} < \zeta_{n+2} \cdots < \zeta_{n+m+1} \quad 2.2.6$$

Then, let  $x = \zeta_{n+1}$ . Using Eqs. 2.2.4-6 it can be shown that

$$f(x) = (n+m+1)! x^n (1-x)^m / n!m! , \quad x \in (0,1).$$

A method that we shall frequently use is a combination of the "composition" and "rejection" techniques (Butler 1956, Hammersley and Handscomb 1964, Kahn 1954). Suppose  $f$  and  $f_i$  are density functions,  $\alpha_i$  are positive real numbers, and  $g_i(x) \in [0,1]$ . We now sample  $\hat{x}$  as follows:

- 1) Pick  $\zeta_1$  and let  $i$  be such that

$$\sum_{j=1}^{i-1} \alpha_j < \zeta_1 \leq \sum_{j=1}^n \alpha_j \leq \sum_{j=1}^m \alpha_j \quad 2.2.7$$

- 2) Pick  $x$  from  $f_i(x)$ , possibly by solving

$$\int_{-\infty}^x f_i(x) dx = \zeta_2 \quad 2.2.8$$

- 3) Pick  $\zeta_3$ . Terminate the algorithm and accept value of  $x$  if

$$\zeta_3 < g_i(x) \quad 2.2.9$$

Otherwise, go back to step 1).

CHAPTER 2

The result of this algorithm is that  $\hat{X}$  will have the density function  $f$  given by

$$f(x) = \sum_{i=1}^n \alpha_i f_i(x) g_i(x) . \quad 2.2.10$$

Thus, if we have a function  $f$  which can be put in this form for which the  $f_i$  can be sampled easily and the  $g_i$  evaluated relatively easily, then we have a good method of sampling from  $f$ . It can be shown that the mean number of tries to accept a value is  $\sum \alpha_i$ . If all the  $g_i = 1$ , we have the pure "composition" method; and if  $n = 1$ , we have the pure "rejection" method. For short we will call this the "mixed" method. We shall sometimes use the mixed method for some of the  $f_i$  also. In these cases we will use the notation (for example)

$$f_2(x) = \sum_{j=1}^{n_2} \alpha_{2j} f_{2j}(x) g_{2j}(x) \quad 2.2.11$$

and so on.

Finally, we consider the problem of sampling from a joint density function  $f(x_1, x_2, \dots, x_n)$ . Define the marginal density functions

$$\begin{aligned} g_m(x_1, x_2, \dots, x_m) &= \int f(x_1, x_2, \dots, x_n) dx_{m+1} dx_{m+2} \dots dx_n \\ &= \int g_{m+1}(x_1, x_2, \dots, x_m, x_{m+1}) dx_{m+1} . \end{aligned} \quad 2.2.12$$

We see that  $g_n = f$ . Now consider  $h_m$  given by

$$h_m(x_m | x_1, x_2, \dots, x_{m-1}) \equiv g_m(x_1, x_2, \dots, x_m) / g_{m-1}(x_1, x_2, \dots, x_{m-1}) . \quad 2.2.13$$



## CHAPTER 2

We see that

$$\int h_m(x_m | x_1, x_2, \dots, x_{m-1}) dx_m = 1 \quad 2.2.14$$

from the definition of the  $g$ 's. We see that  $h_m$  is the conditional density function for  $x_m$  given the specified values for  $x_1, x_2, \dots, x_{m-1}$ . It can be easily seen that  $f$  can be factored into a product of the  $h$ 's; namely,

$$f(x_1, x_2, \dots, x_n) = h_1(x_1) h_2(x_2 | x_1) h_3(x_3 | x_1, x_2) \dots h_n(x_n | x_1, x_2, \dots, x_{n-1}). \quad 2.2.15$$

The procedure then is to get a sample value  $x_1$  using density function  $h_1$ . Then use this value  $x_1$  to determine a density function  $h_2(x_2 | x_1)$  from which to sample  $x_2$ . Similarly, the previously sampled  $x_1, x_2, \dots, x_m$  determine the density function  $h_{m+1}(x_{m+1} | x_1, x_2, \dots, x_m)$  for  $x_{m+1}$ . This scheme is continued until all  $x_i$  have been sampled. Of course, if the  $\hat{x}_i$  are independent random variables, the conditional densities will just be the marginal densities and the variables can be sampled in any order.

There are other methods analogous to the one-dimensional sampling methods which can be used for sampling joint distributions. The reader is referred to the references cited above for more details.

### 2.3 Simulating the Physical Processes--An Overview

In some approaches, the Boltzmann transport equation is written down for a system and from it a Monte Carlo simulation of the system is derived. This method will give correct average quantities, such as fluences, but may not correctly represent fluctuations in the real situation due to variance reduction techniques which have been introduced. The reader is

## CHAPTER 2

referred to Chapter 3 in the book by Carter and Cashwell (1975) for details of this particular method.

We have taken a different and more simple-minded approach in that we attempt to simulate the actual physical processes as closely as possible. We have not introduced any variance reduction techniques, so that fluctuations in the Monte Carlo results should truly be representative of real-life fluctuations. For the design of high-energy particle detectors, this is an important consideration. On the other hand, fluctuations are not usually of interest in radiation shielding-type problems, and the addition of optional variance reduction techniques would make some calculations more efficient. The method used here is generally called analog Monte Carlo.

The correct simulation of an electromagnetic cascade shower can be decomposed into a simulation of the transport and interactions of a single particle, along with some necessary bookkeeping. A last-in-first-out stack is used to store the properties of particles which have yet to be simulated. Initially, only the incident particle is on the stack--or to put it more correctly, the properties of the incident particle are stored in the first position of corresponding arrays. The basic strategy is to transport the top particle until an interaction takes place, or until its energy drops below a predetermined cutoff energy, or until it enters a particular region of space. In the latter two cases, the particle is taken off the stack and simulation resumes with the new top particle. If an interaction takes place, and if there is more than one product particle, the particle with the lowest energy is put on top the stack. This ensures that the depth of the stack need not exceed  $\log_2(E_{\max}/E_{\text{cut}})$  where  $E_{\max}$  is the largest incident energy to be simulated and where  $E_{\text{cut}}$  is the lowest

## CHAPTER 2

cutoff energy. Actually, for the above to be strictly true the particle with the lowest "available" energy should be put on top, where by "available" energy we mean  $E$  for photons,  $E-m$  for electrons, and  $E+m$  for positrons ( $E$  = total energy,  $m$  = electron rest mass energy). When a particle is removed from the stack and none remain, the simulation of the shower (history) is complete.

### 2.4 Particle Transport

The mean free path,  $\lambda$ , of a particle is given in terms of its total cross section,  $\sigma_t$ --or alternatively, in terms of its macroscopic total cross section,  $\Sigma_t$  --according to the expression

$$\lambda = 1/\Sigma_t = [N_a \rho \sigma_t / M]^{-1}, \quad 2.4.1$$

where

$N_a$  = Avogadro's number,

$\rho$  = density,

$M$  = molecular weight,

and  $\sigma_t$  = total cross section per molecule.

The probability of an interaction is given by

$$\text{Pr}\{\text{interaction in distance } dx\} = dx/\lambda.$$

In general, the mean free path may change as the particle moves from one medium to another, or when it loses energy. The number of mean free paths traversed will be

$$N_\lambda = \int_{x_0}^x dx/\lambda(x) \quad . \quad 2.4.2$$

CHAPTER 2

If  $\hat{N}_\lambda$  is a random variable denoting the number of mean free paths from a given point until the next interaction, then it can be shown that  $\hat{N}_\lambda$  has the distribution function

$$\Pr\{\hat{N}_\lambda < N_\lambda\} = 1 - \exp(-N_\lambda), \quad N_\lambda > 0. \quad 2.4.3$$

Using the direct sampling method and the fact that  $1 - \zeta$  is also uniform on (0,1), we can sample  $N_\lambda$  using

$$N_\lambda = -\ln \zeta. \quad 2.4.4$$

This may be used in Eq. 2.4.2 to obtain the location of the next interaction.

Let us now consider the application of the above to the transport of photons. Pair production, Compton scattering (from a "free" electron), and photoelectric processes are presently the only ones considered in EGS. These processes all have finite cross sections that are small enough that all interactions may be simulated. This means that photons travel in a straight line with constant energy between interactions. Thus, if the space in which the simulation takes place is composed of a finite number of regions, in each of which the material is homogeneous and of constant density, then the integral in Eq. 2.4.2 reduces to a sum. If  $x_0, x_1, \dots$  are the boundary distances between which  $\lambda$  is constant, then Eq. 2.4.2 becomes

$$N_\lambda = \sum_{j=1}^{i-1} \left( \frac{x_j - x_{j-1}}{\lambda_j} \right) + \left( \frac{x - x_{i-1}}{\lambda_i} \right), \quad 2.4.5$$

where

$$x \in (x_{i-1}, x_i).$$

## CHAPTER 2

The photon transport procedure is then as follows. First, pick the number of mean free paths to the next interaction using Eq. 2.4.4. Then perform the following steps:

1. Compute  $\lambda$  at the current location.
2. Let  $t_1 = \lambda N_\lambda$ .
3. Compute  $d$ , the distance to the nearest boundary along the photon's direction.
4. Let  $t_2 =$  the smaller of  $t_1$  and  $d$ . Transport by distance  $t_2$ .
5. Deduct  $t_2/\lambda$  from  $N_\lambda$ . If the result is zero (this happens when  $t_2 = t_1$ ), then it is time to interact. Jump out of the loop.
6. This step is reached if  $t_2 = d$ . Thus, a boundary was reached. Do the necessary bookkeeping. If the new region is a different material, go to Step 1. Otherwise, go to Step 2.

In regions where there is a vacuum,  $\sigma = 0$  ( $\lambda = \infty$ ) and special coding is used to account for this situation.

Now, let us consider charged particle transport. The relevant interactions considered in EGS are elastic Coulomb scattering off the nucleus, inelastic scattering off the atomic electrons, bremsstrahlung production, and positron annihilation. Difficulties with charged particle transport arise from the fact that the cross sections for all of the above processes (with the exception of annihilation) become infinite as the energy approaches zero (the infrared catastrophe, etc). In actuality, these cross sections, when various corrections are taken into account (i.e., screening for nuclear scattering, electron binding for electron scattering, and Migdal corrections for bremsstrahlung), are not infinite, but they are very large and

## CHAPTER 2

the exact values for the total cross sections are not well known. Therefore, it is not practical to try to simulate every interaction. On the other hand, the low momentum transfer events which give rise to the large cross section values do not result in large fluctuations in the shower behavior itself. For this reason, they are lumped together and treated in a continuous manner. Cutoff energies are used to distinguish between continuous and discrete interactions.

The electron and photon cutoff energies used by EGS (and PEGS) are given by the variables AE and AP, respectively. Any electron interaction that produces a delta-ray with total energy of at least AE, or a photon with energy of at least AP, is considered to be a discrete event. All other interactions are considered continuous and give rise to continuous energy losses and direction changes to the electron between discrete interactions. The energy losses are due to soft interactions with the atomic electrons (ionization loss) and to the emission of soft bremsstrahlung photons. The changes in direction are mostly due to multiple Coulomb scattering from the nucleus, with some contribution coming from soft electron scattering.

The above considerations complicate charged particle transport in several ways. First of all, due to continuous energy loss the cross section varies along the path of the electron; in addition, the electron path is no longer straight. The fact that the discrete electron total cross section decreases with decreasing energy--and hence, decreases along the path of the electron--makes possible the following trick, which is used to account for the change in  $\lambda$  along the path. An additional fictitious interaction is introduced which, if it occurs, results in straight-ahead scattering (i.e.,

## CHAPTER 2

no interaction at all). The magnitude of this cross section is assumed to be such that the total cross section is constant along the path. That is,

$$\sigma_{t,\text{fict}}(x) = \sigma_{t,\text{real}}(x) + \sigma_{\text{fict}}(x) = \text{constant} = \sigma_{t,\text{real}}(x_0). \quad 2.4.6$$

The location of the next "interaction" is then sampled using Eqs. 2.4.4 and 2.4.2 along with the total fictitious cross section,  $\sigma_{t,\text{fict}}$ . When the point of interaction is reached, a random number is chosen. If it is larger than  $\sigma_{t,\text{real}}(x)/\sigma_{t,\text{real}}(x_0)$ , then the interaction is fictitious and the transport is continued from that point without interaction. Otherwise, the interaction is real and is dealt with in the way described later. It can be shown that this scheme samples the distance between interactions correctly.

The remaining problem in electron transport is in correctly taking into account the multiple scattering of the electrons. This is a difficult problem to which we devote a section later (see Section 2.14). For now, we give the following general explanation. The transport of an electron between interactions is divided into smaller steps. Along each of these steps the electron is assumed to follow a straight line, and the multiple scattering is accounted for by changing the electron's direction at the end of the step. The angle between the initial and final direction is sampled from the appropriate distribution and the azimuthal angle is selected randomly. These steps must be kept small enough so that neglecting the lateral deflection of the electron along a step does not introduce significant errors. A related effect is that of path length correction. The steps must be kept small enough so that the true electron path length is not much larger than the straight line path length. Otherwise, a systematic error in the distance to the next interaction will result.

## CHAPTER 2

### 2.5 Particle Interactions

When a point of (real) interaction has been reached it must be decided which of the competing processes has occurred. The probability that a given type of interaction occurred is proportional to its cross section. Suppose the types of interactions possible are numbered 1 to n. Then  $\hat{i}$ , the number of the interaction to occur, is a random variable with distribution function

$$F(i) = \frac{\sum_{j=1}^i \sigma_j}{\sigma_t} \quad 2.5.1$$

where  $\sigma_j$  is the cross section for the jth type of interaction and  $\sigma_t$  is the total cross section ( $= \sum_{j=1}^n \sigma_j$ ). The  $F(i)$  are the branching ratios. The number of the interaction to occur,  $i$ , is selected by picking a random number and finding the  $i$  which satisfies

$$F(i-1) < \zeta < F(i). \quad 2.5.2$$

Once the type of interaction has been selected, the next step is to determine the parameters for the product particles. In general, the final state of the interaction can be characterized by, say,  $n$  parameters  $\lambda_1, \lambda_2, \dots, \lambda_n$ . The differential cross section is some expression of the form

$$d^n \sigma = g(\vec{\lambda}) d^n \lambda \quad 2.5.3$$

with the total cross section being given by

$$\sigma = \int g(\vec{\lambda}) d^n \lambda \quad 2.5.4$$

Then  $f(\vec{\lambda}) = g(\vec{\lambda}) / \int g(\vec{\lambda}) d^n \lambda$  is normalized to 1 and has the properties of a



## CHAPTER 2

joint density function. This then may be sampled using the method given in Section 2.2 or some of the more general methods mentioned in the literature. Once the value of  $\vec{\lambda}$  determines the final state, the properties of the product particles are defined and can be stored on the stack. As mentioned before, the particle with the least energy is put on top of the stack. The portion of code for transporting particles of the type corresponding to the top particle is then entered.

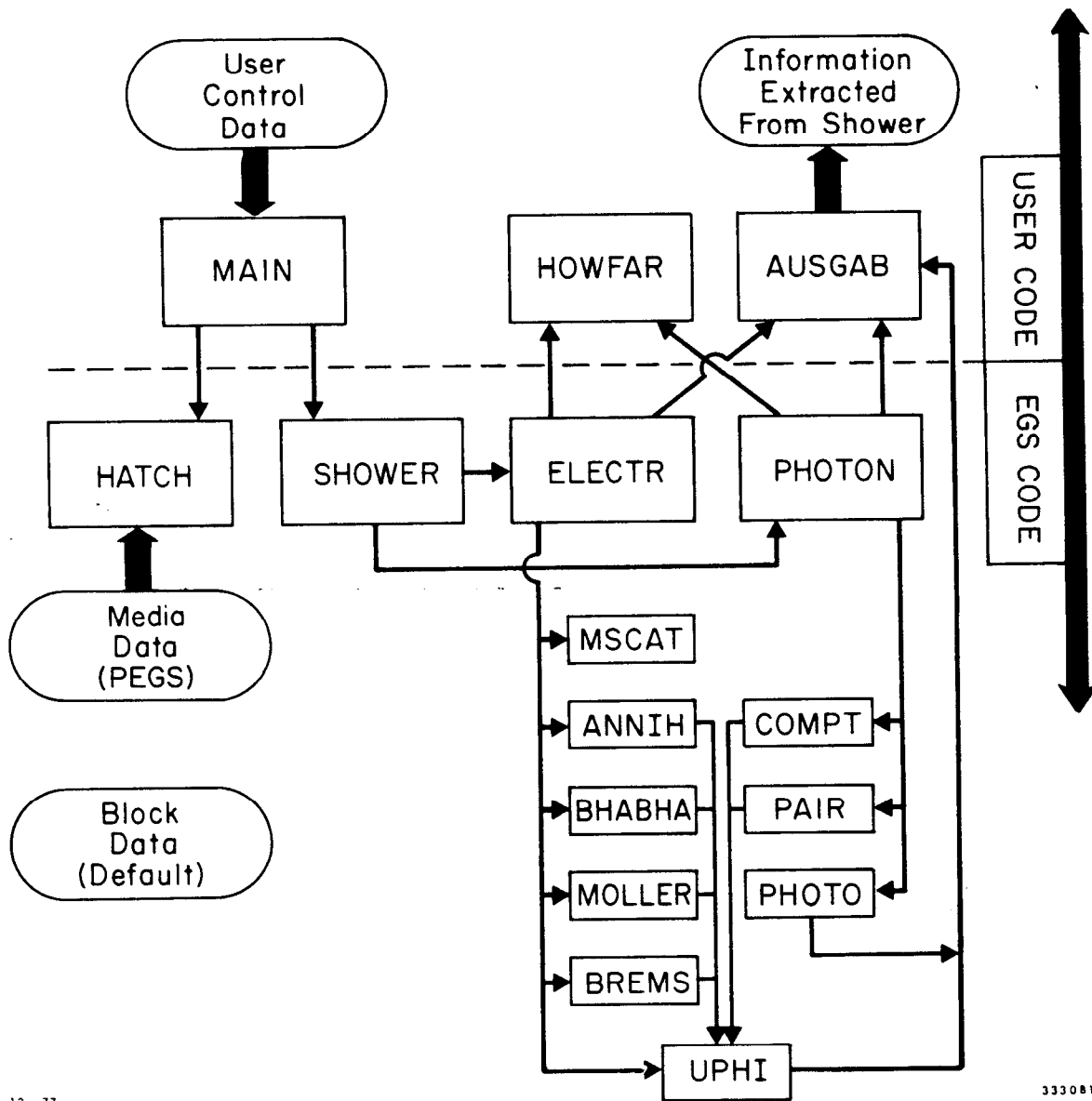
### 2.6 General Implementation Notes

We have seen in the preceding sections how it is possible, given the total cross sections, branching ratios, final state joint density functions, and an endless supply of random numbers, to simulate an electromagnetic shower. Due to the statistical nature of the Monte Carlo method, the accuracy of the results will depend on the number of shower histories run. Generally, the relative errors will be proportional to the inverse square root of the number of histories (Shreider 1966). Thus, to cut errors in half it is necessary to run four times as many histories. Also, for given cutoff energies, the computer time for a shower history is slightly more than linear in the energy of the incident particle. The point to be made here is that Monte Carlo calculations can be very time consuming. It is for this reason that the computational task is divided into two parts. First, a preprocessor code (PEGS) uses theoretical (and sometimes empirical) formulas to compute the various physical quantities needed and prepares them in a form for fast numerical evaluation. Then another code (EGS) uses this data, along with user supplied data and routines, to perform the actual simulation.

## CHAPTER 2

To aid in debugging and to help those interested in studying the various interactions, the EGS Code System has been expanded beyond the minimum coding necessary to simulate showers. With this in mind, PEGS was written in a modular form with over 75 subprograms. These include functions to evaluate physical quantities which are either needed by EGS or are of interest for other reasons. Other routines necessary for the operation of EGS include the fitting routines and the routine to write the data for a given material onto a data set. Included among the routines not needed for the operation of EGS are routines to plot the functions on the line printer or a graphic device, and a routine to compare (on a line printer plot) the theoretical final state density functions with sampled final state distributions (the sampled distributions are produced by the TESTSR (Test Sampling Routine) code as described in Chapter 6). The main program of PEGS calls some once-only initialization routines and then enters an option loop. After reading in the option that is desired, a NAMELIST read establishes other parameters which may be needed. The action requested is then performed and control returns to the beginning of the loop. This continues until the control input has been exhausted.

The EGS code itself consists of two user-callable subroutines, HATCH and SHOWER, which in turn call the other subroutines in the EGS code, some of which call two user-written subroutines, HOWFAR and AUSGAB. The latter determine the geometry and output (scoring), respectively. The user communicates with EGS by means of various COMMON variables. To use EGS, the user must write a MAIN program and the subroutines HOWFAR and AUSGAB. Usually, MAIN will perform any initialization needed for the geometry routine, HOWFAR,



12-77

333081

Fig. 2.6.1 Flow Control with User Using EGS.

## CHAPTER 2

and set the values of certain EGS COMMON variables which specify such things as names of the media to be used, the desired cutoff energies, and the unit of distance (e.g., centimeters, radiation lengths, etc.). MAIN then calls the HATCH subroutine which "hatches" EGS by doing necessary once-only initialization and by reading from a data-set the material data prepared by PEGS for the media requested. This initialization completed, MAIN may now call SHOWER when desired. Each call to SHOWER results in the generation of one Electron Gamma Shower history. The arguments to SHOWER specify the parameters of the incident particle. Thus the user has the freedom to use any source distribution he desires. Figure 2.6.1 illustrates the flow of control and data when a user written program is using the EGS code. The detailed information needed to write such user programs is given in Chapter 4 (the User Manual).

The TESTSR code was written to systematically test EGS' secondary distribution sampling routines; that is, ANNIH, BHABHA, MOLLER, BREMS, COMPT, PAIR, and MSCAT. Figure 2.6.2 illustrates the logical relations between the parts of the TESTSR and EGS codes. The MAIN program of TESTSR reads control information to determine the medium to be used for the test, the routine to be tested, and the primary particle energy. HATCH is called to read in the material data. The SAMPLE routine is then called with appropriate arguments by means of subroutine SELECT. One of SAMPLE's arguments is the name of the external sampling routine to be sampled. Other arguments specify the method of binning the secondary energies and the number of samples or desired precision. SAMPLE repeatedly sets up the particle stack with an appropriate primary particle, calls the sampling routine, and then looks at the stack to see what energies were given to the secondary particles. The value of the energy of one of the secondary particles is used to select the bin to be

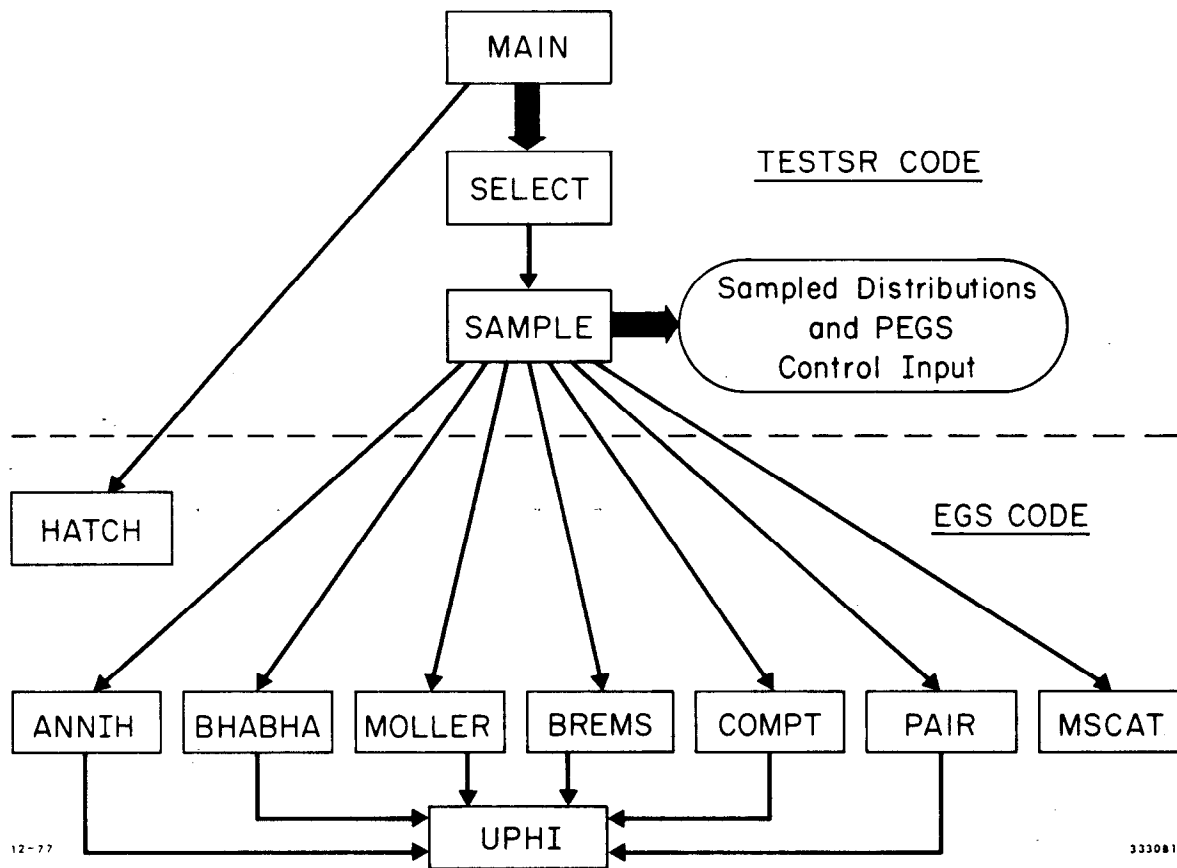


Fig. 2.6.2 Logical Relations Between Parts of EGS and the TESTSR User Code.

## CHAPTER 2

incremented. This process continues until either the number of samples selected is reached, the relative error corresponding to the least counts in any one bin is less than the desired precision, or until the job runs out of time. In any case, SAMPLE then outputs control information for PEGS followed by the sampled distribution. PEGS uses this information to produce a line printer plot comparing the sampled and theoretical distributions. The reader may refer to Chapter 6 for more details regarding TESTSR.

The remainder of this chapter will be devoted to the fundamental interaction processes that are used in the EGS Code System. Classical physics approaches, as well as quantum-mechanical ones, have been used to explain these phenomena, and we assume that the reader is familiar with the basic physics. The CGS system of units is used primarily. However, PEGS scales its outputs in units of radiation lengths and both EGS and PEGS use MeV for the unit of energy. The centimeter is the basic unit of distance in EGS, but transport may be done in some other distance unit by setting the variable DUNIT before calling HATCH. See Chapter 4 for details.

Table 2.6.1 defines some of the mathematical and program symbols for entities in EGS and PEGS, as well as other symbols used in our discussion. The first column gives the item number, the second column shows the mathematical symbol used for the entities, and the third column shows the FORTRAN name for the same thing in the EGS or PEGS code. A 'P', 'E', or both in column four shows whether the item is used in PEGS, EGS, or both. The fifth column contains a definition, explanation, or name of the item.

CHAPTER 2

Table 2.6.1

Symbols in EGS and PEGS

	<u>Math</u>	<u>FORTRAN</u>	<u>Program</u>	<u>Definition</u>
1.	$\pi$	PI	P	3.1415926536
2.	c	C	P	speed of light = $2.997925 \times 10^{10}$ cm/sec
3.	$m_e$	RME	P	electron rest mass = $9.1091 \times 10^{-28}$ g
4.	$\hbar$	HBAR	P	Planck's constant/ $2\pi$ = $1.05450 \times 10^{-27}$ erg-s
5.	$e_{CGS}$	ECGS	P	electronic charge (CGS units) = $4.80298 \times 10^{-10}$ esu
6.	$e_{MKS}$	EMKS	P	electronic charge (MKS units) = $1.60210 \times 10^{-19}$ Coul
7.	$N_a$	AN	P	Avogadro's number = $6.02252 \times 10^{23}$ mole <sup>-1</sup>
8.	(1 Rad)[°]	RADDEG	P	radian expressed in degrees = $180/\pi$
9.	$\alpha$	FSC	P	fine structure constant = $e_{CGS}^2/(\hbar c)$
10.	(1 MeV) [erg]	ERGMEV	P	one MeV expressed in ergs = $e_{MKS} \times 10^{13}$
11.	$r_0$	RO	P	classical electron radius = $e_{CGS}^2/(m_e c^2)$
12.	m	RM	PE	electron rest energy in MeV = $m_e c^2/ERGMEV$
13.	2m	RMT2	PE	2m
14.	$m^2$	RMSQ	PE	$m^2$
15.	'22.9'	A22P9	P	constant in Nagel's formula for $\chi_c$ in degrees. Taken from Moliere's paper in which $\chi_c$ was expressed in grads. So to get $\chi_c$ in degrees, should really use $22.9 \times 360/400$ . Defined as $A22P9 = RADDEG \sqrt{4\pi N_a} e_{CGS}^2/ERGMEV = 22.6960$
16.	'6680'	A6680	P	constant in Bethe's formula for Moliere's b = $4\pi N_a (\hbar/m_e c)^2 (0.885)^2 / (1.167 \times 1.13)$ = 6702.33
17.	k, $k_1$		P	photon energy in ergs
18.	$\check{k}$ , $\check{k}_1$		P	photon energy in MeV

CHAPTER 2

Table 2.6.1 (continued)

	<u>Math</u>	<u>FORTRAN</u>	<u>Program</u>	<u>Definition</u>
19.	$E, E_1$		P	electron total energy in ergs
20.	$\check{E}, \check{E}_1$		P	electron total energy in MeV
21.	T		P	electron kinetic energy in ergs
22.	$\check{T}$		P	electron kinetic energy in MeV
23.	t		P	distance in centimeters
24.	$\check{t}$		P	distance in radiation lengths = $t/X_0$
25.	$\sigma$		P	cross section in $\text{cm}^2/(\text{atom or molecule})$
26.	$\Sigma$		P	macroscopic cross section (probability of interaction/cm) = $N_a \rho \sigma / M$
27.	$\check{\Sigma}$		P	macroscopic cross section [ $X_0^{-1}$ ] units = $X_0 \Sigma$
28.	$\rho$	RHO	PE	material density ( $\text{g}/\text{cm}^3$ )
29.	$N_e$	NE	PE	number of elements in the material
30.	$Z_i$	Z(I)	P	atomic weight of the ith element of the material
31.	$A_i$	WA(I)	P	atomic weight of the ith element of the material ( $\text{g}/\text{mole}$ )
32.	$p_i$	PZ(I)	P	proportion by number of the ith element in the material $\propto p_i/A_i$
33.	$\rho_i$	RHOZ(I)	P	proportion by weight of the ith element in the material $\propto p_i A_i$
34.	M	WM	P	molecular weight ( $\text{g}/\text{mole}$ ) = $\sum_{i=1}^{N_e} p_i A_i$
35.	$C_M$	ZC	P	molecular charge (electrons/molecule) = $\sum_{i=1}^{N_e} p_i Z_i$
36.	n	EDEN	P	electron density ( $\text{electrons}/\text{cm}^3$ ) = $N_a \rho C_M / M$
37.	$X_0$	RLC	PE	radiation length = $(N_a \rho 4 \alpha r_0^2 (Z_A + Z_B - Z_F) / M)^{-1}$



CHAPTER 2

Table 2.6.1 (continued)

<u>Math</u>	<u>FORTRAN</u>	<u>Program</u>	<u>Description</u>
38. $Z_T$	ZT	P	$\sum_{i=1}^{N_e} p_i Z_i (Z_i + \xi_i)$
39. $Z_B$	ZB	P	$\sum_{i=1}^{N_e} p_i Z_i (Z_i + \xi_i) \ln Z_i^{-1/3}$
40. $Z_F$	ZF	P	$\sum_{i=1}^{N_e} p_i Z_i (Z_i + \xi_i) f_c(Z_i)$
41. $Z_S$	ZS	P	$\sum_{i=1}^{N_e} p_i Z_i (Z_i + \xi_{MS})$
42. $Z_E$	ZE	P	$\sum_{i=1}^{N_e} p_i Z_i (Z_i + \xi_{MS}) \ln Z_i^{-2/3}$
43. $Z_X$	ZX	P	$\sum_{i=1}^{N_e} p_i Z_i (Z_i + \xi_{MS}) \ln (1 + 3.34 (\alpha Z_i)^2)$
44. $Z_A$	ZA	P	$Z_T \ln 183$
45. $Z_G$	ZG	P	$Z_B / Z_T$
46. $Z_P$	ZP	P	$Z_B / Z_A$
47. $Z_V$	ZV	P	$(Z_B - Z_F) / Z_T$
48. $Z_U$	ZU	P	$(Z_B - Z_F) / Z_A$
Note: The next four are used in EGS directly and computed in MIX			
49. $b_c$	BLCC	PE	'6680' $\rho Z_S \exp(Z_E / Z_S) X_0 / (M \exp(Z_X / Z_S))$
50. $\chi_{cc}$	XCC	PE	('22.9' / RADDEG) $\sqrt{Z_S \rho X_0 / M}$
51. $t_{eff0}$	TEFFO	PE	$(\exp(B_{min}) / B_{min}) / b_c$
52. $\chi_{r0}$	XRO	PE	$\chi_{cc} \sqrt{t_{eff0} B_{min}}$
53. $\xi_{MS}$	\$FUDGEMS	P	constant used to account for multiple scattering of atomic electrons
54. $\xi_i$	XSI(I)	P	constant for bremsstrahlung and pair production off atomic electrons for element $Z_i$

CHAPTER 2

Table 2.6.1 (continued)

<u>Math</u>	<u>FORTRAN</u>	<u>Program</u>	<u>Description</u>
55. $f_c(Z_i)$	FCOUL(I)	P	bremsstrahlung and pair production Coulomb correction constant for element $Z_i$
56. $B_{\min}$	BMIN	P	
57. $\lambda$	MFP	P	mean free path
58. $A'(Z_i, E)$	APRIME(I)	P	empirical bremsstrahlung correction factor
59. $U(x)$		P	unit step function
60. $\phi_1(\delta)$		P	first screening function
61. $\phi_2(\delta)$		P	second screening function
62. $\delta_i$		P	screening parameter for element $Z_i$
63. $\delta'$		P	average screening parameter for mixture
64. $A_P$	AP	PE	
65. $A_E$	AE	PE	
66. $\Delta$			
67. $\hat{\zeta}, \hat{\zeta}_i,$ $\zeta, \zeta_i$			uniform random variables and sampled values
68. $\alpha_i$			weight of ith element in sampling method
69. $\lambda_0$			Compton wavelength of electron $= 2\pi r_0 / \alpha = 2.4262 \times 10^{-10}$ cm.

## CHAPTER 2

A number of physical, mathematical, and derived constants are used by the codes. We have arrived at their values in a very mnemonic way by means of the PEGS subroutine called PMDCON (Physical, Mathematical, and Derived CONstants). These are items 1 through 16 in Table 2.6.1. As illustrated in items 17 through 27, cupped ( $\cup$ ) energy variables will be in MeV, cupped distance variables will be in radiation lengths, and uncupped quantities will denote CGS units.

A material is specified by giving its density,  $\rho$ , number of elements,  $N_e$ , atomic symbols of its elements,  $S_i$ , and the proportion of the atoms which are of a given type,  $p_i$ . PEGS maintains tables of atomic numbers,  $Z_i$ , and atomic weights,  $A_i$ , for elements 1 through 100. In case the material is a single element, PEGS also has a table of densities. In case the material being used has non-standard isotopes or density, the values supplied by PEGS may be overridden. As an alternative to giving the atomic proportions by number  $p_i$ , they may be given by weight,  $\rho_i$ . The parameters used to define a medium are summarized as items 28 through 33 in Table 2.6.1.

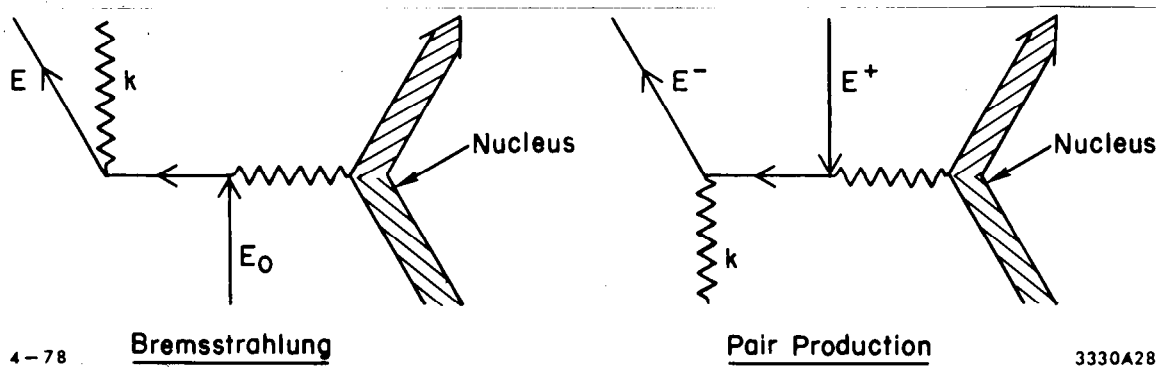
The PEGS subroutine, MIX, takes the material parameters mentioned above and uses them to compute some additional molecular parameters (items 34 through 53 in Table 2.6.1) which are useful in computing cross sections for mixtures. The uses for these parameters will appear later when we discuss the cross sections in detail.

We now proceed to discuss the physical processes and their simulation.

## CHAPTER 2

### 2.7 Bremsstrahlung and Electron-Positron Pair Production

The bremsstrahlung and pair production processes are closely related, as can be seen from the Feynman diagrams below



In the case of bremsstrahlung, an electron or positron is scattered by two photons, a virtual photon from the atomic nucleus and another free photon which is created by the process. In the case of pair production, an electron traveling backward in time (a positron) is also scattered by two similar photons, and one of the collisions scatters it forward in time making it into an electron. The net effect is the absorption of a photon and creation of an electron-positron pair.

The formulas we use for these processes are taken from the review articles by Koch and Motz (1959) on bremsstrahlung and by Motz, Olsen and Koch (1969) on pair production. We also used some ideas from Butcher and Messel (1960) for mixing the cross sections for sampling of the secondary spectra. Below 50 MeV the Born approximation cross sections are used with empirical corrections added to get agreement with experiment. Above 50 MeV the extreme relativistic Coulomb corrected cross sections are used.

## CHAPTER 2

The "shower book" (Messel and Crawford 1970) takes into account the "suppression effect" (Migdal 1956, Fowler 1959, Feinberg 1956) which is expected to be important for energies  $\geq 10^{13}$  eV. We neglect this effect in the present version. One manifestation of the suppression effect is that at these high energies the bremsstrahlung and pair production cross sections are significantly decreased. In addition, an effect due to polarization of the medium (which apparently is effective even at ordinary energies) results in the cutoff of the bremsstrahlung differential cross section at secondary photon energies below a certain fraction of the incident electron energy. This enters in by means of the factor (Messel and Crawford 1970 p. 11).

$$F_P = \left( 1 + \frac{n r_o \lambda_o^2 E_o^2}{\pi k^2} \right)^{-1} \quad 2.7.1$$

where  $n$  is the electron density,  $r_o$  is the classical electron radius,  $\lambda_o$  is the Compton wavelength of an electron, and  $E_o$  and  $k$  are the energies of the electron and photon, respectively. If we define a cutoff energy by

$$k_c = E_o \sqrt{n r_o \lambda_o^2 / \pi} \quad 2.7.2$$

then we see that for  $k \gg k_c$ ,  $F_P$  goes to one; for  $k \approx k_c$ , it is about 1/2; and for  $k \ll k_c$  it goes as  $k^2/k_c^2$ . In the latter case, the  $k^2$  factor multiplied by the usual  $1/k$  dependence results in an overall  $k$  dependence as  $k^{-0}$ . Thus we have finite differential and total cross sections and the infrared catastrophe is averted. It can be seen that the ratio of the cutoff energy to the incident electron energy is independent of energy, and depends on the medium only through its electron density. For lead, the ratio is

## CHAPTER 2

$$\begin{aligned}
 k_c/E_o &= \sqrt{nr_o \lambda_o^2/\pi} \\
 &= 1.195 \times 10^{-4} \quad . \qquad \qquad \qquad 2.7.3
 \end{aligned}$$

The natural log of the inverse of this ratio ( $\approx 9$ ) is then approximately equal to the total bremsstrahlung cross section in units of inverse radiation lengths (if one takes  $d\sigma/dk [X_o^{-1}] = 1/k$  for  $k > k_c$ ,  $= 0$  for  $k < k_c$ ).

We have not taken the time to carefully study and implement these corrections. We therefore now ask what is the expected error from this omission, assuming the Migdal formulas are correct? First, it is clear that at the very high energies ( $\approx 10^{13}$  eV) that the gross behavior of the shower will change as a result of the reduced bremsstrahlung and pair production cross section. We therefore set 100 GeV as a safe upper limit to the present EGS version. Next we see that we are allowing production of photons below the cutoff  $k_c$ . For example, a 10 GeV electron should not omit many photons below 1 MeV; whereas, we would continue production down possibly as low as 1 keV. This should not disturb the general shower behavior much, as there will be many more low energy electrons than high energy, so that the few extra low energy photons produced by the high energy electrons should be insignificant compared to the low energy photons produced by the lower energy electrons. It should be clear, however, that if the user were using EGS to find thin target bremsstrahlung spectrum from high energy electrons, that the results would be in error below the cutoff. An experimental verification of this cutoff, though it might be difficult, would be of interest and could be a strong confirmation of the theory of Migdal (the soft photon cutoff was first obtained by Ter-Mikaelyan (1954a)). A future version of EGS could include these effects and the "shower book" describes their implementation in some detail.

CHAPTER 2

Neglecting possible crystal diffraction effects (Ter-Mikaelyan 1954b, Feinberg 1956), the macroscopic cross section for bremsstrahlung or pair production is given in terms of the microscopic cross sections,  $\sigma_i$ , for the atoms of type  $i$  by

$$\Sigma = \frac{N_a \rho}{M} \sum_i p_i \sigma_i = N_a \rho \frac{\sum_i p_i \sigma_i}{\sum_i p_i A_i} \quad . \quad 2.7.4$$

We see that the macroscopic cross sections do not depend on the absolute normalization of the  $p_i$ 's, only the ratios. With the exception of ionization losses (where polarization effects are important), Eq. 2.7.4 is also valid for the other reactions that are considered (e.g., Møller, Compton, etc.).

For conciseness in what follows we shall use the notation

$$(E_1 \text{ if } B_1, \dots, E_n \text{ if } B_n, E_{n+1}) \quad 2.7.5$$

to denote the conditional expression which takes  $E_i$  for its value if  $B_i$  is the first true expression, and takes  $E_{n+1}$  for its value if no  $B_i$  is true. For example, the Kronecker delta can be defined by

$$\delta_{ij} = (1 \text{ if } i=j, 0). \quad 2.7.6$$

Using this notation, we start with the following formulas for the bremsstrahlung and pair production differential cross sections:

CHAPTER 2

$$\frac{d\sigma_{\text{Brem}}(Z, \check{E}_0, \check{k})}{d\check{k}} = \frac{A'(Z, \check{E}_0) r_o^2 \alpha Z (Z + \xi(Z))}{\check{k}}$$

$$\times \left\{ \left( 1 + (\check{E}/\check{E}_0)^2 \right) \left[ \phi_1(\delta) - \frac{4}{3} \ln Z - (4f_c(Z) \text{ if } \check{E}_0 > 50, 0) \right] \right.$$

$$\left. - \frac{2}{3} \left( \frac{\check{E}}{\check{E}_0} \right) \left[ \phi_2(\delta) - \frac{4}{3} \ln Z - (4f_c(Z) \text{ if } \check{E}_0 > 50, 0) \right] \right\} \quad 2.7.7$$

and

$$\frac{d\sigma_{\text{Pair}}(Z, \check{k}, \check{E}_+) }{d\check{E}_+} = \frac{A'_p(Z, \check{k}) r_o^2 \alpha Z (Z + \xi(Z))}{\check{k}^3}$$

$$\times \left\{ (\check{E}_+^2 + \check{E}_-^2) \left[ \phi_1(\delta) - \frac{4}{3} \ln Z - (4f_c(Z) \text{ if } \check{k} > 50, 0) \right] \right.$$

$$\left. + \frac{2}{3} \check{E}_+ \check{E}_- \left[ \phi_2(\delta) - \frac{4}{3} \ln Z - (4f_c(Z) \text{ if } \check{k} > 50, 0) \right] \right\} \quad 2.7.8$$

where

$$\delta = 136 Z^{-1/3} 2\Delta \quad 2.7.9$$

and

$$\Delta = \frac{\check{k}_m}{2\check{E}_+ \check{E}_-} \quad (\text{for bremsstrahlung}) \quad 2.7.10$$

$$= \frac{\check{k}_m}{2\check{E}_+ \check{E}_-} \quad (\text{for pair production}) \quad 2.7.11$$



To avoid confusion it should be noted that our  $\delta$  is the same as the  $\delta$  of Butcher and Messel (1960) but we use  $\phi_i(\delta)$  to denote their  $f_i(\delta)$ . Rossi (1952) and Koch and Motz (1959) use a variable  $\gamma = \frac{100}{136} \delta$ . Also, note that our  $\phi_i(\delta)$  has the same value as the  $\phi_i(\gamma)$  of Koch and Motz (1959 (Fig. 1)) provided "our  $\delta$ " =  $\frac{136}{100}$  times "their  $\gamma$ ." For arbitrary screening,  $\phi_1$  and  $\phi_2$  are given by

$$\phi_1(\delta) = 4 \int_{\Delta}^1 (q - \Delta)^2 [1 - F(q, Z)]^2 \frac{dq}{q} + 4 + \frac{4}{3} \ln Z \quad 2.7.12$$

$$\phi_2(\delta) = 4 \int_{\Delta}^1 \left[ q^3 - 6\Delta^2 q \ln\left(\frac{q}{\Delta}\right) + 3\Delta^2 q - 4\Delta^3 \right] [1 - F(q, Z)]^2 \frac{dq}{q} + \frac{10}{3} + \frac{4}{3} \ln Z \quad 2.7.13$$

where  $\delta = 272 Z^{-1/3} \Delta$  as before, and where  $F(q, Z)$  is the atomic form factor for an atom with atomic number  $Z$ . Following Nagel (1964), we have used the Thomas-Fermi form factors, for which  $\phi_1$  and  $\phi_2$  are  $Z$  independent and have already been evaluated. Butcher and Messel (1960) have approximated the screening functions to within 1-2% by the formulas

$$\phi_1(\delta) = (20.867 - 3.242 \delta + 0.625 \delta^2 \text{ if } \delta \leq 1, 21.12 - 4.184 \ln(\delta + 0.952)) \quad 2.7.14$$

and

$$\phi_2(\delta) = (20.029 - 1.930 \delta - 0.086 \delta^2 \text{ if } \delta \leq 1, 21.12 - 4.184 \ln(\delta + 0.952)). \quad 2.7.15$$

The Thomas-Fermi screening is quite accurate for high atomic numbers, but at low atomic numbers its accuracy decreases. The Hartree form factors are better for low  $Z$ . Tsai (1974) has given a review of the current state of the

## CHAPTER 2

art in bremsstrahlung and pair production, including best estimates of form factors and the screening functions. EGS could be modified to use these, but since this writeup is already long overdue we shall reserve this modification for a future version.

The  $A'(Z, \check{E}_0)$  in Eq. 2.7.7 is an empirical correction factor. For  $\check{E}_0 > 50$ ,  $A' = 1$  since we use the Coulomb corrected formulas which are accurate to about 3% in this energy range. For  $\check{E}_0 < 50$  we use values interpolated in  $Z$  from the curves of Koch and Motz (1959 (Fig. 23)).  $A'$  is evaluated by the function APRIM in PEGS.

The empirical correction factor  $A'_p(Z, \check{k})$  in Eq. 2.7.8 is defined as:

$$A'_p(Z, \check{k}) = (\text{"Best Estimate of Total Pair Production Cross Section for given } Z, \check{k}\text{"}) / (\text{"Total Pair Production Cross Section obtained by integrating Eq. 2.7.8 with } A'_p \text{ replaced by 1 over all allowed } \check{E}_+ \text{ values"}).$$

For  $\check{k} < 50$ , we take this best estimate to be the data compiled by Storm and Israel (1970), and in fact we use this data directly without resorting to Eq. 2.7.8 whenever pair production total cross sections are needed for  $\check{k} < 50$ . For  $\check{k} > 50$  an integration of Eq. 2.7.8 with  $A'_p \rightarrow 1$  is the best estimate (and agrees with Storm and Israel up to the limiting energy for which they present data); thus

$$A'_p(Z, \check{k} > 50) = 1$$

as in the bremsstrahlung case. Unlike the bremsstrahlung case, however,  $A'_p$  is never explicitly calculated since it is not needed for the total cross section calculation, and, as will be seen later, it is not used in the secondary sampling either.

## CHAPTER 2

The  $f_c(Z)$  in Eqs. 2.7.7 and 2.7.8 is the Coulomb correction term that was derived by Davies, Bethe and Maximon (1954 (formula 36, p. 791)) and is given by

$$f_c(Z) = a^2 \sum_{v=1}^{\infty} \frac{1}{v(v^2 + a^2)} \quad 2.7.16$$

where

$$a = \alpha Z .$$

They also suggest a formula accurate to 4 digits up to  $a = 2/3$  (which corresponds to Uranium); namely,

$$f_c(Z) = a^2 \left\{ (1+a^2)^{-1} + 0.20206 - 0.0369a^2 + 0.0083a^4 - 0.002a^6 \right\} \quad 2.7.17$$

which function FCOULC of PEGS uses to evaluate  $f_c(Z)$ .

$\xi(Z)$  is a function which is used to take into account bremsstrahlung and pair production in the field of the atomic electrons. Strictly speaking, these interactions are different from the corresponding nuclear interaction not only because the mass and charge of an electron are different from the nuclear mass and charge, but also because of the identity of the electrons. Because of the lightness of the electron, it may be ejected from the atom. In the bremsstrahlung case what we really have is radiative Møller or Bhabha scattering. In the case of pair production, if the atomic electron is ejected, we have three rather than two energetic electrons and the reaction is called triplet production. Because of the electron exchange effects and the  $\gamma - e$  interactions between the external photon and the target electron, and also

## CHAPTER 2

because the target can no longer be treated as infinitely heavy, the cross section calculations for these interactions are more complicated than for the corresponding nuclear cases and involve a larger number of approximations (Motz et al., 1969 (p. 631)).

As will be seen below, the ratio of cross sections for the interaction in the electron fields to those in the nuclear field is of the order of  $1/Z$ . Thus, for medium-low to high  $Z$ , the contributions of the atomic electrons are rather minor. On the other hand, for low  $Z$ , such as beryllium and certainly for hydrogen, these interactions are very significant and a more accurate treatment of these interactions is warranted. Nevertheless, we have not treated the bremsstrahlung and pair production in the electronic fields in a special way, primarily because most applications of interest do not involve only very low  $Z$  elements, but rather when low  $Z$  elements are involved, they have usually been mixed with higher  $Z$  elements, in which case the pair production and bremsstrahlung in the low  $Z$  elements are relatively unimportant. This does limit somewhat the universality of the EGS code, however, and if an application that needed, say, an accurate estimate of shower development in pure hydrogen arose, it might be advisable to fix EGS to treat these interactions more completely in the future.

For very high energy incident particles the screening can be considered complete. In this case, relatively simple formulas for the interaction in the atomic field can be obtained (Bethe and Ashkin 1953 (formula 59 on p. 263 and formula 119 on p. 332), Koch and Motz 1959 (formula III-8 on p. 949)). The relative values of the radiation integral

CHAPTER 2

$$\phi_{\text{rad}} \equiv \frac{1}{E} \int_0^{k_{\text{max}}} k \frac{d\sigma_{\text{Brem}}}{dk} dk \quad 2.7.18$$

can be used as an estimate of the relative magnitude of the interactions in the electron or nuclear fields. In the completely screened nuclear field, the radiation integral is (formula 4CS of Koch and Motz (1959))

$$\phi_{\text{rad,nucleus}} = 4\alpha r_0^2 Z^2 [\ln(183Z^{-1/3}) + \frac{1}{18} - f_c(Z)] \quad 2.7.19$$

For  $\phi_{\text{rad}}$  in the completely screened electron field Koch and Motz give (formula III-8 on p. 949)

$$\phi_{\text{rad,electron}} = 4\alpha r_0^2 Z \ln(530Z^{-2/3}) \quad 2.7.20$$

On the other hand, from the formulas of Bethe and Ashkin mentioned above, one would expect

$$\phi_{\text{rad,electron}} = 4\alpha r_0^2 Z \ln(1440Z^{-2/3}) \quad 2.7.21$$

We have not taken the time to resolve this discrepancy but have followed the suggestion of Nagel (1966) and have used Eq. 2.7.21. We neglect the 1/18 in Eq. 2.7.19 and define

$$\xi(Z) = \ln(1440Z^{-2/3}) / [\ln(183Z^{-1/3}) - f_c(Z)] \quad 2.7.22$$

This is the formula used by function XSIF of PEGS to compute  $\xi(Z)$  for use in Eqs. 2.7.7 and 2.7.8. Table 2.7.1 lists the values of  $\xi$  (and other items) for the above formulas for various Z values. We see that the discrepancy results in 15-25% differences in the value of  $\xi$ .

Table 2.7.1

 $\xi(Z)$  and Related Items

Z	1	10	50	92
$\ln Z^{-2/3}$	0	- 1.535	- 2.608	- 3.015
$\ln 1440Z^{-2/3}$	7.272	5.737	4.664	4.258
$\ln 530Z^{-2/3}$	6.273	4.738	3.665	3.258
$\ln 183Z^{-1/3}$	5.209	4.442	3.905	3.702
$f_c(Z)$	$6.404 \times 10^{-5}$	$6.375 \times 10^{-3}$	0.1438	0.3951
$\xi_{BA}$	1.396	1.293	1.240	1.288
$\xi_{KM}$	1.204	1.068	0.9744	0.9852

$$\xi_{BA} = \text{Eq. 2.7.22}$$

$$\xi_{KM} = \text{Eq. 2.7.20/Eq. 2.7.19 (without 1/18)}$$

Now that we have discussed all items appearing in Eqs. 2.7.7. & 8, we mention some additional corrections to Eq. 2.7.7 that have been neglected in this version. First, the differential cross section given in Eq. 2.7.7 goes to zero at the maximum photon energy; whereas, in reality the bremsstrahlung cross section, differential in photon energy, is non-zero at the "high frequency limit" (Koch and Motz 1959 (p. 933)). A more rigorous treatment would modify Eq. 2.7.7 so as to smoothly approach the proper value at the high frequency limit.

Another correction for Eq. 2.7.7 that we have ignored is the "Elwert factor", which Koch and Motz (1959) recommend be applied below  $\gamma=2$ . Our reasons for ignoring it is that our usual electron cutoff

CHAPTER 2

( $\bar{T}=1$ ) is not much below this, and we have not felt it important enough to implement since if one were to try to transport electrons at lower energies, other modifications would be necessary as well, such as abandoning the small angle approximation in multiple scattering in favor of the Goudsmit-Saunderson (1940a,b) formulation. To do a thorough job at lower electron energies would require extensive revisions.

We now discuss the methods we use to sample the secondary energies for bremsstrahlung and pair production interactions. Our methods are based on Eqs. 2.7.7 and 8 with a couple of approximations. For the purpose of our discussion let  $x$  and  $x_0$  be the secondary and incident particle energies, respectively. Then Eqs. 2.7.7 and 8 are of the form

$$\frac{d\sigma_{\text{corrected}}(Z, x_0, x)}{dx} = A'(Z, x_0) \frac{d\sigma_{\text{uncorrected}}(Z, x_0, x)}{dx} \quad 2.7.23$$

According to Eq. 2.7.4 the differential macroscopic cross section, properly weighted with the various constituent materials, will be

$$\frac{d\Sigma(x_0, x)}{dx} = \frac{N_a \rho}{M} \sum_{i=1}^{N_e} p_i \frac{d\sigma_{\text{corrected}}(Z_i, x_0, x)}{dx} \quad 2.7.24$$

and the total macroscopic cross section will be

$$\Sigma(x_0) = \int_{x_{\text{min}}}^{x_{\text{max}}} \frac{d\Sigma(x_0, x)}{dx} dx \quad 2.7.25$$

If the incident particle has undergone an interaction of this type, then the probability density function for  $x$  will be

$$f(x) = \frac{d\Sigma(x_0, x)}{dx} / \Sigma(x_0) \quad 2.7.26$$

## CHAPTER 2

We now observe that any constant factors in the right hand side of Eq. 2.7.24 will cancel out in Eq. 2.7.26, and in particular, if there is only one element then the correction factor  $A'(Z, x_0)$  will be an overall factor, so that it may be ignored. The first approximation which we now make (and which we could avoid if we really wanted to) is that the  $A'(Z, x_0)$  can be ignored for secondary sampling purposes even when there is more than one element. As will be seen, this will allow us to obtain energy independent screening factors. The way we could avoid making this approximation is to have PEGS generate branching ratios among all the constituents as a function of particle energy so that whenever an interaction took place, the first thing done would be to decide with which type of atom the interaction occurred. For complex mixtures this would take a significantly larger amount of data and running time and we have chosen to make the above approximation instead.

Now suppose that the  $f(x)$  in Eq. 2.7.26 is decomposed as in Eq. 2.2.10; that is,

$$\frac{d\Sigma(x_0, x)}{dx} \bigg/ \Sigma(x_0) = \sum_{i=1}^{N_e} \alpha_i' f_i(x) g_i(x) , \quad 2.7.27$$

or

$$\frac{d\Sigma(x_0, x)}{dx} = \sum_{i=1}^{N_e} \alpha_i f_i(x) g_i(x) \quad 2.7.28$$

where

$$\alpha_i = \alpha_i' \Sigma(x_0) . \quad 2.7.28$$

But from Eq. 2.2.7 it can be seen that if all  $\alpha_i$  are multiplied by the same factor, it will not change the function being sampled. We conclude that to properly sample from the p.d.f. (Eq. 2.7.26), it is not necessary



CHAPTER 2

to obtain  $\Sigma(x_0)$ , but it is sufficient to decompose  $d\Sigma(x_0, x)/dx$  as shown in Eq. 2.7.28 without bothering to normalize. We seek decompositions of the form

$$\sum_{j=1}^n \alpha_j f_j(x) g_j(x) = \sum_{i=1}^{N_e} p_i \frac{d\sigma_{\text{uncorrected}}(Z_i, x_0, x)}{dx} . \quad 2.7.29$$

Let us now do this for the bremsstrahlung process (in a manner similar to that of Butcher and Messel (1960)) using Eq. 2.7.7 for  $d\sigma_i/dx$  with  $A'(Z_i, \check{E}_0) = 1$ . The first point to be noted (Nagel 1966) is that  $\phi_1(\delta)$  and  $\phi_2(\delta) \rightarrow 0$  as  $\delta \rightarrow \infty$ , so that the expressions in square brackets in Eq. 2.7.7 go to zero, and in fact go negative, at sufficiently large  $\delta$ . As can be seen from Eq. 2.7.15,  $\phi_2(\delta) = \phi_1(\delta)$  for  $\delta > 1$ . By checking numerical values it is seen that the value of  $\delta$  for which the expressions go to zero is greater than 1, so that both [ ] expressions in Eq. 2.7.7 go to zero simultaneously. Clearly the differential cross section must not be allowed to go negative, so this imposes an upper kinematic limit  $\delta_{\text{max}}(Z_i, \check{E}_0)$  resulting in the condition (from Eq. 2.7.14)

$$21.12 - 4.184 \ln(\delta_{\text{max}}(Z, \check{E}_0) + 0.952) - \frac{4}{3} \ln Z - (4f_c(Z) \text{ if } \check{E}_0 > 50, 0) = 0. \quad 2.7.30$$

Solving for  $\delta_{\text{max}}(Z, \check{E}_0)$  we obtain

$$\delta_{\text{max}}(Z, \check{E}_0) = \exp \left[ \left( 21.12 - \frac{4}{3} \ln Z - (4f_c(Z) \text{ if } \check{E}_0 > 50, 0) \right) / 4.184 \right] - 0.952 . \quad 2.7.31$$

In PEGS routines BREMDZ, BRMSDZ, and BRMSFZ, which compute  $d\sigma_{\text{Brem}}(Z, \check{E}_0, \check{k})/d\check{k}$ , as given by Eq. 2.7.7, it may be seen that the result is set to zero if  $\delta > \delta_{\text{max}}(Z, \check{E}_0)$ . Another way of looking at this is to define

CHAPTER 2

$$\phi_i'(Z, \check{E}_0, \delta) = (\phi_i(\delta) \text{ if } \delta \leq \delta_{\max}(Z, \check{E}_0), \phi_i(\delta_{\max}(Z, \check{E}_0))) \quad . \quad 2.7.32$$

We now define

$$E = \check{k} / \check{E}_0 \quad 2.7.33$$

and use this as the variable to be sampled instead of  $\check{k}$ . The expressions for  $\Delta$  and  $\delta$  then become

$$\Delta = \frac{mE}{2\check{E}_0(1-E)} \quad 2.7.34$$

and

$$\delta_i = \frac{136Z_i^{-1/3} mE}{\check{E}_0(1-E)} \quad . \quad 2.7.35$$

Let us also define a variable (corresponding to DEL in EGS)

$$\Delta_E = \frac{E}{(1-E)\check{E}_0} \quad , \quad 2.7.36$$

so that

$$\delta_i = 136mZ_i^{-1/3} \Delta_E \quad . \quad 2.7.37$$

Since overall factors do not matter let us factorize  $X_0 d\Sigma_{\text{Brem}}/d\check{k}$ . From Eqs.2.7.24 and 2.7.7 with  $A'=1$ , and the definition of  $X_0$  in Table 2.6.1, we obtain

CHAPTER 2

$$\begin{aligned}
 \frac{d\check{\Sigma}_{\text{Brem}}}{d\check{E}} &= X_0 \frac{d\Sigma_{\text{Brem}}}{d\check{E}} \\
 &= \frac{N_{a\rho}}{M} \left( \sum_{i=1}^{N_e} p_i \frac{d\sigma_{\text{uncorrected}}}{d\check{E}} \right) / \left[ (N_{a\rho}/M) 4\alpha r_0^2 (Z_A + Z_B - Z_F) \right] \\
 &= \left\langle \sum_{i=1}^{N_e} p_i \frac{Z_i (Z_i + \xi(Z_i))}{\check{E}} \left\{ (1+(1-\check{E})^2) \left[ \phi'_1(Z_i, \check{E}_0, \delta_i) - \frac{4}{3} \ln Z_i \right. \right. \right. \\
 &\quad \left. \left. - \left( 4f_c(Z_i) \text{ if } \check{E}_0 > 50, 0 \right) \right] - \frac{2}{3}(1-\check{E}) \left[ \phi'_2(Z_i, \check{E}_0, \delta_i) - \frac{4}{3} \ln Z_i \right. \right. \\
 &\quad \left. \left. - \left( 4f_c(Z_i) \text{ if } \check{E}_0 > 50, 0 \right) \right] \right\} \right\rangle / 4(Z_A + Z_B - Z_F) \quad . \quad 2.7.38
 \end{aligned}$$

For brevity let us use

$\phi'_{ji}$  for  $\phi'_j(Z_i, \check{E}_0, \delta_i)$ ,  $f'_{ci}$  for  $(f_c(Z_i) \text{ if } \check{E}_0 > 50, 0)$ , and  $\xi_i$  for  $\xi(Z_i)$  .

Then after some rearrangement Eq. 2.3.38 becomes

$$\begin{aligned}
 \frac{d\check{\Sigma}_{\text{Brem}}}{d\check{E}} &= \frac{1}{4(Z_A + Z_B - Z_F)} \sum_{i=1}^{N_e} p_i Z_i (Z_i + \xi_i) \left\{ \left( \frac{2}{3} \right) \left[ 3\phi'_{1i} - \phi'_{2i} \right. \right. \\
 &\quad \left. \left. + 8(\ln Z_i^{-1/3} - f'_{ci}) \right] \left( \frac{1-\check{E}}{\check{E}} \right) + \left[ \phi'_{1i} + 4(\ln Z_i^{-1/3} - f'_{ci}) \right] \check{E} \right\} \quad 2.7.39
 \end{aligned}$$

Now define

$$\hat{\phi}_j(\Delta_E) = \sum_{i=1}^{N_e} p_i Z_i (Z_i + \xi_i) \phi'_j(Z_i, \check{E}_0, 136Z_i^{-1/3} m \Delta_E) \text{ for } j=1,2 \quad . \quad 2.7.40$$

Also recall from Table 2.6.1 the definition of  $Z_B, Z_F$  . We then can rewrite Eq. 2.7.39 as

CHAPTER 2

$$\frac{d\check{\Sigma}_{\text{Brem}}}{d\check{k}} = \left\{ \left( \frac{2}{3} \right) \left[ 3\hat{\phi}_1(\Delta_E) - \hat{\phi}_2(\Delta_E) + 8(Z_B - (Z_F \text{ if } \check{E}_0 > 50, 0)) \right] \left( \frac{1-E}{E} \right) \right. \\ \left. + \left[ \hat{\phi}_1(\Delta_E) + 4(Z_B - (Z_F \text{ if } \check{E}_0 > 50, 0)) \right] E \right\} \frac{1}{4(Z_A + Z_B - Z_F)} \quad 2.7.41$$

Now let

$$\hat{A}(\Delta_E, \check{E}_0) = 3\hat{\phi}_1(\Delta_E) - \hat{\phi}_2(\Delta_E) + 8(Z_B - (Z_F \text{ if } \check{E}_0 > 50, 0)), \quad 2.7.42$$

$$\hat{B}(\Delta_E, \check{E}_0) = \hat{\phi}_1(\Delta_E) + 4(Z_B - (Z_F \text{ if } \check{E}_0 > 50, 0)) \quad . \quad 2.7.43$$

One can show that  $\phi_j(\delta)$  have their maximum values at  $\delta=0$ , at which they take values (Butcher and Messel 1960)

$$\phi_1(0) = 4 \ln 183, \quad 2.7.44$$

$$\phi_2(0) = \phi_1(0) - 2/3 \quad . \quad 2.7.45$$

The  $\hat{\phi}_j(\Delta_E)$  also are maximum at  $\Delta_E=0$ , and in fact (see Table 2.6.1)

$$\hat{\phi}_1(0) = \sum_{i=1}^{N_e} p_i Z_i (Z_i + \xi_i) \phi_1(0) = 4Z_A, \quad 2.7.46$$

$$\hat{\phi}_2(0) = \sum_{i=1}^{N_e} p_i Z_i (Z_i + \xi_i) \phi_2(0) = 4Z_A - \frac{2}{3} Z_T \quad . \quad 2.7.47$$

The maximum values of  $\hat{A}$  and  $\hat{B}$  are now given by

$$\hat{A}_{\text{max}}(\check{E}_0) = \hat{A}(0, \check{E}_0) = 3(4Z_A) - (4Z_A - \frac{2}{3} Z_T) + 8(Z_B - (Z_F \text{ if } \check{E}_0 > 50, 0)) \\ = \frac{2}{3} Z_T + 8(Z_A + Z_B - (Z_F \text{ if } \check{E}_0 > 50, 0)) \quad , \quad 2.7.48$$

$$\hat{B}_{\text{max}}(\check{E}_0) = \hat{B}(0, \check{E}_0) = 4(Z_A + Z_B - (Z_F \text{ if } \check{E}_0 > 50, 0)) \quad . \quad 2.7.49$$

CHAPTER 2

Now define  $\delta'$  as the weighted geometric mean of the  $\delta_i$ ; that is,

$$\begin{aligned} \delta' &\equiv \left( \prod_{i=1}^{N_e} \delta_i^{p_i Z_i (Z_i + \xi_i)} \right) \left[ \sum_{i=1}^{N_e} p_i Z_i (Z_i + \xi_i) \right]^{-1} \\ &= \exp \left\{ Z_T^{-1} \sum_{i=1}^{N_e} p_i Z_i (Z_i + \xi_i) \ln \delta_i \right\} \end{aligned} \quad 2.7.50$$

$$\begin{aligned} &= 136m\Delta_E \exp \left\{ Z_T^{-1} \sum_{i=1}^{N_e} p_i Z_i (Z_i + \xi_i) \ln Z_i^{-1/3} \right\} \\ &= 136m\Delta_E \exp(Z_B/Z_T) = 136me^{Z_G} \Delta_E \end{aligned}$$

Or if we define

$$\Delta_C = 136me^{Z_G}, \quad 2.7.51$$

we have

$$\delta' = \Delta_C \Delta_E \quad 2.7.52$$

Now define

$$A(\delta') = \hat{A}(\delta'/\Delta_C, \check{E}_0) / \hat{A}_{\max}(\check{E}_0), \quad 2.7.53$$

$$B(\delta') = \hat{B}(\delta'/\Delta_C, \check{E}_0) / \hat{B}_{\max}(\check{E}_0). \quad 2.7.54$$

Then A and B have maximum values of 1 at  $\delta'=0$ , and are thus candidate rejection functions.

We are now ready to explain the reason for introducing the parameter  $\delta'$  and to introduce our final approximation; namely, we assume that the  $\hat{\phi}_j$  can be obtained using

CHAPTER 2

$$\begin{aligned}\hat{\phi}_j(\delta'/\Delta_c) &= \sum_{i=1}^{N_e} p_i Z_i (Z_i + \xi_i) \phi_j'(Z_i, \check{E}_0, 136Z_i^{-1/3} m\delta'/\Delta_c) \\ &\approx \phi_j(\delta') \sum_{i=1}^{N_e} p_i Z_i (Z_i + \xi_i) = \phi_j(\delta') Z_T.\end{aligned}\tag{2.7.55}$$

In order to justify the reasonableness of this approximation, assume for all  $i$  that

$$1 \ll 136Z_i^{-1/3} m\delta'/\Delta_c < \delta_{\max}(Z_i, \check{E}_0).\tag{2.7.56}$$

Then using Eq. 2.7.14 & 15 for the  $\phi_j$  we obtain

$$\begin{aligned}&\sum_{i=1}^{N_e} p_i Z_i (Z_i + \xi_i) \phi_j(136Z_i^{-1/3} m\delta'/\Delta_c) \\ &= \sum_{i=1}^{N_e} p_i Z_i (Z_i + \xi_i) \left[ 21.12 - 4.184 \ln \left( (136Z_i^{-1/3} m\delta'/\Delta_c) + 0.952 \right) \right] \\ &\approx \sum_{i=1}^{N_e} p_i Z_i (Z_i + \xi_i) \left[ 21.12 - 4.184 \ln \left( 136Z_i^{-1/3} m\delta'/\Delta_c \right) \right] \\ &= \left[ 21.12 - 4.184 \ln(136m\delta'/\Delta_c) \right] Z_T^{-4.184} \sum_{i=1}^{N_e} p_i Z_i (Z_i + \xi_i) \ln Z_i^{-1/3} \\ &= \left[ 21.12 - 4.184 \ln(136m\delta'/\Delta_c) + Z_G \right] Z_T \\ &= (21.12 - 4.184 \ln \delta') Z_T \\ &\approx [21.12 - 4.184 \ln(\delta' + 0.952)] Z_T \\ &= \phi_j(\delta') Z_T.\end{aligned}\tag{2.7.57}$$

Q.E.D.

## CHAPTER 2

Butcher and Messel (1960) make this approximation, although they don't mention it explicitly. As with our previous approximation, this approximation could be avoided (i.e., if we were willing to have PEGS fit the A and B functions in some convenient way for EGS).

We proceed now by using Eq. 2.7.55 to eliminate the  $\hat{\phi}_j$  from Eq. 2.7.42 and Eq. 2.7.43 yielding

$$\hat{A}(\Delta_E, \check{E}_0) = [3\phi_1(\delta') - \phi_2(\delta')] Z_T + 8(Z_B - (Z_F \text{ if } \check{E}_0 > 50, 0)) , \quad 2.7.58$$

$$\hat{B}(\Delta_E, \check{E}_0) = \phi_1(\delta') Z_T + 4(Z_B - (Z_F \text{ if } \check{E}_0 > 50, 0)) . \quad 2.7.59$$

If these are now used in Eqs. 2.7.53 and 2.7.54 we obtain

$$A(\delta') = \frac{3\phi_1(\delta') - \phi_2(\delta') + 8(Z_V \text{ if } \check{E}_0 > 50, Z_G)}{\frac{2}{3} + 8[\ln 183 + (Z_V \text{ if } \check{E}_0 > 50, Z_G)]} \quad 2.7.60$$

$$B(\delta') = \frac{\phi_1(\delta') + 4(Z_V \text{ if } \check{E}_0 > 50, Z_G)}{4[\ln 183 + (Z_V \text{ if } \check{E}_0 > 50, Z_G)]} . \quad 2.7.61$$

CHAPTER 2

We now return to Eq. 2.7.41 which we were trying to factor. We have

$$\begin{aligned}
 \frac{d\check{\Sigma}_{\text{Brem}}}{dE} &= \left\{ \frac{2}{3} A(\delta') \hat{A}_{\text{max}}(\check{E}_0) \left( \frac{1-E}{E} \right) + B(\delta') \hat{B}_{\text{max}}(\check{E}_0) E \right\} \frac{1}{4(Z_A + Z_B - Z_F)} \\
 &= \left\{ \frac{2}{3} A(\delta') \left( \frac{1-E}{E} \right) \left[ \frac{2}{3} Z_T + 8(Z_A + Z_B - (Z_F \text{ if } \check{E}_0 > 50, 0)) \right] \right. \\
 &\quad \left. + B(\delta') E [4(Z_A + Z_B - (Z_F \text{ if } E_0 > 50, 0))] \right\} \frac{1}{4(Z_A + Z_B - Z_F)} \\
 &= \frac{[Z_A + Z_B - (Z_F \text{ if } \check{E}_0 > 50, 0)]}{(Z_A + Z_B - Z_F)} \left\{ \left[ \frac{1}{9} \frac{Z_T}{[Z_A + Z_B - (Z_F \text{ if } \check{E}_0 > 50, 0)]} + \frac{4}{3} \right] A(\delta') \left( \frac{1-E}{E} \right) + B(\delta') E \right\} \\
 &= \frac{[Z_A + Z_B - (Z_F \text{ if } \check{E}_0 > 50, 0)]}{(Z_A + Z_B - Z_F)} \left\{ \left[ \ln 2 \left( \frac{4}{3} + \frac{1}{9 \ln 183 [1 + (Z_U \text{ if } \check{E}_0 > 50, Z_P)]} \right) \right] \right. \\
 &\quad \left. \times \left[ \frac{1}{\ln 2} \left( \frac{1-E}{E} \right) \right] [A(\delta')] + \left[ \frac{1}{2} \right] [2E] [B(\delta')] \right\} \quad . \quad 2.7.62
 \end{aligned}$$

We then see that for  $\check{E}_0 \leq 50$ , the case dealt with in Butcher and Messel (1960), we have

$$\begin{aligned}
 \frac{d\check{\Sigma}_{\text{Brem}}}{dE} &= \left\{ \left[ \ln 2 \left( \frac{4}{3} + \frac{1}{9 \ln 183 (1+Z_P)} \right) \right] \left[ \frac{1}{\ln 2} \left( \frac{1-E}{E} \right) \right] [A(\delta')] \right. \\
 &\quad \left. + \left[ \frac{1}{2} \right] [2E] [B(\delta')] \right\} \frac{(Z_A + Z_B)}{(Z_A + Z_B - Z_F)} \quad . \quad 2.7.63
 \end{aligned}$$



CHAPTER 2

This agrees with formula (10) of Butcher and Messel (1960) (except that they do not use  $Z_F$  in their  $X_0$  definition), since our  $Z_A, Z_B, Z_P$  are the same as their  $a, b, p$ . Now ignoring the factor preceding the  $\{\}$  in Eq. 2.7.62, noting that we require  $\check{k} > A_P$  (the photon energy cutoff) and also that energy conservation requires  $\check{k} < \check{E}_0 - m$ , we obtain the factorization (see Eq. 2.7.28)

$$\alpha_1 = \ln 2 \left( \frac{4}{3} + \frac{1}{9 \ln 183 [1 + (Z_u \text{ if } \check{E}_0 > 50, Z_P)]} \right) , \quad 2.7.64$$

$$f_1(E) = \frac{1}{\ln 2} \left( \frac{1-E}{E} \right) \text{ for } E \in (0, 1) , \quad 2.7.65$$

$$g_1(E) = \left( A \left( \delta'(E) \right) \text{ if } E \check{E}_0 \in (A_P, \check{E}_0 - m), 0 \right) , \quad 2.7.66$$

$$\alpha_2 = \frac{1}{2} , \quad 2.7.67$$

$$f_2(E) = 2E \text{ for } E \in (0, 1) , \quad 2.7.68$$

$$g_2(E) = \left( B \left( \delta'(E) \right) \text{ if } E \check{E}_0 \in (A_P, \check{E}_0 - m), 0 \right) . \quad 2.7.69$$

We notice that  $f_2(E)$  is properly normalized, but that  $f_1(E)$  has infinite integral over  $(0, 1)$ . Instead we limit the range over which  $f_1(E)$  is sampled to  $\left( 2^{-N_{\text{Brem}}}, 1 \right)$ , where  $N_{\text{Brem}}$  is chosen such that

$$2^{-N_{\text{Brem}}} \leq \frac{A_P}{\check{E}_0} < 2^{-(N_{\text{Brem}}-1)} . \quad 2.7.70$$

CHAPTER 2

To sample  $f_1(E)$  we further factor it to

$$f_1(E) = \sum_{j=1}^{N_{\text{Brem}}} \alpha_{1j} f_{1j}(E) g_{1j}(E) \quad 2.7.71$$

where

$$\alpha_{1j} = 1 \quad , \quad 2.7.72$$

$$f_{1j}(E) = \left( \frac{1}{\ln 2} 2^{j-1} \text{ if } E < 2^{-j}, \frac{1}{\ln 2} \frac{(1-E2^{j-1})}{E} \text{ if } E \in (2^{-j}, 2^{-j+1}), 0 \right) \quad 2.7.73$$

$$g_{1j}(E) = 1 \quad . \quad 2.7.74$$

The  $f_{1j}$  are properly normalized distributions.

We sample  $f_2(E)$  by selecting the larger of two uniform random variables; namely, (see Section 2.2)

$$E = \max(\zeta_1, \zeta_2) \quad . \quad 2.7.75$$

To sample  $f_1(E)$ , we first select the subdistribution index

$$j = \text{Integer Part } (N_{\text{Brem}} \zeta_1) + 1 \quad . \quad 2.7.76$$

Then to sample from  $f_{1j}(E)$ , first let

$$p = 2^{1-j}, \quad E' = E/p \quad . \quad 2.7.77$$

We then relate the distributions of  $E$  and  $E'$ , as follows. Suppose  $\hat{x}$ ,  $\hat{y}$  are random variables with probability density functions  $f(x)$  and  $g(y)$  and cumulative distribution functions  $F(x)$  and  $G(y)$ . Further, suppose that  $\hat{x}$  is related to  $\hat{y}$  by

$$\hat{x} = h(\hat{y}) \quad 2.7.78$$

with  $h$  monotonic increasing ( $\uparrow$ ) or decreasing ( $\downarrow$ ). Then clearly

CHAPTER 2

$$\begin{aligned}
 F(x) &= \Pr\{\hat{x} < x\} = \Pr\{h(\hat{y}) < x\} \\
 &= \left( \Pr\{\hat{y} < h^{-1}(x)\} \text{ if } h \uparrow, \Pr\{\hat{y} > h^{-1}(x)\} \right) \quad 2.7.79 \\
 &= \left( G(h^{-1}(x)) \text{ if } h \uparrow, 1-G(h^{-1}(x)) \text{ if } h \downarrow \right) .
 \end{aligned}$$

Letting

$$x = h(y), \quad y = h^{-1}(x) \quad , \quad 2.7.80$$

we have

$$F(h(y)) = \left( G(y) \text{ if } h \uparrow, 1-G(y) \text{ if } h \downarrow \right) \quad . \quad 2.7.81$$

Differentiating wrt  $y$ , we obtain,

$$f(h(y)) \frac{dh(y)}{dy} = \left( g(y) \text{ if } h \uparrow, -g(y) \text{ if } h \downarrow \right) \quad . \quad 2.7.82$$

Now

$$\frac{dh(y)}{dy} = \left( \left| \frac{dh(y)}{dy} \right| \text{ if } h \uparrow, - \left| \frac{dh(y)}{dy} \right| \text{ if } h \downarrow \right) \quad . \quad 2.7.83$$

Hence

$$f(h(y)) = g(y) / \left| \frac{dh(y)}{dy} \right| \quad , \quad 2.7.84$$

$$f(x) = g(h^{-1}(x)) / \left| \frac{dh(h^{-1}(x))}{dy} \right| \quad . \quad 2.7.85$$

As an example, we claim that if

$$g(E') = \frac{1}{2n} \left( 1 \text{ if } E' \in (0, \frac{1}{2}), \frac{1-E'}{E'} \text{ if } E' \in (\frac{1}{2}, 1) \right) \quad , \quad 2.7.86$$

and

$$E = h(E') = E'p, \quad E' = h^{-1}(E) = E/p, \quad \frac{dh(E')}{dE'} = p, \quad 2.7.87$$

CHAPTER 2

then

$$f(E) = \frac{1}{\ln 2} \left( \frac{1}{p} \text{ if } E \in (0, p/2), \frac{1-E/p}{E} \text{ if } E \in (p/2, p) \right) . \quad 2.7.88$$

That is, using Eqs. 2.7.86 and 2.7.87 in Eq. 2.7.85, we obtain

$$\begin{aligned} f(E) &= g(h^{-1}(E)) / \left| \frac{dh}{dy} (h^{-1}(x)) \right| \\ &= g(E/p) / p \\ &= \frac{1}{\ln 2} \left( \frac{1}{p} \text{ if } \frac{E}{p} \in (0, \frac{1}{2}), \frac{1-E/p}{E/p} \cdot \frac{1}{p} \text{ if } E/p \in (\frac{1}{2}, 1) \right) \\ &= \frac{1}{\ln 2} \left( \frac{1}{p} \text{ if } E \in (0, p/2), \frac{1-E/p}{E} \text{ if } E \in (p/2, p) \right) \text{ Q.E.D.} \end{aligned} \quad 2.7.89$$

Thus we sample  $f_{1j}(E)$  by first sampling  $E'$  from Eq. 2.7.85 and then letting  $E = E'p$ .

The  $g(E')$  in Eq. 2.7.86 may be decomposed according to

$$g(E') = \sum_{i=1}^2 \alpha'_i f'_i(E') \quad , \quad 2.7.90$$

with

$$\alpha'_1 = \frac{1}{2 \ln 2} \quad , \quad f'_1(E') = (2 \text{ if } E' \in (0, \frac{1}{2}), 0) \quad , \quad 2.7.91$$

$$\alpha'_2 = \left( 1 - \frac{1}{2 \ln 2} \right) \quad , \quad f'_2(E') = \left( \frac{1}{(\ln 2) - \frac{1}{2}} \cdot \frac{1-E'}{E'} \text{ if } E' \in (\frac{1}{2}, 1), 0 \right) . \quad 2.7.92$$

We sample  $f'_1(E')$  by letting  $E' = \zeta/2$ . To sample  $f'_2(E')$  we let  $E' = 1 - \frac{1}{2} x$ ,  $x \in (0, 1)$ , and sample  $x$  from the frequency distribution function

$$h(x) = \alpha'' f''(x) g''(x) \quad 2.7.93$$

CHAPTER 2

where

$$\alpha'' = \frac{1}{(4 \ln 2)^{-2}}, \quad f''(x) = 2x, \quad g''(x) = \frac{1}{2-x} = \frac{0.5}{E'} \quad 2.7.94$$

We already know how to sample  $f''(x)$  (e.g., see Eq. 2.7.75), so this completes the details of sampling the bremsstrahlung spectrum.

Let us now consider the pair production interaction. The general developments are quite analogous to the bremsstrahlung case and we obtain the following formulas:

$$E \equiv \frac{\check{E}}{\check{k}}, \quad 2.7.95$$

where  $\check{E}$  is the energy of one of the secondary electrons,  $\check{k}$  is the incident photon energy,

$$\Delta_E = \frac{1}{\check{k}E(1-E)}, \quad 2.7.96$$

$$\delta' = \Delta_C \Delta_E, \quad 2.7.97$$

$$\begin{aligned} \frac{d\check{Z}_{\text{Pair}}}{dE} &= \left( \frac{Z_A + Z_B - (Z_F \text{ if } \check{k} > 50, 0)}{Z_A + Z_B - Z_F} \right) \\ &\times \left\{ \left[ \frac{2}{3} - \frac{1}{36 \ln 183 [1 + (Z_U \text{ if } \check{k} > 50, Z_P)]} \right] [1] C(\delta') \right. \\ &+ \left. \left[ \frac{1}{12} \left( \frac{4}{3} + \frac{1}{9 \ln 183 [1 + (Z_U \text{ if } \check{k} > 50, Z_P)]} \right) \right] \left[ 12 \left( E - \frac{1}{2} \right)^2 \right] A(\delta') \right\}, \quad 2.7.98 \end{aligned}$$

CHAPTER 2

$$A(\delta') = \text{same as for bremsstrahlung case,} \quad 2.7.99$$

$$C(\delta') = \frac{3\phi_1(\delta') + \phi_2(\delta') + 16(Z_V \text{ if } \check{k} > 50, Z_G)}{-\frac{2}{3} + \left(16 \ln(183 + (Z_V \text{ if } \check{k} > 50, Z_G))\right)}, \quad 2.7.100$$

$$\Delta_C = \text{same as for bremsstrahlung case.} \quad 2.7.101$$

We sample Eq. 2.9.98 by the following decompositions:

$$\alpha_1 = \left[ \frac{2}{3} - \frac{1}{36 \ln 183 [1 + (Z_U \text{ if } \check{k} > 50, Z_P)]} \right], \quad 2.7.102$$

$$f_1(E) = 1, \quad E \in (0, 1) \quad , \quad 2.7.103$$

$$g_1(E) = \left( C(\delta'(E) \text{ if } \check{k} E \in (m, \check{k}-m), 0) \right), \quad 2.7.104$$

$$\alpha_2 = \frac{1}{12} \left( \frac{4}{3} + \frac{1}{9 \ln 183 [1 + (Z_U \text{ if } \check{k} > 50, Z_P)]} \right) \quad 2.7.105$$

$$f_2(E) = 12 \left( E - \frac{1}{2} \right)^2, \quad E \in (0, 1) \quad , \quad 2.7.106$$

$$g_2(E) = \left( A(\delta'(E)) \text{ if } \check{k} E \in (m, \check{k}-m), 0 \right) \quad . \quad 2.7.107$$

As with bremsstrahlung, we ignore the factor ahead of the {} in Eq. 2.7.98 when sampling. This actually has the effect of giving some effective Coulomb correction below 50 MeV, since the factor neglected would have to be larger than 1 for  $\check{k} < 50$ .

CHAPTER 2

We summarize the "run-time" bremsstrahlung and pair production cross sections:

$$\frac{d\check{\Sigma}_{\text{Brem,Run-time}}}{d\check{E}} = \left[ \ln 2 \left( \frac{4}{3} + \frac{1}{9 \ln 183 [1+(Z_U \text{ if } \check{E}_0 > 50, Z_P)]} \right) \right] \times \left[ \frac{1}{\ln 2} \left( \frac{1-\check{E}}{\check{E}} \right) A(\delta') + \left[ \frac{1}{2} \right] [2\check{E}] B(\delta') \right] , \quad 2.7.108$$

$$\frac{d\check{\Sigma}_{\text{Pair,Run-time}}}{d\check{E}} = \left[ \frac{2}{3} - \frac{1}{36 \ln 183 [1+(Z_U \text{ if } \check{k} > 50, Z_P)]} \right] [1] C(\delta') + \left[ \frac{1}{12} \left( \frac{4}{3} + \frac{1}{9 \ln 183 [1+(Z_U \text{ if } \check{k} > 50, Z_P)]} \right) \right] \times \left[ 12 \left( \check{E} - \frac{1}{2} \right)^2 \right] A(\delta') . \quad 2.7.109$$

When these are divided by  $\check{E}_0$  and  $\check{k}$ , respectively, they become

$$\frac{d\check{\Sigma}_{\text{Brem,Run-time}}}{d\check{k}} \quad \text{and} \quad \frac{d\check{\Sigma}_{\text{Pair,Run-time}}}{d\check{E}}$$

which are computed by PEGS functions BREMDR and PAIRD. In general the letter R, as the last letter of a PEGS cross section function, means one of these "run-time" functions. PEGS may be used to plot these for comparison with the more exact BREMDZ and PAIRDZ. See Table 5.2.2 for a complete list of the PEGS functions for bremsstrahlung and pair production.

## CHAPTER 2

It will be observed that the pair production formulas are symmetric about  $\bar{E} = \frac{1}{2}$ . One of the electrons will be given energy  $\check{k}\bar{E}$  and the other  $\check{k}(1-\bar{E})$ . The choice of which one is a positron is made randomly. Since we will want to know which particle has the least energy so we can put it on the top stack position, we may as well restrict the range of  $\bar{E}$  sampled to  $(0, \frac{1}{2})$  and double  $f_1(\bar{E})$  and  $f_2(\bar{E})$ . We then are guaranteed that the  $\bar{E}$  obtained will be for the minimum energy electron. We sample  $f_1(\bar{E})$  by letting  $\bar{E} = \frac{1}{2}\zeta$  and sample  $f_2(\bar{E})$  by letting (see Section 2.2)

$$E = \frac{1}{2} (1 - \max(\zeta_1, \zeta_2, \zeta_3)) \quad . \quad 2.7.110$$

A special approximation which has been carried over from previous versions is that if the incident photon has energy less than 2.1 MeV, one of the electrons is made to be at rest and the other given the rest of the available energy. One possible reason for making this approximation is that the pair sampling routine becomes progressively more inefficient as the pair production threshold is approached. Perhaps a better approximation would be to pick the energy of the low energy electron uniformly from the interval  $(m, \check{k}/2)$ .

We now conclude this section on bremsstrahlung and pair production with a few general remarks. We first note that for  $\delta' \leq 1$ , that  $A(\delta'), B(\delta')$  and  $C(\delta')$  are all quadratic functions of  $\delta'$ . The three coefficients depend on whether the incident energy is above or below 50 MeV. For  $\delta' > 1$ ,  $A(\delta'), B(\delta')$  and  $C(\delta')$  are equal and are given by



CHAPTER 2

$$A,B,C(\delta') = \frac{\phi_1(\delta') + 4(Z_V \text{ if } \check{E}_0, \check{k} > 50, Z_G)}{\phi_1(0) + 4(Z_V \text{ if } \check{E}_0, \check{k} > 50, Z_G)} \quad 2.7.111$$

which will have the form  $c_1 + c_2 \ln(\delta' + c_3)$ . The A,B,C must not be allowed to go negative. PEGS computes a maximum allowed  $\Delta_E$  above which the A,B,C are considered to be zero.

The various parameters needed to sample the secondaries' energies for the bremsstrahlung and pair production interactions are computed in the PEGS routine DIFFER. The parameters are stored for each medium during execution of EGS in COMMON/BREMPR/.

So far we have only discussed the selection of the energy of the secondaries. Since these are interactions with three body final states, the polar angles of the secondary particles are not uniquely determined by the secondary energies, and a complete simulation would sample from some appropriate distributions. However the angles at which products from these reactions are usually emitted are small compared to angular deviations resulting from multiple scattering. We therefore assume that the direction of an electron emitting bremsstrahlung is unchanged, that a bremsstrahlung photon is emitted at an angle relative to the incident electron direction,  $\theta = \frac{m}{\check{E}_0}$ , and that pair produced particles have production angles relative to the incident photon direction given by  $\theta = \frac{m}{\check{k}}$ . The azimuthal angles for the first product particle is chosen randomly and the other product particle is given the opposite azimuth.

One other use for the bremsstrahlung cross section is for computing the mean energy loss per unit length to an electron due to emission of

CHAPTER 2

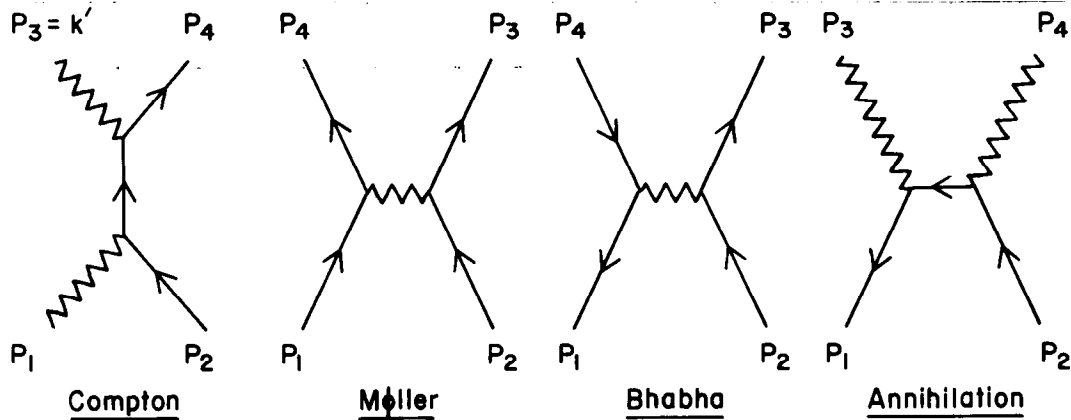
soft photons (i.e., those with energy below the photon cutoff energy  $A_p$ ). This is given by

$$-\left. \frac{d\check{E}}{dx} \right|_{\text{soft brem}} = \int_0^{A_p} \check{k} \left( \frac{d\check{\Sigma}_{\text{Brem}}}{d\check{k}} \right) d\check{k} \quad 2.7.112$$

which will be referred to in Section 2.13.

2.8 Interactions With Atomic Electrons---General Discussion

In this section we consider some general aspects of the two body interactions with the atomic electrons before considering the details of these interactions in subsequent sections. The reactions we consider, Compton, Møller, and Bhabha scattering, and two photon positron-electron annihilation, are illustrated in the Feynman diagrams below.



4-78

3330A26

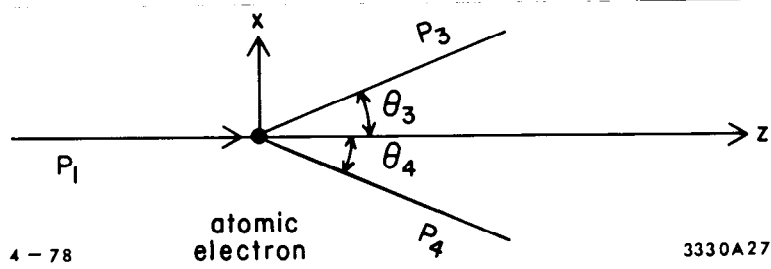
The kinematics of these reactions is given by the four-vector equation

$$P_1 + P_2 = P_3 + P_4 \quad , \quad 2.8.1$$

where we make the convention that  $P_1$  is the incident particle,  $P_2$  is the atomic electron we assume is free and at rest,  $P_3$  is the particle whose energy will be sampled and  $P_4$  is the other final state particle that will get what is left.

CHAPTER 2

Since the reaction is a two body reaction it takes place in a plane. The scattering angles are defined in the figure below where we take the incident particle direction to be the z axis and the reaction is in the x-z plane.



We let  $m_i, E_i, p_i$  be mass, energy, and three-momentum of particle i. The four-momenta are then given by

$$P_1 = (E_1, 0, 0, p_1) \quad 2.8.2$$

$$P_2 = (m, 0, 0, 0) \quad 2.8.3$$

$$P_3 = (E_3, p_3 \sin \theta_3, 0, p_3 \cos \theta_3) \quad 2.8.4$$

$$P_4 = (E_4, -p_4 \sin \theta_4, 0, p_4 \cos \theta_4) \quad 2.8.5$$

If now we want to find the scattering angle  $\theta_3$ , assuming we have found all the energy and momenta, we solve Eq. 2.8.1 for  $P_4$  and take its invariant square to get

$$p_4^2 = p_1^2 + p_2^2 + p_3^2 - 2(P_1 + P_2) \cdot P_3 + 2P_1 \cdot P_2 \quad 2.8.6$$

Now making use of the relation  $P_i^2 = m_i^2$  and Eqs. 2.8.2-5 we obtain

$$m_4^2 = m_1^2 + m^2 + m_3^2 + 2[E_1 m - (E_1 + m)E_3 + p_1 p_3 \cos \theta_3] \quad 2.8.7$$

## CHAPTER 2

Solving for  $\cos \theta_3$  we obtain

$$\cos \theta_3 = \frac{m_4^2 - m_1^2 - m^2 - m_3^2 + 2(E_1 + m)E_3 - 2E_1 m}{2p_1 p_3} . \quad 2.8.8$$

Clearly by symmetry the equation will also be true if we interchange 3 and 4 and obtain a relation for  $\cos \theta_4$ . Therefore, the angles are uniquely determined by the final energies. Once the polar angles have been selected, the azimuthal angle for one particle is selected at random and the other particle is made to have the opposite azimuth.

In the sections that follow we shall concentrate on the differential and total cross sections for these processes and give the sampling methods used to get the secondary energies. We shall also specialize Eq. 2.8.8 to the specific reactions and derive the form used in EGS to get the cosine of the scattering angle. In most cases we get the sines using the formulas

$$\sin \theta_3 = \sqrt{1 - \cos^2 \theta_3} \quad 2.8.9$$

$$\sin \theta_4 = - \sqrt{1 - \cos^2 \theta_4} . \quad 2.8.10$$

The reason for making  $\sin \theta_4$  negative is that this effectively achieves the opposite azimuth within the frame work of the EGS routine UPHI, which will be explained later. In the sections that follow we will drop the subscripts on the angles for simplicity purposes.

### 2.9 Compton Scattering

The differential and total Compton scattering cross sections are given by the formulas originally due to Klein and Nishina (1929)

CHAPTER 2

$$\frac{d\check{\Sigma}_{\text{Compt}}(\check{k}_0)}{d\check{k}} = \frac{X_0 n \pi r_0^2 m}{\check{k}_0^2} \left[ \left( \frac{C_1}{E} + C_2 \right) / E + C_3 + E \right] \quad 2.9.1$$

where

- $X_0$  = radiation length (cm),
- $n$  = electron density (electron/cm<sup>3</sup>),
- $r_0$  = classical electron radius (cm<sup>2</sup>),
- $m$  = electron rest energy (MeV),
- $\check{k}_0$  = incident photon energy (MeV),
- $\check{k}$  = scattered photon energy (MeV),
- $E = \check{k}/\check{k}_0$ ,
- $C_1 = (k'_0)^{-2}$
- $k'_0 = \check{k}_0/m$ ,
- $C_2 = 1 - 2(1+k'_0)/(k'_0)^2$ ,
- $C_3 = (1+2 k'_0)/(k'_0)^2$  .

To obtain the Compton cross section integrated over some range we use

$$\int_{\check{k}_1}^{\check{k}_2} \frac{d\check{\Sigma}_{\text{Compt}}(\check{k}_0)}{d\check{k}} d\check{k} = \frac{X_0 n \pi r_0^2}{k'_0} \left[ C_1 \left( \frac{1}{E_1} - \frac{1}{E_2} \right) + C_2 \ln \frac{E_2}{E_1} + E_2 (C_3 + E_2/2) - E_1 (C_3 + E_1/2) \right] \quad 2.9.2$$

CHAPTER 2

where

$$E_1 = \check{k}_1 / \check{k}_0 \quad ,$$

$$E_2 = \check{k}_2 / \check{k}_0 \quad .$$

To get the total cross section we use Eq. 2.9.2 with  $\check{k}_1$  and  $\check{k}_2$  set to the minimum and maximum possible scattered photon energies. To see what these are, we use Eq. 2.8.8, noting that  $m_1=m_3=0, m_4=m, E_1=p_1=\check{k}_0, E_3=p_3=\check{k}, E_4=\check{E}$ , and  $p_4=\check{p}$ .

$$\cos \theta = \frac{(\check{k}_0+m)\check{k}-\check{k}_0m}{\check{k}_0\check{k}} \quad . \quad 2.9.3$$

Solving for  $\check{k}$  we get the well-known formula

$$\check{k} = \frac{\check{k}_0}{1+(1-\cos \theta)\check{k}_0/m} \quad . \quad 2.9.4$$

We see that for  $\cos \theta = 1, -1$ , we obtain maximum and minimum  $\check{k}$ ; namely,

$$\check{k}_{\max} = \check{k}_0 \quad , \quad 2.9.5$$

$$\check{k}_{\min} = \frac{\check{k}_0}{1+2\check{k}_0/m} \quad . \quad 2.9.6$$

Thus

$$\check{\Sigma}_{\text{Compt, Total}}(\check{k}_0) = \left( \text{Eq. 2.9.2 with } \check{k}_2=\check{k}_0, \check{k}_1 = \frac{\check{k}_0}{1+2\check{k}_0/m} \right) \quad . \quad 2.9.7$$

CHAPTER 2

PEGS functions COMPDM, COMPRM and COMPTM evaluate Eqs. 2.9.1, 2.9.2, and 2.9.7, respectively.

We now consider the sampling of the energy of the scattered gamma ray. We sample the variable

$$E = \check{k}/\check{k}_0 \quad . \quad 2.9.8$$

From Eqs. 2.9.5 and 2.9.6 we see that  $E$  must be in the interval  $(E_0, 1)$ , where

$$E_0 = \frac{1}{1+2 \check{k}_0/m} \quad . \quad 2.9.9$$

We start with a form of the differential cross section similar to that given by Butcher and Messel (1960); namely,

$$\frac{d\check{\Sigma}_{\text{Compt}}}{dE} = \frac{X_0 n \pi r_0^2 m}{\check{k}_0} \left[ \frac{1}{E} + E \right] \left[ 1 - \frac{E \sin^2 \theta}{1+E^2} \right] \propto f(E)g(E) \quad . \quad 2.9.10$$

We will sample  $f(E) = \frac{1}{E} + E$  over  $(E_0, 1)$  and use  $g(E) = \left[ 1 - \frac{E \sin^2 \theta}{1+E^2} \right]$

as a rejection function. We factorize  $\left[ \frac{1}{E} + E \right]$  over  $(E_0, 1)$  as follows

$$f(E) = \frac{1}{E} + E = \sum_{i=1}^2 \alpha_i f_i(E) \quad 2.9.11$$

where

$$\alpha_1 = \ln(1/E_0), \quad f_1(E) = \frac{1}{\ln(1/E_0)} \left( \frac{1}{E} \right), \quad E \in (E_0, 1) \quad 2.9.12$$

$$\alpha_2 = (1-E_0^2)/2, \quad f_2(E) = \frac{2E}{(1-E_0^2)}, \quad E \in (E_0, 1) \quad . \quad 2.9.13$$

CHAPTER 2

We sample  $f_1$  by letting

$$E = E_0 e^{\alpha_1 \zeta} . \quad 2.9.14$$

We could sample  $f_2$  by taking the larger of two random numbers if we were willing to reject sampled values less than  $E_0$ ; but this would get very inefficient for low energy photons. Instead we make a change of variable.

Let

$$E' = \frac{E - E_0}{1 - E_0} . \quad 2.9.15$$

Then in order to give  $E$  the proper distribution,  $E'$  must have the distribution

$$f_2'(E') = f_2(E) \frac{dE}{dE'} = \alpha_1' f_1''(E') + \alpha_2' f_2''(E') \quad 2.9.16$$

where

$$\alpha_1' = \frac{k_0'}{k_0' + 1} , f_1''(E') = 2E' , E' \in (0,1) \quad 2.9.17$$

$$\alpha_2' = \frac{1}{k_0' + 1} , f_2''(E') = 1 , E' \in (0,1) . \quad 2.9.18$$

Both of these subdistributions are easily sampled.

To compute the rejection function it is necessary to get  $\sin^2 \theta$ . Let

$$t = \frac{m(1-E)}{\check{k}_0 E} \quad 2.9.19$$

Then using Eq. 2.9.3, we have

$$\cos \theta = \frac{(\check{k}_0 + m)\check{k} - \check{k}_0 m}{\check{k}_0 \check{k}} = 1 + \frac{mE - m}{\check{k}_0 E} = 1 - t . \quad 2.9.20$$



## CHAPTER 2

Thus

$$\sin^2 \theta = 1 - \cos^2 \theta = (1 - \cos \theta)(1 + \cos \theta) = t(2-t). \quad 2.9.21$$

When the value of  $\bar{E}$  is accepted, then  $\sin \theta$  and  $\cos \theta$  are obtained via

$$\sin \theta = \sqrt{\sin^2 \theta} \quad 2.9.22$$

$$\cos \theta = 1-t \quad 2.9.23$$

The sampling procedure is as follows:

- 1) Compute the parameters depending on  $k'_0$ , but not  $\bar{E}$ ; namely,

$$k'_0, \bar{E}_0, \alpha_1, \alpha_2 \quad .$$

- 2) Sample  $\bar{E}$  in the following way:

$$\text{If } \alpha_1 \geq (\alpha_1 + \alpha_2)\zeta_1 \text{ use } \bar{E} = \bar{E}_0 e^{\alpha_1 \zeta_2}.$$

Else, use  $\bar{E} = \bar{E}_0 + (1 - \bar{E}_0)E'$  where  $E'$  is determined from

$$E' = \max(\zeta_3, \zeta_4) \text{ if } k'_0 \geq (k'_0 + 1)\zeta_2$$

or from

$$E' = \zeta_3 \text{ otherwise.}$$

- 3) Calculate  $t$  and the rejection function  $g(\bar{E})$ .

If  $\zeta_4$  (or  $\zeta_5$ )  $> g(\bar{E})$ , reject and return to Step 2.

After determining the secondary energies, Eq. 2.8.8 is used to obtain the scattering angles and UPHI is called to select random azimuth and to set up the secondary particles in the usual way.

## CHAPTER 2

### 2.10 Møller Scattering

The form of the cross sections and the sampling methods that we use for Møller and Bhabha scattering follow those given by Messel and Crawford (1970 (pp. 13-14)) except that various misprints have been corrected.

The differential Møller (1932) cross section is given by

$$\frac{d\check{\Sigma}_{\text{Møller}}(\check{E}_0)}{d\check{E}} = \frac{X_0 n_2 \pi r_0^2 m}{\beta^2 \check{T}_0^2} \left[ C_1 + \frac{1}{\check{E}} \left( \frac{1}{\check{E}} - C_2 \right) + \frac{1}{\check{E}'} \left( \frac{1}{\check{E}'} - C_2 \right) \right] \quad 2.10.1$$

where

$\check{E}_0$  = incident electron energy (MeV),

$\check{T}_0$  =  $\check{E}_0 - m$  = incident kinetic energy (MeV),

$\check{E}$  = scattered electron energy (MeV),

$\check{T}$  = scattered kinetic energy (MeV),

$\check{E} = \check{T}/\check{T}_0$  = fraction of kinetic energy to scattered electron,

$\check{E}' = 1 - \check{E}$  = fraction of kinetic energy to obtain scattered electron,

$\gamma = \check{E}_0/m$ ,

$C_1 = [(\gamma - 1)/\gamma]^2$ ,

$C_2 = (2\gamma - 1)/\gamma^2$ ,

$\beta^2 = 1 - 1/\gamma^2 = (v/c)^2$ ,

and where other terms have been defined previously.

CHAPTER 2

Because of the identity of the final electrons, the cross section is symmetric with respect to the interchange of  $\check{E}$  with  $\check{E}'$ . Another consequence is that  $\check{E}$  is restricted to lie in the interval  $(0, \frac{1}{2})$ . It can be seen that Eq. 2.10.1 is singular at  $\check{E}=0$  (also at  $\check{E}'=0$  but the range of  $\check{E}'$  is now restricted to  $(\frac{1}{2}, 1)$ ), and the total Møller cross section is infinite. We get around this by only considering, in a discrete way, Møller scatterings for which the scattered electron has at least the electron cutoff energy,  $A_E$  (we also define the cutoff kinetic energy  $T_E = A_E - m$ ). Since the incoming energy is  $\check{E}_0 + m$ , and the minimum final energy is  $2A_E$ , we see that the threshold for discrete Møller scattering is

$$\check{E}_{Th}^{M\ddot{o}ller} = 2A_E - m = 2T_E + m. \quad 2.10.2$$

Møller scattering, in which the secondary electron ( $\delta$ -ray) has less energy than  $A_E$ , is treated continuously as part of the loss (see Section 2.13).

The integral of the Møller cross section over some energy range is given by

$$\int_{\check{E}_1}^{\check{E}_2} \frac{d\check{\Sigma}_{M\ddot{o}ller}(\check{E}_0)}{d\check{E}} d\check{E} = \frac{X_0 n_2 \pi r_0^2 m}{\beta^2 T_0} \left[ C_1 (E_2 - E_1) + \frac{1}{E_1} - \frac{1}{E_2} + \frac{1}{E_2'} - \frac{1}{E_1'} - C_2 \ln \frac{E_2 E_1'}{E_1 E_2'} \right] \quad 2.10.3$$

CHAPTER 2

where

$$E_i = (\check{E}_i - m) / \check{T}_0, \quad i=1,2, \quad 2.10.4$$

$$E_i' = 1 - E_i, \quad i=1,2, \quad 2.10.5$$

and other symbols are the same as in Eq. 2.10.1.

The minimum and maximum energies for the scattered electron (i.e., the one with the lower energy of the two) are  $A_E$  and  $\frac{\check{T}_0}{2} + m$ , respectively. When these limits are used for  $\check{E}_1$  and  $\check{E}_2$  in Eq. 2.10.3, we obtain the total discrete Møller cross section

$$\begin{aligned} \check{\Sigma}_{\text{Møller, Total}}(\check{E}_0) &= (\text{Eq. 2.10.3 with } \check{E}_1 = A_E \text{ \& } \check{E}_2 = (\check{T}_0/2) + m \\ &\text{if } \check{E}_0 > \check{E}_{\text{Th}}^{\text{Møller}}, 0). \end{aligned} \quad 2.10.6$$

PEGS functions AMOLDM, AMOLRM, and AMOLTM evaluate Eqs. 2.10.1, 2.10.3, and 2.10.6, respectively.

For the purpose of sampling, we use  $\bar{E} = \check{T}/\check{T}_0$  as the variable to be sampled and obtain

$$\frac{d\check{\Sigma}_{\text{Møller}}(\check{E}_0)}{d\bar{E}} = \frac{X_0 n 2\pi r_0^2 m}{\check{T}_0 E_0} f(\bar{E}) g(\bar{E}) \quad 2.10.7$$

where

$$f(\bar{E}) = \frac{E_0}{1-2E_0} \frac{1}{\bar{E}^2}, \quad E \in (E_0, \frac{1}{2}), \quad 2.10.8$$

$$g(\bar{E}) = g_1 [1 + g_2 \bar{E}^2 + r(r - g_3)], \quad 2.10.9$$

CHAPTER 2

$$E_0 = T_E / \check{T}_0, \quad 2.10.10$$

$$g_1 = (1-2E_0)/\beta^2, \quad 2.10.11$$

$$g_2 = (\gamma-1)^2/\gamma^2, \quad 2.10.12$$

$$g_3 = (2\gamma-1)/\gamma^2, \quad 2.10.13$$

$$r = E/(1-E). \quad 2.10.14$$

The sampling procedure is as follows:

1. Compute parameters depending on  $\check{E}_0$ , but not  $E$ ; namely

$$E_0, g_1, g_2, g_3.$$

2. Sample  $E$  from  $f(E)$  by using

$$E = T_E / \check{T}_0 - (\check{E}_0 - \check{E}_{th}^{Moller}) \zeta_1. \quad 2.10.15$$

3. Compute  $r$  and the rejection function  $g(E)$ . If  $\zeta_2 > g(E)$ , reject and return to Step 2.

After determining the secondary energies, Eq. 2.8.8 is used to obtain the scattering angles and UPHI is called to select random azimuth and set up the secondary particles in the usual way.

### 2.11 Bhabha Scattering

The differential Bhabha (1936) cross section, as formulated in PEGS, is

CHAPTER 2

$$\frac{d\check{\Sigma}_{\text{Bhabha}}(\check{E}_0)}{d\check{E}_-} = \frac{X_0 n_2 \pi r_0^2 m}{\check{T}_0^2} \left[ \frac{1}{\check{E}} \left( \frac{1}{\check{E}\beta^2} - B_1 \right) + B_2 + \check{E} (B_4 - B_3) \right] \quad 2.11.1$$

where

$\check{E}_0$  = energy of incident positron (MeV),

$\check{T}_0$  = kinetic energy of incident positron (MeV),

$\beta$  =  $v/c$  for incident positron,

$\gamma$  =  $\check{E}_0/m$ ,

$\check{E}_-$  = energy of secondary electron (MeV),

$\check{E} = (\check{E}_- - m)/\check{T}_0 = \check{T}_-/\check{T}_0$ ,

$y = 1/(\gamma+1)$ ,

$B_1 = 2-y^2$ ,

$B_2 = (1-2y)(3+y^2)$ ,

$B_3 = B_4 + (1-2y)^2$ ,

$B_4 = (1-2y)^3$ .

CHAPTER 2

If Eq. 2.11.1 is integrated between  $\check{E}_1$  and  $\check{E}_2$ , we obtain

the formula

$$\int_{\check{E}_1}^{\check{E}_2} \frac{d\check{\Sigma}_{\text{Bhabha}}(\check{E}_0)}{d\check{E}_-} d\check{E}_- = \frac{X_0 n_2 \pi r_0^2 m}{\check{T}_0^2} \left[ \frac{1}{\beta^2} \left( \frac{1}{\check{E}_1} - \frac{1}{\check{E}_2} \right) - B_1 \ln \frac{\check{E}_2}{\check{E}_1} + B_2(\check{E}_2 - \check{E}_1) + \check{E}_2^2(\check{E}_2 B_4/3 - B_3/2) - \check{E}_1^2(\check{E}_1 B_4/3 - B_3/2) \right] \quad 2.11.2$$

where

$$\check{E}_i = (\check{E}_i - m)/\check{T}_0, \quad i = 1, 2 \quad 2.11.3$$

and other symbols are the same as in Eq. 2.11.1.

In the case of Bhabha scattering, the particles in the final state are distinguishable, so the upper limit for  $\check{E}$  is 1. Note that  $\check{E}$  is the fraction of the kinetic energy that the negative atomic electron gets. There is still a singularity at  $\check{E}=0$  which is solved in the same way as for Møller by requiring that the energy transfer to the atomic electron be at least  $T_E = A_E - m$ . It should be noted that there is no singularity at  $\check{E}=1$  as there was for Møller, and in fact, the final positron energy may be less than  $A_E$  (down to  $m$ ). Thus, the threshold for discrete Bhabha scattering is  $A_E$ , and as long as the positron is above the cutoff energy, it will have some non-zero Bhabha cross section. Using the minimum and maximum  $\check{E}_-$  for  $\check{E}_1$  and  $\check{E}_2$  in Eq. 2.11.2, we obtain the total cross section

$$\check{\Sigma}_{\text{Bhabha}}(\check{E}_0) = (\text{Eq. 2.11.2 with } \check{E}_1 = A_E \text{ \& } \check{E}_2 = \check{E}_0 \text{ if } \check{E}_0 > A_E, 0). \quad 2.11.4$$

PEGS functions BHABDM, BHABRM, and BHABTM evaluate Eqs. 2.11.1, 2.11.2, and 2.11.4, respectively.

For the purpose of sampling we use  $\check{E} = \check{T}_- / \check{T}_0$  as the variable to be sampled, and obtain

$$\frac{d\check{\Sigma}_{\text{Bhabha}}(\check{E}_0)}{d\check{E}} = \frac{X_0 n_2 \pi r_0^2 m}{\check{T}_0 \check{E}_0} f(E) g(E)$$

where

$$f(E) = \frac{E_0}{1-E_0} \frac{1}{E^2}, \quad E \in (E_0, 1),$$

$$g(E) = (1-E_0) \left[ \frac{1}{\beta^2} - E \left( B_1 - E \left( B_2 - E \left( B_3 - E B_4 \right) \right) \right) \right], \quad 2.11.7$$

$$E_0 = T_E / \check{T}_0, \quad 2.11.8$$

$$y = 1/(\gamma+1), \quad 2.11.9$$

[Note: EGS uses variable YY to avoid conflict with Y-coordinate of particle.]

$$B_4 = (1-2y)^3, \quad 2.11.10$$

$$B_3 = C_4 + (1-2y)^2, \quad 2.11.11$$

$$B_2 = (1-2y)(3+y^2), \quad 2.11.12$$

$$B_1 = 2-y^2. \quad 2.11.13$$

The sampling method is as follows:

1. Compute parameters depending on  $\check{E}_0$  but not  $E$ ; namely,

$$E_0, \beta, \gamma, B_1, B_2, B_3, B_4.$$

2. Sample  $E$  from  $f(E)$  by using

$$E = E_0 / [1 - (1-E_0)\zeta_1]. \quad 2.11.14$$

3. Compute the rejection function  $g(E)$ . If  $\zeta_2 > g(E)$ , reject and return to Step 2.



## CHAPTER 2

The rest of the routine is similar to the Møller routine except that now the delta ray may have the most energy, in which case the contents of the two top locations of the particle stack must be interchanged to ensure that the particle of lower energy is on top.

2.12 Two Photon Positron-Electron Annihilation

The two photon positron-electron annihilation cross sections we have used are taken from Heitler (1954, p. 268-270). Taking Heitler's formula (6) (on p. 269), translating to the laboratory frame, integrating over azimuth, and changing from angle to energy variable, we obtain the following form of the differential cross section used in PEGS:

$$\frac{d\check{\Sigma}_{\text{Annih}}(\check{E}_0)}{d\check{k}} = S_1(k') + S_1(A-k') \quad 2.12.1$$

where

$$\check{E}_0 = \text{energy of incident positron (MeV)}, \quad 2.12.2$$

$$\check{k} = \text{energy of secondary photon of lower energy (MeV)},$$

$$\gamma = \check{E}_0/m, \quad 2.12.3$$

$$A = \gamma + 1 = (\text{available energy})/m, \quad 2.12.4$$

$$T'_0 = \gamma - 1 = (\text{kinetic energy})/m, \quad 2.12.5$$

$$p'_0 = \check{p}_0/m = \sqrt{\gamma^2 - 1} = \sqrt{AT'_0} \quad 2.12.6$$

$$k' = \check{k}/m, \quad 2.12.7$$

$$S_1(x) = C_1 [-1 + (C_2 - 1/x)/x], \quad 2.12.8$$

$$C_1 = \frac{X_0 n \pi r_0^2}{AT'_0 m}, \quad 2.12.9$$

$$C_2 = A + 2\gamma/A \quad . \quad 2.12.10$$

We see that Eq. 2.12.1 satisfies, in a manifest way, the symmetry under exchange of the annihilation photons.

In order to get the value of Eq. 2.12.1 integrated between  $\check{k}_1$  and  $\check{k}_2$  we integrate the  $S_1$  functions and obtain

$$\int_{\check{k}_1}^{\check{k}_2} \frac{d\check{\Sigma}_{\text{Annih}}}{d\check{k}} d\check{k} = S_2(k'_2) - S_2(k'_1) + S_2(A - k'_1) - S_2(A - k'_2) \quad 2.12.11$$

where

$$k'_i = \check{k}_i / m \quad , \quad i = 1, 2, \quad 2.12.12$$

$$S_2(x) = m \int S_1(x) dx = m C_1 [-x + C_2 \ln x + 1/x] \quad . \quad 2.12.13$$

For the total cross section we use Heitler's formula directly with appropriate changes to take into account units and notation. We have

$$\check{\Sigma}_{\text{Annih}}(\check{E}_0) = \frac{X_0 n \pi r_0^2}{\gamma + 1} \left[ \frac{\gamma^2 + 4\gamma + 1}{\gamma^2 - 1} \ln(\gamma + \sqrt{\gamma^2 - 1}) - \frac{\gamma + 3}{\sqrt{\gamma^2 - 1}} \right] \quad 2.12.14$$

PEGS functions ANIHDM, ANIHRM, and ANIHTM evaluate Eqs. 2.12.1, 2.12.11, and 2.12.14, respectively.

We did not find any references in the literature for sampling schemes that would sample this distribution exactly. We will sample the parameter  $E$  defined by

$$E = \frac{k'}{A} = \frac{\check{k}}{\check{E}_0 + m} \quad . \quad 2.12.15$$

To find the limits over which we sample  $E$ , let us compute the limits for  $k'$ . We use Eq. 2.8.8 with  $m_1 = m$ ,  $E_1 = \check{E}_0$ ,  $p_1 = \check{p}_0$ ,  $m_3 = m_4 = 0$ ,  $E_3 = p_3 = \check{k}$ , so

$$\cos \theta = \frac{(\check{E}_0 + m)\check{k} - \check{E}_0 m - m^2}{\check{p}_0 \check{k}} \quad . \quad 2.12.16$$

Solving for  $\check{k}$  and dividing by  $m$  we obtain

$$k' = \frac{A}{A - (\check{p}_0/m) \cos \theta} = \frac{1}{1 - \sqrt{T'_0/A} \cos \theta} \quad . \quad 2.12.17$$

Thus, setting  $\cos \theta_3 = \pm 1$  in Eq. 2.12.17 we see that

$$k'_{\min} = \frac{1}{1 + \sqrt{T'_0/A}} = \frac{A}{A + p'_0} \quad , \quad 2.12.18$$

$$k'_{\max} = \frac{1}{1 - \sqrt{T'_0/A}} = \frac{A}{A - p'_0} \quad . \quad 2.12.19$$

Also,

$$\begin{aligned} k'_{\min} + k'_{\max} &= \frac{1}{1 + \sqrt{T'_0/A}} + \frac{1}{1 - \sqrt{T'_0/A}} \\ &= \frac{1 - \sqrt{T'_0/A} + 1 + \sqrt{T'_0/A}}{1 - T'_0/A} = \frac{2A}{\gamma + 1 - (\gamma - 1)} \\ &= A \quad . \quad 2.12.20 \end{aligned}$$

That is, when one photon is at the minimum the other is at the maximum and the sum is the available energy (divided by  $m$ ).

Now, due to the identity of the two photons, we restrict  $E < \frac{1}{2}$ ; moreover,  $E > E_0$ , where

$$E_0 = \frac{k'_{\min}}{A} = \frac{1}{A + \sqrt{AT'_0}} = \frac{1}{A + p'_0} \quad . \quad 2.12.21$$

The cross section to be sampled is

$$\frac{d\check{\Sigma}_{\text{Annih}}}{dE} = mA \left[ S_1(AE) + S_1(A(1-E)) \right] \quad . \quad 2.12.22$$

Due to the symmetry in  $E$ , we can expand the range of  $E$  that we sample from  $(E_0, \frac{1}{2})$  to  $(E_0, 1-E_0)$  and throw away the second  $S_1$ . Then if we get a sampled  $E > \frac{1}{2}$ , we use  $1-E$  instead.

Thus the distribution to be sampled now is given by

$$\frac{d\check{\Sigma}_{\text{Annih}}}{dE} = mA C_1 \left[ -1 + (C_2 - \frac{1}{AE}) / AE \right], \quad E \in (E_0, 1-E_0) \quad . \quad 2.12.23$$

Using the value of  $C_2$  and rearranging, we obtain

$$\frac{d\check{\Sigma}_{\text{Annih}}}{dE} = \frac{X_0 n \pi r_0^2 m}{\check{I}_0} \ln \left[ (1-E_0)/E_0 \right] f(E) g(E) \quad 2.12.24$$

where

$$f(E) = \frac{1}{\ln \left[ (1-E_0)/E_0 \right]} \frac{1}{E} \quad , \quad 2.12.25$$

$$g(E) = 1-E + \frac{1}{A^2} \left( 2\gamma - \frac{1}{E} \right) \quad . \quad 2.12.26$$

To see that  $g(E)$  is a valid rejection function we find its extrema.

$$g'(E) = -1 + \frac{1}{A^2 E^2} = 0 \quad \rightarrow \quad E = \frac{1}{A} \quad . \quad 2.12.27$$

$$g''(E) = \frac{-2}{A^2 E^3} < 0 \quad .$$

Thus, we see that  $g(E)$  has a maximum at  $E = \frac{1}{A} \geq E_0$  with maximum value

$$g\left(\frac{1}{A}\right) = 1 - \frac{2}{A^2} < 1 \quad . \quad 2.12.28$$

The sampling procedure is then as follows:

1. Compute parameters depending on  $\check{E}_0$  only; namely,

$$A, \gamma, T'_0, P'_0, E_0, \ln\left(\frac{1-E_0}{E_0}\right) \quad .$$

2. Sample  $E$  using

$$E = E_0 e^{\zeta_1 \ln\left(\frac{1-E_0}{E_0}\right)} \quad . \quad 2.12.29$$

3. Compute  $g(E)$ . Then reject  $E$  and return to Step 2 if  $\zeta_2 > g(E)$ .
4. Get larger and smaller  $E$  values using

$$E_{\text{Bigger}} = \max(E, 1-E) \quad , \quad 2.12.30$$

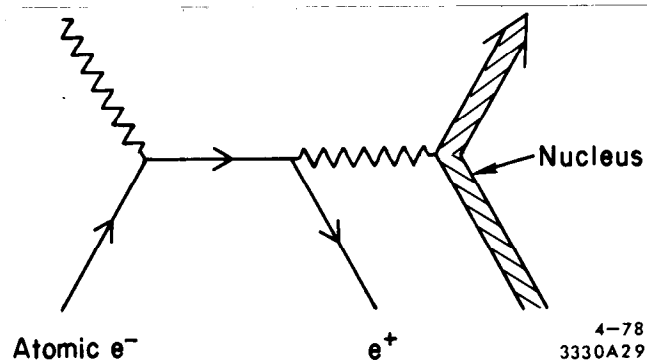
$$E_{\text{Smaller}} = 1 - E_{\text{Bigger}} \quad . \quad 2.12.31$$

Use these to set up the photons.

The polar angles are determined by the energies using Eq. 2.8.8 and UPHI is called to select random azimuth.

A special case arises when a positron falls below the cutoff energy before annihilating. In this case it is assumed that it comes to rest before annihilating. Then each gamma has energy  $\check{k}=m$  and the angular distribution is isotropic with gammas going in opposite directions.

We should perhaps mention at this point that a positron can also annihilate and give off only one photon via the process below.



Messel and Crawford (1970) make the point that the ratio of one photon annihilation to two photon annihilation is small until higher energies are reached, at which point the absolute value of the cross section is small. Thus, we ignore one photon positron annihilation.

It is also possible to have annihilation accompanied by three or more photons, but these interactions are even less likely than one photon annihilation and will not be considered further.

### 2.13 Continuous Electron Energy Loss

We have made the distinction between discrete and continuous energy losses to electrons and positrons. In the discrete case, secondary particles with energies above their cutoff energies are created (taking some energy from the electron or positron) and subsequently transported. The continuous loss is the result of interactions in which the energy transfer to the secondary particles is not sufficient to put them above the discrete transport energy thresholds. The secondary particles are either soft bremsstrahlung photons, or atomic electrons which absorb some energy. The mean total continuous energy loss per unit length is thus given by

$$-\left(\frac{dE_{\pm}}{dx}\right)_{\text{Total Continuous}} = -\left(\frac{dE_{\pm}}{dx}\right)_{\text{Soft Bremsstrahlung}} + -\left(\frac{dE_{\pm}}{dx}\right)_{\text{Sub-cutoff Atomic Electrons}} \quad 2.13.1$$

where  $\pm$  denotes for positive or negative electrons. The first term on the right-hand side of Eq. 2.13.1 is the same for electrons and positrons (to the accuracy with which we treat bremsstrahlung) and is given by Eq. 2.7.112).

The second term may be expressed as the integral of the differential cross section for transferring a specified amount of energy,  $T$ , to an atomic electron, times the amount of the energy transfer over the range of energy transfers which still give rise to soft final state secondary electrons.

That is

$$-\left(\frac{dE_{\pm}}{dx}\right)_{\text{Sub-cutoff Atomic Electrons}} = \int_0^{T_{\text{max}}} T \frac{d\Sigma_{\pm}}{dT} dT \quad 2.13.2$$

For values of  $T$  on the order of the atomic excitation levels, the frequencies and strengths of the atomic oscillators must be taken into account and the integration is quite complicated. On the other hand, for values of  $T$  large enough that the atomic electrons may be considered free, the cross section can be the Møller or Bhabha cross section. Let  $T_{\text{med}}$  be a value of  $T$  which is sufficiently above the atomic excitation level, but is still small compared to  $T_{\text{max}}$ . Then

$$\left(-\frac{dE_{\pm}}{dx}\right) = \int_0^{T_{\text{med}}} T \frac{d\Sigma_{\pm}}{dT} dT + \int_{T_{\text{med}}}^{T_{\text{max}}} T \frac{d\Sigma_{\text{Møller}}}{dE} dT \quad 2.13.3$$



and

$$\left(-\frac{dE_+}{dx}\right) = \int_0^{T_{\text{med}}} T \frac{d\Sigma_+}{dT} dT + \int_{T_{\text{med}}}^{T_{\text{max}}} T \frac{d\Sigma_{\text{Bhabha}}}{dE} dE \quad . \quad 2.13.4$$

When certain appropriate approximations are made it turns out that Eqs. 2.12.3 and 4 are independent of  $T_{\text{med}}$ . We use the formulas recommended by Berger and Seltzer (1964 (formula 22)) for restricted stopping power which are based on the Bethe-Bloch formula (Bethe 1930, 1932, Bloch 1933) (except that we corrected errors in their formula for  $F^+(\tau, \Delta)$ ). Other references (used in double checking our formulas) are Rohrlich and Carlson (1953), Jauch and Rohrlich (1955), Turner (1964), Sternheimer (1952, 1953, 1956, 1966, 1967, 1971), Evans (1955 (to check Bhabha and Møller cross sections)), Armstrong and Alsmiller (1970), and Messel and Crawford (1970).

The formula that we use for the restricted stopping power (i.e., due to sub-cutoff electrons) is

$$\left(-X_0 \frac{d\check{E}_{\pm}}{dx}\right)_{\text{Sub-cutoff Atomic Electrons}} = \frac{X_0 n 2\pi r_0^2 m}{\beta^2} \left[ \ln \frac{2(\tau+2)}{(\bar{I}_{\text{adj}}/m)} + F^{\pm}(\tau, \Delta) - \delta \right] \quad 2.13.5$$

where

$$\gamma = \check{E}_0/m = \text{usual relativistic factor}, \quad 2.13.6$$

$$\eta = \sqrt{\gamma^2 - 1} = \beta\gamma = \check{p}_0 c/m, \quad 2.13.7$$

$$\beta = \sqrt{1 - \gamma^{-2}} = v/c \text{ for incident particle}, \quad 2.13.8$$

$$T'_E = T_E/m = \text{kinetic energy cutoff in electron mass units}, \quad 2.13.9$$

$$\tau = \gamma - 1, \quad 2.13.10$$

$$y = (\gamma + 1)^{-1} \text{ (See Bhabha formulas)}, \quad 2.13.11$$

$$T'_{\text{max}} = \text{maximum possible energy transfer}$$

$$= (\tau \text{ if positron, } \tau/2 \text{ if electron}), \quad 2.13.12$$

CHAPTER 2

$$\Delta = \min(T'_E, T'_{\max}) = \text{restricted maximum energy transfer,} \quad 2.13.13$$

$$\bar{I}_{\text{adj}} = \text{average adjusted mean ionization energy,} \quad 2.13.14$$

$$\delta = \text{density effect correction,} \quad 2.13.15$$

$$F^-(\tau, \Delta) = -1 - \beta^2 + \ln [(\tau - \Delta)\Delta] + \tau / (\tau - \Delta) \quad 2.13.16$$

$$+ \left[ \frac{\Delta^2}{2} + (2\tau + 1) \ln \left( 1 - \frac{\Delta}{\tau} \right) \right] / \gamma^2$$

$$F^+(\tau, \Delta) = \ln(\tau\Delta) - \frac{\beta^2}{\tau} \left\{ \tau + 2\Delta - \frac{3\Delta^2 y}{2} \right. \\ \left. - (\Delta - \Delta^3/3)y^2 - (\Delta^2/2 - \tau\Delta^3/3 + \Delta^4/4)y^3 \right\} \quad 2.13.17$$

The density effect correction has been treated extensively by Sternheimer, first for specific materials and finally in 1971 for arbitrary materials. We were not aware of Steinheimer's general formulas until after the parts of PEGS dealing with ionization loss had already been written. As a result, this general scheme has not been incorporated into PEGS, although it is a straightforward job which could be done at some point.

There are therefore currently two alternate schemes for computing the density effect. If the material is one which has specifically been studied by Sternheimer, then his formulas can be used, including his value for  $\bar{I}_{\text{adj}}$ . Otherwise an asymptotic density effect correction is used as suggested by Armstrong and Alsmiller (1970).

According to Sternheimer the density effect is given by the formula

$$\delta = \begin{cases} 0 & \text{if } x < x_0 & 2.13.18a \\ 2(\ln 10)x + C + a(x_1 - x)^{m_s} & \text{if } x \in (x_0, x_1) & 2.13.18b \\ 2(\ln 10)x + C & \text{if } x > x_1 & 2.13.18c \end{cases}$$

where

$$x = \log_{10}(\bar{p}c/m) = \ln \eta / \ln 10, \quad 2.13.19$$

$$C = -2 \ln(\bar{I}_{adj}/h\nu_p) - 1, \quad 2.13.20$$

$$\nu_p = \text{plasma frequency} = \sqrt{nr_0^2 c^2 / \pi} \quad 2.13.21$$

and  $x_0, x_1, a, m_s$  are parameters computed by Sternheimer from atomic oscillator strengths for specific materials.

The recommended values for  $\bar{I}_{adj}$ , which are used by Berger and Seltzer (1964) and Sternheimer (1971), but which differ from values previously used by Sternheimer, are given by

$$\ln \bar{I}_{adj} = \left( \sum_{i=1}^{Ne} p_i Z_i (\ln I_{adj}(Z_i)) \right) / \left( \sum_{i=1}^{Ne} p_i Z_i \right) \quad 2.13.22$$

with

$$I_{adj}(Z) = \begin{cases} \text{Values in Table 2.13.1 if } Z \leq 12 \\ Z(9.76 + 58.8Z^{-1.19}) \times 10^{-6} \text{ MeV if } Z > 12. \end{cases} \quad 2.13.23$$

The values of  $I_{adj}$  in Table 2.13.1 were taken from Berger and Seltzer (1964), Sternheimer (1966), and Turner (1964).

As noted by Berger and Seltzer, "the values of  $x_0, x_1, C, a$ , and  $m_s$  depend, among other things, on the value of the mean excitation energy. Two sets of these parameters have been given by Sternheimer: in his 1952 paper with the use of one set of I-values, and in his 1956 paper with

## CHAPTER 2

the use of another set. Following his recommendation, we have adjusted the density effect correction to the  $I_{adj}$ -values adopted in the present work through the following interpolation procedure: Let  $\delta_1$  and  $\delta_2$  denote the corrections for a given medium and energy, evaluated with mean excitation energies  $I_1$  and  $I_2$ . The desired value, corresponding to mean excitation energy  $I_{adj}$ , is calculated as

$$\delta = [\delta_1 \log(I_2/I_{adj}) + \delta_2 \log(I_{adj}/I_1)] / \log(I_2/I_1) \quad . \quad 2.13.24$$

We have also followed this procedure. Tables 2.13.2 and 2.13.3 show the materials for which PEGS has Sternheimer parameters along with their values.

The approximation suggested by Armstrong and Alsmiller (1970), for use when no Sternheimer parameters are available, is to neglect the term " $a(x_1-x)^m$ " in Eq. 2.13.18b and neglect  $\delta$  if it is negative. This has the effect of turning the density effect on sharply at  $x = -C/2 \ln 10$  rather than spreading the turn-on over the interval  $x \in (x_0, x_1)$ . When  $x$  is outside the interval  $(x_0, x_1)$  the formula thus obtained is the same as Sternheimer's formula, and within this interval the error in stopping power is at most about 3-6% (near the center of the interval).

Sternheimer's (1971) general formula, which we have not implemented in Version 3, consists of a prescription for computing  $x_0, x_1$ ,  $a$  and  $m_s$  for arbitrary material.

PEGS routine SPINIT initializes the stopping power routines for a particular medium. Routine SPIONB ( $\check{E}_0, A_E$ , POSITR) evaluates Eq. 2.13.5 for a positron if POSITR is true, and for an electron if POSITR is false.

## CHAPTER 2

Table 2.13.1

Values of  $I_{adj}$  (eV) for  $Z \leq 12$  Elements\*

Element	Z	$I_{adj}$
H	1	18.7
He	2	42.0
Li	3	38.0
Be	4	60.0
B	5	73.0
C	6	78.0
N	7	85.0
O	8	89.0
F	9	117.
Ne	10	131.
Na	11	143.
Mg	12	156.

\*Taken from Turner (1964), Berger and Seltzer (1964), and Sternheimer (1966).

Routines SPIONE and SPIONP use SPIONB to evaluate Eq. 2.13.5 for electrons and positrons, respectively. Routines SPTOTE and SPTOTP evaluate Eq. 2.13.1 for electrons and positrons, respectively, for specified electron and photon cutoff energies. Routines EDEDX(E) and PDEDX(E) use SPTOTE and SPTOTP to evaluate Eq. 2.13.1 using the user specified  $A_E$  and  $A_P$  as the cutoff energies.

Table 2.13.2

Sternheimer Parameters for Elements

Element	Z	$\bar{I}_{adj}^*$	I	-C	10a	$m_s$	$x_1$	$x_0$
He	2	42.0	26.9/44.1	10.19/11.18	9.8/21.3	4.11/3.22	3/3	2.00/2.21
Li	3	38.0	34.0/39.0	2.81/3.07	3.56/3.74	2.99/3.05	2/2	-0.10/-0.05
Be	4	60.0	60.4/64.1	2.70/2.83	2.60/4.13	3.38/2.82	2/2	0.00/-0.10
C	6	78.0	77.1/78.1	2.82/3.22	3.18/5.31	3.15/2.63	2/2	0.04/-0.05
Ne	10	131.	120/130	11.52/11.72	2.17/2.58	3.34/3.18	4/4	2.10/2.14
Mg	12	156.	-/156	-/4.54	-/0.938	-/3.56	-/3	-/0.10
Al	13	163.	150/163	4.06/4.21	0.38/0.906	4.25/3.51	3/3	0.39/0.05
Si†	14	172.	172	4.38	0.874	3.59	3	0.10
A	18	210.	192/228	11.92/12.27	3.89/0.255	2.80/4.36	4/5	1.96/2.02
Fe	26	285.	243/337	3.97/4.62	0.88/1.27	3.47/3.29	3/3	-0.01/0.10
Cu†	29	314.	314	4.43	1.09	3.39	3	0.20
Ge†	32	343.	343	5.10	1.67	3.14	3	0.10
Kr	36	381.	340/494	12.37/13.12	5.37/0.771	2.56/3.57	4/5	2.00/2.12
Ag	47	487.	428/660	4.88/5.75	1.62/2.51	3.10/2.88	3/3	-0.03/0.20
Sn	50	516.	479/709	5.49/6.28	2.43/4.04	2.85/2.52	3/3	0.17/0.20
Xe	54	555.	509/758	12.77/13.57	7.94/1.50	2.19/3.07	4/5	1.72/1.90
W	74	748.	698/991	5.33/6.03	2.14/0.283	2.93.3.91	3/4	0.21/0.30
Au	79	797.	743/1136	5.45/6.31	2.54/0.436	2.80/3.62	3/4	0.25/0.30
Pb†	82	826.	826	6.21	3.55	2.64	3	0.40
U	92	923.	881/1325	5.86/6.69	3.27/0.652	2.64/3.37	3/4	0.20/0.30

Key: \*From Table 2.13.1 or Eq. 2.13.23.

†Sternheimer (1966).

All other numbers refer to Sternheimer (1952)/Sternheimer (1956) and should be used with Eq. 2.13.24.

Table 2.13.3

Sternheimer Parameters for Compounds

Compound	$\bar{I}^*_{adj}$	I	-C	10a	$m_s$	$x_1$	$x_0$
NaI	433.	392/562	5.77/6.49	2.78/4.52	2.77/2.44	3/3	0.09/0.18
LiI	473.	360/636	5.52/6.66	2.77/5.25	2.72/2.32	3/3	-0.07/0.08
Liq.H <sub>2</sub> <sup>†</sup>	18.7	18.7	2.91	0.569	6.22	2	0.42
Propanet	50.3	50.3	3.48	5.55	2.57	2	0.24
Freont <sup>†</sup>	205.	205.	5.30	1.79	3.10	3	0.42
Anthracene	67.0	64.6/67.2	3.03/3.11	4.3/4.20	2.79/2.86	2/2	0.09/0.11
Stilbene	65.2	62.5/65.4	3.03/3.12	4.0/4.23	2.90/2.86	2/2	0.09/0.12
Polystyrene	63.8	-/63.8	-/3.15	-/4.29	-/2.85	-/2	-/0.13
Polyethylene	54.9	-/54.9	-/2.94	-/3.93	-/2.86	-/2	-/0.12
Lucite	69.1	-/69.1	-/3.21	-/4.56	-/2.78	-/2	-/0.14
Toluene	62.1	59.7/62.3	3.20/3.30	4.6/4.54	2.77/2.83	2/2	0.12/0.17
Xylene	61.0	57.9/61.2	3.14/3.25	4.5/4.44	2.77/2.84	2/2	0.12/0.16
H <sub>2</sub> O	65.1	68.0/74.1	3.30/3.47	3.77/5.19	3.15/2.69	2/2	0.08/0.23
AgCl	384.	348/491	5.08/5.77	1.39/0.177	3.30/4.21	3/4	0.18/0.33
AgBr	434.	383/574	5.14/5.95	1.60/0.235	3.18/4.03	3/4	0.10/0.30
Emulsion	320.	286/373	5.02/5.55	1.56/0.220	3.17/4.01	3/4	0.17/0.23
H <sub>2</sub>	18.7	15.6/19.0	9.11/9.50	3.4/5.05	5.01/4.72	3/3	1.76/1.85
N <sub>2</sub>	85.0	87.7/91.0	10.60/10.68	1.12/1.25	3.84/3.72	4/4	1.81/1.86
Methane	44.5	-/44.5	-/9.56	-/0.552	-/4.22	-/4	-/1.55
Ethylene	54.9	-/54.9	-/9.52	-/0.700	-/3.94	-/4	-/1.54
Acetylene	63.8	-/63.8	-/9.95	-/0.841	-/3.91	-/4	-/1.61
LiF <sup>†</sup>	88.9	88.9	3.07	4.56	2.76	2	-0.072

Key: \* $\bar{I}^*_{adj}$  from Table 10 of Berger and Seltzer (1964) if two I-values listed; otherwise, used single I-value for  $\bar{I}^*_{adj}$ .

<sup>†</sup>Data from Sternheimer (1966)

All other numbers refer to Sternheimer (1952)/Sternheimer (1956) and should be used with Eq. 2.13.24.

## CHAPTER 2

As a final comment on continuous energy loss, we mention that when an electron is transported a given distance, it is assumed that its loss of energy due to sub-cutoff secondaries is equal to the distance traveled times the mean loss per unit length as evaluated using Eq. 2.13.1. In actuality, the energy loss over a transported distance is subject to fluctuations and gives rise to a Landau distribution. A future improvement to EGS would be the ability to optionally sample from the Landau distribution in determining energy loss. It should be noted that the proper distribution would be a restricted Landau distribution, and not one determined by the full range of energy transfers. Such an enhancement would probably not affect the overall shower development significantly, but could give significantly different results for single electrons passing through thin slabs (scintillators, for example). Of course, fluctuations due to the discrete interactions are already properly accounted for.

### 2.14 Multiple Scattering

When an electron passes through matter, it undergoes a large number of elastic collisions with the atomic nuclei. These have the effect of changing the electrons' direction, but do not significantly change its energy. To take into account these scatterings we use Moliere's (1948) theory of multiple scattering as formulated by Bethe (1953). For the details of computing multiple scattering in mixtures, and for a good introduction to the subject, we have made frequent use of the review article by Scott (1963). In Versions 1 and 2 of EGS the method of sampling scattering angles was based on a scheme of Nagel's whereby one



## CHAPTER 2

of 29 discrete representative reduced angles was selected and then used to obtain the real scattering angle. In EGS3 we depart from this scheme to use a method similar to that of Messel and Crawford (1970), whereby the scattering angles are chosen in a truly continuous way. This method also allows us to transport over variable step lengths while still taking multiple scattering properly into account.

The cross section for elastic scattering off the nucleus is proportional to  $Z^2$ . Scattering from atomic electrons is taken into account by replacing  $Z^2$  by  $Z(Z + \xi_{MS})$ . Scattering from atomic electrons that results in discrete delta rays is already properly taken into account, so the  $\xi_{MS}$  need only account for the sub-cutoff scatterings. Scott (1963) has outlined the procedures for taking into account scattering from atomic electrons in a more rigorous way, but we have not implemented it here. Instead we treat  $\xi_{MS}$  more as a "fudge factor" to get our multiple scattering as consistent with experiment as possible. In the developments to follow we shall need the parameters

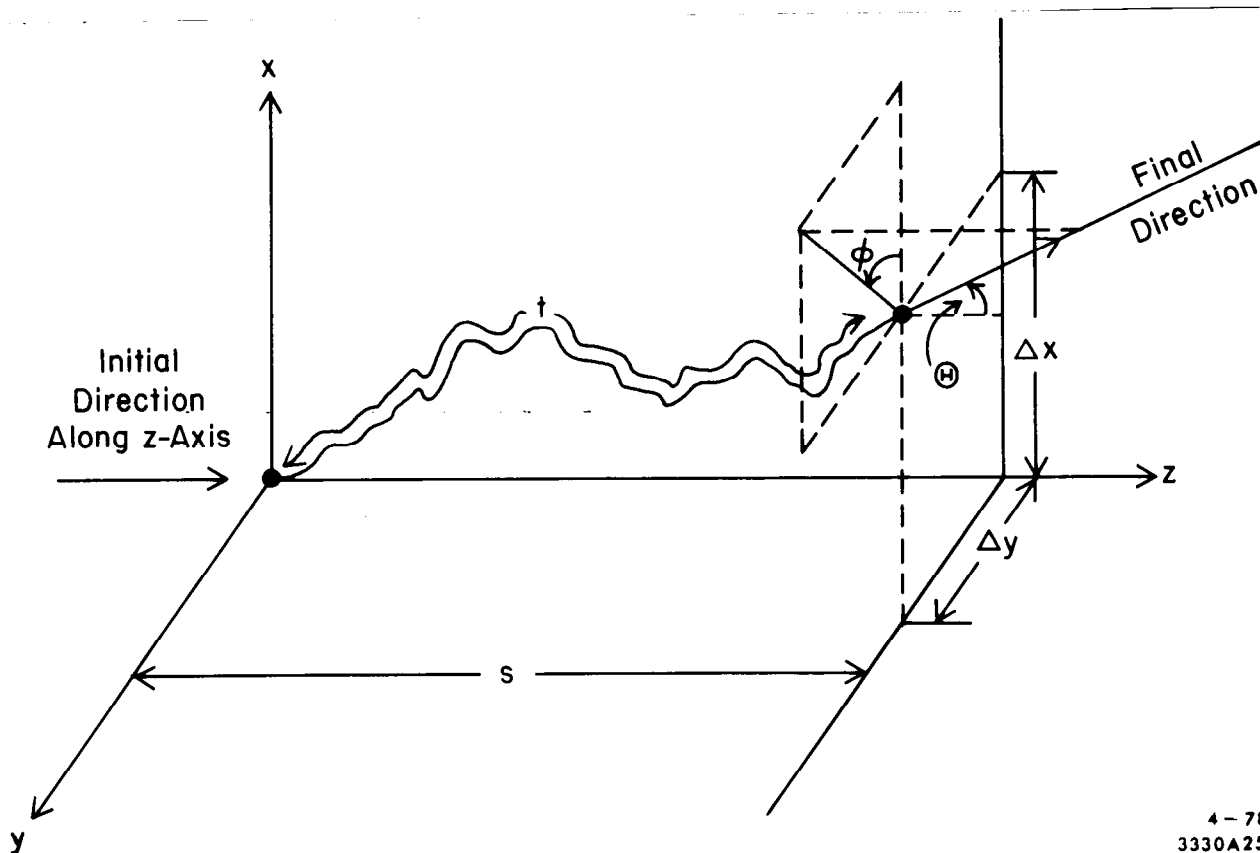
$$Z_S = \sum_{i=1}^{N_e} p_i Z_i (Z_i + \xi_{MS}) \quad 2.14.1$$

$$Z_E = \sum_{i=1}^{N_e} p_i Z_i (Z_i + \xi_{MS}) \ln Z_i^{-2/3} \quad 2.14.2$$

$$Z_X = \sum_{i=1}^{N_e} p_i Z_i (Z_i + \xi_{ms}) \ln \left[ 1 + 3.34 (\alpha Z_i)^2 \right] \quad 2.14.3$$

## CHAPTER 2

Suppose an electron is normally incident on a slab of thickness  $s$ (cm), as shown in Fig. 2.14.1. When the electron reaches the other side of the slab, it will have traveled a total distance of  $t$ (cm), will have achieved lateral displacements from its initial direction of  $\Delta x$  and  $\Delta y$ , and will be headed in a direction specified by  $\Theta$  and  $\phi$ .



4-78  
3330A25

That is, the final position is  $(\Delta x, \Delta y, s)$ , and the final direction is  $(\sin \Theta \cos \phi, \sin \Theta \sin \phi, \cos \Theta)$ . We call  $s$  the straight line distance and  $t$  the total distance traveled. In our simulation we neglect the lateral deflections  $\Delta x$  and  $\Delta y$ , but correct for the difference between

## CHAPTER 2

s and t. In order to be able to do this without introducing significant errors we must restrict the size of the electron transport steps to be less than certain limits, which we will derive later. Our procedure then is to transport the electron in a straight line a distance (step size) s along its initial direction. The scattering angle  $\Theta$  is sampled from a p.d.f. which depends on the material, the total distance traveled, t, and on the particle energy. The azimuthal angle  $\phi$  is then chosen randomly and the direction of the electron is adjusted using EGS subroutine UPHI. We shall now discuss the p.d.f. for  $\Theta$ , and then we will derive various limits on s and suggest possible future improvements.

One of the advantages of Moliere's theory is that the energy-dependent p.d.f. of  $\Theta$  can be expressed in terms of an energy-independent p.d.f. of a reduced angle  $\theta$ , where

$$\theta = \frac{\Theta}{\chi_c B^{1/2}}, \quad 2.14.4$$

and where  $\chi_c$  and B are parameters that depend on energy, material, and t. The p.d.f. of  $\Theta$  is given by

$$f(\Theta) = f_M(\Theta) (\sin \Theta / \Theta)^{1/2}, \quad 2.14.5$$

which is like Bethe's formula (58) except that we define our  $f_M(\Theta)$  to be their  $f_M(\Theta)$  times  $\Theta$ ; that is, we include the phase space factor in ours. The factor  $(\sin \Theta / \Theta)^{1/2}$  is less than one and is used as a rejection function to correct the Moliere distribution at large angles. In addition, we reject all sampled  $\Theta > 180^\circ$ . The p.d.f.  $f_M(\Theta)$  is sampled

CHAPTER 2

by first sampling  $\theta$ , the reduced angle, from its p.d.f.,  $f_r(\theta)$ , and then using Eq. 2.14.4 to get  $\Theta$ . This is equivalent to saying that

$$f_M(\Theta)d\Theta = f_r(\theta)d\theta \quad . \quad 2.14.6$$

For the reduced angle p.d.f. we use the first three terms of Bethe's Eq. (25); namely,

$$f_r(\theta) = \left[ f^{(0)}(\theta) + \frac{1}{B} f^{(1)}(\theta) + \frac{1}{B^2} f^{(2)}(\theta) \right] \quad . \quad 2.14.7$$

The general formula for the  $f^{(i)}$  is (Bethe, Eq. (26))

$$f^{(n)}(\theta) = (n!)^{-1} \int_0^\infty u du J_0(\theta u) \times \exp(-u^2/4) \left[ \frac{1}{2} u^2 \ln(u^2/4) \right]^n \quad . \quad 2.14.8$$

For  $n=0$  this reduces to

$$f^{(0)}(\theta) = 2e^{-\theta^2} \quad . \quad 2.14.9$$

Instead of using the somewhat complicated expressions when  $n=1$  and 2, we have elected to use a) the numerical values presented in Bethe's paper (for 29 selected values of  $\theta$  from 0 to 10), b) the fact that  $f^{(i)}(\theta)$  behaves as  $\theta^{-2i-2}$  for large  $\theta$ , and c) the fact that  $f^{(1)}(\theta)$  goes over into the single scattering law at large  $\theta$ . That is,

$$\lim_{\theta \rightarrow \infty} f^{(1)}(\theta)\theta^4 = 2 \quad . \quad 2.14.10$$

This also implies that

$$\lim_{\theta \rightarrow \infty} f^{(2)}(\theta)\theta^4 = 0 \quad . \quad 2.14.11$$

The  $f^{(i)}(\theta)$  functions are not needed in EGS directly, but rather PEGS needs the  $f^{(i)}(\theta)$  to create data that EGS does use. Let

CHAPTER

$$\eta = 1/\theta \quad 2.14.12$$

and

$$f_{\eta}^{(i)}(\eta) = f^{(i)}(1/\eta)\eta^{-4} = f^{(i)}(\theta(\eta))\theta(\eta)^4 \quad 2.14.13$$

As a result of Eqs. 2.14.11 and 2.14.12 we see that  $f_{\eta}^{(1)}(0) = 2$  and  $f_{\eta}^{(2)}(0) = 0$ . We now do a cubic spline fit to  $f^{(i)}(\theta)$  for  $\theta \in (0,10)$  and  $f_{\eta}^{(i)}(\eta)$  for  $\eta \in (0,5)$ . If we use  $\hat{f}^{(i)}(\theta)$  and  $\hat{f}_{\eta}^{(i)}(\eta)$  to denote these fits, then we evaluate the  $f^{(i)}(\theta)$  as

$$f^{(i)}(\theta) = \left( \hat{f}^{(i)}(\theta) \text{ if } \theta < 10, \frac{1}{\theta^4} \hat{f}_{\eta}^{(i)}(1/\theta) \right) \quad 2.14.14$$

Similarly if we want  $f_{\eta}^{(i)}(\eta)$  for arbitrary  $\eta$  we use

$$f_{\eta}^{(i)}(\eta) = \left( \hat{f}_{\eta}^{(i)}(\eta) \text{ if } \eta < 5, \frac{1}{\eta^4} \hat{f}^{(i)}(1/\eta) \right) \quad 2.14.15$$

To complete the mathematical definition of  $f(\theta)$  we now give additional formulas for the evaluation of  $\chi_c$  and  $B$ . We have

$$B - \ln B = b, \quad 2.14.16$$

$$b = \ln \Omega_0, \quad 2.14.17$$

$$\Omega_0 = b_c t / \beta^2, \quad 2.14.18$$

$$b_c = \frac{.6680 \rho Z_S e^{Z_E/Z_S}}{Me^{Z_X/Z_S}} \quad 2.14.19$$

[Note: PEGS computes  $\check{b}_c = X_0 b_c$ ],

CHAPTER 2

$$'6680' = 4\pi N_a \left( \frac{\hbar}{m_e c} \right)^2 \left[ \frac{(0.885)^2}{1.167 \times 1.13} \right] = 6702.33 \quad , \quad 2.14.20$$

$$\rho = \text{material mass density (g/cm}^3) \quad , \quad 2.14.21$$

$$M = \text{molecular weight} = \sum_{i=1}^{N_e} p_i A_i \quad , \quad 2.14.22$$

$$\chi_c = \frac{\chi_{cc} \sqrt{t}}{\check{E}_{MS} \beta^2} \quad , \quad 2.14.23$$

$$\chi_{cc} = \frac{'22.9'}{(180/\pi)} \sqrt{\frac{Z_S \rho}{M}} \quad (\text{cm}^{-1/2} \text{MeV}) \quad 2.14.24$$

$$\left[ \text{Note: PEGS computes } \chi_{cc} = \chi_{cc} \sqrt{X_0} (\text{r.l.}^{-1/2} \text{MeV}) \right] \quad ,$$

$$'22.9' = (180/\pi) \sqrt{4\pi N_a} r_0 m = 22.696 \quad (\text{cm-MeV}) \quad . \quad 2.14.25$$

$\check{E}_{MS}$  is the energy (in MeV) of the electron that is scattering and may be set equal to the energy at the beginning or end of the step (or something in between) to try to account for ionization loss over the step. Equations 2.14.23-25 are based on formula 7.4 of Scott (1963) which is equivalent to

$$\chi_c^2 = \frac{N_a \rho}{M} 4\pi r_0^2 \left[ \sum_{i=1}^{N_e} p_i Z_i (Z_i + \xi_{MS}) \right] \int_0^t \frac{m^2 dt'}{\check{E}(t')^2 \beta(t')^4} \quad . \quad 2.14.26$$

CHAPTER 2

From this we see that, to be proper, we should replace  $\sqrt{t}/\check{E}_{MS}\beta^2$  using

$$\frac{\sqrt{t}}{\check{E}_{MS}\beta^2} = \left( \int_0^t \frac{dt'}{\check{E}(t')^2\beta(t')^4} \right)^{1/2}, \quad 2.14.27$$

where  $\check{E}(t')$  is the particle's energy (in MeV) after going a distance  $t'$  along its path. Likewise,  $\beta(t') = \sqrt{1-m^2/\check{E}(t')^2}$  is the particle's velocity, at the same point, divided by the speed of light. We assume that our steps are short enough and the energy high enough that Eqs. 2.14.23-25 are sufficiently accurate.

For completeness, we give a derivation of Eqs. 2.14.18-21. We start with the definition of  $\Omega_0$ , (which differs somewhat from Scott's definition),

$$\Omega_0 \equiv e^b. \quad 2.14.28$$

According to Bethe's formula(22)

$$e^b = \frac{\chi_c^2}{\chi_\alpha^2} = \frac{\chi_c^2}{1.167' \chi_\alpha^2}. \quad 2.14.29$$

From the derivation in Bethe it is seen that

$$1.167' = e^{2C-1} \quad 2.14.30$$

where

$$C = 0.577216 \text{ is Euler's constant.} \quad 2.14.31$$

CHAPTER 2

Scott's formula (7.25) for  $\chi_\alpha$  is

$$\chi_c^2 \ln \chi_\alpha = 4\pi \int_0^t \frac{dt'}{k^2(t')} \sum_{i=1}^{N_e} N_i \alpha_i^2 \left[ \ln \chi_{\alpha_i} + \frac{\ln \chi_i^{el}}{Z_i} \right], \quad 2.14.32$$

where

$$k = p/\hbar, \quad 2.14.33$$

$p$  = particle momentum,

$$N_i = \frac{N_a \rho}{M} p_i = \text{density of atoms of type } i, \quad 2.14.34$$

$$\alpha_i = \alpha Z_i / \beta = Z_i e^2 / \hbar v, \quad 2.24.35$$

$\chi_{\alpha_i}$  = the screening angle for atoms of type  $i$

$$= \left[ \chi_0^2 (1.13 + 3.76 \alpha_i^2) \right]^{1/2}, \quad 2.14.36$$

$$\chi_0 = \frac{\bar{\chi}_0}{r_{TF}}, \quad 2.14.37$$

$$\bar{\chi}_0 = \lambda_0 / 2\pi = \hbar / p = \text{wavelength of electron} / 2\pi, \quad 2.14.38$$

$r_{TF}$  = Thomas-Fermi radius of atom

$$= 0.885 a_0 Z_i^{-1/3}, \quad 2.14.39$$

$$a_0 = \text{Bohr radius} = \hbar^2 / m_e e^2 \quad 2.14.40$$

$\chi_i^{el}$  = screening angle for the atomic electrons for atoms of type  $i$ .



CHAPTER 2

The next step is to let  $\beta=1$  in the  $\alpha_i$  that are in the  $\chi_{\alpha_i}$ , to delete the term with  $\chi_i^{e\ell}$ , and to let  $Z_i^2 \rightarrow Z_i(Z_i + \xi_{MS})$ . Recalling that  $p=E\beta/c$ ,

Eq. 2.14.32 now becomes

$$\chi_c^2 \ln \chi_\alpha = \frac{N_a \rho}{M} 4\pi e^4 \left[ \sum_{i=1}^{N_e} p_i Z_i (Z_i + \xi_{MS}) \ln \chi_{\alpha_i} \right] \int_0^t \frac{dt'}{E^2 \beta^2} \quad . \quad 2.14.41$$

Since  $e^2 = r_0 m_e c^2$ , and using Eq. 2.14.27, we obtain

$$\chi_c^2 \ln \chi_\alpha = \frac{N_a \rho}{M} 4\pi r_0^2 \left[ \sum_{i=1}^{N_e} p_i Z_i (Z_i + \xi_{MS}) \ln \chi_{\alpha_i} \right] \frac{m^2 t}{E_{MS}^2 \beta^4} \quad . \quad 2.14.42$$

Dividing by Eq. 2.14.26 and multiplying by 2, we get

$$\ln \chi_\alpha^2 = \left[ \sum_{i=1}^{N_e} p_i Z_i (Z_i + \xi_{MS}) \ln \chi_{\alpha_i}^2 \right] Z_S^{-1} \quad . \quad 2.14.43$$

But using Eqs. 2.14.36-40,

$$\ln \chi_{\alpha_i}^2 = \ln \chi_0^2 + \ln \left[ 1.13 + 3.76(\alpha Z_i)^2 \right] \quad , \quad 2.14.44$$

$$\ln \chi_0^2 = \ln \left[ \frac{\hbar^2 m^2 e^4}{p^2 (0.885)^2 \hbar^4 Z_i^{-2/3}} \right] = \ln \left[ \frac{m^2 e^4}{p^2 \hbar^2 (0.885)^2} \right] - \ln Z_i^{-2/3} \quad , \quad 2.14.45$$

$$\ln \left[ 1.13 + 3.76(\alpha Z_i)^2 \right] = \ln 1.13 + \ln \left[ 1 + 3.34(\alpha Z_i)^2 \right] \quad . \quad 2.14.46$$

CHAPTER 2

Hence,

$$\ln \chi_{\alpha}^2 = \left[ Z_S \ln \left( \frac{m_e^2 e^4 1.13}{p^2 \hbar^2 (0.885)^2} \right) + Z_X - Z_E \right] Z_S^{-1} , \quad 2.14.47$$

so that

$$\chi_{\alpha}^2 = \frac{m_e^2 e^4 1.13 e^{Z_X/Z_S}}{p^2 \hbar^2 (0.885)^2 e^{Z_E/Z_S}} . \quad 2.14.48$$

Now, recalling that Eqs. 2.14.23-25 are equivalent to

$$\chi_C^2 = \frac{N_a \rho}{M} 4\pi r_0^2 Z_S t \left( m_e^2 c^4 / E^2 \beta^4 \right) , \quad 2.14.49$$

and using Eqs. 2.14.28, 29, 48, 49, we obtain

$$\begin{aligned} \Omega_0 &= \frac{\frac{N_a \rho}{M} 4\pi r_0^2 Z_S t m_e^2 c^4 (E^2 \beta^2 / c^2) \hbar^2 (0.885)^2 e^{Z_E/Z_S}}{m_e^2 (r_0^2 m_e^2 c^4) e^{Z_X/Z_S} E^2 \beta^4 (1.167) (1.13)} \\ &= '6680' \left[ \frac{\rho Z_S e^{Z_E/Z_S}}{M e^{Z_X/Z_S}} \right] \frac{t}{\beta^2} \\ &= b_c t / \beta^2 . \quad \text{Q.E.D.} \end{aligned} \quad 2.14.50$$

## CHAPTER 2

Moliere's B parameter is related to b by the transcendental Eq. 2.14.16. For a given value of b, the corresponding value of B may be found using Newton's iteration method. As a rough estimate,  $B=b + \ln b$ . It can be seen that b, and hence B, increases logarithmically with increasing transport distance.

The intuitive meaning of  $\Omega_0$  is that it may be thought of as the number of scatterings that take place in the slab. If this number is too small, then the scattering is not truly multiple scattering and various steps in Moliere's derivation become invalid. In Moliere's (1948) original paper, he considered his theory valid for

$$\Omega_0 \text{ (his } \Omega_b) \geq 20 \quad , \quad 2.14.51$$

which corresponds to

$$B \geq 4.5, \quad \text{and} \quad b \geq 3 \quad . \quad 2.14.52$$

From Eqs. 2.14.50 and 2.14.51 we arrive at the condition

$$t/\beta^2 \geq 20/b_c = (t_{\text{eff}})_0 \quad .$$

Another restriction on the validity of Eq. 2.14.5 is mentioned by Bethe (1953); namely,

$$\chi_c^2 B < 1 \quad . \quad 2.14.53$$

This means that the slab must not become so thick that  $\Theta/\theta = \chi_c \sqrt{B}$  becomes larger than one radian. We must include Eq. 2.14.53 in the list of restrictions on the size of the transport step s,t.

Resuming our presentation of the method used to sample  $\Theta$  , we return now to the problem of sampling  $\theta$  from  $f_r(\theta)$  given by Eq. 2.14.7. It might

CHAPTER 2

at first appear that  $f_r(\theta)$  is already decomposed into sub-distribution functions. However,  $f^{(1)}(\theta)$  and  $f^{(2)}(\theta)$  are not always positive, and thus, are not candidate distribution functions. Graphs of  $f^{(1)}(\theta)$  and  $f^{(2)}(\theta)$  are shown in Fig. 2.14.1. We now adopt a strategy similar to that used by Messel and Crawford (1970); namely, mix enough of  $f^{(0)}(\theta)$  with  $f^{(1)}(\theta)$  and  $f^{(2)}(\theta)$  to make them everywhere positive. Unlike Messel and Crawford, who dropped the term involving  $f^{(2)}(\theta)$ , we have been able to retain all of the first three terms in the expansion.

The factorization we use is

$$f_r(\theta) = \sum_{i=1}^3 \alpha_i f_i(\theta) g_i(\theta) , \quad 2.14.54$$

where

$$\alpha_1 = 1 - \lambda/B, \quad 2.14.55$$

$$f_1(\theta) = 2e^{-\theta^2} \text{ for } \theta \in (0, \infty), \quad 2.14.56$$

$$g_1(\theta) = 1, \quad 2.14.57$$

$$\alpha_2 = \mu g_{2, \text{Norm}} / B, \quad 2.14.58$$

$$f_2(\theta) = 1/\mu \text{ for } \theta \in (0, \mu), \quad 2.14.59$$

$$g_2(\theta) = \frac{\theta}{g_{2, \text{Norm}}} \left( \lambda f^{(0)}(\theta) + f^{(1)}(\theta) + f^{(2)}(\theta)/B \right), \quad 2.24.60$$

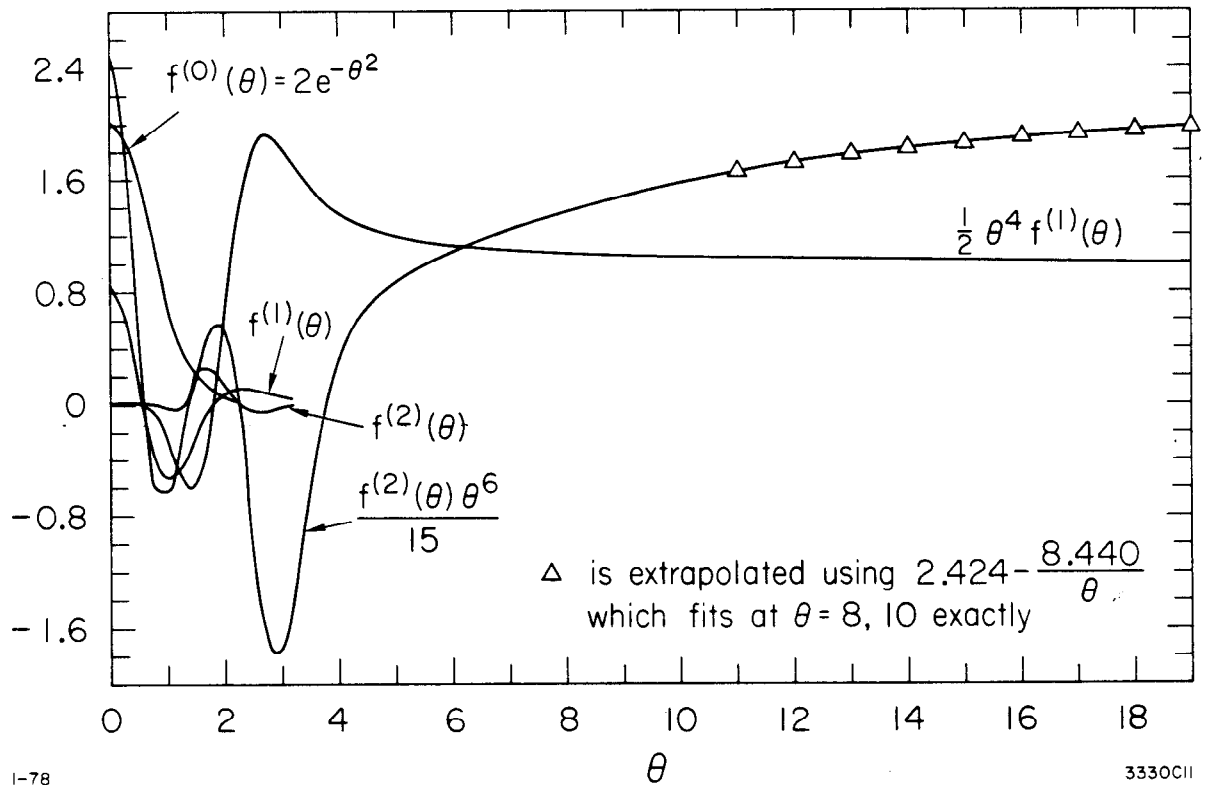


Fig. 2.14.1 Plots of  $f^{(0)}$ ,  $f^{(1)}$ , and  $f^{(2)}$ .

CHAPTER 2

$$\alpha_3 = g_{3, \text{Norm}} / 2\mu^2 B, \quad 2.14.61$$

$$f_3(\theta) = 2\mu^2 \theta^{-3} \text{ for } \theta \in (\mu, \infty), \quad 2.14.62$$

$$g_3(\theta) = \frac{\theta^4}{g_{3, \text{Norm}}} \left( \lambda f^{(0)}(\theta) + f^{(1)}(\theta) + f^{(2)}(\theta)/B \right). \quad 2.14.63$$

When the third sub-distribution function is selected, we first sample  $\eta=1/\theta$  using  $f_{\eta 3}(\eta)$  and  $g_{\eta 3}(\eta)$  given by

$$f_{\eta 3}(\eta) = 2\mu^2 \eta \text{ for } \eta \in (0, 1/\mu), \quad 2.14.64$$

$$g_{\eta 3}(\eta) = \frac{\eta^{-4}}{g_{3, \text{Norm}}} \left( \lambda f^{(0)}(1/\eta) + f^{(1)}(1/\eta) + f^{(2)}(1/\eta)/B \right). \quad 2.14.65$$

Then we let  $\theta = 1/\eta$ .

As presented above, this scheme contains four parameters,  $\lambda$ ,  $\mu$ ,  $g_{2, \text{Norm}}$ , and  $g_{3, \text{Norm}}$ ; the latter two are so chosen that  $g_2(\theta)$  and  $g_{\eta 3}(\eta)$  have maximum values (over the specified ranges) which are not greater than 1. The first sub-distribution is the gaussian (actually exponential in  $\theta^2$ ) distribution that dominates for large  $B$  (thick slabs). The third sub-distribution represents the "single scattering tail." The second sub-distribution can be considered as a correction term for central  $\theta$  values. The parameter  $\mu$  separates the central region from the tail. The parameter  $\lambda$  determines the admixture of  $f^{(0)}$  in the second and third sub-distribution

## CHAPTER 2

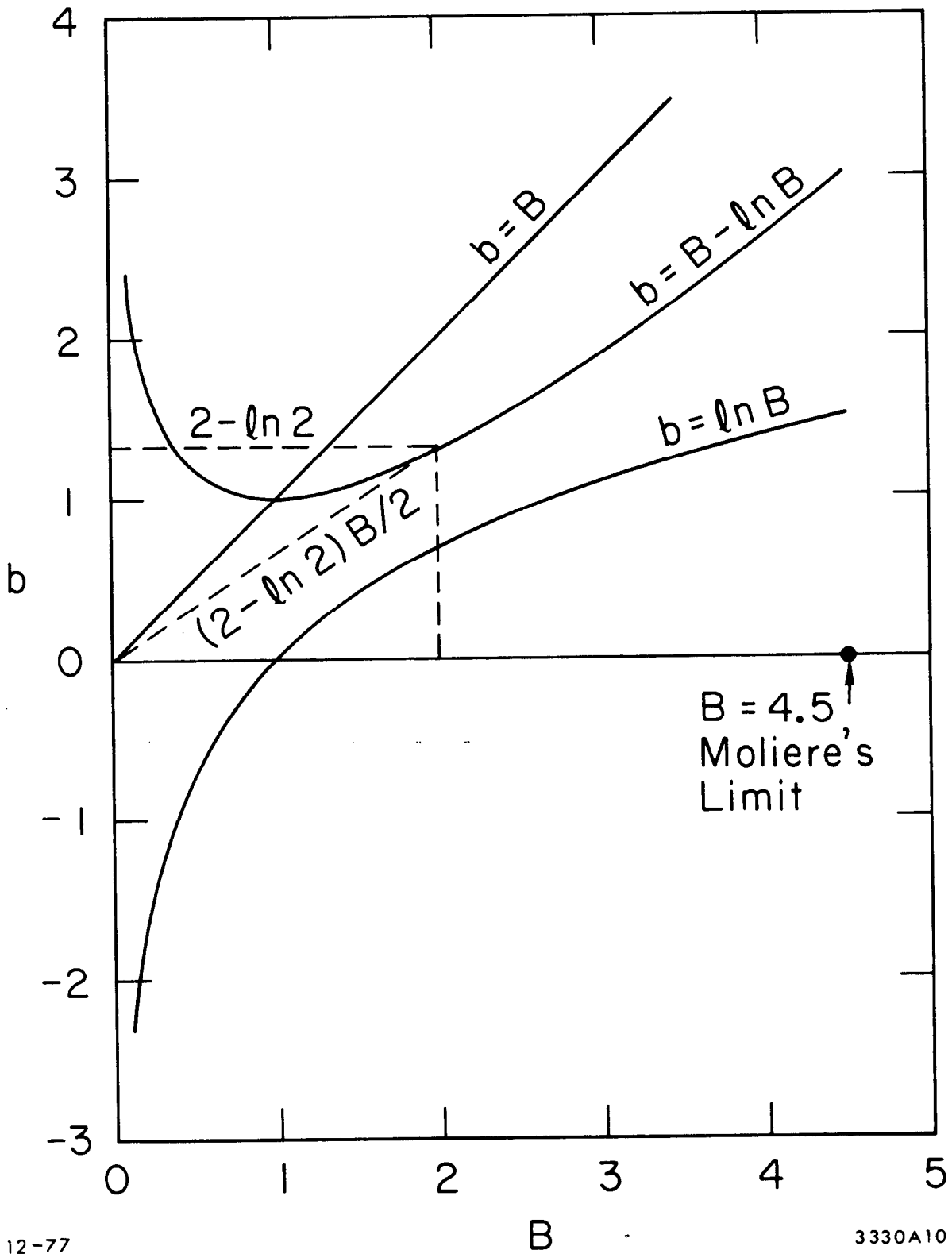
functions. It must be large enough to ensure that  $g_2(\theta)$  and  $g_3(\theta)$  are always positive. It will also be noted that  $\alpha_1$  becomes negative if  $B < \lambda$  so that this case must be specially treated. After studying the variation of the theoretical sampling efficiency with the variation of these parameters, the values

$$\lambda=2, \mu=1, g_{2,\text{Norm}} = 1.80, g_{3,\text{Norm}} = 4.05 \quad 2.14.66$$

were chosen. These values do not give the absolute optimum efficiency, but the optimum  $\mu$  values were usually close to one, so we chose  $\mu=1$  for simplicity.  $\lambda$  could not have been chosen much lower while still maintaining positive rejection functions. Furthermore it was desired to keep  $\lambda$  as low as possible since this would allow Moliere's distribution to be simulated for as low values of  $B$  as possible. Although Moliere's theory becomes less reliable for  $B < 4.5$ , it was felt that it was probably as good an estimate as could easily be obtained even in this range.

Since  $\alpha_1 < 0$  for  $B < \lambda$ , some modification of the scheme must be devised in this case. What we have done is to use the computed value of  $B$  in computing  $\chi_c \sqrt{B}$ , but for sampling we set ' $1/B$ ' = ' $1/\lambda$ '. This has the effect of causing the gaussian not to be sampled.

Our next point is best made by means of Fig. 2.14.2 which is a graph of Eq. 2.14.16, the transcendental equation relating  $B$  and  $b$ . It will be observed that when viewed as defining a function of  $b$  the resulting function is double valued. We of course reject the part of the curve for  $B < 1$ . We would, however, like to have a value of  $B$  for any thickness



12-77

3330A10

Fig. 2.14.2 Plot of Eq. 2.14.16 ( $B - \ln B = b$ ).



CHAPTER 2

of transport distance (i.e., any value of  $b$ ). In order to obtain a smooth transition to zero thickness we join a straight line from the origin, ( $B=0, b=0$ ), to the point on the curve ( $B=2, b=2 - \ln 2$ ).  $B$  is then determined by

$$B = \left\{ \begin{array}{l} \frac{2}{2 - \ln 2} b \text{ if } b < 2 - \ln 2, \\ \text{the } B > 1 \text{ satisfying } B - \ln B = b, \\ \text{if } b > 2 - \ln 2. \end{array} \right\} \quad 2.14.67$$

For rapid evaluation,  $B$  has been fit using a piecewise quadratic fit for  $b \in (2, 30)$  ---  $b=30$  corresponding roughly to a thickness of  $10^7$  radiation lengths, which should be sufficient for any application.

Actually,  $b=0$  does not correspond to  $t=0$ , but rather to  $t \approx 2 \times 10^{-6} X_0$ . We nevertheless set  $\theta=0$  if  $b \leq 0$ . The case where  $b \in (0, 3)$  is not too likely either, since  $b=3$  roughly corresponds to  $t \approx 10^{-4} X_0$ , and is not very important since the scattering angles should be small.

To complete our discussion on sampling we note that  $f_1(\theta)$  is sampled directly by means of

$$\theta = \sqrt{-\ln \zeta}. \quad 2.14.68$$

The p.d.f. of  $f_2(\theta)$  is sampled by merely choosing a uniformly distributed random number. The p.d.f. of  $\hat{f}_3(\eta)$  is sampled by taking the larger of two uniformly distributed random numbers. Finally,  $g_2(\theta)$  and  $g_{\eta 3}(\eta)$  are divided into "B-independent" parts

## CHAPTER 2

$$g_2(\theta) = g_{21}(\theta) + g_{22}(\theta)/B \text{ for } \theta \in (0,1), \quad 2.14.69$$

$$g_{n3}(\theta) = g_{31}(\eta) + g_{32}(\eta)/B \text{ for } \eta \in (0,1). \quad 2.14.70$$

The functions  $g_{21}$ ,  $g_{22}$ ,  $g_{31}$ , and  $g_{32}$  have been fit by PEGS over the interval (0,1) using a piecewise quadratic fit. This completes our discussion of the method used to sample  $\theta$ .

We now consider what limits should or must be placed on the size of the transport step. One condition is that  $\chi_c^2 B < 1$ . Another requirement might be that the difference between the straight line and total distance traveled by an electron be less than some fraction of  $t$ ; that is,  $(t-s) < \epsilon t$ . The reason for this restriction is that we are using an approximate correction method so we would like to keep the correction from getting too large. Another condition might be that the expected lateral deflection over one step be kept below some value; that is,  $\Delta x_{\text{rms}} < \Delta x_{\text{max}}$ . Other restrictions that are independent of multiple scattering are that the step must not exceed the distance to the next interaction, or geometry boundary, or the range of the electron. Also, if the material density were a function of position and the density over-ride facility were being used (see Chapter 4.), or if the modifications necessary to simulate showers in electric and magnetic fields were made and the electric and magnetic fields were functions of position, then the transport step size should be kept small enough to adequately take into account the

## CHAPTER 2

inhomogenities. It is for such reasons as these that the TMXS (i.e. maximum transport step) over-ride (see Chapter 4) has been provided to allow the user to decide on the desired limits to the transport step length. We now consider the multiple scattering restrictions on transport step size one at a time.

The maximum total step size consistent with Bethe's condition,  $t_B$ , is determined by the condition

$$\chi_c^2(t_B)B(t_B) = 1 \quad . \quad 2.14.71$$

From Eq. 2.14.16 we can write

$$e^b = e^{B/B} \quad , \quad 2.14.72$$

and using Eqs. 2.14.17, 18, 23 with Eqs. 2.14.71 and 2.14.72, we have

$$\frac{b_c t_B}{\beta^2} = \frac{\exp [(\check{E}_{MS} \beta^2)^2 / \chi_{cc}^2 t_B] \chi_{cc}^2 t_B}{(\check{E}_{MS} \beta^2)^2} \quad . \quad 2.14.73$$

Solving for  $t_B$  we obtain

$$t_B = \frac{(\check{E}_{MS} \beta^2 / \chi_{cc})^2}{\ln [b_c (\check{E}_{MS} \beta / \chi_{cc})^2]} \quad . \quad 2.14.74$$

It can be seen that the energy variation of  $t_B$  is dominated by the  $\check{E}_{MS}^2$  factor. PEGS function TMXB evaluates Eq. 2.14.74.

CHAPTER 2

Now let  $t_p(\bar{E})$  be the transport distance such that on the average

$$(t_p - \bar{s}_p) / t_p = \bar{E} \quad , \quad 2.14.75$$

where  $\bar{s}_p$  is the average "straight line" distance traveled when the total distance is  $t_p$ . Since we are making a rough estimate, we shall use the Fermi-Eyges scattering theory. Messel and Crawford (1970) discuss the path length correction (we use their correction method but not necessarily their limit). In analogy to their equations we obtain

$$t = s + \frac{1}{2} \int_0^t \overline{\Theta^2}(t') dt' \quad , \quad 2.14.76$$

$$\overline{\Theta^2}(t) = \frac{\check{E}_S^2(t/X_0)}{\beta^4 \check{E}^2} \quad , \quad 2.14.77$$

$$\check{E}_S = m \sqrt{\frac{4\pi}{\alpha}} = 21.2 \text{ MeV} \quad , \quad 2.14.78$$

$$t = s + \left( \frac{\check{E}_S}{2\check{E}\beta^2} \right)^2 \frac{t^2}{X_0} \quad , \quad 2.14.79$$

$$(t-s)/t = \left( \frac{\check{E}_S}{2\check{E}\beta^2} \right)^2 \frac{t}{X_0} \quad . \quad 2.14.80$$

Comparing Eq. 2.14.75 and 2.14.80 we see that

$$t_p(\bar{E}) = t_s(\check{E})\bar{E} \quad , \quad 2.14.81$$

CHAPTER 2

where we have defined

$$t_s(\check{E}) = X_0 \left( \frac{2\check{E}\beta^2}{\check{E}_S} \right)^2 . \quad 2.14.82$$

For the purposes of making corrections we now have

$$s' = t'(1-t') \quad , \quad 2.14.83$$

$$t' = s' [2/(1 + \sqrt{1-4s'})] \quad , \quad 2.14.84$$

where

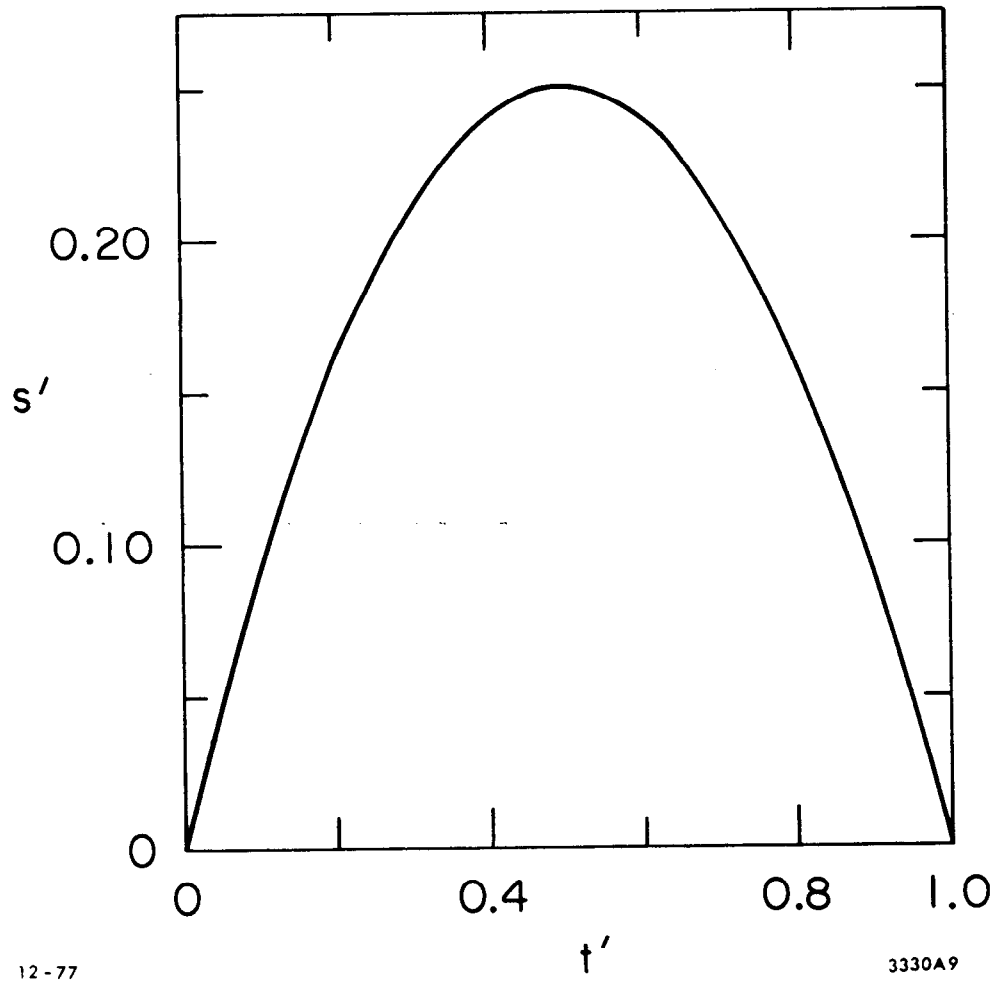
$$s' = s/t_s(\check{E}) \quad , \quad 2.14.85$$

$$t' = t/t_s(\check{E}) \quad . \quad 2.14.86$$

Figure 2.14.3 shows a graph of Eq. 2.14.83. It can be seen that, after a distance  $t=t_s$ , there has been so much scattering that according to our simple model the electron has traveled a net distance of zero. It also can be seen that the largest achievable  $s'$  is  $\frac{1}{4}$ , which occurs for  $t'=\frac{1}{2}$ . Thus we must at least require  $t' \leq \frac{1}{2}$ , and this part of the curve is a graph of Eq. 2.14.84. We fit Eq. 2.14.84 with a piecewise quadratic fit for greater speed. Because Eq. 2.14.84 is singular at  $s'$  near 0.25, we restrict our fit to  $s' < 0.22$ . We now also select our path length restriction to be

$$t < t_{Pmax} = t_s E_{Pmax} \quad 2.14.87$$

where we select  $E_{Pmax}=0.3$  as default in EGS. But this may be over-ridden by users to smaller (but not larger) values if desired.



12-77

3330A9

Fig. 2.14.3 Plot of Eq. 2.14.83  
( $s' = t'(1-t')$ ).

## CHAPTER 2

We now direct our attention to path-length corrections. According to Fermi-Eyges theory\*, if  $r_{\text{rms}}$  is the root-mean-square lateral deflection after traveling distance  $t$ , then

$$\begin{aligned} r_{\text{rms}} &= t^{\oplus}_{\text{rms}}(t)/\sqrt{3} \\ &= \frac{t^{3/2} \check{E}_S}{\sqrt{3X_0} \check{E}\beta^2} . \end{aligned} \tag{2.14.88}$$

If we define  $t_{\ell d}(E_{\ell d})$  to be the transport distance which on the average gives rise to a lateral deflection of  $E_{\ell d}X_0$ , then we have

$$t_{\ell d}(\bar{r}_{\ell d}) = X_0 \left( \check{E}\beta^2 \sqrt{3} E_{\ell d} / \check{E}_S \right)^{2/3} . \tag{2.14.89}$$

It can be seen that, whereas  $t_B$  and  $t_{P_{\text{max}}}$  vary as  $E^2$  for large energy,  $t_{\ell d}$  varies as  $E^{2/3}$ , and thus it must be the smallest upper limit on the path length above some energy. We now seek to obtain more quantitative information relating these restrictions.

Since  $t_P$  and  $t_{\ell d}$  are expressed in terms of radiation lengths it would be useful if  $t_B$  could be also. We make the same approximations that were probably made in obtaining  $\oplus^2$  in terms of radiation lengths; namely, that the difference between the  $\xi_{\text{MS}}$  and  $\xi(Z_i)$  can be ignored and that the Coulomb correction terms of the radiation length can be neglected. It is then true that  $Z_T \approx Z_S$  and it can be shown that

---

\*For a short review of Fermi-Eyges theory see Kase and Nelson (1972).

CHAPTER 2

$$\chi_{cc}^{-2} = X_0 \frac{\alpha}{\pi m^2} \ln \left[ 183/\bar{Z}_{\text{geom}}^{1/3} \right] \quad 2.14.90$$

where

$$\bar{Z}_{\text{geom}} = e^{-3Z_G} \quad 2.14.91$$

= the weighted geometric mean atomic number.

Moreover, it can be shown that

$$\frac{b_c}{\chi_{cc}^2} \approx \frac{(\bar{Z}_{\text{geom}})^{-2/3}}{1.5 \alpha^2 m^2 (1+3.34 \alpha^2 \bar{Z}_{\text{geom}}^2)} \quad 2.14.92$$

The expression for  $t_B$  now becomes

$$t_B \approx X_0 \frac{\alpha}{\pi} \frac{\check{E}^2 \beta^4 \ln \left[ 183/\bar{Z}_{\text{geom}}^{1/3} \right]}{m^2 \ln \left[ \check{E}^2 \beta^2 / 1.5 \bar{Z}_{\text{geom}}^{2/3} \alpha^2 m^2 (1+3.34 \alpha^2 \bar{Z}_{\text{geom}}^2) \right]}$$

$$\approx X_0 \frac{\alpha}{2\pi} \frac{\check{E}^2 \beta^4}{m^2} \ln \left[ 183/\bar{Z}_{\text{geom}}^{1/3} \right] / \ln \left[ 90 \check{E} \beta / m \bar{Z}_{\text{geom}}^{1/3} \right] \quad 2.14.93$$

For  $\check{E} \beta / m > 1$ , the logarithm in 2.14.93 is always greater than about 3, so

$$t_B \lesssim X_0 \frac{\alpha}{2\pi} \frac{\check{E}^2 \beta^4}{m^2} \ln \left[ 183/\bar{Z}_{\text{geom}}^{1/3} \right] / \left[ 3 + \ln (\check{E} \beta / m) \right] \quad 2.14.94$$

The expression for  $t_{P_{\text{max}}}$  can be rewritten as

$$t_{P_{\text{max}}} = X_0 \frac{\alpha E_{P_{\text{max}}}}{\pi} \frac{\check{E}^2 \beta^4}{m^2} \quad 2.14.95$$

For  $E_{P_{\text{max}}} = 0.3$  we thus see that  $t_B \lesssim \frac{1}{2} t_{P_{\text{max}}}$ . Thus we expect  $t_B$  to be more restrictive unless  $E_{P_{\text{max}}}$  is chosen quite a bit smaller.



## CHAPTER 2

We now consider at what energies  $t_{\ell d}$  becomes the significant restriction. Setting  $t_B = t_{\ell d}$ , using the equality form of Eq. 2.14.94, letting  $L = 3 + \ln(\check{E}\beta/m)$ , and letting  $L_g = \ln[183/\bar{Z}^{1/3}_{geom}]$ , we obtain

$$\check{E}\beta^2 = m \left[ \frac{6\pi^2 L^3 E_{\ell d}^2}{\alpha^2 L_g^3} \right]^{1/4} . \quad 2.14.96$$

For  $E_{\ell d} = 0.001$  and  $L = L_g$  we find  $\check{E}\beta^2 = 0.5$  MeV.

PEGS should have functions to evaluate all of these path length restrictions; namely, TMXB, TMXP and TMXLD for  $t_B$ ,  $t_{Pmax}$ , and  $t_{\ell d}$ , respectively, and another function TMXS which takes the minimum of these. However, PEGS currently has only TMXB and a TMXS which computes the minimum of TMXB and 10 radiation lengths. The latter restriction was used to make TMXS easier to fit. PEGS fits  $TMXS(\check{E})$  with a piecewise linear fit so that the maximum recommended step size is easily evaluated.

The effect of using these path length restrictions needs to be studied further. It will be seen in Section 3.5 that the choice of path length restriction can be very important depending on the problem. For the experiments we have tested EGS3 against, the path length limitation that has been most effective has been a combination of the TMXB restriction and a requirement that the path length be less than  $200(t_{eff})_0$ , the latter being the maximum step size used in EGS2.

### 2.15 Photoelectric Effect

The total photoelectric cross sections that we use are taken from Storm and Israel (1970) and are available for elements 1 through 100. The data read from the data file is in units of barns/atom. PEGS routine PHOTTZ computes

CHAPTER 2

$$\check{\Sigma}_{\text{photo,partial}}(Z, \check{k}) = \frac{N_a \rho}{M} X_0 \left( \frac{1 \times 10^{-24} \text{cm}^2}{\text{barn}} \right) \sigma_{\text{photo}}(Z, \check{k}) \text{ (barns)} \quad , \quad 2.15.1$$

where  $\sigma_{\text{photo}}(Z, \check{k})$  is obtained by using PEGS function AINTP to do a log-log interpolation in energy of the cross sections in the data base. The total cross section, as computed by PEGS routine PHOTTE, is given by

$$\check{\Sigma}_{\text{photo}}(\check{k}) = \sum_{i=1}^{N_e} P_i \check{\Sigma}_{\text{photo,partial}}(Z_i, \check{k}) \quad . \quad 2.15.2$$

This total photoelectric cross section is then used in the computation of the photon mean free path and branching ratio.

The run-time implementation of the photoelectric effect is presently rather crude. In the first two versions of EGS the photoelectric effect was treated in subroutine PHOTON, but in EGS3 subroutine PHOTO has been created to deal with it. This should facilitate in developing more general photoelectric routines in the future.

At present the only data available at run time to EGS is a weighted average K-edge energy given by

$$\check{E}_{\text{K-edge}} = \frac{\sum_{i=1}^{N_e} P_i \check{\Sigma}_{\text{photo}}(A_P) \check{E}_{\text{K-edge}}(Z_i)}{\sum_{i=1}^{N_e} P_i \check{\Sigma}_{\text{photo}}(A_P)} \quad . \quad 2.15.3$$

Whenever it has been determined that a photoelectric event has occurred, a photoelectron is created with total energy

$$\check{E} = \check{k} - \check{E}_{\text{K-edge}} + m \quad , \quad 2.15.4$$

## CHAPTER 2

and with the same direction as the incident photon. To preserve the energy balance, a photon of energy  $\bar{E}_{K\text{-edge}}$  is created and then forcibly discarded.

Recently, a substitute PHOTO routine, which uses the  $E_{K\text{-edge}}$  of the highest Z constituent rather than a weighted average, has been written (Clark 1977). If the incident photon is below this edge, it is merely discarded. Otherwise a photoelectron is created with the appropriate energy. The fluorescent yield and branching ratios between  $K_\alpha$  and  $K_\beta$  photons are then consulted, resulting in the decision to create either no photons, one average  $K_\alpha$  photon or one average  $K_\beta$  photon. In any case, excess energy is tallied by creating a photon with the leftover energy and forcibly discarding it.

### 3. COMPARISON BETWEEN EGS CALCULATIONS AND VARIOUS EXPERIMENTS AND OTHER MONTE CARLO RESULTS

#### 3.1 Conversion Efficiency of Lead for 30-200 MeV Photons

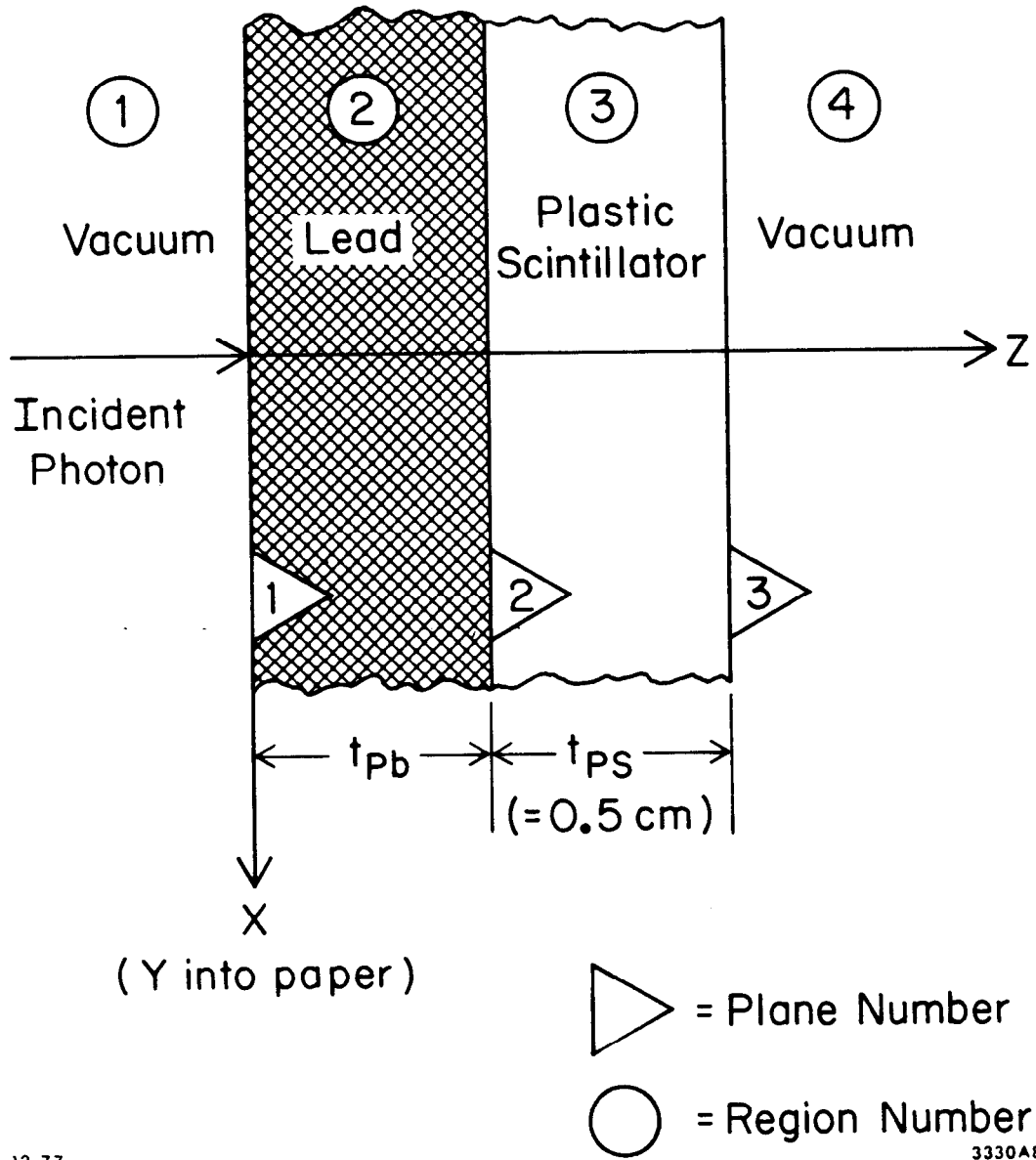
We begin this chapter by describing an EGS simulation of a recent experiment (Darriulat 1975) that measured the conversion efficiency for 44, 94, and 177 MeV photons incident upon lead. By tagging the photons the mean energy was determined to an accuracy of  $\pm 4$  Mev. The photon beam, with an area less than 15 cm x 15 cm, struck a lead plate of desired thickness (1 to 20 mm) and area (20 cm x 20 cm). Immediately following the lead was a large plastic scintillation detector, 28 cm x 40 cm in area and 5 mm thick. An event was counted as a conversion if more than 60 keV was deposited in the scintillator for each incoming photon.

To calculate the conversion efficiency with EGS, the geometry layout shown in Fig. 3.1.1 was used, consisting of four regions separated by three semi-infinite planes. Polystyrene, with a density of  $1.032 \text{ g-cm}^{-3}$  and consisting of hydrogen and carbon with an atomic ratio H/C = 1.10, was used as the medium for plastic scintillator in region 3. The density of lead was taken to be  $11.34 \text{ g-cm}^{-3}$ . PEGS was used to create the necessary material data with cutoff energies of 1.5 MeV and 0.1 MeV for electrons and photons, respectively.

The actual User Code\* that was used in this calculation is called UCCONEFF and is given in Appendix UC. The HOWFAR subprogram portion of UCCONEFF utilizes three auxiliary subroutines PLANE2, PLANE1, and CHGTR,

---

\*The reader is encouraged to read Chapter 4 (the "User Manual") first in order to gain an understanding of the role of the User Code.



12-77

3330A8

Fig. 3.1.1 Geometry Layout Used in HOWFAR for Simulation of Conversion Efficiency Experiment.

## CHAPTER 3

that should be self-explanatory to the reader after studying the code listing. Although HOWFAR could have been written in a simpler manner without using these auxiliary subroutines, we prefer to introduce them here because they will become very useful in later examples where geometries can be somewhat more complicated.

The AUSGAB (scoring and/or outputing) subroutine was setup to sum the energy deposition in the plastic for each incident photon. Upon completion of a photon shower generation initiated by a CALL SHOWER statement in MAIN, a conversion event was scored provided that the energy sum in the plastic exceeded 0.060 MeV as dictated by the experiment. The conversion efficiency was calculated by dividing the event count (NSCINT) by the total number of photon histories incident (NCOUNT).

The results of the calculations are compared with the experimental data in Fig. 3.1.2. Needless to say, the agreement is extremely good over the entire lead thickness range for the two energies shown.

In the text describing the experimental results, Darriulat et al point out that the energy spectrum in the scintillator showed characteristic peaks corresponding to the production of one, two, or three secondary electrons. To check out this observation the total energy deposition in the scintillator per incident photon was histogrammed\*. Fig. 3.1.3 is representative of the results obtained and indeed shows three peaks. Assuming an energy loss of about  $2 \text{ MeV/g-cm}^{-2}$  for a

---

\*The histogramming package that was used is a SLAC facility code called DPAK/HPAK (Logg et al 1976) and, for simplicity purposes, the programming that relates to it is not shown in the User Code.

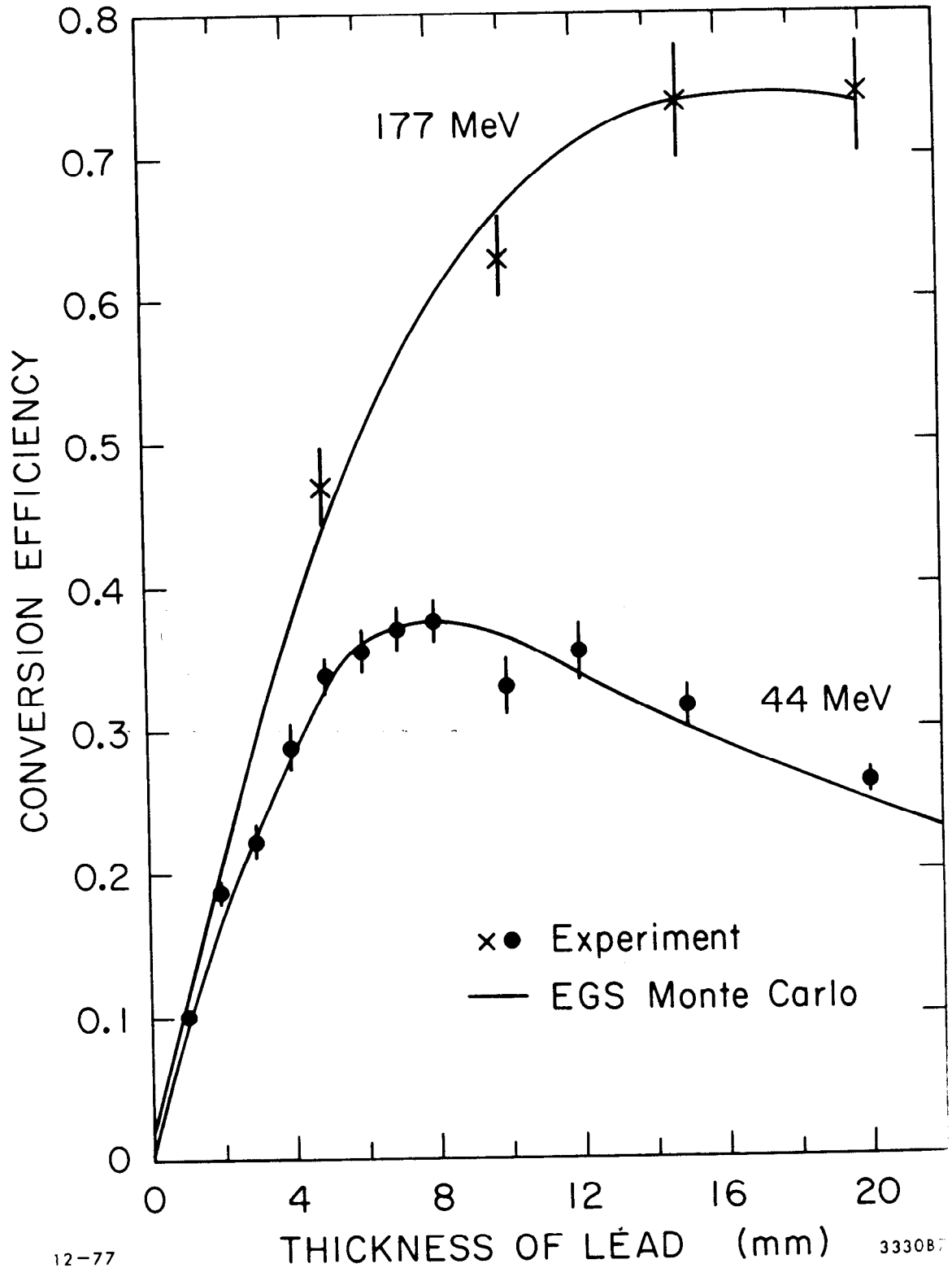
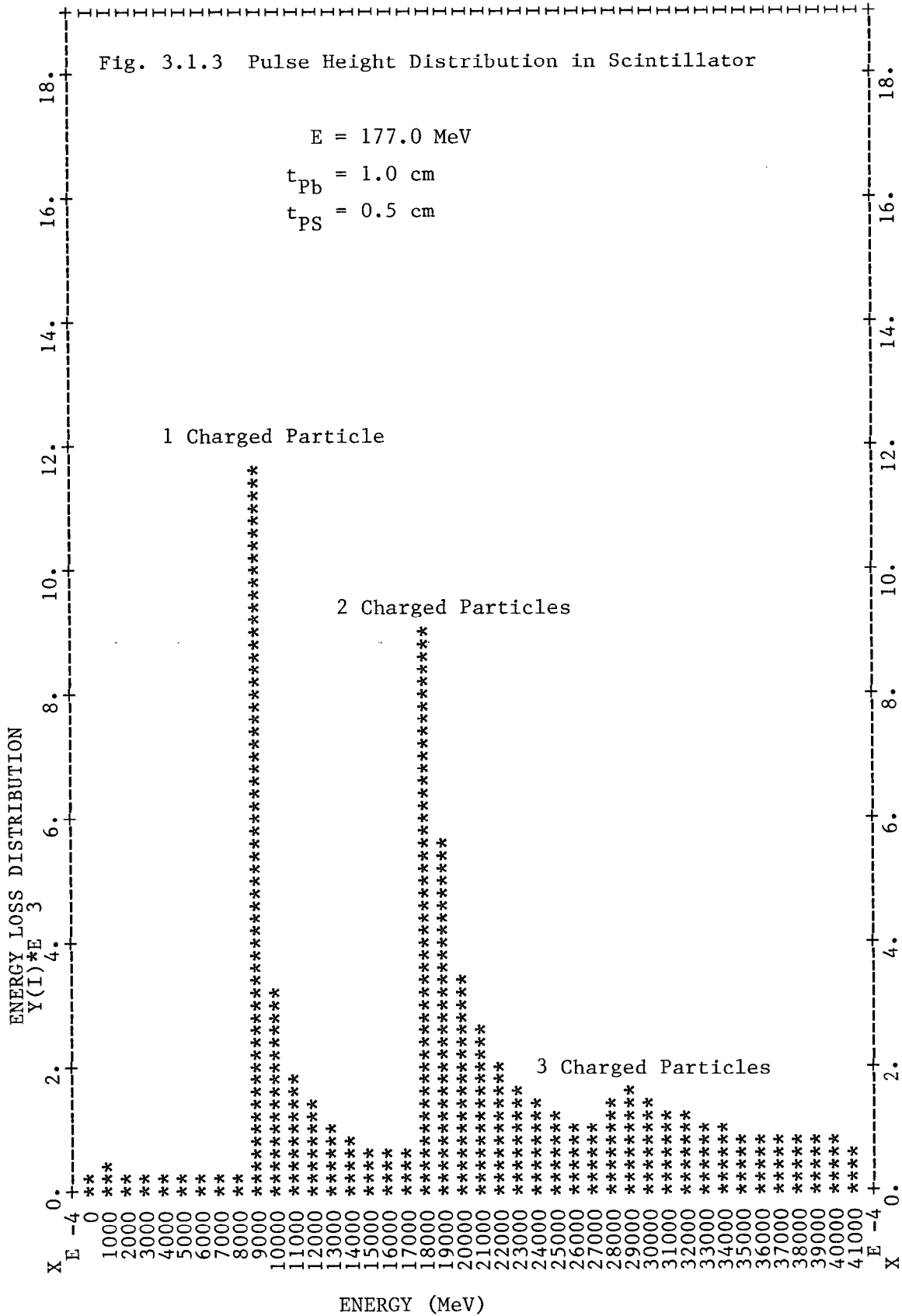


Fig. 3.1.2 Conversion Efficiency Experiment and Comparison with EGS Monte Carlo Simulation of Results.



76%



single electron traversing the plastic thickness (0.5 cm), the peaks are also seen to be in their expected energy locations (1, 2, and 3 MeV).

In conclusion, EGS can predict photon conversion efficiencies rather well, at least in the energy range 30-200 MeV and for geometries similar to the one described here.

### 3.2 The Charged Component of 1 GeV Electron Showers

The longitudinal development of electromagnetic cascade showers has been analytically modeled and solved under various approximations (Rossi 1952). Typically, the mean number of charged particles, when plotted as a function of the thickness of the absorber in radiation lengths, starts at unity, rises to a maximum, and exhibits a tail corresponding to attenuation of the photon component. The height of the curve at the maximum can be parameterized in terms of the ratio,  $E/E_0$ , where  $E_0$  is the incident energy and  $E$  is the lower limit at which charged particles are considered in the estimate. The smaller the value of  $E$  the larger the height of the shower curve. Such curves can be obtained rather easily with EGS, and we shall illustrate this by comparing such a calculation with an experiment that was designed to sort the secondary charged particle component in terms of  $E$ .

The experiment (Drickey 1968) was performed by observing the secondary charged particle tracks traversing a streamer chamber located around a stack of lead plates that were placed in a beam of 1 GeV electrons ( $e^+$  in this case). The streamer chamber arrangement is depicted in Fig. 3.2.1 showing three sections with lengths 11, 13, and 15 cm. The upbeam section was used to ensure that one and only one electron was

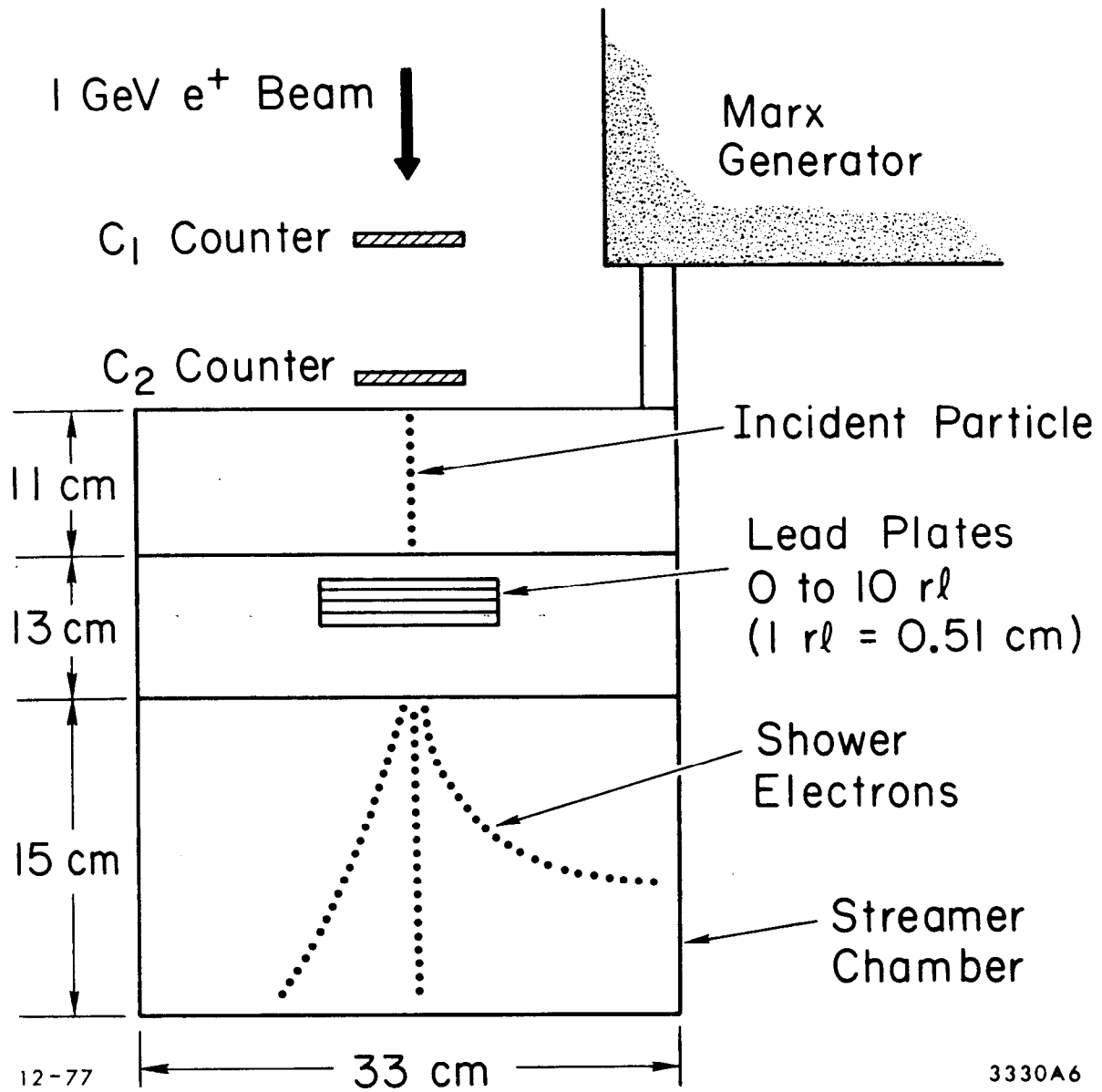
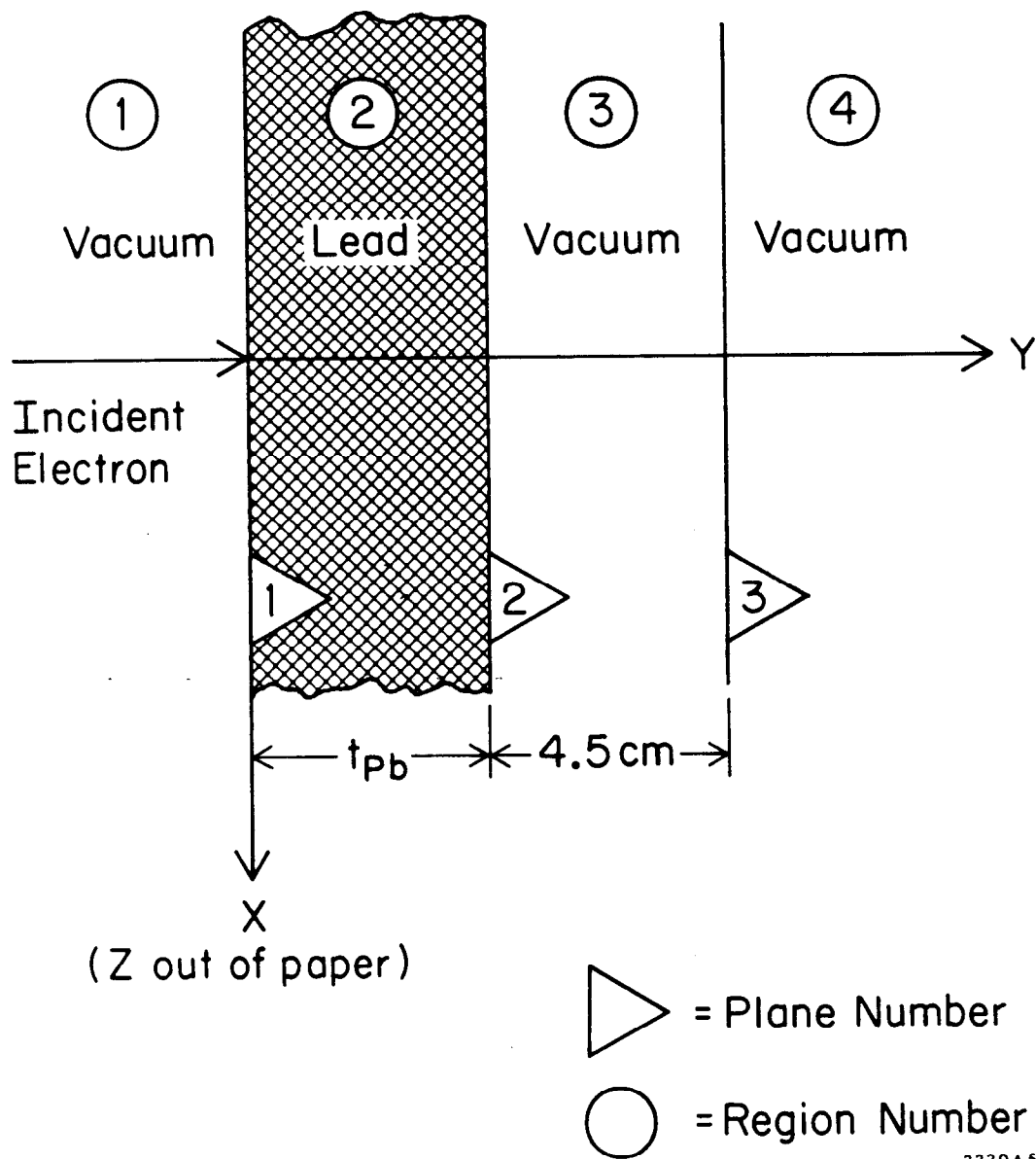


Fig. 3.2.1 Streamer Chamber Arrangement Used in the Experiment by Drickey et al. (1968) (Note: 12 cm chamber gap in the direction of normal to plane of figure; magnetic field in that direction too).

## CHAPTER 3

incident at a time, and also eliminated confusion between those cases when no charged particle emerged from the lead and when the chamber fired improperly. The downbeam surface of the lead converter was 4.5 cm upbeam from the entrance to the third section (15 cm long) in which the shower particles were observed and measured. Data were taken with lead thicknesses out to 10 radiation lengths. A magnetic field of 1665 G, perpendicular to the chamber plane shown in Fig. 3.2.1, was established (uniformly we will assume) in the third section only. This provided a means of determining the momentum of the individual secondaries that were photographed in stereo. The 12 cm chamber gap (in the direction of the magnetic field vector), the chamber width (33 cm), and a scanning criteria (namely, tracks had to penetrate at least 2.54 cm into the third section in order to be scored) essentially established the geometric acceptance for this experiment, although the helical trajectory of the particles was a contributing influence, as we shall soon see.

The geometry layout that was used is shown in Fig. 3.2.2. It is essentially the same as the one used in the previous example (see Fig. 3.1.1) and the HOWFAR subroutines are identical to one another. Differences are accounted for in the MAIN code in the form of coordinate-axis identification, dimensions, and region-media definitions. The AUSGAB subroutine plays a key role in this problem. As particles reach plane number 3, they are discarded in HOWFAR. Upon entering AUSGAB charged particles with IARG=3 (User Discard) and IR(NP)=4 are further analyzed provided that they are within the lateral (X-Z) extents of the chamber. Having passed this test, trajectories are calculated (with and without magnetic field) and particles that leave the



12-77

3330A5

Fig. 3.2.2 Geometry Layout Used in HOWFAR for Simulation of Streamer Chamber Experiment.

## CHAPTER 3

chamber prior to reaching the 2.54 cm Z-position are eliminated from further analysis. Those that remain are sorted by energy. Details of the calculation are given in the AUSGAB portion of the User Code (UCSPARK) that is given in Appendix UC.

The results are shown in Figs. 3.2.3 through 3.2.5. The experimental points essentially lie between the B=0 and B-1665 G curves obtained by EGS. The agreement is not as good as we had expected, but this can be attributed to the following facts:

1. The magnetic field was assumed to be constant in region 4 and we know that it generally is not. It usually drops off near the edges (perhaps this is why the experimentalists required particles to penetrate 2.54 cm into the chamber where momentum analysis could be properly made).
2. The magnetic field in region 3 was taken to be zero, and this is generally not true either. Fringe field effects could change the acceptance calculation.
3. The experimentalists did not select tracks that were either too dark or too light. The EGS calculation does not make this check ---all tracks are sorted.

The conclusion reached is that the EGS code does a reasonable job in simulating the results obtained by Drickey---although refinements could probably be made in the EGS analysis if additional information were provided by the experimentalists.

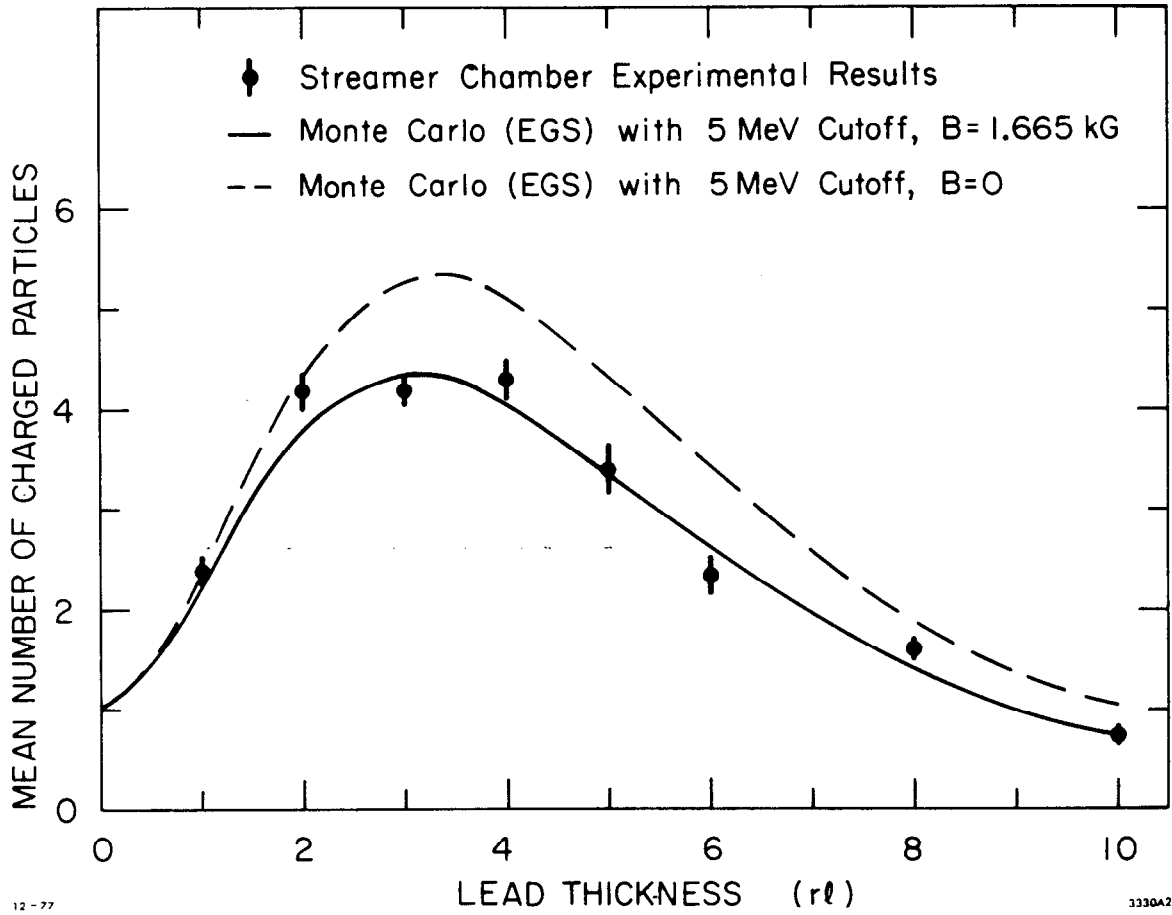


Fig. 3.2.3 Streamer Chamber Experimental and Monte Carlo (with and without magnetic field) Results for Secondaries of 5 MeV or Greater.

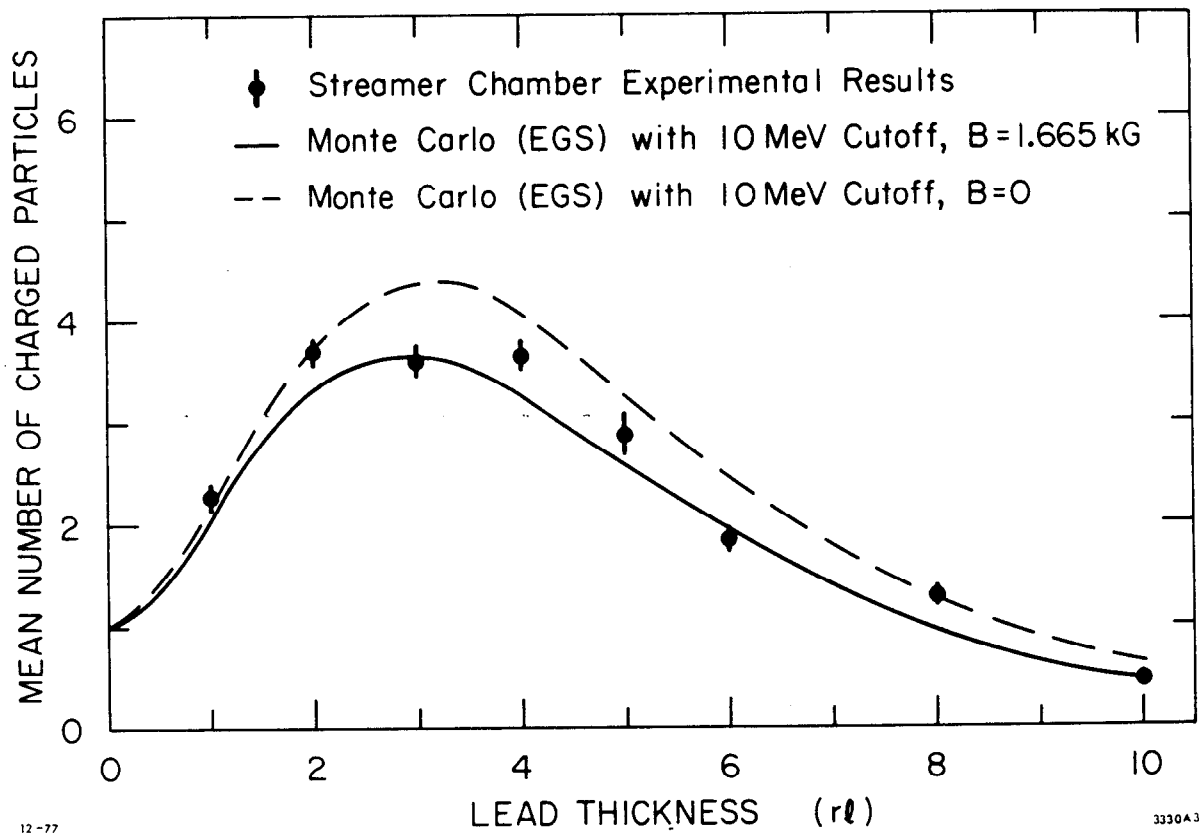


Fig. 3.2.4 Streamer Chamber Experimental and Monte Carlo (with and without magnetic field) Results for Secondaries of 10 MeV or Greater.

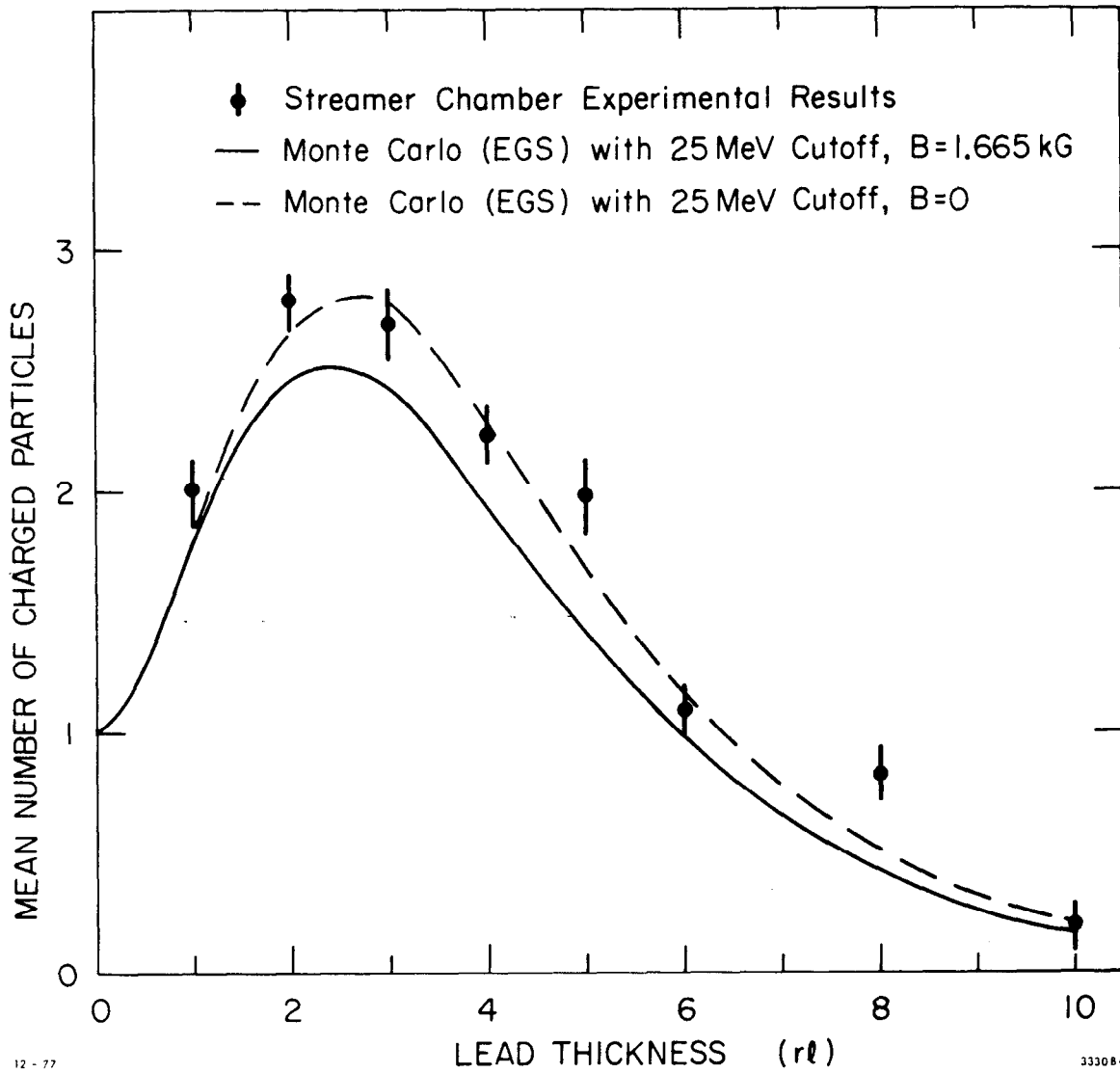


Fig. 3.2.5 Streamer Chamber Experimental and Monte Carlo (with and without magnetic field) Results for Secondaries of 25 MeV or Greater.



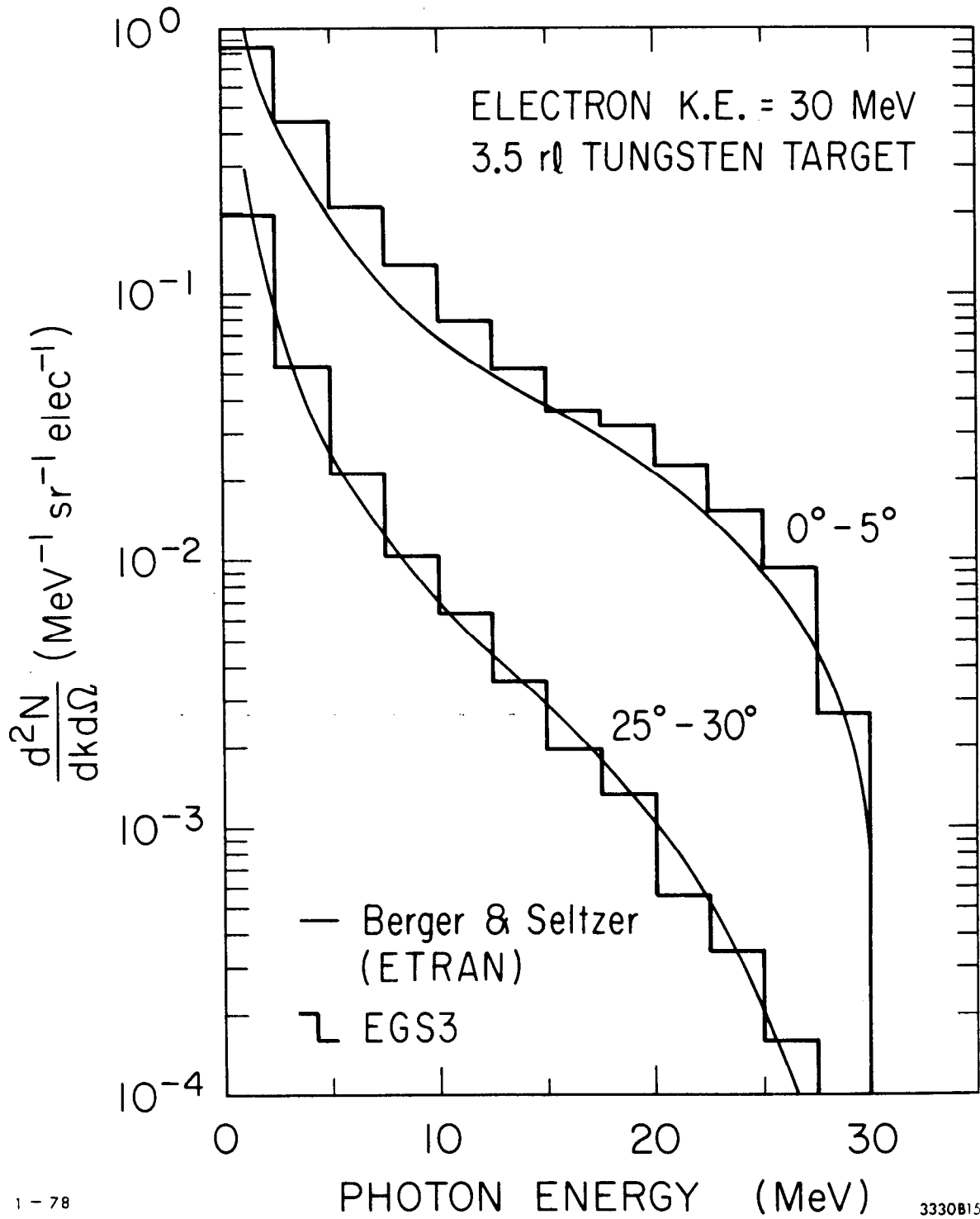
### 3.3 Low Energy Bremsstrahlung from High-Z Targets

#### 3.3.1 Comparison of EGS with ETRAN

Bremsstrahlung energy-angle distribution calculations have been performed using the Monte Carlo electron-photon transport code called ETRAN (Berger and Seltzer 1970). This code was described somewhat in Chapter 1. The results of interest here are for 30 MeV electrons incident upon a thick (3.5 radiation lengths), semi-infinite, tungsten target. We have performed similar calculations using EGS. Photons that emanate from the lead are sorted by energy and by polar angle relative to the direction of the incident beam. When sorting by polar angle, the lateral position of the particle at the target surface was not considered in the analysis.

In Fig. 3.3.1 we plot the bremsstrahlung spectrum on an absolute scale (photons/(MeV-sr-electron)) for two angular bins. The agreement between EGS and ETRAN is quite good at the larger of the two angles. In the forward bin EGS is somewhat higher than ETRAN. In Fig. 3.3.2 we plot the angular distribution of bremsstrahlung, again on an absolute basis (MeV/(sr-electron)), and the agreement between EGS and ETRAN is excellent everywhere, with the possible exception of the angular region past  $90^{\circ}$  where EGS gives results that are 50% lower than ETRAN.

The ETRAN code uses the Goudsmit-Saunderson (1940a,b) multiple scattering formulism as compared to our Bethe-corrected Moliere approach (Bethe 1953, Moliere 1947, 1948). Whether this is the reason for the difference in the backward direction results is subject for further investigation. The slight increase in the  $0^{\circ}$ - $5^{\circ}$  spectrum over that calculated by ETRAN will be discussed in the next section dealing with experimental results. All in all, the two programs give



1 - 78

3330B15

Fig. 3.3.1 Comparison of EGS and ETRAN Monte Carlo Bremsstrahlung Spectrum Results.

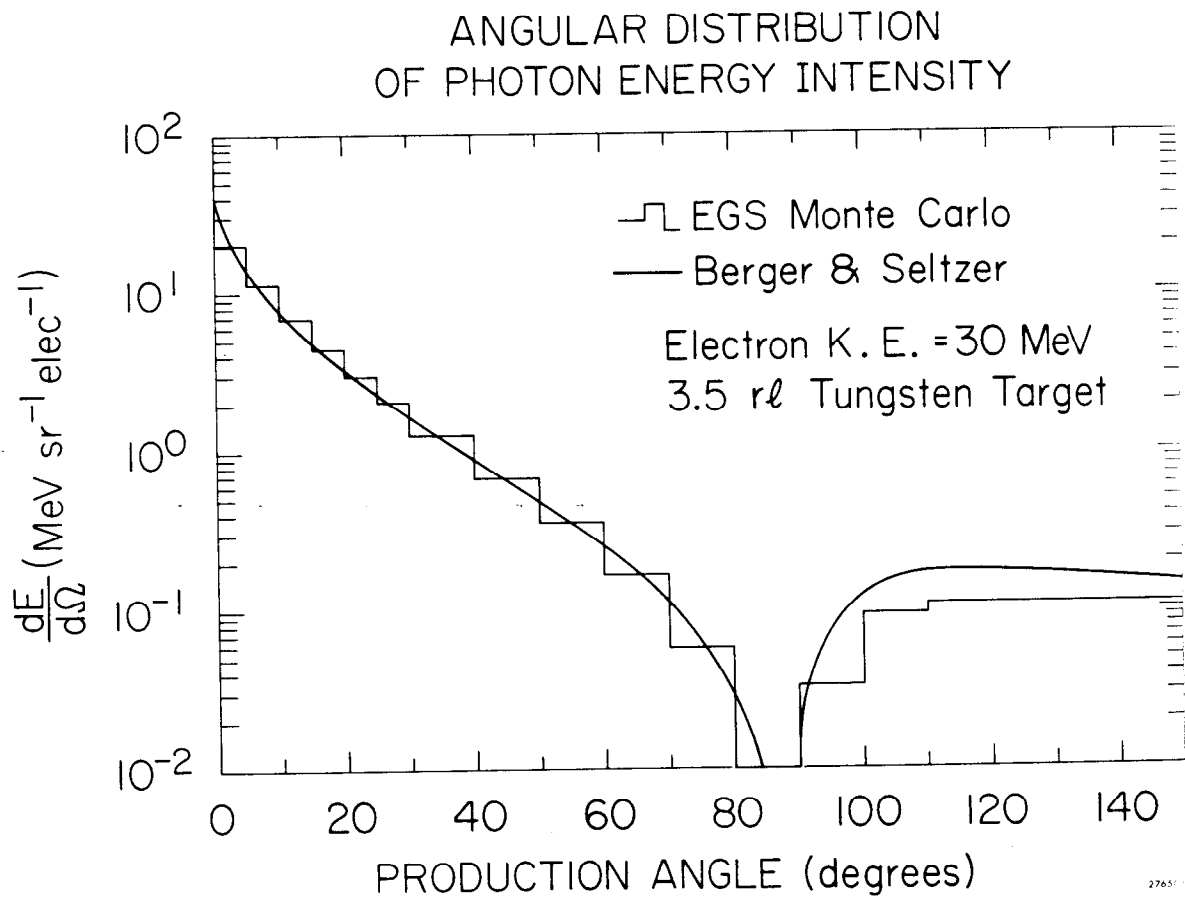


Fig. 3.3.2 Comparison of the Angular Distribution of Bremsstrahlung Results Obtained with EGS and ETRAN.

essentially the same thick-target, high-Z, low energy bremsstrahlung results.

We have not included the User Code (UCB&S) listing in Appendix UC because of its similarity to other examples and because of its mere simplicity.

### 3.3.2 Comparison of EGS with Experimental Results

Although agreement with another Monte Carlo code is comforting, obviously it is desirable to compare with experimental data in this energy realm as well. A recent experiment by Levy (1974) has measured the thick target bremsstrahlung photon spectrum from a 25 MeV electron beam incident on a 6 radiation length lead target. The results are shown in Fig. 3.3.3 along with the EGS spectrum produced for these conditions. The data has been normalized to the EGS spectrum in the high-energy region. The agreement is good except perhaps in the low-energy portion where there seem to be fewer photons calculated than measured. The experimental setup consisted of a well-shielded sodium iodide crystal that looked at the bremsstrahlung after it scattered from a carbon scatterer, the purpose of the latter being two-fold: to shift the energy of the photons by Compton scattering and to reduce the intensity of the bremsstrahlung overall. By using two-body kinematics and the Klein-Nishina cross section, the spectrum emanating from the lead and scattering from the carbon into the angle defined by a pinhole in the detector shield was thus determined. Because Compton scattered electrons could also contribute to the signal processed by the detector, especially to the low-energy portion, we offer this as a possible

## PHOTON SPECTRUM

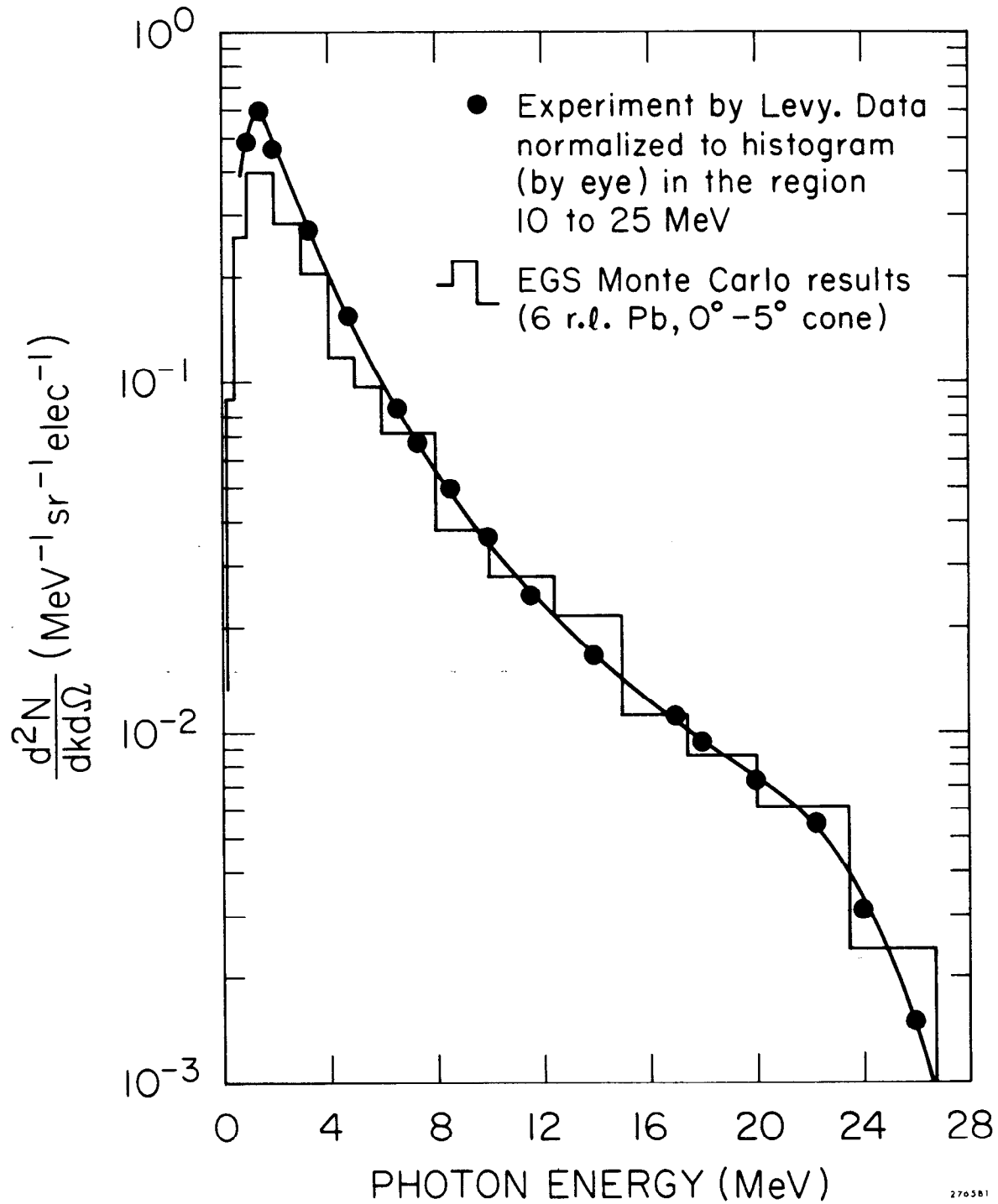
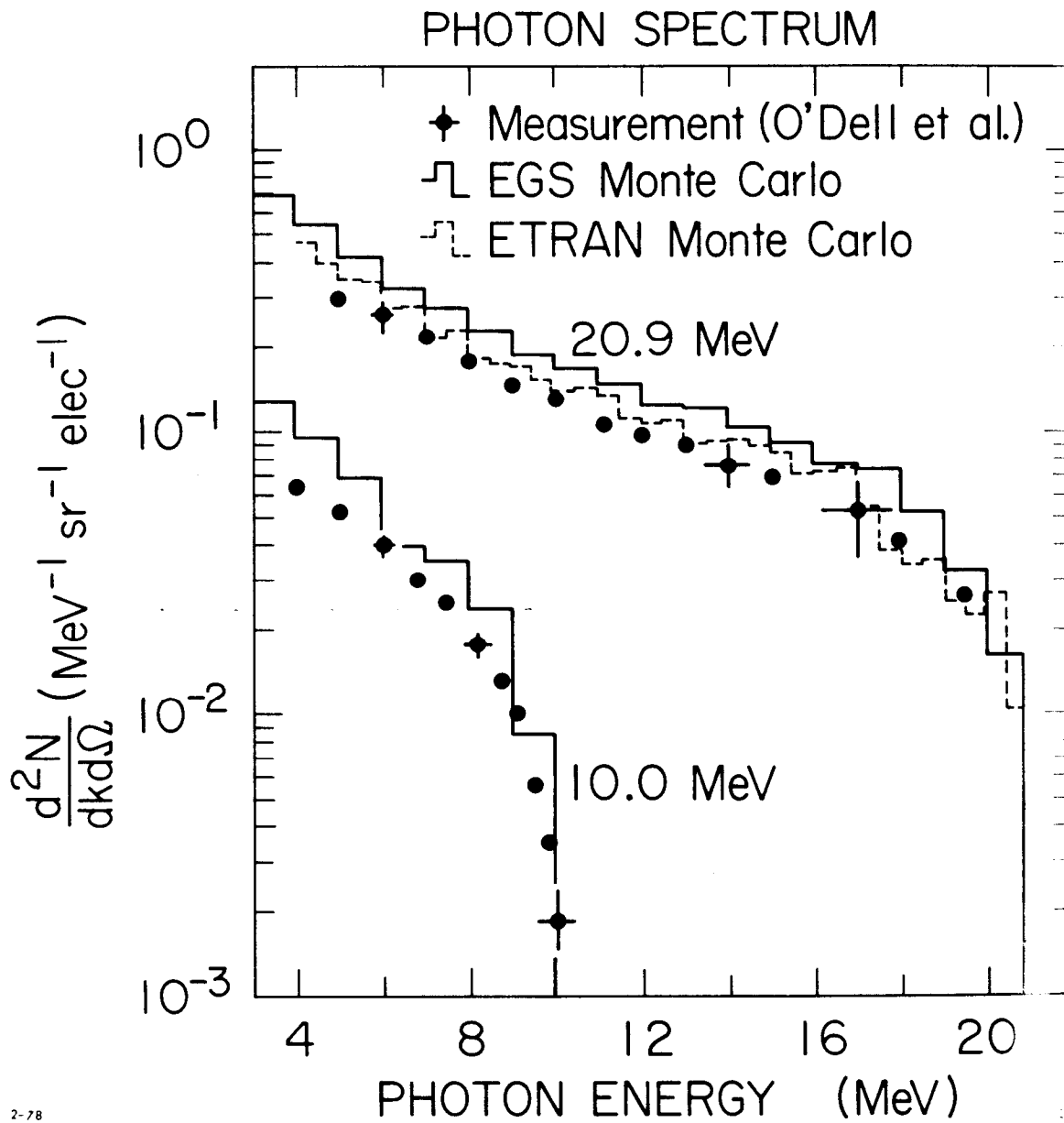


Fig. 3.3.3 Comparison of EGS Monte Carlo Bremsstrahlung Spectrum with Experiment by Levy (1974).

explanation to the slight discrepancy observed in Fig. 3.3.3. In general, the agreement is reasonably good.

A similar comparison, but this time with an absolute photon spectrum measurement (O'Dell 1968), is shown in Fig. 3.3.4. The EGS histograms and experimental points shown are for 20.9 and 10 MeV electron beams incident on a tungsten-gold target ( $0.490$  and  $0.245 \text{ g-cm}^{-2}$ , respectively). Also shown are the Monte Carlo results using ETRAN (Berger and Seltzer 1970). In this comparison one observes that the bremsstrahlung shape is excellent, but the absolute results are about 25% too high in the case of EGS. The experimental error bars are in the range of 10-20%, depending on energy, and the ETRAN results seem to be in better agreement, although still slightly higher for the 20.9 MeV case. As we have seen in a previous example (see Fig. 3.3.1 ( $0^\circ-5^\circ$ )), one observes that EGS is slightly higher (15%) than ETRAN. Berger (1978) suggests that both ETRAN and EGS might be using inaccurate bremsstrahlung cross sections for high-Z media and energies less than 50 MeV, with the ETRAN choice being fortuitously better. This remains to be studied, however, and will not be considered in this version of EGS.

The conclusion reached is that EGS will accurately predict the shape of low-energy bremsstrahlung from high-Z targets, but may overestimate the magnitude by 10-25%. EGS will also accurately predict the angular distribution, with the exception of the backward direction which may be a factor of two too low.



2-78

Fig. 3.3.4 Comparison of EGS and ETRAN Monte Carlo Bremsstrahlung Spectrum with Experiment by O'Dell (1968).

### 3.4 Comparison of EGS with Large, Modularized NaI(Tl) Detector

#### Experiment

The application of large, modularized NaI(Tl) detectors to physics experiments, particularly those involving the gamma-ray spectroscopy of the newly discovered psi particles at high energy electron-positron storage rings, has increased considerably during the last few years. A recent paper by Ford et al (1976) describes an experiment that was performed at SLAC to measure, among other things, the energy resolution of a typical detector array consisting of 19 NaI(Tl) hexagonal modules. Although each module itself cannot be expected to provide good energy resolution at high gamma-ray or electron energies, due to the transverse spread of energy in the secondary electromagnetic shower (i.e., leakage), this problem is overcome in a detector made up of an array of modules, such as that shown in Fig. 3.4.1 (taken from Ford et al (1976)). Each hexagon is encapsulated in a stainless steel container with 20 mil wall thickness. The individual crystals are optically coupled at one end to a 0.5 inch thick glass window, through which the crystal volume is viewed by a 3 inch diameter photomultiplier tube.

The properties of this composite detector were explored by Ford et al using electron beams in the range 0.1 to 4 GeV. The observed response of the modular array of 19 hexagons to electrons incident along the axis of the central module is summarized in Fig. 3.4.2. This figure shows not only the energy resolution obtained when the energies deposited in all 19 crystals are summed, but also those obtained when only the energies in the central 7 modules or in the central module alone are used. Also shown in this figure is the EGS Monte Carlo simulation of





Figure 3.4.1 A photograph of a detector consisting of 19 hexagonal modules (from Ford et al (1976)).

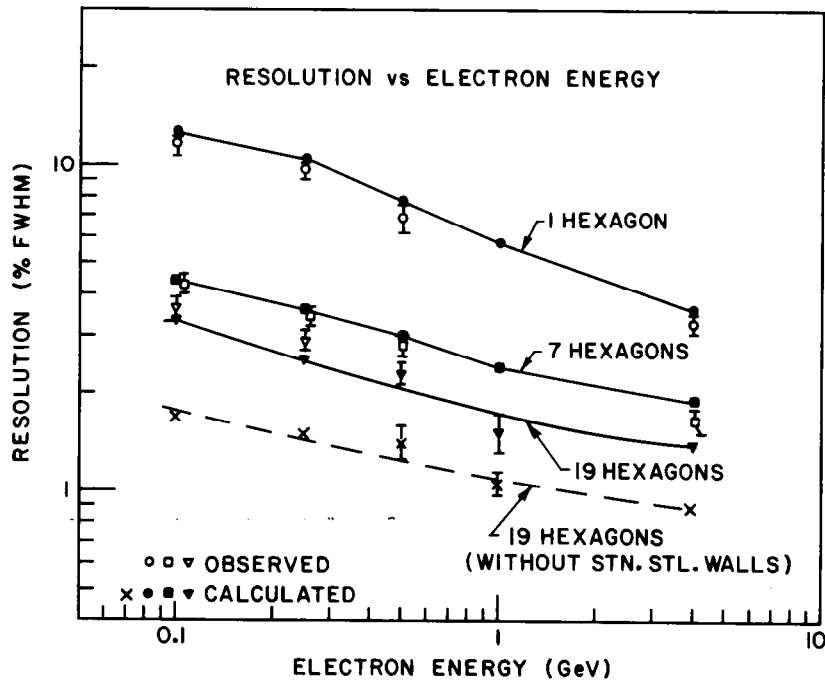


Figure 3.4.2 A comparison between the observed and calculated (EGS) resolution for detectors consisting of 1, 7, or 19 hexagons (taken from Ford et al (1976)).

7/13

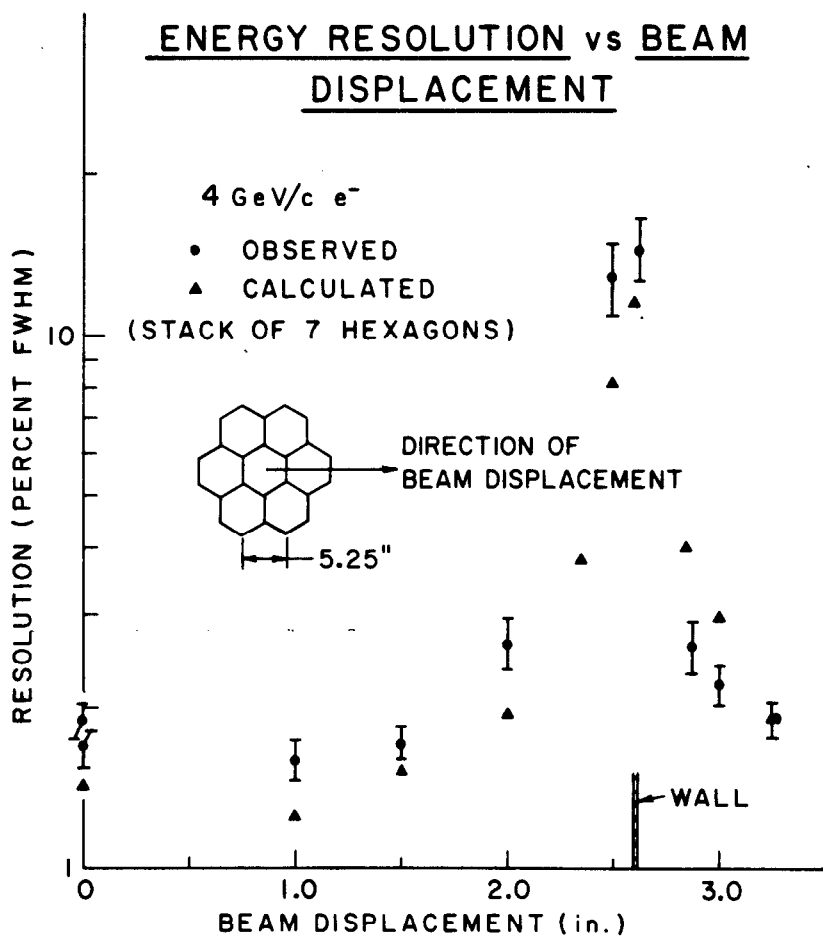


Fig. 3.4.3 A comparison between the observed and calculated (EGS) resolution as a function of beam displacement for a  $1/4$  inch  $\times$   $1/4$  inch electron beam of 4 GeV/c (taken from Ford et al (1976)).

## CHAPTER 3

the electromagnetic shower in this detector. The agreement is observed to be very good. EGS takes into account both the energy leakage fluctuations from the detector volume and fluctuations due to energy absorption in the stainless steel walls surrounding each crystal module.

The 20 mil thick stainless steel walls cause undesirable effects when the trajectory approaches closely or intercepts these walls, as illustrated in Fig. 3.4.3. In this figure the variation of the energy resolution is shown as a function of the displacement of the trajectory from the axis of an array of 7 modules. No significant loss in the resolution is experienced until the trajectory approaches within about 0.5 inch of the nearest wall. It can be seen that the agreement between measurement and calculation is very good and gives confidence in the ability of the EGS Code System to predict the response of the detector for any incident trajectory.

In conclusion, the resolution provided by assemblies of these hexagonal NaI(Tl) crystals is well-accounted for by the EGS simulation of the electromagnetic cascade in the detector.

### 3.5 Comparison of EGS with Longitudinal and Radial Shower Experiment at 1 GeV in Water and Aluminum

An experiment was performed by Crannell et al (1969) to measure the three-dimensional distribution of energy deposition for 1 GeV showers in water and aluminum. The water target consisted of a steel tank containing 8000 liters of distilled water. The incident beam entered the water through a 0.13 mm aluminum window centered on the square end of the tank ( $122 \times 122 \times 460 \text{ cm}^3$ ). The aluminum target, on

## CHAPTER 3

the other hand, consisted of plates varying in thickness from 0.64 to 2.5 cm. The plates were pressed together to simulate a solid target (61 x 61 x 180 cm<sup>3</sup>). Details concerning the detectors used and other related items are in the publication and will not be discussed here. Differential, as well as integral, energy block diagram data obtained from this experiment afford a good opportunity to test the EGS Code System---this is particularly of interest to us for two reasons:

1. A reasonably good comparison was made by Alsmiller and Moran (1969), who used the Zerby and Moran (1962a,b, 1963) Monte Carlo code mentioned in Chapter 1.
2. Crannell indicates in the paper that the Nagel code does not give radial distributions in agreement with the experiment.

Whether or not the Nagel code (SHOWER1---see Chapter 1) is correct will not be the subject of our discussion here. However, since Version 3 descends from the Nagel code, we feel obligated to attempt to simulate the experiment performed and published by Crannell.

The User Code for this calculation is actually quite simple and gives us a chance to make use of two more subprograms that may turn out to be of use to EGS-users. The first routine is called SUBROUTINE CYLNDR and is called by HOWFAR whenever cylindrical (shell) geometries are employed. The code is listed as part of the User Code (UCH20&AL) and is given in Appendix UC.

The second routine is SUBROUTINE ECONSV, which is a mnemonic for energy conservation. Whenever Monte Carlo shower calculations are performed all of the input energy should be accounted for. ECONSV

## CHAPTER 3

provides a convenient way to implement this into most User Codes, as illustrated in UCH20&AL. Subroutine ECONSV sorts the energy-deposited according to

i.) particle type (IQ = -1, 0, + 1),

ii.) region (IR = 1 to maximum-IR),

and

iii.) reason (IARG = 0, 1, 2, 3, or 4),

with appropriate "column and row" totals plus a grand total (normalized to fraction).

A comparison of the Crannell data with EGS is given in Figs. 3.5.1 and 3.5.2 for water and aluminum, respectively. The agreement is extremely good everywhere for the water case, and reasonably good for the aluminum experiment. The slight discrepancy at large radii in the aluminum comparison might be accounted for by the fact that the detector used,  $\text{CaF}_2(\text{Eu})$ , was not as "well-matched" with the absorber as in the water experiment where an anthracene detector was used. Crannell goes into considerable discussion on this in the paper, and the reader is referred to this reference.

Alsmiller and Moran (1969) found a slight disagreement with their comparison, although all-in-all, the differences were truly not too significant. In Fig. 3.5.3 we show the comparison of EGS with Alsmiller and Moran, and with the experiment for the first radial interval data in water. Alsmiller and Moran attribute their difference at small depths to the fact that the density effect correction was not included in the electron stopping power formulation used in their code. They state that the correction would reduce the energy deposited at small

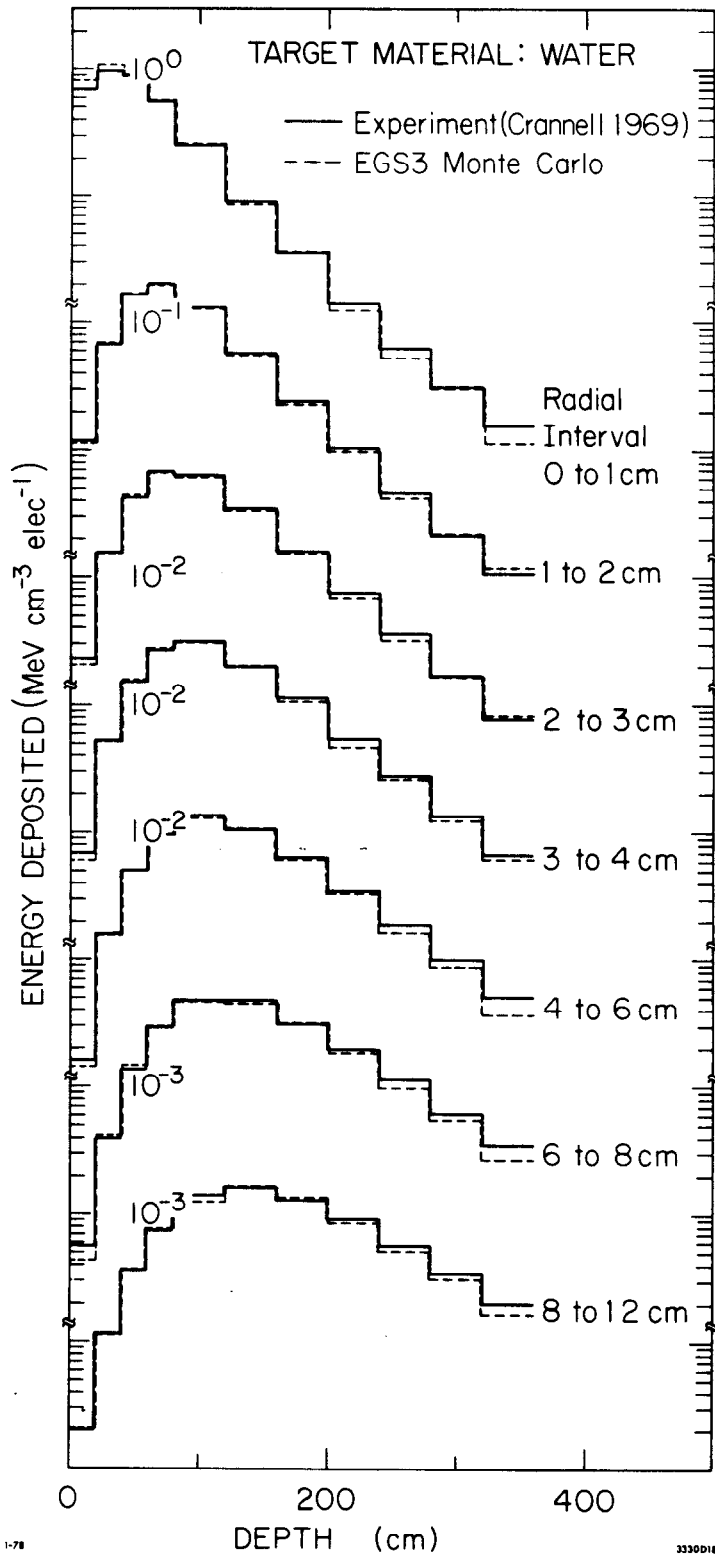


Fig. 3.5.1 Comparison of EGS with Crannell (1969) Shower Experiment in Water.

CHAPTER 3

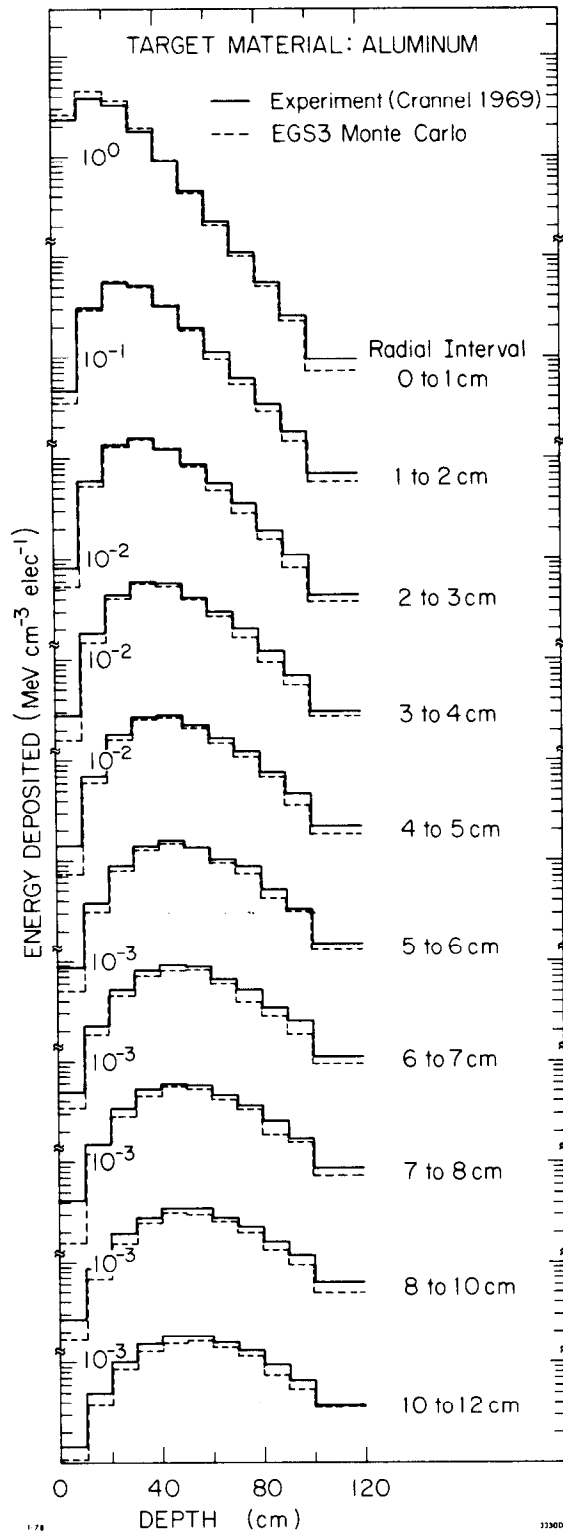


Fig. 3.5.2 Comparison of EGS with Cramwell (1969) Shower Experiment in Aluminum.



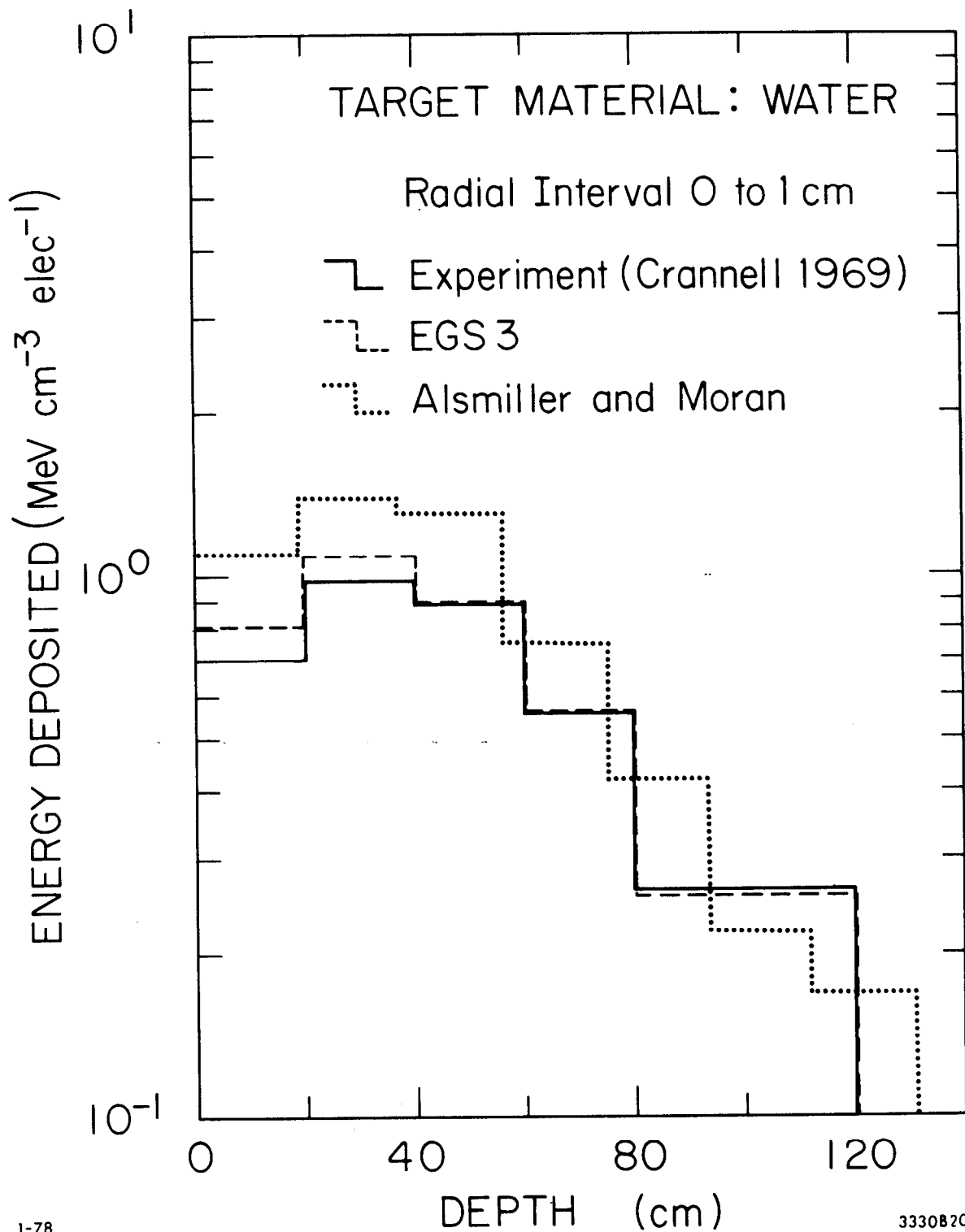


Fig. 3.5.3 Comparison of EGS with Monte Carlo Calculation by Alsmiller and Moran (1969) and with the Crannell (1969) Water Experiment for the First Radial Interval.

depths and radii and result in the effect seen in Fig. 3.5.3. We concur with this analysis. The EGS code accounts for the density effect in the correct manner, and the fact that we get better agreement with Crannell in this figure supports the argument of Alsmiller and Moran.

Before concluding this section, the role of the maximum step size (TMXS) should be discussed, particularly since the Crannell water shower experiment provides a good example for demonstration. The reader is referred to the last few pages of Section 2.14 for a somewhat detailed discussion of path-length restrictions in general. What we wish to show here, however, is that because of the small radial bins employed in the water-shower experiment ( $\sim 0.03$  r.l.), the maximum step size must be limited. If not, systematic discrepancies will occur as a result of neglecting the lateral deflection of the charge particle as it multiple scatters along its track.

Table 3.5.1 compares EGS2 and EGS3 with the Crannell data for the center radial bin (0 to 1 cm). Both EGS2 and EGS3(a) are alike in that (see Section 2.14)

$$\text{TMXS} \leq 200(t_{\text{eff}})_0 \approx 0.015 \text{ r.l. for water.}$$

By removing this restriction, as in EGS3(b), TMXS is only limited by the Bethe restriction (see Section 2.14) and the resultant step sizes can be correspondingly larger (by a factor of 10, say). The net result is that the calculated energy deposition is systematically higher than that of the experiment at longitudinal depths out to a few hundred cm. At greater depths the effect is somewhat less noticeable because of statistical accuracy. In contrast, restricting the step size results

TABLE 3.5.1

Depth Bin (cm)	Experiment (Crannell 1969)	EGS2	EGS3(a)	EGS3(b)
0 - 20	0.702	0.800 (12%)	0.802 (12%)	0.826 (15%)
20 - 40	0.976	1.11 (12%)	1.08 (10%)	1.19 (18%)
40 - 60	0.886	0.948 (7%)	0.923 (4%)	1.06 (16%)
60 - 80	0.562	0.567 (< 1%)	0.566 (< 1%)	0.680 (17%)
80 - 120	0.264	0.261 (1%)	0.253 (4%)	0.309 (14%)
120 - 160	0.0923	0.0930 (< 1%)	0.0891 (3%)	0.111 (17%)
160 - 200	0.0358	0.0341 (5%)	0.0356 (< 1%)	0.0385 (7%)
200 - 240	0.0143	0.0162 (12%)	0.0123 (14%)	0.0154 (7%)
240 - 280	6.37-3	6.72 x 10 <sup>-3</sup> (5%)	5.14 x 10 <sup>-3</sup> (19%)	8.04 x 10 <sup>-3</sup> (21%)
280 - 320	3.18-3	2.71 x 10 <sup>-3</sup> (15%)	3.06 x 10 <sup>-3</sup> (4%)	2.87 x 10 <sup>-3</sup> (10%)
320 - 360	1.59-3	6.06 x 10 <sup>-4</sup> (62%)	1.13 x 10 <sup>-3</sup> (29%)	1.00 x 10 <sup>-3</sup> (37%)
	<u>Time/Case</u>	<u>1.10sec/case</u>	<u>1.03sec/case</u>	<u>0.69sec/case</u>

See text for explanation of table.

Percentages were obtained from the experiment and respective EGS numbers using  $\% = 100 \left( 1 - \frac{\text{smaller no.}}{\text{larger no.}} \right)$

## CHAPTER 3

in a slower running code, as indicated in Table 3.5.1. Additional discrepancies show up in other radial bins as well, but will not be described here.

We have selected the above TMXS restriction as the default in EGS3 based on the present good agreement with the Crannell data, and because it was the one used in EGS2. As a point of fact, however, there could be situations that dictate choosing an even smaller TMXS limitation. This can be most easily accomplished by introducing the proper macro in the User Code (see Section 4.4.1d). On the other hand, when circumstances require a faster running code with spatial resolution not being an important consideration, a macro could be used to raise the TMXS limitation to larger values.

We conclude this section by stating that EGS3 accurately predicts longitudinal and radial cascades in low-Z elements, at least in the 1 GeV energy range.

### 3.6 Track Length Calculations

Track length calculations are most easily done with EGS3 by summing the variable TVSTEP\* in subroutine AUSGAB each time a simple transport (IARG=0) takes place. In the case of photon track lengths the calculation is simplified because the photon does not lose energy during transport. Charged particles, on the other hand lose energy along the entire TVSTEP, and the method of scoring is correspondingly more complicated. In the following two sub-sections differential track lengths are obtained

---

\*In EGS2, use VSTEP.

using EGS and are compared with similar results using the Zerby and Moran shower code.

### 3.6.1 Differential Photon Track Length

Alsmiller (1969) has used the Zerby and Moran (1962a,b, 1963) code in order to calculate the differential photon track length for the specific case of 18 GeV electrons incident on a cylindrical copper target having a radius of 11.5 cm and a thickness of 24.5 cm. The results are compared with similar data obtained using EGS3 as shown in Fig. 3.6.1 where agreement between the codes is quite apparent. Also shown in the figure is a solid line corresponding to the track length formula of Clement (1963). The User Code for this calculation is not given here because of its simplicity and similarity to previous ones.

### 3.6.2 Differential Electron Track Length

In order to properly score the charged particle track length in subroutine AUSGAB, account must be taken of the continuous energy loss along the track. By determining the energy of the particle at the beginning and the end of the track ( $E(NP)$  and  $E(NP)-EDEP$ , respectively), the total track length ( $TVSTEP$ )\* can be fractionated, sorted, and summed in histogram bins corresponding to energy. The particular algorithm that was used in the present set of calculations is given below.

---

\* In EGS2, use VSTEP.

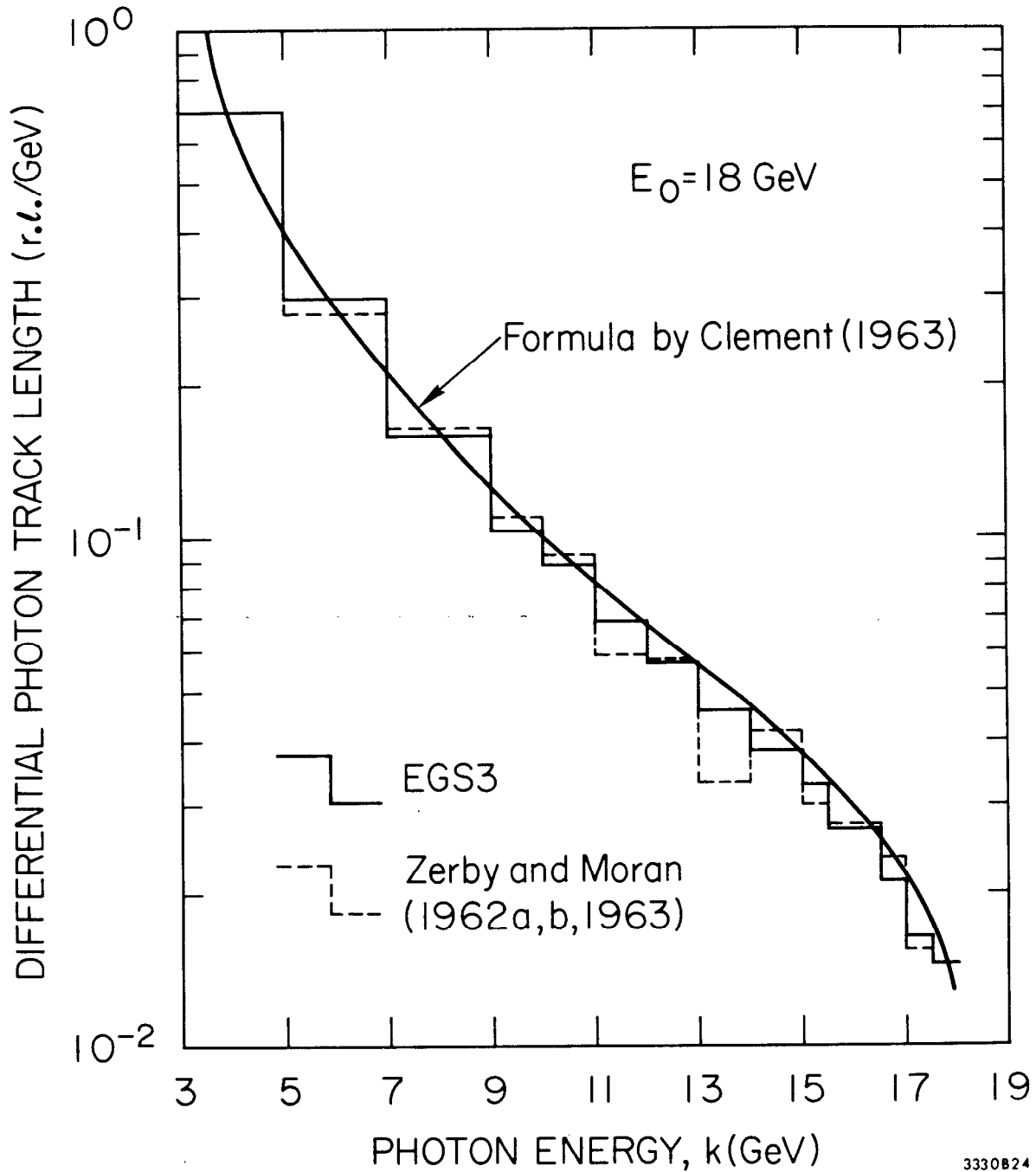


Fig. 3.6.1 Differential Photon Track Length — Comparison of EGS with Zerby and Moran (1962a,b, 1963) Monte Carlo Results.

## CHAPTER 3

```

SUBROUTINE AUSGAB(IARG);
COMMON/EPCONT,STACK/;
COMMON/BINS/EBIN($MXBIN), TLSUM($MXBIN),NBINS:
.
.
.
.
IF (IARG.EQ.0.AND.IQ(NP).NE.0)<
    EHIGH=E(NP);
    EL0W=E(NP)-EDEP;
    DO I=1,NBINS<
        EH=AMIN1(EHIGH,EBIN(I+1));
        EL=AMAX1(EL0W,EBIN(I));
        DELE=EH-EL;
        IF(DELE.GT.0.0)<
            TL=DELE*TVSTEP/EDEP;
            TLSUM(I)=TLSUM(I)+TL;
        >
    >
    >
    >
RETURN;
END;

```

Fig. 3.6.2 compares the charged particle track length, as calculated by EGS3, with that of Zerby and Moran (1962a, 1963) for three incident electron energies (50, 200, 700 MeV) and for an infinite copper medium. EGS3 is seen to agree with Zerby and Moran.

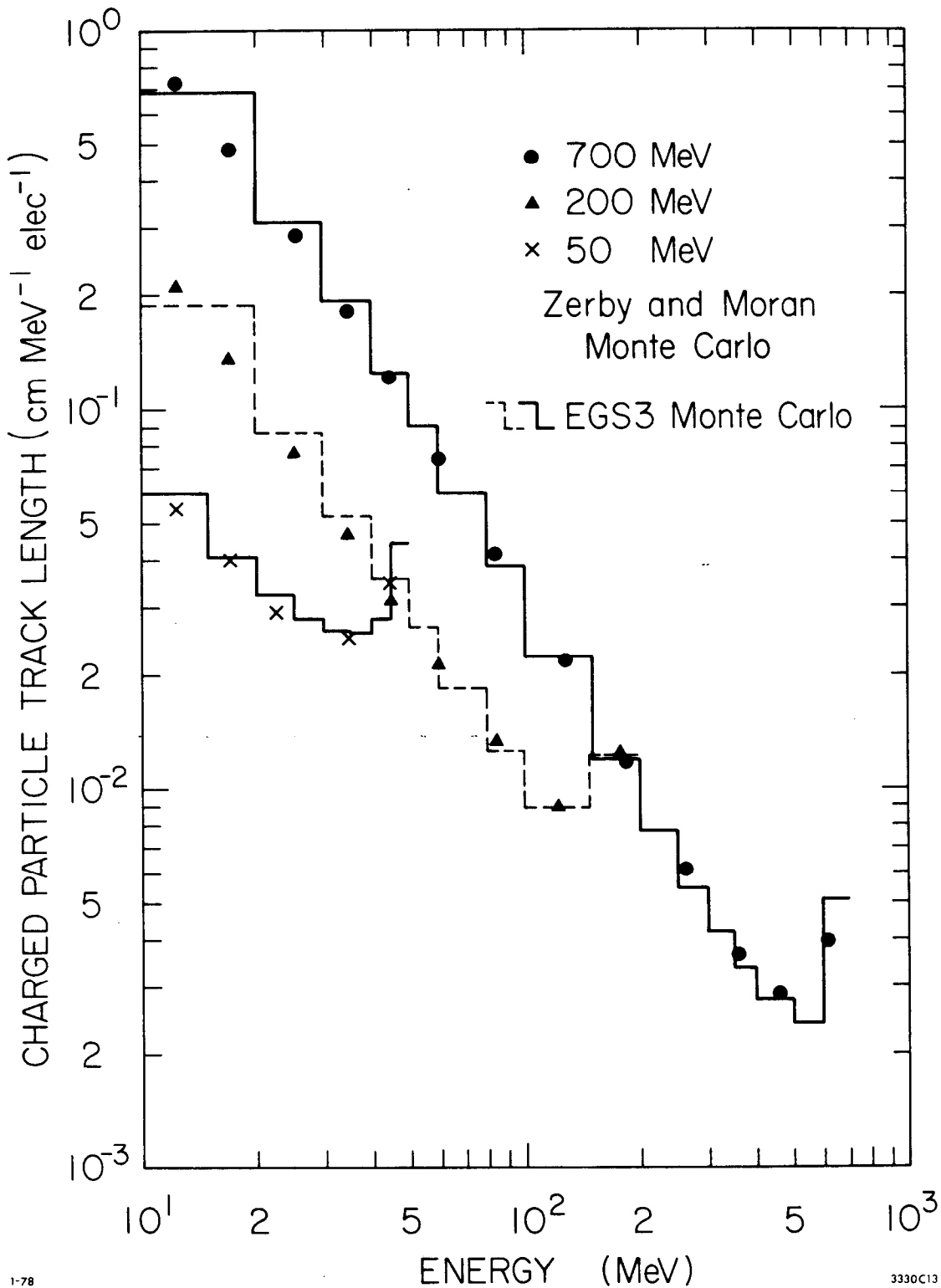


Fig. 3.6.2 Differential Electron Track Length — Comparison of EGS with Zerby and Moran (1962a, 1963) Monte Carlo Results.



### 3.7 Multiple Scattering of 15.7 MeV Electrons in Thin Foils

An experiment that is considered by many to be a benchmark for testing electron multiple scattering at low energies (15.7 MeV) was reported by Hanson et al (1951), who found excellent agreement with the theory of Moliere. Details of the experiment are left to the reader. In Figs. 3.7.1 and 2 we present calculational results obtained with gold foil thicknesses of 18.66 and 37.28  $\text{mg}\text{-cm}^{-2}$ , respectively. In addition to the experimental results (solid line), we have plotted both EGS2 and EGS3 histograms. In both figures, EGS3 is observed to agree with experiment in a smooth manner over the entire angular range. EGS2, on the other hand, calculates less scattering after  $12^\circ$  and is somewhat erratic at the tails. This is not caused by statistical variations, but is due to the fact that the multiple scattering reduced angle is sampled from a discrete distribution in EGS2, as mentioned in Section 1.1. The sampling of the reduced angle, in the case of EGS3, is done in a continuous fashion as described in Section 2.14, and the result is quite apparent in the figures.

In conclusion, EGS3 will accurately calculate low-energy electron scattering from thin foils.

CHAPTER 3

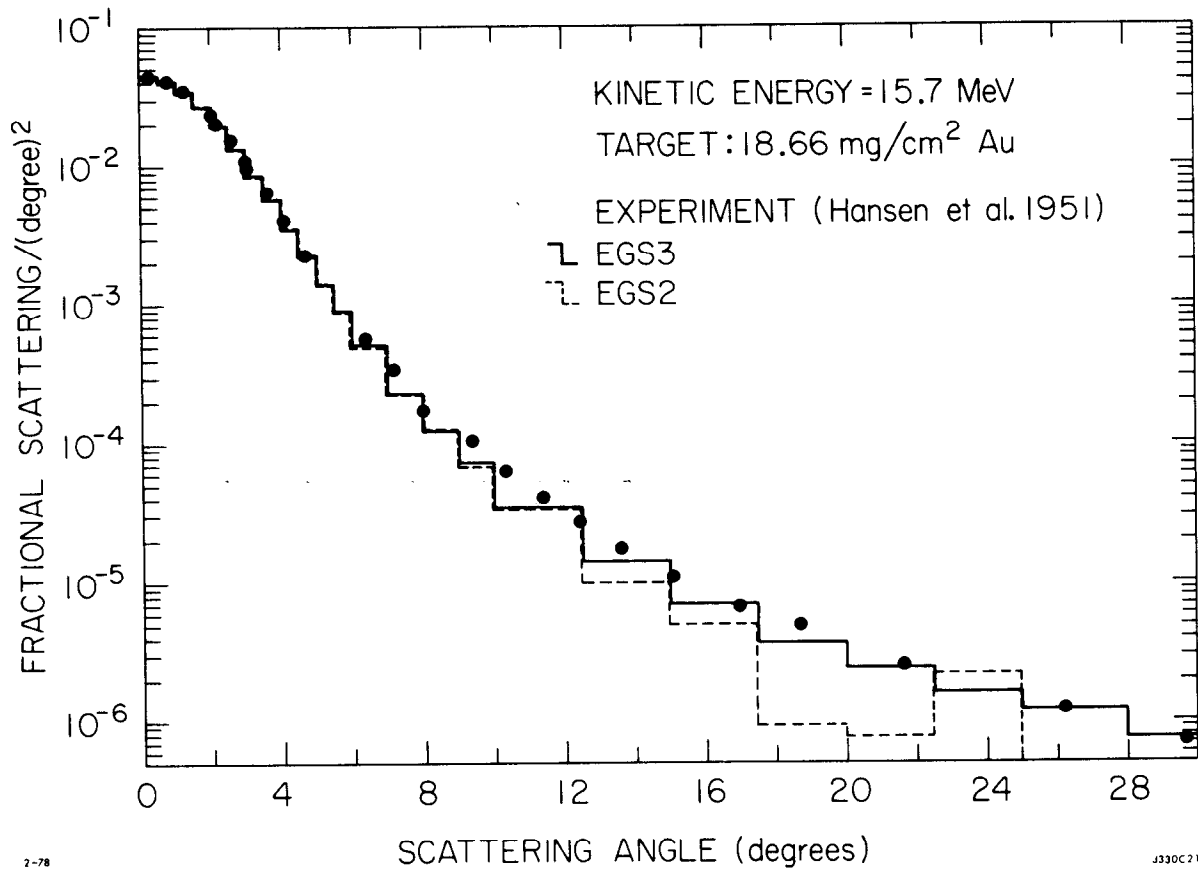


Fig. 3.7.1 Multiple Scattering of 15.7 MeV Electrons in a Gold Foil (18.66 mg/cm<sup>2</sup>) — Comparison of EGS Monte Carlo (Versions 2 and 3) with Experiment by Hanson (1951).

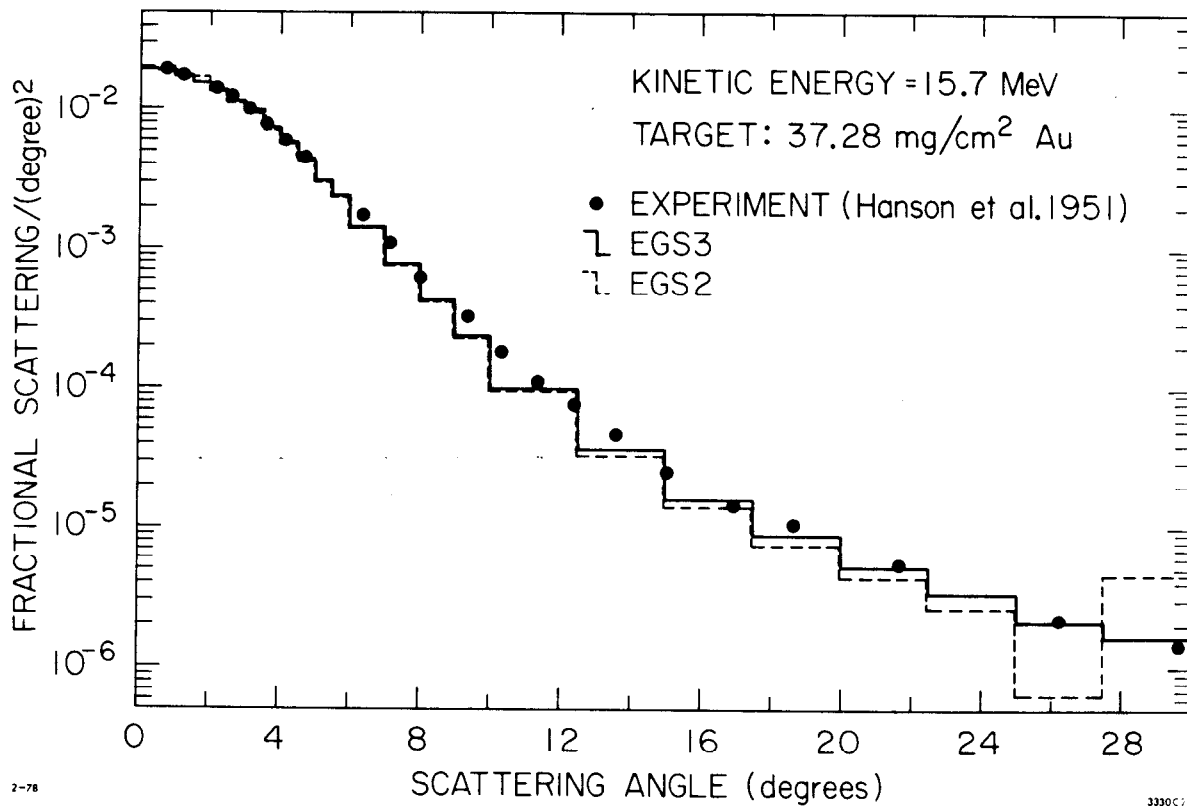


Fig. 3.7.2 Multiple Scattering of 15.7 MeV Electrons in a Gold Foil (37.28 mg/cm<sup>2</sup>) — Comparison of EGS Monte Carlo (Version 2 and 3) with Experiment by Hanson (1951).

3.8 Concluding Remarks

In this chapter we have attempted to demonstrate the validity, as well as the capability, of the EGS Code System (Version 3) to accurately simulate electromagnetic cascade showers in media. We believe that the examples presented here do just that. Additional input from EGS-users at SLAC and elsewhere also confirm this. The various User Code examples, in conjunction with the EGS User Manual (see Chapter 4), should be of benefit to those who wish to perform similar calculations.

## CHAPTER 4

### 4. USER MANUAL FOR EGS3 \*

#### 4.1 Introduction

Starting with Version 2, the EGS Code System has been written in an extended FORTRAN language known as MORTRAN \*\*. The reasons for converting to MORTRAN include the following:

- i.) Flexibility of user interaction with EGS by means of the MORTRAN input unit number stack and macro facility.
- ii.) The possibility of using MORTRAN macros for program parameters which might need changing (e.g., dimensions for various arrays).
- iii.) The possibility of using macros to define the method used to approximate functions---the main code of EGS then becomes independent of the approximate method used. For example, to change from piecewise linear fits to piecewise quadratic fits only requires a change in the definition of a few macros, and does not require any changes in the main code.
- iv.) In the past, with the form of output and geometry fixed within EGS, anyone who wanted to make some non-standard use of EGS had to get "their fingers" in the inner workings of the code. Often they did not want the form of output already provided, so they either had to take out some of the code, at the peril of throwing out too much, or else keep the "dead wood." All of this tended to introduce bugs into the code---and bugs are not easy to spot when looking at the output of a Monte Carlo program!

---

\* This manual, which applies to EGS2 as well, will be kept up-to-date as a WYLBUR data set in the EGS\$RP account at the Stanford Linear Accelerator Center.

\*\* To be more specific, we are presently using MORTRAN2. The reader is encourage to study the article by Cook and Shustek (1975) on the MORTRAN2 language. An article by Zahn (1975) is also useful.

## CHAPTER 4

For these reasons it was decided to remove all old output and geometry checking, and to make well defined spots in EGS where interaction with the user is allowed. The use of macros allows EGS to be flexible in various ways without danger of having the internal logic of EGS inadvertently changed.

In addition, MORTRAN is a structured programming language. It is implemented by means of a set of macros which are used by a macro processor to translate the language into FORTRAN. The resultant FORTRAN is then run like any other FORTRAN code. Because the language is structured, the codes that are written tend to be more logical in appearance and much easier to read---especially to an outsider, or the author himself at a later time. Another feature is that one can switch back and forth between MORTRAN and FORTRAN with ease by means of the %M and %F control statements.

Although there might be some resistance by users of EGS to learn another language, we would like to point out two facts:

- 1.) The MORTRAN language (excluding macros) is trivial to learn by those who program in FORTRAN.
- 2.) EGS can be set-up and run by writing entirely in FORTRAN should the user so desire.

We would encourage EGS users not to do the latter, however, for this would truly defeat the real purpose for using MORTRAN---namely, the macro facility. Admittedly, MORTRAN macros can be difficult to read and understand, depending on their complexity. In most cases, however, the user should not have to understand the more complicated ones, and should be able to master the few that he will use with his particular problem.

Before describing the ways to use EGS to create electromagnetic cascade showers, we would like to state that this User Manual is designed with the SLAC physics and engineering community in mind. In order to document the EGS Code System for the SLAC user, we have sacrificed some generality in description. Even without the present writeup, however, several copies of EGS have gone out to public use at other facilities and, to our best knowledge, have been used quite successfully. We feel, therefore, that even lacking generality, this manual will be of use outside of SLAC.

## CHAPTER 4

Although written with Version 3 of the EGS Code System in mind, this manual can be used in conjunction with EGS2 as well. Differences between the two versions have been noted in the text.

### 4.2 General Description of Implementation

As we have described in Chapter 2 and demonstrated by means of examples in Chapter 3, the EGS code itself consists of two User-Callable subroutines, HATCH and SHOWER, which in turn call the other subroutines in the EGS code, some of which call two User-Written subroutines, HOWFAR and AUSGAB. This is best illustrated with the aid of Fig. 4.2.1, which we have borrowed from Chapter 2.

To use EGS the user must write a "User Code." This consists of a MAIN program and the subroutines HOWFAR and AUSGAB, the latter two determining the geometry and output (scoring), respectively. Additional auxiliary subprograms might be included in the User Code to facilitate matters. The user can communicate with EGS by means of various COMMON variables. Usually MAIN will perform any initialization needed for the geometry routine, HOWFAR, and sets the values of certain EGS COMMON variables which specify such things as names of the media to be used, the desired cutoff energies, and the distance unit to be used (e.g., inches, centimeters, radiation lengths, etc.). MAIN then calls the HATCH subroutine which "hatches EGS" by doing necessary once-only initialization and by reading material data for the media from a data set that had been previously created by PEGS. This initialization completed, MAIN may then call SHOWER when desired. Each call to SHOWER results in a generation of one history (often referred to as a "case"). The arguments to SHOWER specify the parameters of the incident particle initiating the cascade.

In addition, macro definitions can be included in MAIN in order to control or over-ride various functions in EGS as well as in the User-Written codes.

A list of EGS subroutines and their functions is given in Section 4.8.

CHAPTER 4

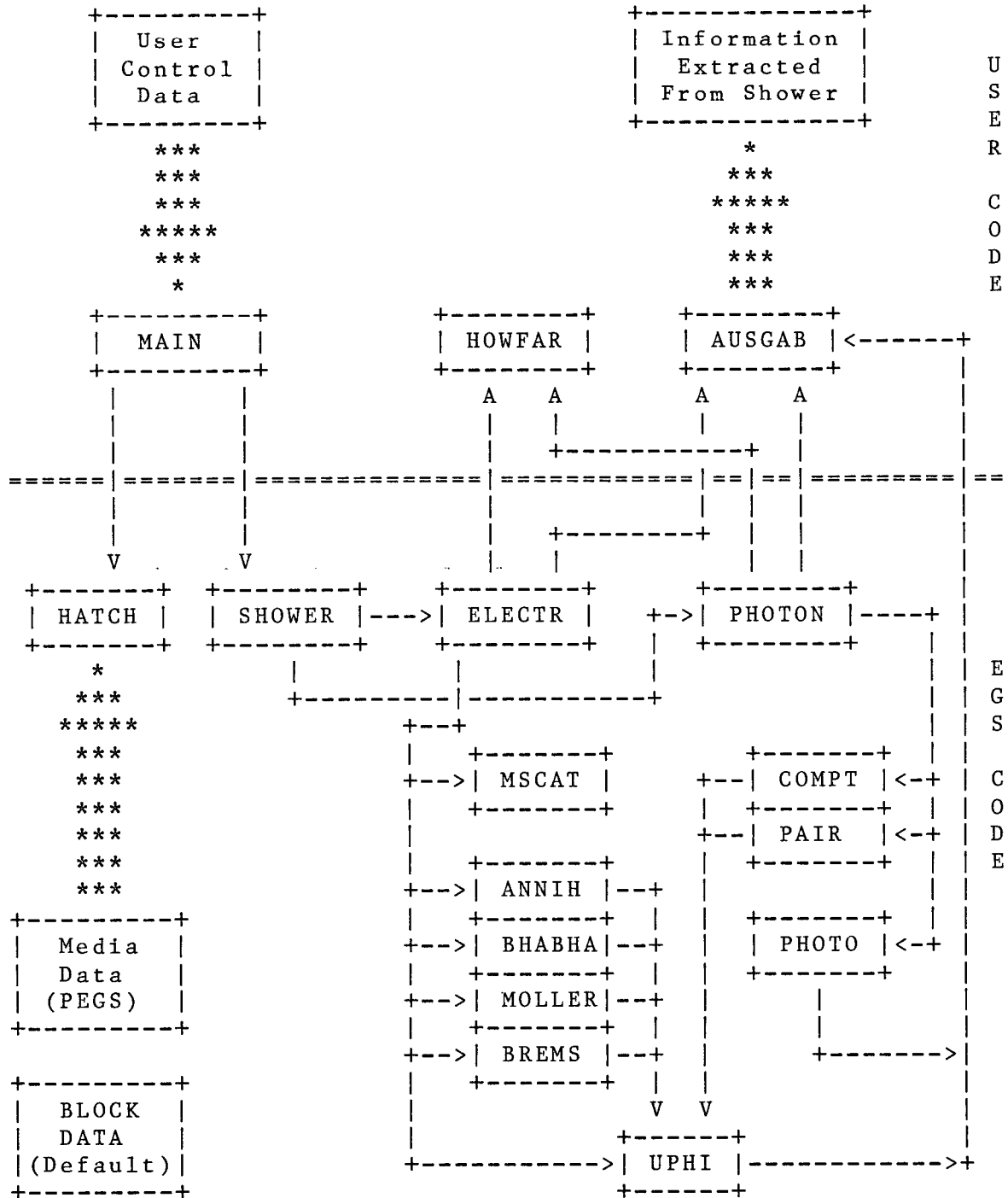


Fig. 4.2.1 Flow Control with User Using EGS



## CHAPTER 4

In summary, the user communicates with EGS by means of:

- 1.) Subroutines HATCH --- to establish media data  
SHOWER --- to initiate the cascade  
HOWFAR --- to specify the geometry  
AUSGAB --- to score and output the  
          results
- 2.) COMMON blocks --- by changing values of variables
- 3.) Macro definitions --- re-definition of pre-defined  
          features.

To reiterate, we shall refer to the MAIN/HOWFAR/AUSGAB combination (plus auxiliary subprograms and macros) as the User Code. The following sections discuss these things in greater detail.

### 4.3 The COMMON Blocks

Listed here are the names of the COMMON blocks relevant to the user (and relevant variables contained in them) with a brief description of their functions. Their usage will be discussed in more detail in subsequent sections.

Table 4.3.1

COMMON BLOCK	VARIABLE	FUNCTION
BOUNDS	ECUT	Array of regions' charged particle cutoff energies in MeV.
	PCUT	Array of regions' photon cutoff energies in MeV.
	VACDST	Distance to transport in vacuum (default=1.E8).

CHAPTER 4

Table 4.3.1  
(continued)

COMMON BLOCK	VARIABLE	FUNCTION
EPCONT	EDEP	Energy deposited in MeV (Double Precision).
	TUSTEP	Total (curved) step length requested.
	USTEP	User (straight line) step length requested and granted.
	TVSTEP	Actual total (curved) step length to be transported.
	VSTEP	Actual (straight line) step length to be transported.
	IDISC	User discard request flag. IDISC=1 means user requests immediate discard, IDISC=-1 means user requests discard after completion of transport, and IDISC=0 (default) means no user discard requested.
	IROL	Index of previous region.
	IRNEW	Index of new region.
	EOLD	Charged particle (total) energy at beginning of step in MeV.
	ENEW	Charged particle (total) energy at end of step in MeV.
	BETA	Beta for present particle.
	BETA2	Beta squared for present particle.
	IAUSFL	Array of flags for turning-on various calls to AUSGAB.

CHAPTER 4

Table 4.3.1  
(continued)

COMMON BLOCK	VARIABLE	FUNCTION
EPCONT (continued)	EKE	Kinetic energy of charged particle in MeV.
	ELKE	Natural logarithm of EKE.
	GLE	Natural logarithm of photon energy.
	TSCAT	See Eq. 2.14.82.
MEDIA	NMED	Number of media being used (default=1).
	MEDIA	Array containing names of media (default is NaI).
	RLC	Array containing radiation lengths of the media in cm.
	RLDU	Array containing radiation lengths of the media in distance units established by DUNIT.
	RHO	Array containing density of the media in g/cu.cm.
MISC	MED	Array containing medium index for each region.
	DUNIT	The distance unit to be used. DUNIT=1 (default) establishes all distances in cm; whereas, DUNIT=2.54 establishes all distances in inches.
	KMPI	FORTTRAN unit number from which to read material data (default=12).
	KMPO	FORTTRAN unit number on which to "echo" (e.g., print out) material data (default=8).

## CHAPTER 4

Table 4.3.1  
(continued)

COMMON BLOCK	VARIABLE	FUNCTION
MISC (continued)	RHOR	Array containing the density for each region (g/cu.cm.). If this is different than the default density for the medium for that region, the cross sections and stopping powers are scaled appropriately. The user may also let the density vary continuously by means of the subroutine RHASET. CALL RHASET(RHOL) should return the local density, RHOL, at the position of the current particle. The default RHASET uses RHOL=RHOR(IR(NP)).
RANDOM	IXX	Random number generator seed (default=123456789).
STACK	Note:	This COMMON block contains the information about the particles currently in the shower. All of the following variables are arrays except NP.
	E	Total energy in MeV (Double Precision).
	X,Y,Z	Position of particle in units established by DUNIT.
	U,V,W	Direction cosines of particle (not necessarily normalized---see Section 4.1.1c).
	DNEAR	A lower bound of distance from (X,Y,Z) to nearest surface of current region.

CHAPTER 4

Table 4.3.1  
(continued)

COMMON BLOCK	VARIABLE	FUNCTION
STACK (continued)	WT	Statistical weight of current particle (default=1.0). To be used in conjunction with importance sampling as determined by user.
	IQ	Integer charge of particle (+1,0,-1).
	IR	Index of particle's current region.
	NP	The stack pointer (i.e., the particle currently being pointed to). Also, the number of particles on the stack.
THRESH	RMT2	Twice the electron rest mass energy in MeV.
	RMSQ	Electron rest mass energy squared in MeV-squared.
	AP	Array containing PEGS lower photon cutoff energy for each medium in MeV.
	UP	Array containing PEGS upper photon cutoff energy for each medium in MeV.
	AE	Array containing PEGS lower charged particle cutoff energy for each medium in MeV.
	UE	Array containing PEGS upper charged particle cutoff energy for each medium in MeV.
	TE	Same as AE except kinetic energy rather than total energy.
THMOLL	Array containing the Moller threshold energy (THMOLL=AE+TE) for each medium in MeV.	

## CHAPTER 4

Table 4.3.1  
(continued)

COMMON BLOCK	VARIABLE	FUNCTION
UPHIOT	THETA	Collision scattering angle (polar).
	SINTHE	Sine of THETA.
	COSTHE	Cosine of THETA.
	SINPHI	Sine of PHI (the azimuthal scattering angle of the collision).
	COSPHI	Cosine of PHI.
	PI	Pi.
	TWOPI	Twice pi.
USEFUL	MEDIUM	Index of current medium. If vacuum, then MEDIUM=0.
	MEDOLD	Index of previous medium.
	RM	Electron rest mass energy in MeV.
	PRM	"Precision" electron rest mass energy in MeV (Double Precision).
	PRMT2	Twice PRM (Double Precision).

### 4.4 The Sequence of Operations

The sequence of operations needed for the correct operation of EGS is shown below along with sections in this chapter for additional details.

- Step 1. User-Over-Ride-Of-EGS-Macros (4.4.1).
- Step 2. Pre-HATCH-Call-Initialization (4.4.2).
- Step 3. HATCH-Call (4.4.3).
- Step 4. Initialization-For-HOWFAR (4.4.4).
- Step 5. Initialization-For-AUSGAB (4.4.5).
- Step 6. Determination-Of-Incident-Particle-Parameters (4.4.6).
- Step 7. SHOWER-Call (4.4.7).
- Step 8. Output-Of-Results (4.4.8).

## CHAPTER 4

The following are restrictions on the order of these operations:

- i.) Step 1 must precede use of EGS macros by user.
- ii.) Step 2 must precede Step 3.
- iii.) Steps 3 through 6 must precede Step 7.
- iv.) Step 5 may be repeated as often as desired, depending on whether information on single showers or many showers is desired (e.g., for shower fluctuation or conversion efficiency calculations).
- v.) At least one Step 7 must precede the first Step 8.

Details for the above steps are given in the following sub-sections.

### 4.4.1 User-Over-Ride-Of-EGS-Macros (Step 1)

EGS macros which the user might want to over-ride include the following:

#### a.) Array Dimensions

\$MXMED Maximum number of media (default=10).  
\$MXREG Maximum number of regions (default=2000).

For example, to extend the number of media to 7, include the statement

```
%'$MXMED'='7'
```

in the User Code.

#### b.) Pseudo-Random Number Generation

Whenever EGS (or the User Code) requires a floating point random number uniform in the interval (0,1) in a variable, say RNUMBR, the following statement type is included:

```
$RANDOMSET RNUMBR;
```

For efficiency purposes, EGS currently uses an "in-line" simulation of the SLAC system routine called RAN6. If the user desires to use some other random number generator (e.g., RAN10), this can be most easily accomplished by including

## CHAPTER 4

the over-ride macro

```
%'$RANDOMSET#;'=#1=RAN10(0);'
```

in the User Code at Step 1 (prior to any corresponding pattern). Of course, the user must make sure that the random number generator is properly initialized. As an example, suppose we wish to "seed" the random number generator in the User Code by the statement

```
IXX=987654321;
```

which could be included at any step prior to Step 7. To properly initialize, however, the associated COMMON block, RANDOM, would have to be included in the declaration section of the User Code. This is best done with the statement

```
COMIN/RANDOM/;
```

If no initialization is provided, EGS automatically seeds with IXX=123456789 in BLOCK DATA (default). The user should note that RAN6 must be re-seeded (with an odd integer number) for any new run of the same problem in order to avoid getting identical statistical results.

### c.) Sines and Cosines

To increase calculational speed, sines and cosines are not determined by function (e.g., SINTHE=SIN(THETA)) in EGS. Instead, the sine is looked-up in a sine-table and the cosine is determined from the sine. However, it is quite easy to revert back to the standard method (such as was done in EGS1) by means of the macros

```
%'$EVALUATE#USING SIN(#);'=#1=SIN(#2);'  
%'$SET INTERVAL#,SINC;'=#';'
```

which are thereby included at Step 1 of the User Code. The reader is referred to the paper by Cook and Shustek (1975) as an aid in understanding the above macros.

It should be pointed out that due to the precision involved in the table look-up, the direction cosines can become slightly unnormalized.



## CHAPTER 4

Depending on the problem at hand, this can lead to incorrect results---such as when two direction cosines are simultaneously involved in an angular sort of particles. The problem can generally be remedied by renormalizing the direction cosines prior to using them.

### d.) Charged Particle Transport

The pattern \$CHARGED-TRANSPORT; has been included in subroutine ELECTR in order to allow transport of the charged particles by means other than what has normally been considered in this version. For example, if it were desired to simulate showers in a magnetic field, the macro

```
%$CHARGED-TRANSPORT;='CALL MAGTRN;'
```

could be included in Step 1 of the User Code, and an appropriate subroutine MAGTRN would need to be provided by the user.

Another pattern that has been included in ELECTR is \$TMXS-OVER-RIDE;, which is there in case the user wants to impose an additional constraint on the lowest level electron transport step size. It can be used, for example, to revert back to the method used in EGS1 in which step sizes were taken discretely (rather than randomly as is done in both EGS2 and EGS3). To do this one uses the macro

```
%$TMXS-OVER-RIDE;=';IF(E(NP).GT.5.0)  
<TMXS=0.01*RLDU(MEDIUM);> ELSE <TMXS=  
0.001*RLDU(MEDIUM);>'
```

(Note: When the above macro is used with EGS2, use RLC(MEDIUM) in place of RLDU(MEDIUM)).

The macro

```
%$TMXS-OVER-RIDE;='TP=1.335E-3*EKE**2  
*RLDU(MEDIUM); TMXS=AMIN1(TMXS,TP);'
```

can be used to limit path length corrections (see Section 2.14) to values less than 15 per cent (whether or not this is important depends on the problem being solved). On the other hand, to remove the path length correction entirely (as in EGS1 and EGS2), one can use the macro-pair

## CHAPTER 4

```
%'$SET-USTEP;'='USTEP=TUSTEP;'  
%'$SET-TVSTEP;'='TVSTEP=VSTEP;'
```

Finally, the macro

```
%'$TMXS-OVER-RIDE;'='TP=200.0*TEFFO(MEDIUM);  
TMXS=AMIN1(TMXS,TP);'
```

limits the step size essentially in the manner done in EGS2, and we use this as the default macro for EGS3 for reasons discussed and demonstrated at the end of Section 3.5.

### 4.4.2 Pre-HATCH-Call-Initialization (Step 2)

This step consists of setting EGS COMMON variables that are used by HATCH in its initialization operations. All of these variables are initialized to some reasonable value in the BLOCK DATA subprogram. Therefore, if different values are desired they should be set with executable code (as opposed to another BLOCK DATA). Concurrently, the various COMMON blocks (i.e., BOUNDS, MEDIA, MISC) will have to be included in the declaration section of the MAIN program of the User Code. These variables are:

- a.) NMED --- This must be initialized to the number of media to be used in the shower generation (default=1).
- b.) MEDIA --- This array contains the names of the media required and is dimensioned MEDIA(24,\$MXMED), where \$MXMED is an EGS macro that is currently defined to be 10 (default), and whose value is the maximum number of media for which array space has been allocated (see Section 4.4.1a above). The media names are stored in MEDIA in alphanumeric field specification A1 to ensure transportability. Each medium name is 24 characters long. For the convenience of users compiling with EGS' macros, there is a macro to generate A1 strings. For example,

```
$S'STRING' expands to 'S','T','R','I','N','G'.
```

One way of implementing this in the User Code is demonstrated in the next example, which is for three media: lead, steel, and air at NTP.

## CHAPTER 4

A temporary array is declared and initialized in MAIN by

```
INTEGER TEMP(24,3)/$S'PB',          22*' ',
                $S'STEEL',          19*' ',
                $S'AIR AT NTP',14*' ';/;
```

Then at Step 2 one puts

```
NMED=3;          "NUMBER OF MEDIA USED"
DO J=1,NMED <DO I=1,24 <MEDIA(I,J)=TEMP(I,J);>>
```

- c.) MED --- This array, which is dimensioned MED(\$MXREG), contains the medium indices for each region. A medium index of zero means a region is filled with a vacuum (default values: \$MXREG\*1). For instance, if we consider the three media example above along with vacuum to define four regions, we might have

```
MED(1)=3; "FIRST REGION IS AIR AT NTP"
MED(2)=1; "SECOND REGION IS LEAD"
MED(3)=0; "THIRD REGION IS VACUUM"
MED(4)=2; "FOURTH REGION IS STEEL"
```

in Step 2 of the User Code.

- d.) ECUT and PCUT --- These arrays contain the cutoff energies (in MeV) for charged particles and photons, respectively, for each region. They are dimensioned ECUT(\$MXREG) and PCUT(\$MXREG). At the time that data for each medium is generated in the pre-processing code, PEGS, two parameters (AE and AP) are set to the lowest energies at which it will be desired to transport electrons and photons. HATCH will raise the values of ECUT and/or PCUT---supplied by the user or set by default in EGS BLOCK DATA---if necessary in order to assure that ECUT and PCUT in each region are not smaller than the AE or AP for the medium corresponding to that region. The AE and AP corresponding to vacuum are zero (default values for both arrays: \$MXREG\*0.0). These defaults, after being raised, give the lowest possible cutoffs consistent with the data from PEGS. For instance, consider the four region example from above. The statement

```
DO I=1,3 <ECUT(I)=10.0; PCUT(I)=100.0;>
```

## CHAPTER 4

when put in Step 2 of the User Code results in charged particles being cutoff at 10.0 MeV (total energy) and photons being cutoff at 100.0 MeV in the first three regions only. In the fourth region the respective cutoffs are set by AE and AP as established by PEGS. Of course COMMON/BOUNDS/ will have to be declared at the beginning of the MAIN code. Combined with COMMON/MEDIA/ and COMMON/MISC/, the macro declaration might look like

```
COMIN/BOUNDS,MEDIA,MISC/;
```

- e.) DUNIT --- This parameter determines the unit of distance to be used in the shower simulation. On input to HATCH, this parameter will be interpreted as follows:
- 1.) DUNIT > 0 means that DUNIT is the length of the distance unit expressed in centimeters. For example, setting DUNIT=2.54 would mean that the distance unit would be one inch.
  - 2.) DUNIT < 0 means that the absolute value of DUNIT will be interpreted as a medium index. The distance unit used will then be the radiation length for this medium, and on exit from HATCH, DUNIT will be equal to the radiation length of that medium in centimeters. The obvious use of this feature is for the case of only one medium with DUNIT=-1. Then the shower is expressed entirely in radiation lengths of the first medium.

The distance unit used by PEGS is the radiation length. After HATCH interprets DUNIT, it scales all distance-type data from PEGS in the proper way, so that all subsequent operations in EGS will be correctly performed with all distances in units of DUNIT (default value: 1.0 cm).

## CHAPTER 4

### 4.4.3 HATCH-Call (Step 3)

This step is very simple---HATCH has no arguments, so all one has to do is:

```
CALL HATCH;
```

The following output, for example, will indicate that the media data was found and scaled, and that the next step can be taken:

```
DUNIT REQUESTED & USED ARE:  1.00000E+00  1.00000E+00(CM.)  
EGS SUCCESSFULLY HATCHED FOR ONE MEDIUM.
```

Failure to "hatch" will result in messages to indicate the difficulty followed by a STOP in HATCH.

### 4.4.4 Initialization-For-HOWFAR (Step 4)

As stated previously, HOWFAR is the routine that determines the geometry of the regions. Although initialization for items that are taken up in HOWFAR can be done at any step prior to calling SHOWER (Step 7), Step 4 allows a space in MAIN to consider if such initialization need be performed. For example, if regions are defined by semi-infinite planes, data defining each plane (e.g., coordinates and unit normal vectors) can be established here. The data may be referred to in HOWFAR or by user-written subprograms called by HOWFAR.

It may be that some of the dimensions of the regions are determined at run-time, or the geometry may be so complex that it is desirable to use executable code to generate tables for use by HOWFAR. In such cases, initialization for HOWFAR will probably consist of filling up some user-written COMMON blocks for HOWFAR.

### 4.4.5 Initialization-For-AUSGAB (Step 5)

This step is similar to Step 4 above in that it provides a specified location in the MAIN code where quantities used in AUSGAB can be initialized. For example, suppose that we wished to create an array, ESUM, to keep track of the total energy deposited in each of the regions. We could declare

```
COMMON/TOTALS/ESUM($MXREG);
```

in both the MAIN code and in AUSGAB, with the statement

## CHAPTER 4

```
DO I=1,$MXREG <ESUM(I)=0.0;>
```

included in the MAIN code at Step 5. To complete the example, the statement

```
ESUM(IR(NP))=ESUM(IR(NP)) + EDEP;
```

in AUSGAB would keep a running total of the energy deposited in each region under consideration (Note: for a more complicated example, see subroutine ECONSV---described in Section 3.5 and listed in the User Code UCH20&AL in Appendix UC).

This would be a good time to point out that EDEP is a double precision variable---established as such via a macro. Therefore, one might wish to establish ESUM as double precision (in both MAIN and AUSGAB) as well. The authors have dealt with problems, particularly back in the days of SHOWER2-SHOWER4 (see Chapter 1), in which energy balancing could not be accounted for due to round-off error difficulties. This was particularly evident for large shower-history problems involving the addition of small energy values to large numbers in various regions. As a result of this experience, we have established certain key energy variables in the EGS code as double precision. The user may take advantage of this at his discretion (see example in Section 4.7).

### 4.4.6 Determination-Of-Incident-Particle-Parameters (Step 6)

This step is really self-explanatory---particularly when looked at in conjunction with Step 7 below. A specific example of such coding might be useful and is given as follows:

```
IQI=-1; "INCIDENT PARTICLE IS AN ELECTRON"  
EI=1000.0; "TOTAL ENERGY (MEV)"  
XI=0.0; YI=0.0; ZI=0.0; "PARTICLE COORDINATES"  
UI=0.0; VI=0.0; WI=1.0; "DIRECTION COSINES"  
IRI=2; "REGION NUMBER 2 IS THE INCIDENT REGION"  
WTI=1.0; "WEIGHT FACTOR IN IMPORTANCE SAMPLING"  
IXX=987654321; "RANDOM NUMBER GENERATOR SEED"  
NCASES=10; "NUMBER OF HISTORIES TO RUN"
```

## CHAPTER 4

### 4.4.7 SHOWER-Call (Step 7)

The calling sequence for SHOWER is:

```
CALL SHOWER(IQI,EI,XI,YI,ZI,UI,VI,WI,IRI,WTI);
```

The types of the arguments are given by their starting letter in accordance with standard FORTRAN convention. These arguments specify the charge, total energy, position, direction, region index, and statistical weight (generally taken as unity in this version) of the incident particle, and are used to fill the corresponding stack variables (see COMMON/STACK/ in Section 4.3). Section 4.4.6 above might be of some aid in understanding the parameter list. The subroutine may be called repeatedly by means of statements like

```
DO I=1,NCASES <CALL SHOWER(IQI,EI,XI,.....,etc.);>
```

### 4.4.8 Output-Of-Results (Step 8)

This step has been added for completeness and is self-explanatory.

## 4.5 Specifications for HOWFAR

On entry to the geometry subprogram, HOWFAR, EGS has determined that it would like to transport the top particle on the stack by a straight line distance USTEP. All of the parameters of the particle are available to the user via COMMON/STACK/ as described earlier. The user controls the transport by setting the following variables:

USTEP, IDISC, IRNEW, and DNEAR(NP).

Except for the last variable (which is in COMMON/STACK/), these are available to the user via COMMON/EPCONT/. The ways in which these may be changed, and the way EGS will interpret these changes, will now be discussed in detail.

- a.) If the user decides that the current particle should be discarded, then he should set IDISC nonzero (the usual convention is to set IDISC=1). A positive value for IDISC will cause the particle to be discarded immediately. A negative value for IDISC will cause EGS to discard the particle when

## CHAPTER 4

it completes the transport\*. EGS initializes IDISC to zero, and if left zero no user requested discard will take place.

- b.) If immediate discard was not requested, then the user should check to see whether transport by distance USTEP would cause a region boundary to be crossed. The presence of the region index, IR(NP), for the current particle should make this task much easier than if only the position of the particle were known. If no boundary would be crossed, then USTEP and IRNEW may be left as they are. If a boundary would be crossed, then USTEP should be set to the distance to the boundary from the current position along the current direction, and IRNEW should be set to the region index of the region on the other side of the boundary.
  
- c.) The setting of DNEAR(NP) by the user is optional. However, its use is recommended for efficiency purposes---for reasons that will now be explained. First of all, it is clear that boundary checking takes time and should be avoided whenever possible. If EGS had no way of knowing how far it was from a boundary, then it would have to ask the user how far to go every time it wanted to transport a particle. This would not be too serious for photons since they usually go relatively far on each transport. However, the transport of a charged particle from one interaction to the next requires the path-length to be split-up into smaller lengths in order to properly simulate the multiple scattering process. If the particle is a fairly good distance from the nearest boundary relative to the small steps being taken, clearly checking for boundary crossings on each transport is a waste of time. In order to avoid this inefficiency, each particle has stored on the stack a variable called DNEAR, which is used by EGS to store a lower bound to the distance from the particle's current position to the nearest region boundary. This variable is used by EGS in the following ways:

-----  
\* Note: In Version 2 (EGS2) the particle will only be discarded, as a result of setting IDISC negative, provided the particle is able to travel the whole distance USTEP without multiple scattering.



## CHAPTER 4

- i.) DNEAR for the incident particle is initialized to zero.
- ii.) Whenever a particle is actually moved (by a straight line distance VSTEP) the path length transported is deducted from the DNEAR for the particle.
- iii.) Whenever a particle interacts, the DNEAR's for the product particles are set from the DNEAR value of the parent particle.
- iv.) When EGS has decided it would like to transport the current particle by a distance USTEP (which will be the distance to the next interaction), subroutine HOWFAR will be called to get the user's permission to go that far only if USTEP is larger than DNEAR.
- v.) (Note: This item applies ONLY to EGS2).

Once EGS has obtained an approved value for an electron USTEP, it checks to see what is the largest "very small step" (VSTEP) it can use consistent with the multiple scattering calculation. If this value (variable TMXS) is larger than USTEP, then VSTEP is set to USTEP, the electron is transported by the whole USTEP, and everything is fine. More usually, however, TMXS will be smaller than USTEP. In this case, VSTEP is set equal to TMXS and the electron is transported this distance. The amount of the step (VSTEP) is then deducted from USTEP to give the remaining distance for the current USTEP. At this point DNEAR is compared to the expected size of the next VSTEP. If it is larger, the next small step is taken without consulting HOWFAR further. These small steps continue without further consultation with HOWFAR until either USTEP is exhausted, or until DNEAR becomes less than the expected size of the next step.

## CHAPTER 4

### c.) (continued---EGS2 and EGS3)

In conclusion, to take advantage of these efficiency features, the user should set DNEAR(NP) equal to the distance to the nearest region boundary from the particle's current position. If it is easier for the user to compute some quick lower bound to the actual nearest distance, this could be used to set DNEAR with time savings depending on how close the lower bound is to the actual nearest distance on the average. If the medium for a region is vacuum, the user need not bother computing DNEAR, as EGS will always transport to the next boundary in only one step in this case.

### d.) (Note: This item applies ONLY to EGS2).

With this background on the multiple scattering problem we are now ready to discuss some fine points. On return from HOWFAR, EGS assumes that all of the distance USTEP, starting with the current position, will be in the current region, except possibly the end point. The latter will be in a new region if and only if IRNEW is different from the current region index. It is also assumed that the switch to a new region, and any requests for deferred discard, are to take effect only if the end point of this path is reached. If more than one VSTEP is required to exhaust either USTEP or DNEAR, then EGS concludes that the end point of the path was not reached because of multiple scattering. Thus EGS resets IRNEW to the current region index, and will have to call HOWFAR one or more times in order to cross the boundary, or perform the deferred discard.

Consider, as an example of how to write a HOWFAR sub-program, the three region geometry in Fig. 4.5.1. A particle is shown in Region 2 with coordinates (X,Y,Z) and direction cosines (U,V,W). We will assume that the slab of thickness ZTHICK is semi-infinite (x and y-directions), and that particles are immediately discarded whenever they go into

CHAPTER 4

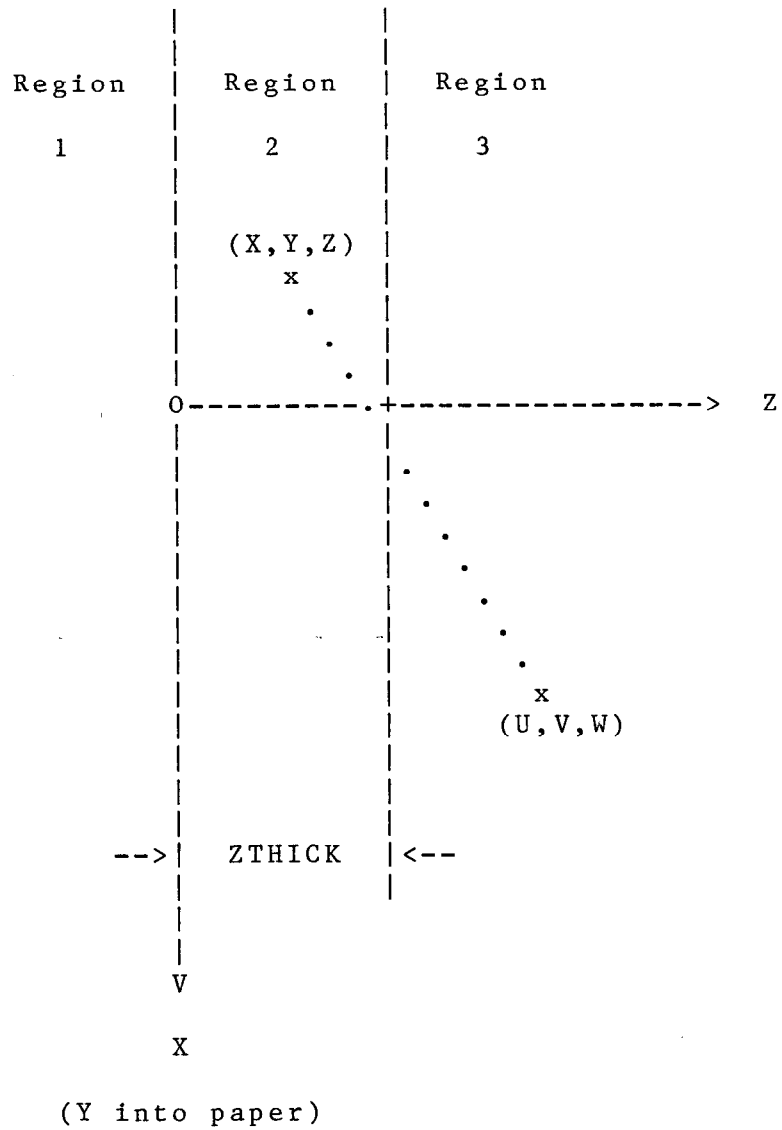


Fig. 4.5.1 A Three Region Geometry Example for HOWFAR

## CHAPTER 4

Region 1 or Region 3. The following HOWFAR code is then applicable:

```
SUBROUTINE HOWFAR;
COMIN/EPCONT,STACK/; "COMMON BLOCKS NEEDED IN CALCULATIONS"
COMMON/PASSIT/ZTHICK; "SLAB THICKNESS DEFINED IN MAIN"
IF(IR(NP).NE.2) <IDISC=1; RETURN;>
"MIGHT AS WELL SET DNEAR NEXT"
DNEAR(NP)=AMIN1(Z(NP),ZTHICK-Z(NP));
IF(W(NP).EQ.0.0) <RETURN; "PARTICLE GOING PARALLEL TO PLANES">
"CHECK FORWARD PLANE FIRST SINCE SHOWER HEADING THAT WAY"
"MOST OF THE TIME"
IF(W(NP).GT.0.0) <DELTAZ=(ZTHICK-Z(NP))/W(NP); IRNEXT=3;>
"OTHERWISE, PARTICLE MUST BE HEADING IN BACKWARDS DIRECTION"
ELSE <DELTAZ=-Z(NP)/W(NP); IRNEXT=1;>
"NOW CHECK WITH USTEP AND RESET THINGS IF NECESSARY"
IF(DELTAZ.LE.USTEP) <USTEP=DELTAZ; IRNEW=IRNEXT;>
RETURN; END;
```

Other HOWFAR examples can be found in the code listings given in Appendix UC corresponding to the various comparison studies presented in Chapter 3.

### 4.6 Specifications for AUSGAB

The subroutine AUSGAB is called by EGS with the statement:

```
CALL AUSGAB(IARG);
```

The argument IARG indicates the situation under which AUSGAB is being called. In this version, as opposed to Version 2 (EGS2), IARG can take on 23 values starting from zero (i.e., IARG=0 through IARG=22). The first five IARG values are consistent with EGS2, and we shall discuss them first---the remaining 18 IARG values must be "switched-on" by means of the array IAUSFL. The value for IARG and the corresponding situations are given in Table 4.6.1:

## CHAPTER 4

Table 4.6.1

IARG	Situation
0	Particle is going to be transported by distance TVSTEP (or VSTEP in the case of EGS2).
1	Particle is going to be discarded because its energy is below the cutoff ECUT (for charged particles) or PCUT (for photons)---but its energy is larger than the corresponding PEGS cutoff AE or AP, respectively.
2	Particle is going to be discarded because its energy is below both ECUT and AE (or PCUT and AP).
3	Particle is going to be discarded because the user requested it (in HOWFAR usually).
4	A (fluorescent) photon is going to be discarded with the binding energy of a photoelectron.

The above IARG values are the ones generally required in the majority of situations in which EGS is used to simulate electromagnetic cascade shower development. In particular, IARG=0 is useful whenever track lengths are being calculated or when charged particle ionization loss is needed. Also, as a check on energy conservation, EDEP can be summed in AUSGAB for all IARG values less than 5. We have extended the IARG range in Version 3 in order to allow the user to extract additional information without making changes to the EGS coding. To do this we have created the integer flag array, IAUSFL(J), for J=1 through 23. It takes on values of 1 or 0 depending on whether AUSGAB is called or not, respectively. For J=1 through 5, which corresponds to IARG=0 through 4, IAUSFL(J)=1 (default). In other words, AUSGAB is always called for the situations listed in Table 4.6.1, and EGS2 and EGS3 are identical in this respect. For the remaining values of J, corresponding to IARG=5 through 22, IAUSFL(J)=0 (default). The value for IARG and the corresponding situations for this upper set of IARG values are shown in Table 4.6.2.

## CHAPTER 4

Table 4.6.2

IARG	Situation
5	Particle has been transported by distance TVSTEP (or VSTEP in the case of EGS2).
6	A bremsstrahlung interaction has occurred and a call to BREMS is about to be made in ELECTR.
7	Returned to ELECTR after a call to BREMS was made.
8	A Moller interaction has occurred and a call to MOLLER is about to be made in ELECTR.
9	Returned to ELECTR after a call to MOLLER was made.
10	A Bhabha interaction has occurred and a call to BHABHA is about to be made in ELECTR.
11	Returned to ELECTR after a call to BHABHA was made.
12	An in-flight annihilation of the positron has occurred and a call to ANNIH is about to be made in ELECTR.
13	Returned to ELECTR after a call to AHHIH was made.
14	A positron has annihilated at rest.
15	A pair production interaction has occurred and a call to PAIR is about to be made in PHOTON.
16	Returned to PHOTON after a call to PAIR was made.
17	A Compton interaction has occurred and a call to COMPT is about to be made in PHOTON.
18	Returned to PHOTON after a call to COMPT was made.
19	A photoelectric interaction has occurred and a call to PHOTO is about to be made in PHOTON.
20	Returned to PHOTON after a call to PHOTO was made (assuming NP is non-zero).
21	Subroutine UPHI was just entered.
22	Subroutine UPHI was just exited.

## CHAPTER 4

As an example of how to write an AUSGAB subprogram, consider the previous three region geometry (Fig. 4.5.1). Suppose that we wish to score (i.e., output on the line printer) only photons that emanate from Region 2 into Region 3. The AUSGAB subprogram that will accomplish this is given below. In this example we print out the stack variables plus IARG.

```
SUBROUTINE AUSGAB(IARG);
COMIN/STACK/;
"ONLY OUTPUT INFORMATION FOR PHOTONS THAT ARE DISCARDED"
"IN REGION 3"
IF(IARG.EQ.3.AND.IQ(NP).EQ.0.AND.IR(NP).EQ.3) <
    OUTPUT E(NP),X(NP),Y(NP),Z(NP),U(NP),V(NP),W(NP),
        IQ(NP),IR(NP),IARG; (7G15.7,3I5);>
RETURN; END;
```

### 4.7 UCSAMPLE --- An Example of a "Complete" User Code

The following User Code, called UCSAMPLE, simulates electromagnetic cascade showers initiated by 1 GeV electrons that are incident (normally) on a 3 cm, semi-infinite slab of iron. The upstream region of the slab is vacuum and the downstream region is air at NTP. A particle is discarded whenever it exits the slab (on either side), or whenever its total energy falls below a preset cutoff energy of 100 MeV. The stack variable information E(NP), Z(NP), W(NP), IQ(NP), IR(NP), plus the IARG value, is outputted on the line printer (first 15 lines only) for photons reaching Region 3.

The maximum number of regions is changed from 2000 (default) to 20 by means of an over-ride macro at Step 1 in the User Code. Furthermore, the distance unit (DUNIT) is changed (at Step 2) so that distances are in radiation lengths of iron rather than in centimeters.

A total of 10 cases of incident electrons is run and the total energy fraction for each region is summed and printed out at the end of the run for an energy balance check. Finally, the last random number generator (integer) that was used is printed out for possible use in avoiding statistically identical results in future runs of the same problem.

The UCSAMPLE User Code is given below.

CHAPTER 4

```
%E "EJECT (START NEW PAGE) IN MORTRAN LISTING"
"*****"
"***** UCSAMPLE *****"
"*****"
"*** MAIN ***"
"*****"

"STEP 1. USER-OVER-RIDE-OF-EGS-MACROS"

% '$MXREG'='20' "OVER-RIDING THE MAXIMUM NUMBER OF REGIONS"

"DECLARATIONS:"

COMIN/BOUNDS,MEDIA,MISC,RANDOM,USEFUL/; "COMMONS NEEDED"
COMMON/PASSIT/ZTHICK; "SLAB THICKNESS...NEEDED IN HOWFAR"
COMMON/LINES/NLINES,NWRITE; "TO KEEP TRACK OF LINES-PRINTED"
COMMON/TOTALS/ESUM($MXREG); "FOR ENERGY CONSERVATION CHECK"
$ENERGY PRECISION EI,ESUM,EKIN,TOTKE,ETOT; "DOUBLE PRECISION"

"CREATE A TEMPORARY ARRAY AND DEFINE THE MEDIA, NEXT"
INTEGER TEMP(24,2)/$S'FE',22*' ', $S'AIR AT NTP',14*' '/;

"STEP 2. PRE-HATCH-CALL-INITIALIZATION"

NREG=3; "THE NUMBER OF REGIONS---A LOCAL VARIABLE ONLY"
NMED=2; "TWO MEDIA WILL BE USED"
DO J=1,NMED <DO I=1,24 <MEDIA(I,J)=TEMP(I,J);>>

MED(1)=0; "REGION 1 IS VACUUM"
MED(2)=1; "REGION 2 IS IRON"
MED(3)=2; "REGION 3 IS AIR AT NTP"

"SET ENERGY CUTOFFS FOR EACH REGION NEXT"
DO I=1,NREG <ECUT(I)=100.0; PCUT(I)=100.0;>

DUNIT=-1; "DISTANCES WILL BE IN RADIATION LENGTHS (OF IRON)"

"STEP 3. HATCH-CALL"

CALL HATCH;

"STEP 4. INITIALIZATION-FOR-HOWFAR"

ZTHICK=3.0; "SLAB THICKNESS IN CENTIMETERS"
ZTHICK=ZTHICK/RLC(1); "CONVERT TO RADIATION LENGTHS"

"STEP 5. INITIALIZATION-FOR-AUSGAB"
```



## CHAPTER 4

```
DO I=1,$MXREG <ESUM(I)=0.DO;> "ZERO THE ENERGY BALANCE ARRAY"
NLLINES=0; "INITIALIZE THE NLLINES-COUNTER"
NWRITE=15; "THE NUMBER OF LINES TO PRINT OUT"
```

"STEP 6. DETERMINATION-OF-INCIDENT-PARTICLE-PROPERTIES"

```
IQI=-1; "INCIDENT PARTICLE IS AN ELECTRON"
EI=1000.DO; "INCIDENT ENERGY (TOTAL) IN MEV"
EKIN=EI-PRM; "K.E. OF ELECTRON---PRM IS THE REST MASS"
XI=0.0; YI=0.0; ZI=0.0; "COORDINATES OF INCIDENT PARTICLE"
UI=0.0; VI=0.0; WI=1.0; "DIRECTION COSINES---ALONG Z=AXIS"
IRI=2; "INCIDENT PARTICLE STARTS OUT IN REGION 2---IRON"
WTI=1.0; "WEIGHT FACTOR---NOT USED IN CALCULATION, BUT"
"      IS A PARAMETER IN SUBROUTINE SHOWER; HENCE DEFINE"
"      AS UNITY"
IXX=987654321; "RANDOM NUMBER GENERATOR SEED"
NCASES=10; "NUMBER OF HISTORIES (CASES) TO RUN"
IARG=-1; "IARG (HERE ONLY), INVENTED TO MARK THE"
"      INCIDENT PARTICLES"
```

"STEP 7. SHOWER-CALL"

```
OUTPUT; (/,' SHOWER RESULTS:',///,7X,'E',14X,
'Z',14X,'W',10X,'IQ',3X,'IR',2X,'IARG',/);
```

```
DO I=1,NCASES <
  IF(NLLINES.LT.NWRITE) <
    OUTPUT EI,ZI,WI,IQI,IRI,IARG;
    (3G15.7,3I5);
    NLLINES=NLLINES+1;>

  CALL SHOWER(IQI,EI,XI,YI,ZI,UI,VI,WI,IRI,WTI);
```

"END OF SHOWER-CALL LOOP">

"STEP 8. OUTPUT-OF-RESULTS"

```
TOTKE=NCASES*EKIN; "TOTAL K.E. INVOLVED IN RUN"
```

```
OUTPUT EI,ZTHICK,NCASES,IXX;
(//,' INCIDENT TOTAL ENERGY OF ELECTRON=',F12.1,' MEV',/,
' IRON SLAB THICKNESS=',F6.3,' RADIATION LENGTHS',/,
' NUMBER OF CASES IN RUN=',I3,/, ' LAST RANDOM NUMBER=',
I12,//,' ENERGY DEPOSITION SUMMARY:',//);
```

```
"CALCULATE AND PRINT OUT THE FRACTION OF ENERGY"
"DEPOSITED IN EACH REGION"
```

CHAPTER 4

```

ETOT=0.D0;
DO I=1,NREG <
  ETOT=ETOT+ESUM(I);
  ESUM(I)=ESUM(I)/TOTKE;  "FRACTION IN EACH REGION"

  OUTPUT I, ESUM(I);  (' FRACTION IN REGION',I3,'=',F10.7);
>

ETOT=ETOT/TOTKE;  "THE TOTAL FRACTION OF ENERGY IN RUN"

OUTPUT ETOT;  (//,' TOTAL ENERGY FRACTION IN RUN=',G15.7,/,
  ' WHICH SHOULD BE CLOSE TO UNITY');

STOP;
END;  "LAST STATEMENT OF MAIN"

%E  "EJECT (START NEW PAGE) IN MORTRAN LISTING"

SUBROUTINE AUSGAB(IARG);
COMIN/EPCONT,STACK/;  "COMMONS NEEDED IN AUSGAB"
COMMON/LINES/NLINES,NWRITE;  "TO KEEP TRACK OF LINES-PRINTED"
COMMON/TOTALS/ESUM($MXREG);  "FOR ENERGY CONSERVATION CHECK"
$ENERGY PRECISION ESUM;  "DOUBLE PRECISION"

"KEEP A RUNNING SUM OF THE ENERGY DEPOSITED IN EACH REGION"
ESUM(IR(NP))=ESUM(IR(NP)) + EDEP;

"PRINT OUT THE FIRST NLINES OF STACK INFORMATION, ETC."
"BUT, ONLY FOR PHOTONS THAT ARE DISCARDED IN REGION 3"

IF(NLINES.LT.NWRITE) <
  IF(IARG.EQ.3.AND.IQ(NP).EQ.0.AND.IR(NP).EQ.3) <
    OUTPUT E(NP),Z(NP),W(NP),
      IQ(NP),IR(NP),IARG;  (3G15.7,3I5);

    NLINES=NLINES+1; >>

RETURN;
END;  "LAST STATEMENT OF SUBROUTINE AUSGAB"

%E  "EJECT (START NEW PAGE) IN MORTRAN LISTING"

SUBROUTINE HOWFAR;
COMIN/EPCONT,STACK/;  "COMMON NEEDED IN HOWFAR"
COMMON/PASSIT/ZTHICK;  "SLAB THICKNESS DEFINED IN MAIN"

IF(IR(NP).NE.2) <IDISC=1; RETURN;>

```

CHAPTER 4

```
"MIGHT AS WELL SET DNEAR NEXT"
DNEAR(NP)=AMIN1(Z(NP),ZTHICK-Z(NP));

IF(W(NP).EQ.0.0) <RETURN; "PARTICLE GOING PARALLEL TO PLANES">

"CHECK FORWARD PLANE FIRST SINCE SHOWER HEADING THAT WAY"
"MOST OF THE TIME"
IF(W(NP).GT.0.0) <DELTAZ=(ZTHICK-Z(NP))/W(NP); IRNEXT=3;>
"OTHERWISE, PARTICLE MUST BE HEADING IN BACKWARDS DIRECTION"
ELSE <DELTAZ=-Z(NP)/W(NP); IRNEXT=1;>
"NOW CHECK WITH USTEP AND RESET THINGS IF NECESSARY"
IF(DELTAZ.LE.USTEP) <USTEP=DELTAZ; IRNEW=IRNEXT;>

RETURN;
END; "LAST STATEMENT OF SUBROUTINE HOWFAR"

"*****
***** END OF UCSAMPLE *****
*****"
```

The results of running this User Code are given below:

```
DUNIT REQUESTED&USED ARE: -1.00000E+00 1.76045E+00(CM.)
EGS SUCCESSFULLY HATCHED FOR 2 MEDIA.
```

SHOWER RESULTS:

E	Z	W	IQ	IR	IARG
1000.000	.0	1.000000	-1	2	-1
163.9964	1.704107	.9999205	0	3	3
236.1858	1.704108	.9993746	0	3	3
147.1114	1.704108	.9993164	0	3	3
123.6111	1.704108	.9997739	0	3	3
194.9223	1.704108	.9987965	0	3	3
1000.000	.0	1.000000	-1	2	-1
107.8580	1.704108	.9981059	0	3	3
1000.000	.0	1.000000	-1	2	-1
129.2727	1.704107	.9994448	0	3	3
1000.000	.0	1.000000	-1	2	-1
373.1440	1.704108	.9994652	0	3	3
492.3091	1.704108	.9998357	0	3	3
1000.000	.0	1.000000	-1	2	-1
718.2241	1.704107	.9998002	0	3	3

CHAPTER 4

INCIDENT TOTAL ENERGY OF ELECTRON= 1000.0 MEV  
IRON SLAB THICKNESS= 1.704 RADIATION LENGTHS  
NUMBER OF CASES IN RUN= 10  
LAST RANDOM NUMBER= 571026837

ENERGY DEPOSITION SUMMARY:

FRACTION IN REGION 1= 0.0  
FRACTION IN REGION 2= 0.3525439  
FRACTION IN REGION 3= 0.6474561

TOTAL ENERGY FRACTION IN RUN= 1.000000  
WHICH SHOULD BE CLOSE TO UNITY

## CHAPTER 5

### 5. USER MANUAL FOR PEGS3 \*

#### 5.1 Introduction

The PEGS (Processor for EGS) code is a stand alone utility program, written in MORTRAN \*\*, whose purpose is to generate material data for the EGS code, and to provide other services for the user who is studying or simulating electromagnetic interactions. The active operations of PEGS are functionals; that is, they are operations whose arguments are functions (the functions related to high energy physics interactions). Included among these operations are:

- Fitting of functions by means of piecewise linear fits
- Production of print plots of selected functions
- Evaluation of functions at selected points
- Comparision of functions with sampled spectra

Associated with these active functionals are other operations; namely,

- Selection of material to which the functions refer
- Selection of energy cutoffs for fits
- Punching of fit data
- Generation of material independent multiple scattering data (EGS2 only)

-----  
\* This manual, which essentially applies to PEGS2 as well, will be kept up-to-date as a WYLBUR data set in the EGS\$RP account at the Stanford Linear Accelerator Center.

\*\* To be more specific, we are presently using MORTRAN2. The reader is encourage to study the article by Cook and Shustek (1975) on the MORTRAN2 language. An article by Zahn (1975) is also useful. The introduction to Chapter 4 discusses the reasons for choosing MORTRAN.

## CHAPTER 5

### 5.2 Structural Organization of PEGS

The PEGS code contains over 3200 MORTRAN source lines which are the source for a MAIN program, BLOCK DATA subprogram, about 13 subroutines, and about 80 functions. Despite the large number of subprograms, PEGS has a simple structure. Fig. 5.2.1 shows a flowchart of the MAIN program of PEGS. After the once-only initializations an option loop is entered. Each time through the option loop, an option is read (option names are four characters and are read as 4A1), numeric control parameters are read (using NAMELIST/INP/), and then the option name is looked up in the option table. If not found, the job is aborted. If found, the appropriate code is executed and return is passed to the beginning of the option loop. Normal exit from the loop is by selection of the STOP option, or detection of an End of File condition on the control input file. The details for the use of the options are contained in Section 5.3.

Fig. 5.2.2 shows the subprogram relationships of PEGS. Boxed items are subprograms, and option names (i.e., :CALL:) are used to show which subprograms correspond to which options. It can be seen that the physical routines are accessed directly for the PWLF option. For utility options (TEST, PLTN, PLTI, HPLT, and CALL) the physical routines are referenced using the function FI---the so-called "function multiplexer". Function FI has five arguments. The first argument (I) tells which physical function to invoke, and the other four arguments (X1, X2, X3, X4) are used as needed as arguments for the called function. FI then returns the value returned by the called function.

This method of implementing options that are functionals was selected to avoid the necessity of having a separate call to the associated utility routines for each physical function on which it might be desired to operate. It was also desired to be able to refer to the particular function symbolically, both at compile time and at run-time, and to know the number of arguments to each function. In order to have these conveniences and also allow easy insertion or deletion of functions to the list of functions accessible to FI, a MORTRAN macro (\$FUNCTIONS) was written which takes a list of names of functions (each of which is immediately preceded by the number of arguments it has) and generates other macros containing the desired information. In particular,



CHAPTER 5

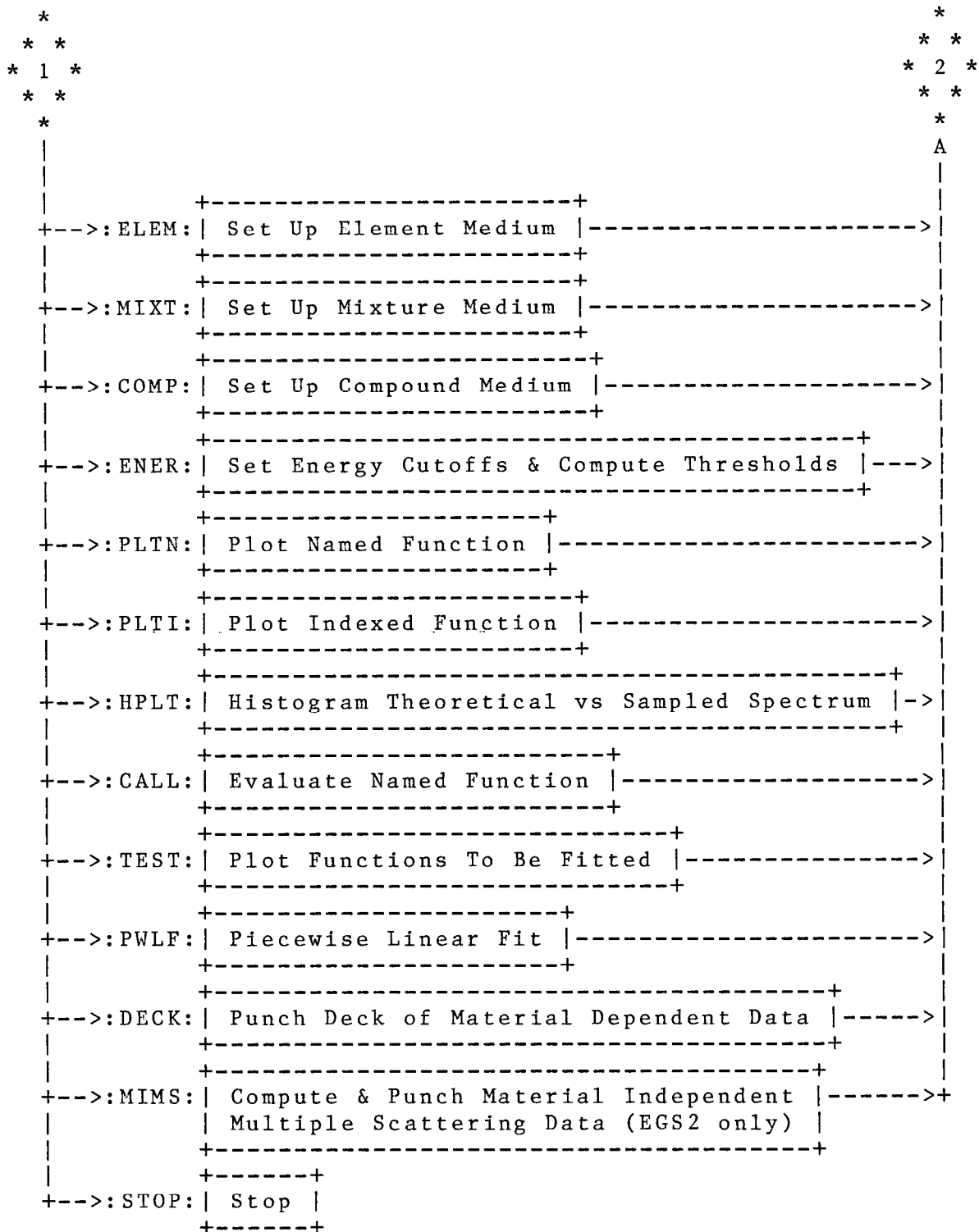


Fig. 5.2.1 Flowchart of the MAIN Program of PEGS  
(continued from previous page)





CHAPTER 5

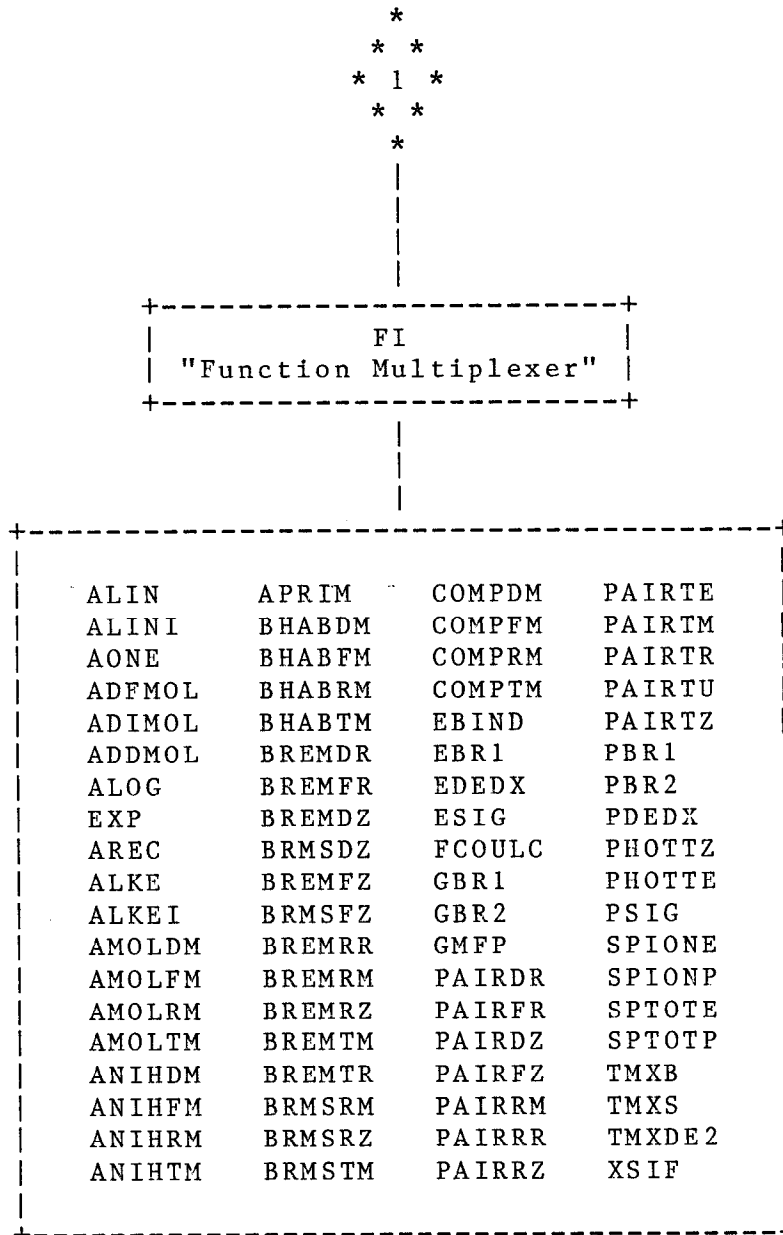


Fig. 5.2.2 Subprogram Relationships of PEGS  
(continued from previous page)

## CHAPTER 5

the following macros are defined:

`$NFUNS` - Gives the number of functions.

`$FLIST$DATA(FNAME)` - Generates a data statement initializing the array `FNAME(6,$NFUNS)` so that `FNAME(i,j)` has the *i*th character of the name of the *j*th function.

`$FLIST$NARGS` - Gives a list of the number of arguments for each function, which is used to initialize the runtime array `NFARG($NFUNS)`.

`$FLIST$FNUMS` - Gives a list of numbers from 1 to `$NFUNS`, which is used to generate the computed GO TO in FI.

`$FLIST$FCALLS` - Generates the function calls in FI with the proper number of arguments for each function taken from the list X1, X2, X3, X4.

`$FN(function name)` - Gives the function index of the specified function.

`$NA(function name)` - Gives the number of arguments for the specified function.

It should also be noted that there are relationships between the functions shown in Fig. 5.2.2 that are not indicated there. We show the most complicated of these in Figs. 5.2.3a,b (Bremsstrahlung Related Functions) and in Figs. 5.2.4a,b (Pair Production Related Functions). One reason for the complexity of these is that the higher level forms of the cross sections must be obtained by numerical integration of the more differential forms.

CHAPTER 5

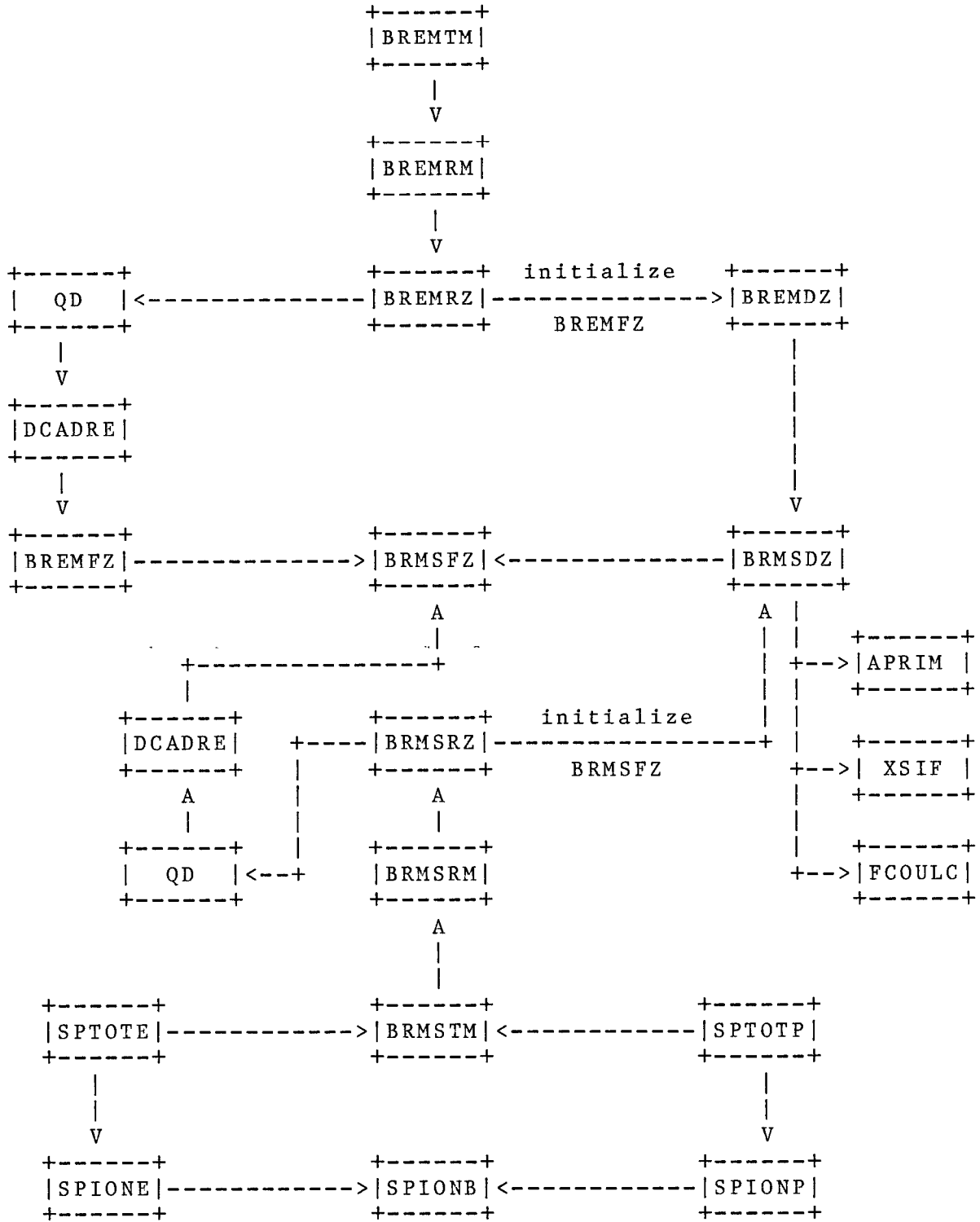


Fig. 5.2.3a Bremsstrahlung Related Functions---Most Accurate Form (Used to Produce the Total Cross Sections and Stopping Power).

CHAPTER 5

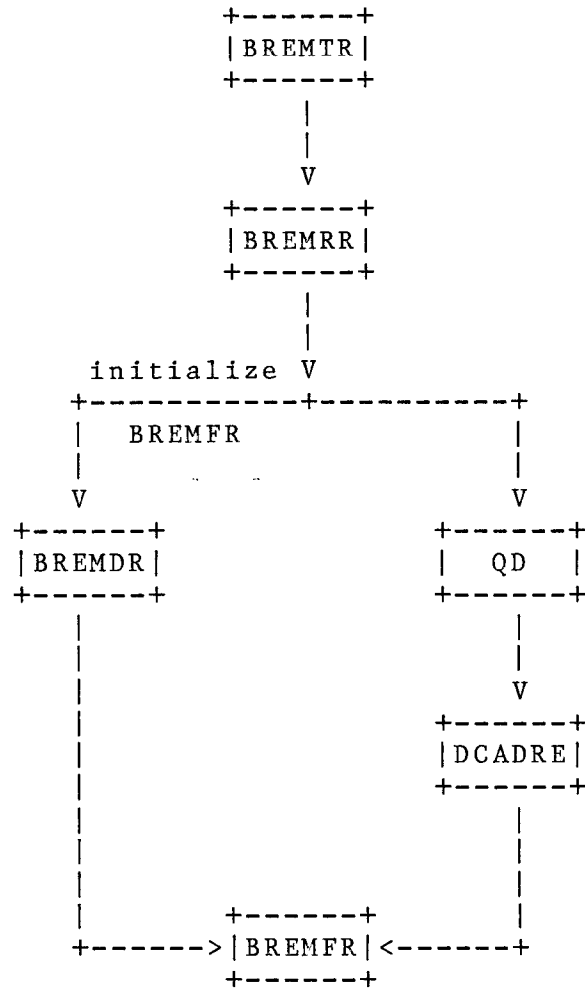


Fig. 5.2.3b Bremsstrahlung Related Functions---With Run-Time Approximations (For Comparison with Sampled Spectra).

CHAPTER 5

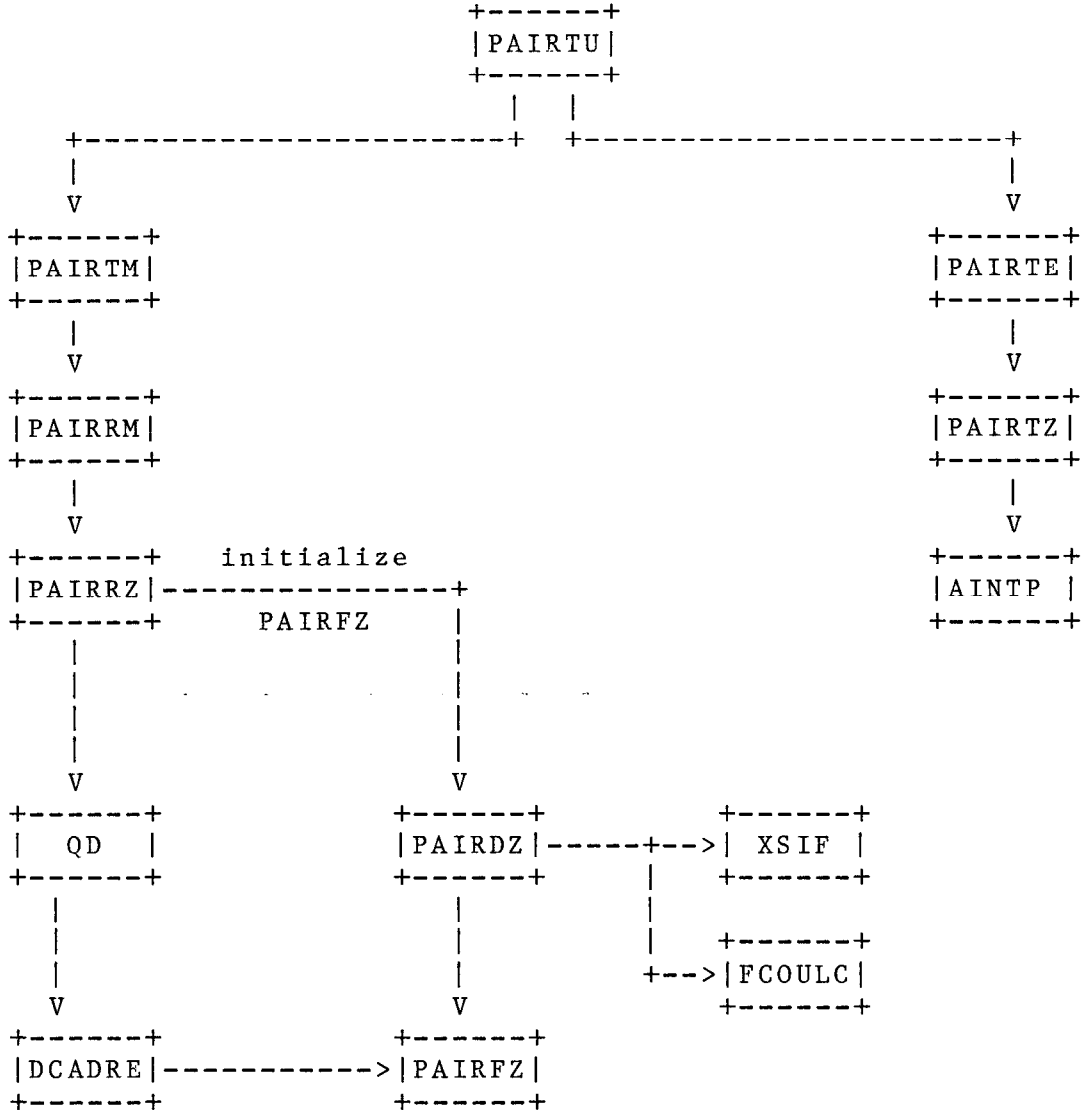


Fig. 5.2.4a Pair Production Related Functions---Most Accurate Form (Used to Produce the Total Cross Sections and Stopping Power).

CHAPTER 5

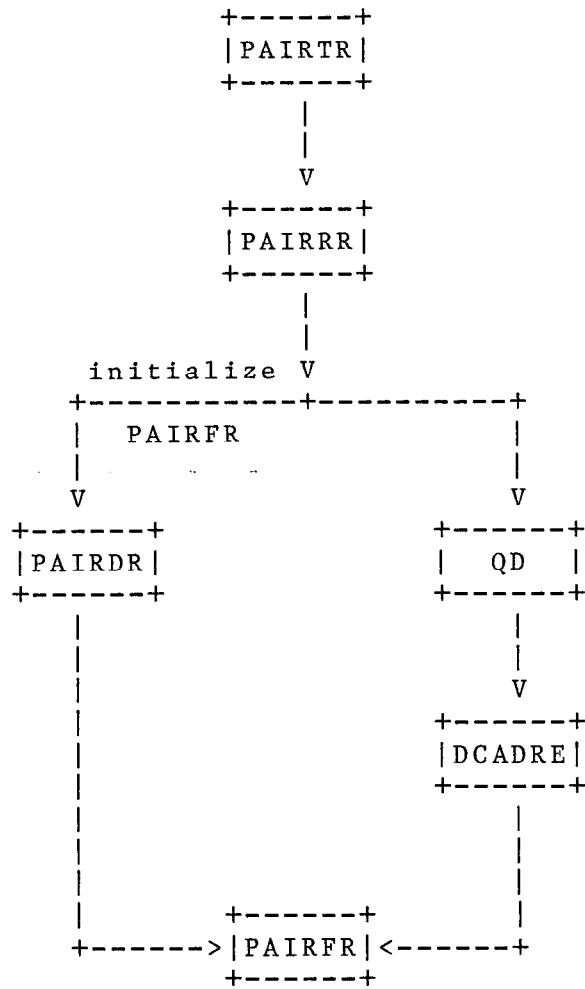


Fig. 5.2.4b Pair Production Related Functions---With Run-Time Approximations (For Comparison with Sampled Spectra).

## CHAPTER 5

Table 5.2.1 lists the SUBROUTINES used in PEGS. A brief description of their use and page references for a fuller discussion is given.

Table 5.2.2 lists the FUNCTIONS used in PEGS along with their mathematical symbols, definitions, and locations in this report for a fuller discussion. The names of most of the functions have been chosen in a rather mnemonic way. The first three or four letters suggest the process being considered. The last letter designates the form of the cross section (Z for element, M for mixture, and R for "run-time" mixture). The next to last letter describes either the particular form of the cross section (such as D for differential, T for total or R for range-integrated), or it indicates that only the secondary energy is to vary, with other data being passed through a common. The letter F is used in such cases and the data in common is initialized using the corresponding function that has a next to last letter of D. If the function word begins with an I through N (i.e., the FORTRAN integer convention) the word is prefixed with the letter A. A few examples are given below:

- AMOLDM is the differential Moller cross section for a mixture of elements.
- BREMDR is the differential bremsstrahlung cross section for a "run-time" mixture of elements.
- BREMRM is the bremsstrahlung cross section, integrated over some energy range, for a mixture of elements.
- BRMSTM is the soft bremsstrahlung total cross section for a mixture of elements.
- PAIRRR is the pair production cross section, integrated over some energy range, for a "run-time" mixture of elements.
- PAIRTZ is the total cross section for pair production for an element.

This method of naming is not strictly adhered to, however. For example, SPIONE is the ionization stopping power for an electron, PBR1 and PBR2 are positron branching ratios, and GMFP is the gamma-ray mean free path.



## CHAPTER 5

### Table 5.2.1

#### SUBROUTINES Used In PEGS

NAME	DESCRIPTION	PAGES
DECK	Subprogram to produce a deck of material dependent data (for subsequent use by EGS).	5.2-4, 5.3-16
DIFFER	Determines the various parameters needed for bremsstrahlung and pair production energy sampling.	2.7-30, 5.2-4, 5.3-10
EFUNS	Subprogram to compute electron functions to be fit in a way that avoids repetition.	5.2-4
GFUNS	Subprogram to compute photon functions to be fit in a way that avoids repetition.	5.2-4
HPLT	Creates line printer plot comparisons of EGS-sampled data (via TESTSR code) and theoretical functions of PEGS.	5.2-4, 5.3-20
MIX	Computes Z-dependent parameters that reside in COMMON/MOLVAR/.	5.2-4, 5.3-10
MOLIER	Computes material independent multiple scattering data (for EGS2 only).	5.2-4
PLOT	Subprogram to plot a given function (referenced by number).	5.2-4
PMDCON	Determines the physical, mathematical, and derived constants in a very mnemonic way.	2.6-11, 5.2-4
PWLF	Subprogram to piecewise linearly fit up to 10 functions simultaneously on an interval (XL,XU).	5.3-13, 5.3-14
SPINIT	Initializes stopping power functions for a particular medium.	2.13-6, 5.2-4, 5.3-10

CHAPTER 5

Table 5.2.2

FUNCTIONS Used In PEGS

NAME	DESCRIPTION	PAGES
AINTP	Linear or log interpolation function.	2.15-2, 5.2-9
ALKE	Log of kinetic energy (ALOG(E-RM)), used as a cumulative distribution function for fits and plots.	5.2-5, 5.3-19
ALKEI	Inverse of ALKE (=EXP(X)+RM).	5.2-5
ALIN	Linear cumulative distribution func- tion for plots (ALIN(X)=X).	5.2-5, 5.3-19
ALINI	Inverse of ALIN (=same as ALIN). Used as inverse cumulative distri- bution function in plots.	5.2-5
AONE	Derivative of ALIN (AONE(X)=1). Used as probability density function for plots.	5.2-5
ADFMOL	Approximate cumulative distribution function for Moller and Bhabha cross sections (ADFMOL(E)=-1/(E-RM)).	5.2-5, 5.3-19
ADIMOL	Inverse of ADFMOL.	5.2-5
ADDMOL	Derivative of ADFMOL.	5.2-5
AMOLDM	Moller differential cross section for a mixture of elements.	2.10-3, 5.2-5

CHAPTER 5

Table 5.2.2  
(continued)

FUNCTIONS Used In PEGS

NAME	DESCRIPTION	PAGES
AMOLFM	"One argument" form of AMOLDM.	5.2-5
AMOLRM	Moller cross section, integrated over some energy range, for a mixture of elements.	2.10-3, 5.2-5
AMOLTM	Moller total cross section for a mixture of elements.	2.10-3, 5.2-4, 5
ANIHDM	Annihilation differential cross section for a mixture of elements.	2.12-2, 5.2-5
ANIHFM	"One argument" form of ANIHDM.	5.2-5
ANIHDM	Annihilation cross section, integrated over some energy range, for a mixture of elements.	2.12-2, 5.2-5
ANIHTM	Annihilation total cross section for a mixture of elements.	2.12-2, 5.2-4, 5
APRIM	Empirical correction factor in bremsstrahlung cross section.	2.7-7, 5.2-5, 7
AREC	Reciprocal function (=derivative of $A_{LOG}(X)$ ). Used as probability density function in log plots ( $AREC(X)=1/X$ ).	5.2-5
BHABDM	Bhabha differential cross section for a mixture of elements.	2.11-3, 5.2-5
BHABFM	"One argument" form of BHABDM.	5.2-5

CHAPTER 5

Table 5.2.2  
(continued)

FUNCTIONS Used In PEGS

NAME	DESCRIPTION	PAGES
BHABRM	Bhabha cross section, integrated over some energy range, for a mixture of elements.	2.11-3, 5.2-5
BHABTM	Bhabha total cross section for a mixture of elements.	2.11-3, 5.2-4,5
BREMDR	Bremsstrahlung differential cross section for a "run-time" mixture of elements.	2.7-28, 5.2-5,8
BREMFZ	"One argument" form of BREMDR.	5.2-5,8
BREMDZ	Bremsstrahlung differential cross section for an element.	2.7-14,28 5.2-5,7
BREMFZ	"One argument" form of BREMDZ.	5.2-5,7
BREMRM	Bremsstrahlung cross section, integrated over some energy range, for a mixture of elements.	5.2-5,7
BREMRZ	Bremsstrahlung cross section, integrated over some energy range, for a "run-time" mixture of elements.	5.2-5,8
BREMRZ	Bremsstrahlung cross section, integrated over some energy range, for an element.	5.2-5,7
BREMTM	Bremsstrahlung total cross section for a mixture of elements.	5.2-4,5,7

CHAPTER 5

Table 5.2.2  
(continued)

FUNCTIONS Used In PEGS

NAME	DESCRIPTION	PAGES
BREMTR	Bremsstrahlung total cross section for a "run-time" mixture of elements.	5.2-5,8
BRMSDZ	Soft bremsstrahlung differential cross section for an element.	2.7-14, 5.2-5,7
BRMSFZ	"One argument" form of BRMSDZ.	2.7-14,
BRMSRM	Soft bremsstrahlung cross section, integrated over some energy range, for a mixture of elements.	5.2-5,7
BRMSRZ	Soft bremsstrahlung cross section integrated over some energy range, for an element.	5.2-5,7, 5.3-19
BRMSTM	Soft bremsstrahlung total cross section for a mixture of elements.	5.2-5,7
COMPDM	Compton differential cross section for a mixture of elements.	2.9-4, 5.2-5
COMPFM	"One argument" form for COMPDM.	5.2-5
COMPRM	Compton cross section, integrated over some energy range, for a mixture of elements.	2.9-4, 5.2-5
COMPTM	Compton total cross section for a mixture of elements.	2.9-4, 5.2-4,5
DCADRE	Quadrature routine to integrate $f(x)$ between a and b using cautious Romberg extrapolation.	5.2-7-10
EBIND	Function to get an average photo-electric binding energy.	5.2-4,5

## CHAPTER 5

Table 5.2.2  
(continued)

### FUNCTIONS Used In PEGS

NAME	DESCRIPTION	PAGES
EBR1	Function to determine the electron(-) branching ratio (Brem/Total).	5.2-5
EDEDX	Evaluates SPTOTE with cutoff energies of AE and AP.	2.13-7, 5.2-5
ESIG	Determines the total electron(-) interaction cross section (probability per radiation length).	5.2-5
FCOULC	Coulomb correction term in pair production and bremsstrahlung cross sections.	2.7-8, 5.2-5,7,9
FI	Function multiplexer.	5.2-1,5,6
GBR1	Function to determine the gamma-ray branching ratio (Pair/Total).	5.2-5
GBR2	Function to determine the gamma-ray branching ratio ((Pair+Compton)/Total).	5.2-5
GMFP	Function to determine the gamma-ray mean free path.	5.2-4, 5.3-18
IFUNT	Given PEGS function name, it looks it up name in table and returns the function index. Used by options that specify functions by name.	
PAIRDR	Pair production differential cross section for a "run-time" mixture of elements.	2.7-28, 5.2-5,10
PAIRDZ	Pair production differential cross section for an element.	2.7-5,28, 5.2-5,9

CHAPTER 5

Table 5.2.2  
(continued)

FUNCTIONS Used In PEGS

NAME	DESCRIPTION	PAGES
PAIRFR	"One argument" form of PAIRDZ.	5.2-5,10
PAIRFZ	"One argument" form of PAIRDZ.	5.2-5,9
PAIRRM	Pair production cross section, integrated over some energy range, for a mixture of elements.	5.2-5,9
PAIRRR	Pair production cross section, integrated over some energy range, for a "run-time" mixture of elements.	5.2-5,10
PAIRRZ	Pair production cross section, integrated over some energy range, for an element.	5.2-5,9
PAIRTE	"Empirical" total pair production production cross section for a mixture (=SUM(PZ(I)*PAIRTZ(Z(I))).	2.7-7, 5.2-5,9
PAIRTM	Pair production total cross section for a mixture of elements, obtained by numerical integration of differential cross section.	2.7-5,7, 5.2-5,9
PAIRTR	Pair production total cross section for a "run-time" mixture of elements.	5.2-5,10
PAIRTU	Pair production total cross section actually "used". Same as PAIRTE for primary energy less than 50 MeV; otherwise, same as PAIRTM.	2.7-7, 5.2-4,5,9
PAIRTZ	Computes contribution to empirical pair production total cross section for an element assuming one atom per molecule. It is obtained by log-linear interpolation of Israel-Storm data.	5.2-5,9
PBR1	Function to determine the positron branching ratio (Brem/Total).	5.2-5

CHAPTER 5

Table 5.2.2  
(continued)

FUNCTIONS Used In PEGS

NAME	DESCRIPTION	PAGES
PBR2	Function to determine the positron branching ratio ((Brem+Bhabha)/Total).	5.2-5
PDEDX	Evaluates SPTOTP with cutoff energies of AE and AP.	2.13-7, 5.2-5
PHOTTE	Determines the proper mix of PHOTTZ's for a mixture.	2.15-2, 5.2-4,5
PHOTTZ	Determines the interpolated total photoelectric cross section from tabulated data.	2.15-1, 5.2-5
PSIG	Determines the total positron interaction cross section (probability per radiation length).	5.2-5
QD	Driver function for DCADRE, the numerical integration routine.	5.2-7-10
QFIT	Utility logical function for the piecewise linear fit subroutine, PWLF. It returns .TRUE. if a given partition gives a good fit.	5.2-4, 5.3-14,15
SPIONB	Does the work for SPIONE and SPIONP. One argument tells whether to compute stopping power for electron or positron.	2.13-6,7, 5.2-7
SPIONE	Calculates the stopping power due to ionization for electrons(-).	2.13-7, 5.2-5,7
SPIONP	Calculates the stopping power due to ionization for positrons.	2.13-7, 5.2-5,7
SPTOTE	Calculates the total stopping power (ionization plus soft bremsstrahlung) for electrons(-) for specified cutoffs.	2.13-7, 5.2-4,5,7



CHAPTER 5

Table 5.2.2  
(continued)

FUNCTIONS Used In PEGS

NAME	DESCRIPTION	PAGES
SPTOTP	Calculates the total stopping power (ionization plus soft bremsstrahlung) for positrons for specified cutoffs.	2.13-7, 5.2-4,5,7
TMXB	Determines the maximum total step length consistent with Bethe's criterion.	2.14-20, 2.15-1, 5.2-5
TMXS	Determines the minimum of TMXB and 10 radiation lengths.	2.15-1, 5.2-5
TMXDE2	Included for possible future modification purposes ( $=TMXB/(E^{**2}*BETA^{**4})$ ). It might be easier to fit this quantity than to fit TMXB and then apply the denominator in EGS at run-time.	5.2-5
XSIF	Function to account for bremsstrahlung and pair production in the field of the atomic electrons.	2.7-10, 5.2-5,7,9
ZTBL	Given the atomic symbol for an element, it returns the atomic number.	

## CHAPTER 5

### 5.3 PEGS Options and Input Specifications

#### 5.3.1 Interrelations Between Options

Fig. 5.3.1 illustrates the logical relationship between options of PEGS. For example, in order to be able to use the PLTN option, one of the material specification options (ELEM, MIXT, COMP) must have already been processed. The PWLF option requires that both the ENER option and one of the material specification options precede it. To use the DECK option, it is sufficient to have validly invoked the PWLF option. The STOP and MIMS options are seen to be independent of the others.

In the following sections, for each option we will give its function, parameters which control it, the format of cards needed to invoke it, and an explanation of the routines (if any) that are used to implement it. The cards for a given option are named with the first part of their name being the option name, and the last part the card number. For example, MIXT2 is the name of the second card needed for the MIXT option. The information is summarized in Table 5.3.1. It should be noted that IBM and CDC require different formats for NAMELIST data. Also, the single card referred to as being read by NAMELIST may in fact be several cards, provided that the proper convention for continuing NAMELIST cards is followed. Once the first card (indicating the option) has been read in, however, the second card (i.e., NAMELIST/INP/) must follow (see examples at the end of Section 5.3.2). We will use the IBM form of NAMELIST in our examples.

#### 5.3.2 The ELEM, MIXT, COMP Options

The purpose of the ELEMENT, MIXTURE, and COMPOUND options is to specify the material used by the PEGS functions. As mentioned in Section 2.6, the parameters needed to specify a material are its density (RHO), the number of different kinds of atoms (NE), and, for each different kind of atom, its atomic number (Z(I)), its atomic weight (WA(I)), and its proportion either by number (PZ(I)) or by weight (RHOZ(I)). PEGS has tables for the atomic symbol (ASYMT(1:100)) and the atomic weight (WATBL(1:100)) for elements I=1 through I=100, so the type of atom is specified by giving its atomic symbol (ASYM(I)). PEGS also has a table of the densities of the elements (RHOTBL(1:100)).

CHAPTER 5

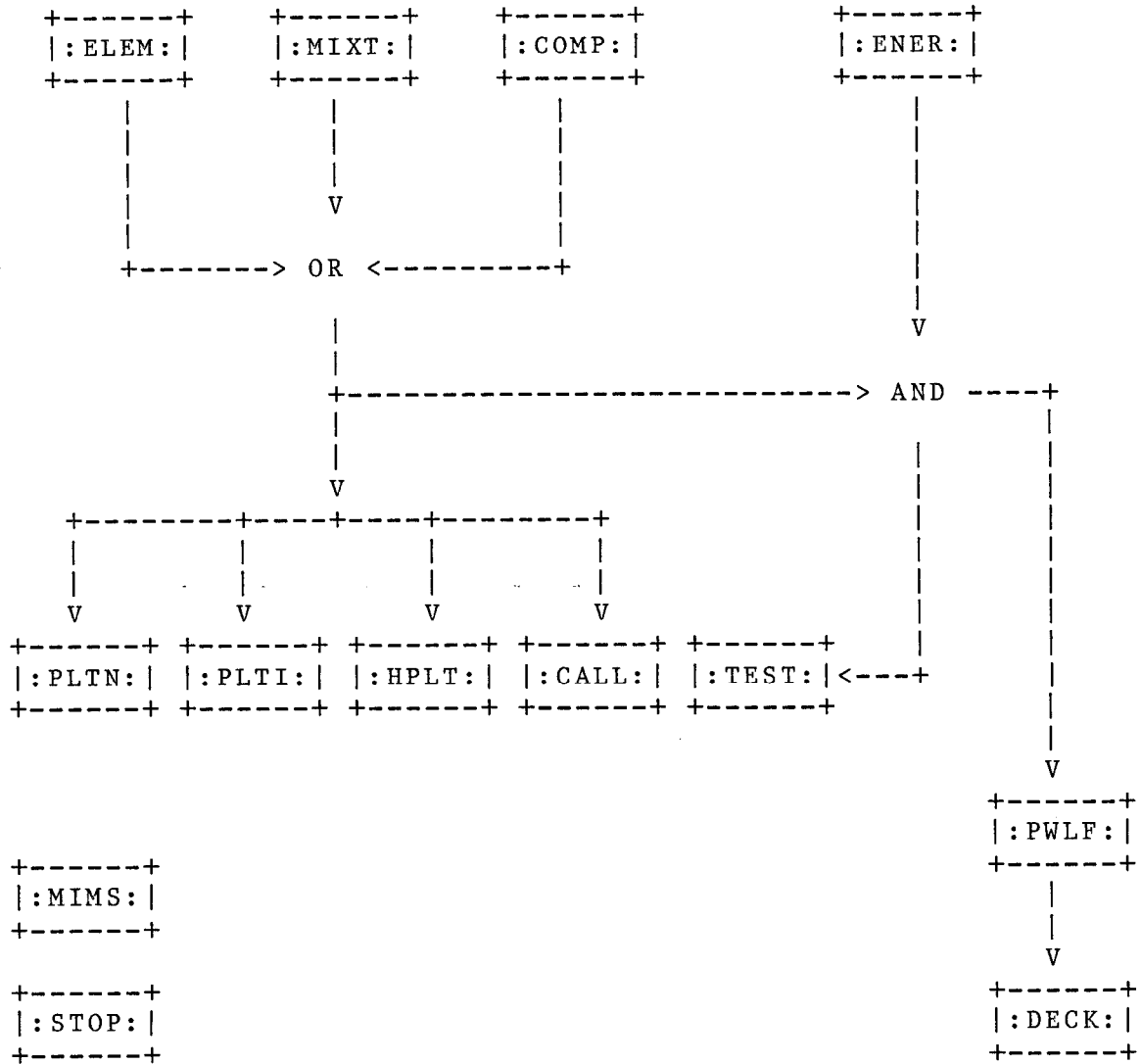


Fig. 5.3.1 Logical Relationship Between the Options of PEGS

CHAPTER 5

Table 5.3.1

PEGS Control Cards

CARD	FORMAT	VARIABLES READ	COMMENTS
ELEM1	(4A1)	OPT(1:4)	'ELEM'. Means "select material that is an element."
ELEM2	NAMELIST/INP/	RHO	Optional. If given, this over-rides the PEGS default density (g/cc) for the element.
		WA(1)	Optional. Atomic weight of element. If given, this over-rides the PEGS default.
ELEM3	(24A1, 6X,24A1)	MEDIUM(1:24)	Identifier assigned to data set to be produced.
		IDSTRN(1:24)	Optional. Identifier of medium name under which desired Sternheimer coefficients are catalogued in PEGS. If not specified, the identifier in MEDIUM(1:24) is used.
ELEM4	(24(A2,1X))	ASYM(1)	Atomic symbol for element.
COMP1	(4A1)	OPT(1:4)	'COMP'. Means "select material that is a compound."
COMP2	NAMELIST/INP/	NE	Number of elements in compound.
		RHO	Density (g/cc) of compound.
		(PZ(I),I=1,NE)	Relative numbers of atoms in compound.
		(WA(I),I=1,NE)	Optional. May be used to over-ride default atomic weights (e.g., to allow for special isotopes).

CHAPTER 5

Table 5.3.1  
(continued)

PEGS Control Cards

CARD	FORMAT	VARIABLES READ	COMMENTS
COMP3	(24A1, 6X,24A1)	MEDIUM, IDSTRN	Same as ELEM3.
COMP4	(24(A2, 1X))	(ASYM(I), I=1, NE)	Atomic symbols for the atoms in the compound. Duplicates are allowed if several isotopes of the same element are present.
MIXT1	(4A1)	OPT(1:4)	'MIXT'. Means "select material that is a mixture."
MIXT2	NAMELIST/INP/	NE	Number of elements in mixture.
		RHO	Density (g/cc) of mixture.
		(RHOZ(I), I=1, NE)	Relative amount of atom in mixture (by weight).
		(WA(I), I=1, NE)	Optional. May be used to over-ride default atomic weights.
MIXT3	(24A1, 6X,24A1)	MEDIUM, IDSTRN	Same as ELEM3.
MIXT4	(24(A2, 1X))	(ASYM(I), I=1, NE)	Same as COMP4.
ENER1	(4A1)	OPT(1:4)	'ENER'. Means "select energy limits."
ENER2	NAMELIST/INP/	AE	Lower cutoff energy (total) for charged particle transport (MeV).

CHAPTER 5

Table 5.3.1  
(continued)

PEGS Control Cards

CARD	FORMAT	VARIABLES READ	COMMENTS
		UE	Upper limit energy (total) for charged particle transport (MeV).
		AP	Lower cutoff energy for photon transport (MeV).
		UP	Upper limit energy for photon transport (MeV).
<p>Note: If the user supplies negative values for the energy limits above, the absolute values given will be interpreted as in units of the electron rest mass energy. Thus, AE=-1 is equivalent to AE=0.511 MeV.</p>			
PWLF1	(4A1)	OPT(1:4)	'PWLF'. Means "select piecewise linear fit."
PWLF2	NAMelist/INP/		Note: The following PWLF parameters (see Section 5.3.4) are optional and may be over-ridden by the user. The default values (in BLOCK DATA) are indicated below.
		EPE/0.01/	Electron EP parameter.
		EPG/0.01/	Gamma EP parameter.
		ZTHRE(1:8)/8*0./	Electron ZTHR parameter.
		ZTHRG(1:3)/0.,.1,0./	Gamma ZTHR parameter.
		ZEPE(1:8)/8*0./	Electron ZEP parameter.
		ZEPG(1:3)/0.,.01,0./	Gamma ZEP parameter.

CHAPTER 5

Table 5.3.1  
(continued)

PEGS Control Cards

CARD	FORMAT	VARIABLES READ	COMMENTS
		NIFE/20/	Electron NIP parameter.
		NIPG/20/	Gamma NIP parameter.
		NALE/\$MXEKE/	Electron NIMX parameter.
		NALG/\$MXGE/	Gamma NIMX parameter.
DECK1	(4A1)	OPT(1:4)	'DECK'. Means "punch fit data and other useful parameters."
DECK2	NAMelist/INP/		No parameters.
MIMS1	(4A1)	OPT(1:4)	'MIMS'. Means "Calculate Material Independent Multiple Scattering Data" (for EGS2 only).
MIMS2	NAMelist/INP/		MIMS is controlled by macro settings and by data in BLOCK DATA that is not accessible to the NAMelist.
TEST1	(4A1)	OPT(1:4)	'TEST'. Means "Plot the fitted functions."
TEST2	NAMelist/INP/	NPTS	Optional. Number of points to plot per function (Default=50).
CALL1	(4A1)	OPT(1:4)	'CALL'. Means "Call the designated function and print value."

CHAPTER 5

Table 5.3.1  
(continued)

PEGS Control Cards

CARD	FORMAT	VARIABLES READ	COMMENTS
CALL2	NAMelist/INP/	XP(1:4)	Values for up to four arguments of the function.
CALL3	(6A1)	NAME(1:6)	Name of function to be evaluated.
PLTI1	(4A1)	OPT(1:4)	'PLTI'. Means "Plot function given its index and the index of the distribution function."
PLTI2	NAMelist/INP/	IFUN	The index of the function to be plotted.
		XP(1:4)	Values for the static arguments (parameters).
		IV	Variable telling which argument is to be varied (e.g., IV=2 means plot function vs. its second argument).
		VLO	Lower limit for argument being varied.
		VHI	Upper limit for argument being varied.
		NPTS	Number of points to plot.
		IDF	Index of distribution function used to select independent variable.
		MP	May be used to select printer vs. graphic plot output. Not currently operational (i.e., only print plots are produced).



CHAPTER 5

Table 5.3.1  
(continued)

PEGS Control Cards

CARD	FORMAT	VARIABLES READ	COMMENTS
PLTN1	(4A1)	OPT(1:4)	'PLTN'. Means "Plot the named function."
PLTN2	NAMELIST/INP/	XP(1:4),IV, VLO,VHI,NPTS, IDF,MP	Same as PLTI2.
PLTN3	(2(6A1))	NAME(1:6)  IDFNAM(1:6)	Name (6 characters) of function to be plotted.  Name of distribution function to be used.
HPLT1	(4A1)	OPT(1:4)	'HPLT'. Means "Plot histogram to compare the sampled spectrum with the range-integrated and the differential theoretical values."
HPLT2	NAMELIST/INP/	EI  ISUB	Total energy of test particle (MeV).  Variable telling which function is being tested: 1=PAIR 2=COMPT 3=BREMS 4=MOLLER 5=BHABHA 6=ANNIH 7=MSCAT (not implemented).
HPLT3	( ' TEST DATA FOR ROUTINE=',12A1,' ,#SAMPLES=', I10,' ,NBINS=',I5)	NAMESB(1:12)  NTIMES  NBINS	Name of subroutine tested.  Number of samples.  Number of histogram bins.

CHAPTER 5

Table 5.3.1  
(continued)

PEGS Control Cards

CARD	FORMAT	VARIABLES READ	COMMENTS
HPLT4	(' IQI=',I2,',RNLO,RNHI=',2F12.8,',IRNFLG=',I2)		
		IQI	Charge of test particle.
		RNLO,RNHI	Lower and upper limits to random number preceding call to test function.
		IRNFLG	Non-zero means to "apply above limits to preceding random number to test for correlation." Zero value means "don't do this."
HPLT5...etc.	(9I8)	NH(1:NBINS)	The sampled data (from TESTSR).

-----  
(text continued from page 5.3-1)

The ELEMent option is used if the material in question has only one type of atom. In this case PEGS knows that NE=1, has the density in a table, sets PZ(1)=1, and deduces Z(1) and WA(1) from ASYM(1). Thus the atomic symbol (ASYM(1)) is the only information that the user need supply. Before each option, RHO and the WA(I) are saved and then cleared so that it can be determined whether these have been set by the user. If so, they over-ride the table values in PEGS. This allows the different atoms to be non-standard isotopes and/or allows the overall density to be adjusted to the experimental state. For options other than ELEM, MIXT, or COMP, RHO and WA(I) are restored after reading the NAMELIST.

(Note: This method of saving and restoring is a hold-over from a previous time when the option was also read by NAMELIST. It would now be possible to selectively clear RHO and WA(I) after reading OPT but before reading the NAMELIST card(s)).

## CHAPTER 5

The COMPound option is used when there is more than one different kind of atom and it is desired to give the proportions by relative number of atoms (PZ(I)). The only required data is NE, ASYM(I), and PZ(I) (for I=1,NE). Optionally, any of the WA(I) can be over-ridden.

The MIXTure option is similar to the COMPound option except that the relative atomic proportions are given by weight (RHOZ(I)) rather than by number.

When the PZ(I) values have been specified, PEGS obtains the RHOZ(I) using  $RHOZ(I)=PZ(I)*WA(I)$ ; otherwise, the PZ(I) are obtained from  $PZ(I)=RHOZ(I)/WA(I)$ . The absolute normalization of the PZ(I) and RHOZ(I) values is not important because of the way the quantities are used. For example, the macroscopic cross sections contain factors like

$$PZ(I)/SUM(PZ(I)*WA(I))$$

where the denominator is the "molecular weight".

In addition to physically specifying the material being used, a name for it must be supplied (MEDIUM(1:24)) for identification purposes. This name is included in the output deck when the DECK option is selected. The name can be different for any two data sets that are created, even though the same material has been used. For example, one might produce PEGS output using a particular material but different energy limits (or fit tolerances, density effect parameters, etc.), with separate identification names for each (e.g., FE1, FE2, etc.).

The quantity IDSTRN(1:24) is used to identify the Sternheimer density effect parameters that are tabulated in BLOCK DATA. If IDSTRN(1) is blank, then IDSTRN is given the same value as MEDIUM. If this name is not identifiable with any of those in BLOCK DATA, the Sternheimer density effect scheme is replaced by an asymptotic one (as discussed in Section 2.13).

After reading the input data for these options, subroutine MIX is called in order to compute the Z-related parameters that reside in COMMON/MOLVAR/, subroutine SPINIT is called to initialize the stopping power routines for this material, and subroutine DIFFER is called to compute run-time parameters for the pair production and bremsstrahlung sampling routines. The reader might find the comments in subroutine MIX useful.

## CHAPTER 5

The following are examples of sets of data cards that can be used with the ELEM, MIXT, and COMP options:

(Note: The NAMELIST data starts in column 2).

A. Material---Element is Iron with defaults taken.

```

                                Column
Card   123456789112345678921234567893123456789412345678..etc.

ELEM1  ELEM
ELEM2  &INP &END
ELEM3  IRON                FE
ELEM4  FE
```

B. Material---Element is Helium-3 with the density and atomic weight over-ridden by user.

```

                                Column
Card   123456789112345678921234567893123456789412345678..etc.

ELEM1  ELEM
ELEM2  &INP RHO=1.E-2,WA(1)=3 &END
ELEM3  HELIUM-3           HE
ELEM4  HE
```

C. Material---Compound is sodium iodide with IDSTRN(1:24) defaulting to MEDIUM(1:24).

```

                                Column
Card   123456789112345678921234567893123456789412345678..etc.

COMP1  COMP
COMP2  &INP NE=2,RHO=3.667,PZ(1)=1,PZ(2)=1 &END
COMP3  NAI
COMP4  NA I
```

CHAPTER 5

D. Material---Compound is polystyrene scintillator (e.g., PILOT-B or NE-102A) with data taken from the booklet:

"Particle Properties - April 1976"

by the Particle Data Group (LBL/CERN).  
The asymptotic density effect is used.

Column  
Card 123456789112345678921234567893123456789412345678..etc.  
COMP1 COMP  
COMP2 &INP NE=2,RHO=1.032,PZ(1)=1,PZ(2)=1.1 &END  
COMP3 POLYSTYRENE SCINTILLATOR  
COMP4 C H

E. Material---Mixture is lead glass, consisting of five specified elements (and 1 per cent of the trace elements unspecified). The asymptotic density effect is used.

Column  
Card 123456789112345678921234567893123456789412345678..etc.  
MIXT1 MIXT  
MIXT2 &INP NE=5,RHO=3.61,PZ=41.8,21.0,29.0,5.0,2.2 &END  
MIXT3 LEAD GLASS  
MIXT4 PB SI O K NA

F. Material---Mixture is U-235, U-238, and carbon (not a real material) with the asymptotic density effect used.

Column  
Card 123456789112345678921234567893123456789412345678..etc.  
MIXT1 MIXT  
MIXT2 &INP NE=3,RHO=16,WA=235,238,RHOZ=50,30,10 &END  
MIXT3 JUNK  
MIXT4 U U C

## CHAPTER 5

### 5.3.3 The ENER Option

The ENERGY option is used to define the electron and photon energy intervals over which it is desired to transport particles, and hence, over which fits to total cross sections and branching ratios must be made. The electron energy interval is (AE,UE) and the photon interval is (AP,UP). If any of these is entered negative, it is multiplied by  $-RM=-0.511$  MeV; that is, the absolute magnitude is assumed to be the energy in units of the electron rest mass energy. The quantities  $TE=AE-RM$ ,  $TET2=2*TE$ , and  $TEM=TE/RM$ , as well as the bremsstrahlung and Moller thresholds ( $RM+AP$  and  $AE+TM$ , respectively), are then computed and printed out.

The following are examples of sets of data cards that can be used with the ENER option:

(Note: The NAMELIST data starts in column 2).

- A. Electron and photon cutoff energies are 1.5 MeV and 10 keV, respectively. The upper energy limit for both is set at 100 GeV. (Note: All energies are in MeV and are total energies).

```

                                Column
Card      123456789112345678921234567893123456789412345678..etc.
ENER1     ENER
ENER2     &INP AE=1.5,UE=100000.,AP=0.01,UP=100000. &END
```

- B. Same as above, except  $AE=3*RM$ .

```

                                Column
Card      123456789112345678921234567893123456789412345678..etc.
ENER1     ENER
ENER2     &INP AE=-3,UE=100000.,AP=0.01,UP=100000. &END
```

### 5.3.4 The PWLF Option

The PieceWise Linear Fit option performs a simultaneous piecewise linear (vs.  $\ln(E-RM)$ ) fit of eight electron functions over the energy interval (AE,UE) and a simultaneous piecewise linear (vs.  $\ln E$ ) fit of three photon functions over the energy interval (AP,UP). Each simultaneous fit over several functions is accomplished by a single call to subroutine PWLF---once for the electrons and once for the photons.

## CHAPTER 5

By simultaneous fit we mean that the same energy sub-intervals are used for all of the functions of a set. Alternatively, we could describe it as fitting a vector function. The PWLF subroutine is an executive routine that calls the function QFIT. Function QFIT, which does most of the work, tries to perform a fit to the vector function by doing a linear fit with a given number of subintervals. It returns the value .TRUE. if the fit satisfies all tolerances and .FALSE. otherwise. Subroutine PWLF starts out doubling the number of subintervals until a successful fit is found. Additional calls to QFIT are then made to determine the minimum number of subintervals needed to give a good fit. Sometimes, because of discontinuities in the functions being fitted, a fit satisfying the specified tolerances cannot be obtained within the constraints of the number of subintervals allowed by the array sizes of EGS. When this happens, PEGS prints out the warning message (for example):

```
NUMBER OF ALLOCATED INTERVALS(= 150) WAS INSUFFICIENT
TO GET MAXIMUM RELATIVE ERROR LESS THAN      0.01
```

Even in this case a fit is produced which is sufficient most of the time.

Let NFUN be the number of components to the vector function  $F(IFUN, E(J))$  (where  $IFUN=1, NFUN$ ), and let  $E(J)$  be a sequence of points ( $J=1, NI$ ) covering the interval being fitted. The number of points ( $NI$ ) is about ten times the number of fit intervals ( $NINT$ ) in order that the fit will be well tested in the interiors of the intervals. If  $FEXACT(IFUN, J)$  and  $FFIT(IFUN, J)$  are the exact and fitted values of the  $IFUN$ -th component at  $E(J)$ , then the logical function QFIT may be given as follows:

```
LOGICAL FUNCTION QFIT(NINT);
COMMON.....etc.
QFIT=.TRUE.;
REM=0.0; "RELATIVE ERROR MAXIMUM"
NI=10*NINT;
DO J=1, NI <
  DO IFUN=1, NFUN <
    AER=ABS(FEXACT(IFUN, J)-FFIT(IFUN, J));
    AF=ABS(FEXACT(IFUN, J));
    IF(AF.GE.ZTHR(IFUN))<IF(AF.NE.0.0) REM=AMAX1(REM, AER/AF);>
    ELSE <IF(AER.GT.ZEP(IFUN)) QFIT=.FALSE.;>
  >
>
QFIT=QFIT.AND.REM.LE.EP;
RETURN; END;
```

## CHAPTER 5

Thus we see that EP is the largest allowed relative error for those points where the absolute computed value is above ZTHR(IFUN), and ZEP(IFUN) is the largest allowed absolute error for those points where the absolute computed value is less than ZTHR(IFUN).

Other features of the QFIT routine include provisions for aligning a subinterval boundary at a specified point in the overall interval (in case the fitted function has a discontinuous slope such as at the pair production or Moller thresholds), and computation of fit parameters in bins flanking the main interval to guard against truncation errors in subinterval index computations.

The net result of the fit is to obtain coefficients AX, BX, AF(IFUN,J), and BF(IFUN,J) such that

$$FVALUE(E)=AF(IFUN,INTERV)*XFUN(E) + BF(IFUN,INTERV)$$

is the value of the IFUN-th function, and where

$$INTERV=INT(AX*XFUN(E) + BX).$$

XFUN is called the distribution function and is  $\ln(E-RM)$  for electrons and  $\ln(E)$  for photons.

The coding of EGS and its original \$EVALUATE macros are designed to allow a "mapped PWLF" in which we have AX, BX, AF(IFUN,J), BF(IFUN,J), and M(I), such that when

$$I=INT(AX*XFUN(E)+BX)$$

and

$$J=M(I),$$

then

$$FVALUE(E)=AF(IFUN,J)*XFUN(E) + BF(IFUN,J)$$

for the IFUN-th function. This kind of fit has the advantage that it could get a better fit with a smaller amount of stored data. However, this fitting scheme has never been implemented in PEGS. With the present scheme more data than necessary is used in describing the functions at the higher energies where they vary quite smoothly.



## CHAPTER 5

The following is an example of the data cards that can be used with the PWLF option:

```

                                Column
Card      123456789112345678921234567893123456789412345678..etc.

PWLF1     PWLF
PWLF2     &INP &END
```

### 5.3.5 The DECK Option

The DECK option prints and punches the data needed to specify the current material, the energy intervals specified, various computed molecular parameters (e.g., the radiation length), the run-time parameters for pair production and bremsstrahlung, and the fit data produced by the PWLF option. In other words, DECK prints and punches anything that might be of use to EGS in simulating showers, or to the user in his analysis routines. The macros ECHOREAD and ECHOWRITE have been written to give nicely captioned print-outs of data (read or written) and to eliminate the need for creating separate write statements to echo the values.

Subroutines DECK (in PEGS) and HATCH (in EGS) are a matched pair in that HATCH reads what DECK writes (perhaps subroutine DECK should be renamed LAY...?). Thus, if the user would like to get more information at EGS run-time, he need only modify DECK and HATCH accordingly.

DECK should be invoked when either ELEM, MIXT, or COMP and ENER and PWLF have been run for the current material and before any of these have been executed for the next material (see Fig. 5.3.1).

The following is an example of the data cards that can be used with the DECK option:

```

                                Column
Card      123456789112345678921234567893123456789412345678..etc.

DECK1     DECK
DECK2     &INP &END
```

## CHAPTER 5

### 5.3.6 The MIMS Option and the CMS Code

The MIMS option produces a data set for EGS (Version 2 only) that contains Material Independent Multiple Scattering data. A stand alone program, CMS (Continuous Multiple Scattering), performs an analogous function for EGS3, except that the data is held in a BLOCK DATA subprogram in the EGS code itself rather than in an external data set.

In the sense that these data sets are produced already, the MIMS option and CMS code are now dispensable. However, as documentation for the origin of the present data, they are valuable and they will be maintained with the EGS Code System. It might be desirable to incorporate the CMS code into future versions of PEGS since it has various functions related to multiple scattering which one might want to plot.

The following is an example of the data cards that can be used with the MIMS option:

```

                                Column
Card      123456789112345678921234567893123456789412345678..etc.

MIMS1     MIMS
MIMS2     &INP &END
```

### 5.3.7 The TEST Option

The TEST option is used as an easy way to obtain plots of all the functions that the PWLF option fits. These plots are valuable in getting a feel for the magnitudes and variations of the fitted functions.

The following is an example of the data cards that can be used with the TEST option:

```

                                Column
Card      123456789112345678921234567893123456789412345678..etc.

TEST1     TEST
TEST2     &INP NPTS=50 &END
```

## CHAPTER 5

### 5.3.8 The CALL Option

The CALL option is used whenever one desires to have PEGS evaluate a particular function and print out the results.

The following is an example of the data cards that can be used with the CALL option in order to test for discontinuities in GMFP (Gamma Mean Free Path) near 50 MeV. (Note: In this example we have included the (necessary) ELEM option cards for Lead).

Card	Column
ELEM1	ELEM
ELEM2	&INP &END
ELEM3	PB
ELEM4	PB
CALL1	CALL
CALL2	&INP XP(1)=49.99 &END
CALL3	GMFP
CALL1	CALL
CALL2	&INP XP(1)=50.01 &END
CALL3	GMFP

The resulting output from PEGS is:

```
OPT=CALL
FUNCTION CALL:      1.95297      = GMFP   OF      49.9900
OPT=CALL
FUNCTION CALL:      1.97129      = GMFP   OF      50.0100
```

### 5.3.9 The PLTI and PLTN Options

The PLTI and PLTN options may be used to obtain printer--- and with some work, possibly graphic---plots of any of the functions in the PEGS function table. The PLTI option is rather primitive in that the functions involved must be specified by number, so we shall instead concentrate on the PLTN option in which the functions are specified by name.

## CHAPTER 5

Consider the function  $BRMSRZ(Z,E,K1,K2)$  which is the soft bremsstrahlung cross section (for an electron of total energy  $E$  and element  $Z$ ) integrated over the photon energy range  $(K1,K2)$ . Suppose we would like to see a plot of  $BRMSRZ(2,E,0.0,1.5)$  for values of  $E$  from 5 to 100 MeV. Also assume we want the data points evenly spaced in  $\ln(E)$ . Then (see Table 5.3.1) the function name is 'BRMSRZ', the distribution function name is  $IDNAM='ALOG'$ , the static arguments are  $XP(1)=2.$ ,  $XP(3)=0.0$ ,  $XP(4)=1.5$ , the independent variable is the second argument (i.e.,  $IV=2$ ), and its limits are  $VLO=5.0$  and  $VHI=100.0$ . If we want 100 points on the plot we let  $NPTS=100$ . No graphics are currently implemented, so we ignore  $MP$ . The cards necessary to accomplish this plot are:

Card	Column
PLTN1	PLTN
PLTN2	&INP XP(1)=2.,XP(3)=0.0,XP(4)=1.5,IV=2,VLO=5., VHI=100.,NPTS=100 &END
PLTN3	BRMSRZALOG

Distribution functions that are available are indicated below:

IDFNAM	Purpose
'ALIN'	Linear plot.
'ALOG'	Natural log plot.
'ALKE'	Natural log of electron kinetic energy plot.
'ADFMOL'	Approximation to Moller and Bhabha distributions (i.e., $1/K.E.$ distribution).

### 5.3.10 The HPLT Option

The Histogram PLoT option is designed to be used in conjunction with the TESTSR (TEST Sampling Routine) program (see Section 2.6 and Chapter 6).

The basic idea is that a probability density function (see Section 2.1),  $PDF(X)$ , is to be sampled by EGS (note:  $PDF(X)$  will have other static arguments which we ignore for this discussion). Let  $CDF(X)$  be the cumulative distribution function associated with  $PDF(X)$ . If  $PDF(X)$  drops sharply with increasing  $X$ , we will not get many samples in the bins with

## CHAPTER 5

large X unless we make the bins themselves larger in such regions. We accomplish this by finding another p.d.f. and c.d.f., PDG(X) and CDG(X), respectively, such that PDG(X) approximates PDF(X). If we want N bins, we then pick the X(I) such that

$$CDG(X(I+1)) - CDG(X(I)) = (CDG(X(N+1)) - CDG(X(I))) / N.$$

For all I, this implies that

$$X(I) = CDGI((CDG(X(N+1)) - CDG(X(1))) * I / (N+1) + CDG(X(1)))$$

where CDGI is the inverse function of CDG. Thus, if PDG(X) is a reasonable approximation, the histogram bins at large X should have the same order of magnitude of counts as those at lower X. The function CDG(X) is called the "distribution function" in the context of the HPLT option. CDG(X), CDGI(X), and PDG(X) are used by the TESTSR and HPLT programs. If we let SPDF(X) and SCDF(X) be the "sampled" data, and PDF(X) and CDF(X) be the theoretical data, then the routine HPLT can be summarized by the pseudo-code:

```
DO I=1,N <
  PLOT((SCDF(X(I+1))-SCDF(X(I)))/(CDG(X(I+1))-CDG(X(I))));
  PLOT((CDF(X(I+1))-CDF(X(I)))/(CDG(X(I+1))-CDG(X(I))));

DO....X(I) at 10 points in the interval (X(I),X(I+1)) <
  PLOT(d(SCDF)/d(CDG)=PDF(X)/PDG(X));>
>
RETURN; END;
```

Thus the theoretical and sampled distributions can be compared and problems with the sampling routine (or the random number generator, for example) can be detected.

All of the control cards for the HPLT option are punched directly by the TESTSR routine. The reader should consult Chapter 6 for an example of how the HPLT option of PEGS can be used in conjunction with EGS by means of the User Code TESTSR.

## CHAPTER 5

### 5.4 Concluding Remarks

In the previous sections we have seen the various uses for PEGS. We summarize by giving the option sequences most generally used.

- A. Minimal material data set creation (for use by EGS).
  - 1. ELEM (or MIXT, or COMP)
  - 2. ENER
  - 3. PWLF
  - 4. DECK
  
- B. Same as A. with default plots of all the functions that the PWLF option fits.
  - 1. ELEM (or MIXT, or COMP)
  - 2. ENER
  - 3. TEST
  - 4. PWLF
  - 5. DECK
  
- C. Comparison of theoretical and sampled distributions by means of the HPLT option.
  - 1. ELEM (or MIXT, or COMP)  
Note: Data cards should agree with those used with the TESTSR run.
  - 2. HPLT  
Note: Data cards come directly from TESTSR.
  
- D. Selective plotting of various functions.
  - 1. ELEM (or MIXT, or COMP) - for material 1
  - 2. PLTN - for function 1
  - 3. PLTN - for function 2,....etc.
  
  - 4. ELEM (or MIXT, or COMP) - for material 2,....etc.
  - 5. PLTN - for function 1
  - 6. PLTN - for function 2,....etc.

## CHAPTER 6

### 6. TESTSR---A USER CODE TO TEST THE SAMPLING ROUTINES

#### 6.1 Introduction

TESTSR (Test Sampling Routine) is a User Code designed to systematically test the secondary energy distribution sampling routines of EGS---namely, PAIR, COMPT, BREMS, MOLLER, BHABHA, and ANNIH. TESTSR also samples the multiple scattering angle by means of subroutine MSCAT.

Figure 6.1.1 illustrates the logical relationships between parts of TESTSR and EGS. The MAIN program of TESTSR reads (or sets) control information to determine the medium to be used for the test, the routine to be tested, and the primary particle energy. Subroutine HATCH is called to read in the material data. The SAMPLE routine is then called with appropriate arguments by means of subroutine SELECT. One of SAMPLE's arguments is the name of the external routine to be sampled. Other arguments specify the method of binning the secondary energies and the number of samples (or the desired precision).

SAMPLE repeatedly sets up the particle stack with an appropriate primary particle, calls the sampling routine, and then looks at the stack to see what energies were given to the secondary particles. The value of the energy of one of the secondary particles is used to select the bin to be incremented. This process continues until either the number of samples that had been requested is obtained, the relative error corresponding to the least counts in any one bin is less than the desired precision, or until the job runs out of time. In any case, SAMPLE then outputs control data that can be used by PEGS in order to produce a line printer plot comparing the sampled and theoretical distributions (see Section 5.3.10). A listing of the TESTSR code is given in the next section.

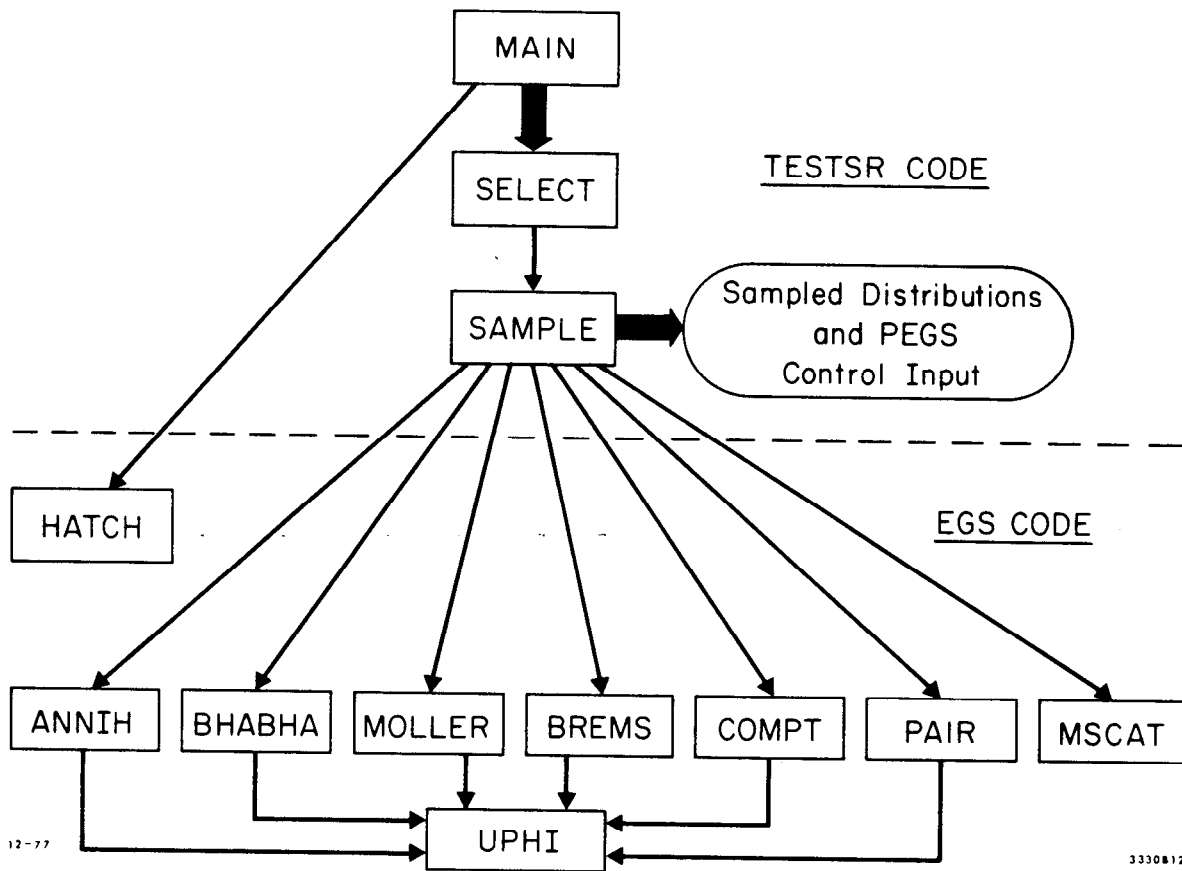


Fig. 6.1.1 Logical Relations Between Parts of EGS and the TESTSR User Code.



## CHAPTER 6

### 6.2 TESTSR Code Listing

The following is a typical TESTSR code listing. In this example, the secondary energy distribution of Compton photons is sampled for 10 MeV primaries incident on aluminum. The reader can refer to the code listing for an explanation of the other parameters that are involved.

```
%E
"TESTSR---USER CODE TO TEST COMPTON SCATTERING (ISUB=2)"

%'$TIMEOUT<'='CALL LEFT1(KTIMEL);IF(KTIMEL.LT.1500)<'

"SHORT MAIN PROGRAM TO CALL SUBROUTINES HATCH AND SELECT"
;COMIN/EPCONT,MEDIA,MISC,THRESH,USEFUL/;
INTEGER MEDARR(24)/$S'AL',22*' '/;

DO J=1,24 <MEDIA(J,1)=MEDARR(J);>
CALL HATCH;
ISUB=2; "COMPT"
EI=10.0; "INCIDENT TOTAL ENERGY"
IQI=0; "PHOTON"
IMED=1;
IRNFLG=0;
PRECN=1000000.;
NBINS=20;
CALL SELECT(ISUB,EI,IQI,IMED,IRNFLG,PRECN,NBINS);
STOP;
END; "END OF MAIN PROGRAM OF TESTSR"

%E
SUBROUTINE SELECT(ISUB,EI,IQI,IMED,IRNFLG,PRECN,NBINS);

"ROUTINE TO TEST EGS SAMPLING ROUTINES"
"ISUB TELL WHICH ONE TO TEST"
" =1 PAIR"
" =2 COMPT"
" =3 BREMS"
" =4 MOLLER"
" =5 BHABHA"
" =6 ANNIH"
" =7 MSCAT"
"EI IS THE ENERGY(IN MEV) AT WHICH TO TEST"
"IQI IS CHARGE OF PARTICLE. "
"IMED IS INDEX OF MEDIUM"
```

## CHAPTER 6

```
"IRNFLG DETERMINES THE CONDITIONS UNDER WHICH THE ROUTINES"
"   ARE SAMPLED.  IRNFLG.NE.0 MEANS REQUIRE THE RANDOM"
"   NUMBER SELECTED BEFORE THE SAMPLING ROUTINE IS CALLED"
"   TO BE IN THE LIMITS DETERMINED BY BRANCHING RATIOS."
"   IRNFLG=0 MEANS THIS REQUIREMENT IS NOT MADE."
"PRECN DETERMINES THE PRECISION OF THE TEST"
"  >1 MEANS SAMPLE PRECN TIMES."
"  <1 MEANS SAMPLE UNTIL RELATIVE ERROR IS < PRECN."
"NBINS IS THE NUMBER OF BINS IN THE HISTOGRAM."
```

```
;COMIN/ELECIN,PHOTIN,THRESH,USEFUL/;
EXTERNAL PAIR,COMPT,BREMS,MOLLER,BHABHA,ANNIH,ALIN,ALOG,EXP,
AMOLD,AMOLI,MSCAT;
```

```
"PREPARE TO EVALUATE BRANCHING RATIOS"
```

```
MEDIUM=IMED;
IF(ISUB.LE.2)<ELN=ALOG(EI);$SET INTERVAL ELN,GE,GEM;>
ELSE<ELN=ALOG(EI-RM);$SET INTERVAL ELN,EKE,EEM;>
```

```
GO TO (:PAIR:, :COMPT:, :BREMS:, :MOLLER:, :BHABHA:, :ANNIH:,
      :MSCAT:), ISUB;
OUTPUT ISUB;(' ILLEGAL ISUB=', I10);
STOP;
```

```
:PAIR:
RNLO=0.0;
$EVALUATE RNHI USING GBRI(ELN);
CALL SAMPLE(ISUB, PAIR, ALIN, ALIN, RM, EI-RM,
EI, IQI, RNLO, RNHI, IRNFLG, PRECN, NBINS);
RETURN;
```

```
:COMPT:
$EVALUATE RNLO USING GBRI(ELN);
$EVALUATE RNHI USING GBR2(ELN);
CALL SAMPLE(ISUB, COMPT, ALOG, EXP, EI/(1.+2.*EI/RM), EI,
EI, IQI, RNLO, RNHI, IRNFLG, PRECN, NBINS);
RETURN;
```

```
:BREMS:
RNLO=0.0;
IF(IQI.LT.0)<$EVALUATE RNHI USING EBRI(ELN);>
ELSE<$EVALUATE RNHI USING PBRI(ELN);>
CALL SAMPLE(ISUB, BREMS, ALOG, EXP, AP(MEDIUM), EI-RM,
EI, IQI, RNLO, RNHI, IRNFLG, PRECN, NBINS);
RETURN;
```

## CHAPTER 6

```
:MOLLER:
$EVALUATE RNLO USING EBRI(ELN);
RNHI=1.0;
CALL SAMPLE(ISUB,MOLLER,AMOLD,AMOLI,AE(MEDIUM),RM+(EI-RM)/2.,
EI,IQI,RNLO,RNHI,IRNFLG,PRECN,NBINS);
RETURN;
```

```
:BHABHA:
$EVALUATE RNLO USING PBR1(ELN);
$EVALUATE RNHI USING PBR2(ELN);
CALL SAMPLE(ISUB,BHABHA,AMOLD,AMOLI,AE(MEDIUM),EI,
EI,IQI,RNLO,RNHI,IRNFLG,PRECN,NBINS);
RETURN;
```

```
:ANNIH:
$EVALUATE RNLO USING PBR2(ELN);
RNHI=1.0;
PINC=SQRT(EI**2-RM**2);
CALL SAMPLE(ISUB,ANNIH,ALOG,EXP,(EI+RM)*RM/(EI+RM+PINC),
(EI+RM)/2.0,EI,IQI,RNLO,RNHI,IRNFLG,PRECN,NBINS);
RETURN;
```

```
:MSCAT:
CALL SAMPLE(ISUB,MSCAT,ALIN,ALIN,0.,3.14159/5.,
EI,IQI,0.,1.,0,PRECN,NBINS);
RETURN;
```

```
END; "END OF SUBROUTINE SELECT"
```

```
FUNCTION ALIN(X);
ALIN=X;
RETURN;
END;
```

```
FUNCTION AMOLD(X);
COMIN/USEFUL/;
AMOLD= 1./(X-RM);
RETURN;
END;
```

```
FUNCTION AMOLI(X);
COMIN/USEFUL/;
AMOLI= 1./X + RM;
RETURN;
END;
```

CHAPTER 6

```

%E
SUBROUTINE SAMPLE(ISUB,FUN,XDF,XDFI,ELO,EHI,EI,IQI,RNLO,RNHI,
IRNFLG,P,N);

"ROUTINE TO CALL A SAMPLING ROUTINE MANY TIMES AND HISTOGRAM"
"THE RESULTING SPECTRUM. THE RESULTS ARE OUTPUT IN A FORM"
"WHICH CAN BE PROCESSED BY PEG'S OPTION HPLT."
"FUN IS THE SAMPLING ROUTINE BEING TESTED."
"XDF IS A CUMULATIVE DISTRIBUTION FUNCTION WHICH APPROXIMATES"
" THE CUMULATIVE DISTRIBUTION FUNCTION OF FUN."
"XDFI IS THE INVERSE OF FUNCTION XDF"
"ELO IS THE LOWEST 2NDARY ENERGY THAT SHOULD BE GENERATED."
"EHI IS THE HIGHEST 2NDARY ENERGY THAT SHOULD BE GENERATED."
"IF IRNFLG IS NON-ZERO, THEN BEFORE EACH CALL THE FUN,"
"RANDOM NUMBERS WILL BE SELECTED UNTIL ONE IS FOUND BETWEEN"
"RNLO AND RNHI. IF PRECN>1, FUN WILL BE CALLED PRECN TIMES."
"IF PRECN<1, FUN WILL BE CALLED UNTIL THE LARGEST RELATIVE"
" ERROR IN ANY BIN IS LESS THAN PRECN."
"N IS THE NUMBER OF BINS"

INTEGER NAME(12),NAMET(12,7),NMAX/500/,NH(500),B(100)
,XC/'X'/,BLNK/' '/;
DATA NAMET/SS'PAIR E+ ',SS'COMPT G ',
SS'BREMS G ',SS'MOLLER ELO ',
SS'BHABHA E- ',SS'ANNIH G ',SS'MULT SCAT '/;
LOGICAL PRFLG;
;COMIN/EPCONT,RANDOM,STACK,UPHIOT/;
DATA XI/0./,YI/0./,ZI/0./,UI/1./,VI/0./,WI/0./,DNEARI/0./,
WTI/1./;
DATA IRI/1/;
INTEGER IQF(2,6);
DATA IQF/1,-1,0,-1,0,-1,-1,-1,-1,1,0,0/;
IQF(2,3)=IQI;
DO ICH=1,12 <NAME(ICH)=NAMET(ICH,ISUB);>
PRFLG=P.LT.1.0;
IPREC=P;
NP1=N+1;
NP2=N+2;
DO IBIN=1,NP2 <NH(IBIN)=0;>
NTIMES=0;
XFMN=XDF(ELO);
XFMX=XDF(EHI);
AX=N/(XFMX-XFMN);
BX=2.0-XFMN*AX;
: OUTER: LOOP<"CHECK TIMEOUT OR OTHER TERMINATION AFTER"
" EACH OUTER LOOP."

```

## CHAPTER 6

```

IF (PRFLG) <NLOOP=200;>
ELSE <NLOOP=MIN0(200, IPREC-NTIMES);>

:INNER:DO IS=1, NLOOP <
NP=1;
E(1)=EI; IQ(1)=IQI; U(1)=UI; V(1)=VI; W(1)=WI;
$TRANSFER PROPERTIES TO (1) FROM I;

"NOW CONDITION RANDOM NUMBER GENERATOR, IF REQUESTED"
IF (IRNFLG.NE.0) <
LOOP <$RANDOMSET RN;> UNTIL (RNLO.LE.RN).AND.(RN.LE.RNHI);
>

CALL FUN; "CALL SAMPLING ROUTINE"

"NOW CHECK RESULTS"
IF (NP.NE.2.AND.ISUB.LT.7.OR.NP.NE.1.AND.ISUB.EQ.7) <
  OUTPUT NP; (' NP ERROR, FINAL NP=', I10);>
IF (ISUB.LT.7) <
IF (IQF(1, ISUB).EQ.IQ(NP)) <"DESIRED RESULT IS ON TOP OF STACK"
IF (IQF(2, ISUB).NE.IQ(1)) <
: IQERROR: OUTPUT IQ(1), IQ(2); (' IQ ERROR, IQS=', 2I3); STOP;>
XV=E(2);>
ELSE <"RESULT IS ON NEXT TO TOP"
IF ((IQF(1, ISUB).NE.IQ(1)).OR.(IQF(2, ISUB).NE.IQ(2)))
GO TO :IQERROR:;
XV=E(1);>
>
ELSE <XV=THETA;>

"NOW ACCUMULATE INTO HISTOGRAM"
IBIN=MAX0(1, MIN0(NP2, IFIX(AX*XDF(XV)+BX)));
NH(IBIN)=NH(IBIN)+1;
> "END OF INNER LOOP"

NTIMES=NTIMES+NLOOP;
"SEE IF WE ARE RUNNING OUT OF TIME"
$TIMEOUT <EXIT :OUTER:;>
"NOW TEST FOR DESIRED PRECISION"
IF (PRFLG) <"TEST FOR DESIRED RELATIVE ERROR"
MIN=NH(2); DO IBIN=3, NP1 <MIN=MIN0(MIN, NH(IBIN));>
RE=1./SQRT(FLOAT(MAX0(MIN, 1)));
IF (RE.LE.P) EXIT :OUTER:;
>
ELSE <"SPECIFEC NUMBER OF CALLS WAS REQUESTED."
IF (NTIMES.GE.IPREC) EXIT :OUTER:;
>

```

CHAPTER 6

```

>REPEAT "OUTER LOOP"

"      FIND MAXIMUM NUMBER OF COUNTS FOR SCALING.  "
MAX=NH(1); DO IBIN=2, NP2 <MAX=MAX0(MAX, NH(IBIN)); >
SCLY=100./FLOAT(MAX);
"      PUT OUT CAPTION AND ALSO PUNCH OUT VALUES  "
UOUTPUT(7)EI, ISUB, NAME, NTIMES, N, IQI, RNLO, RNHI, IRNFLG, TVSTEP,
(NH(IBIN+1), IBIN=1, N);
('HPLT', /, ' &INP EI=', F10.3, ', ISUB=', I2, ', &END' /
' TEST DATA FOR ROUTINE=', I2A1, ', #SAMPLES=', I10, ', NBINS=', I5 /
' IQI=', I2, ', RNLO, RNHI=', 2F12.8, ', IRNFLG=', I2, ', TVSTEP=',
G15.7/(9I8));
OUTPUT NAME, NTIMES, EI, ELO, EHI, P, N, IQI, RNLO, RNHI, IRNFLG;
('1PLOT OF TEST DATA FOR ROUTINE ', I2A1, ', #SAMPLES=', I10 /
 1X, 'EI=', 1PG10.5, ', ELO=', G12.5, 'EHI=', G12.5, ', REQ'D PRECN=',
G9.2, ', NBINS=', I3 /
' IQI=', I2, ', RNLO, RNHI=', 2F12.8, ', IRNFLG=', I2 /
3X, 'ABCISSA', 6X, 'COUNTS', 3X, 'F(X)      ....5...10...15...20..',
'.25...30...35...40...45...50...55...60...65...70...75..',
'.80...85...90...95..100' /);
"      INITIALIZE PLOT VECTOR  "
DO ICOL=1, 100 < B(ICOL)=BLNK; >
"      NOW DO THE PLOT  "
DO IBIN=1, NP2 <
ICOL=MAX0(1, MIN0(100, IFIX(SCLY*NH(IBIN))+1));
B(ICOL)=XC;
XV=0.0;
IF(IBIN.GT.1)XV=XDFI((IBIN-BX)/AX);
FX=NH(IBIN)/FLOAT(NTIMES);
OUTPUT XV, NH(IBIN), FX, B; (1X, 1PE14.5, I7, OPF10.6, 100A1);
B(ICOL)=BLNK;
> "END IBIN LOOP"

"CALCULATE AND OUTPUT MULTIPLE SCATTERING DATA FOR"
"MSCAT OPTION."

IF(ISUB.EQ.7) <"FOR MSCAT OPTION, WRITE-OUT TABLE FOR"
"      FRACTION/SQ.DEG."
OUTPUT; ('MULTIPLE SCATTERING TABLE OF FRACTION/SQ.DEGREE:'
, //);

DO IBIN=2, NP1 <
  XV1=XDFI((IBIN-BX)/AX);
  XV2=XDFI((IBIN+1-BX)/AX);
  OMEGA=2*PI*(COS(XV1)-COS(XV2))*(180./PI)**2; "SOLID ANGLE"
"      IN SQ. DEG."

```

## CHAPTER 6

```
FX=NH(IBIN)/FLOAT(NTIMES);
FXN=FX/OMEGA; "FRACTION/SQ.DEG."
XV1=XV1*180./PI; XV2=XV2*180./PI; "CHANGE TO DEGREES"
"                                     FOR PRINT OUT."

OUTPUT XV1,XV2,FX,FXN;
(1X,G15.7,' TO ',G15.7,' DEGREES',5X,'FRACTION=',G15.7,5X,
'FRACTION/SQ.DEG.=' ,G15.7);
>
>

RETURN;
END; "END OF SUBROUTINE SAMPLE"

"DUMMY AUSGAB AND HOWFAR NEEDED AND DEFINED BELOW"

SUBROUTINE AUSGAB;
RETURN;
END;

SUBROUTINE HOWFAR;
RETURN;
END;
```

### 6.3 Output from TESTSR

In addition to data cards that can be used for the HPLT option of PEGS (see Section 6.4), a plot of the sampled secondary energy distribution for the routine in question is given as output from the TESTSR User Code. Figure 6.3.1 shows the line printer plot obtained by using the TESTSR code listed in Section 6.2 above.

For subroutine MSCAT, the sampled secondary energy distribution is not the quantity of interest. Instead, the TESTSR User Code plots the result of sampling the multiple scattering angle, and no data card output is presently available for use in PEGS.

PLOT OF TEST DATA FOR ROUTINE COMPT G ,#SAMPLES= 748600  
 EI=10.000 ,ELO= .24914 EHI= 10.000 ,REQ'D PRECN= 1.0E+06,NBINS= 20  
 IQI= 0,RNLO,RNHI= 3.59964252 10.0000286 ,IBNPLG= 0  
 ABCISSA COUNTS F(X) ....5...10...15...20...25...30...35...40...45...50...55...60...65...70...75...80...85...90...95...100

ABCISSA	COUNTS	F(X)	
0.0	0	0.0	X
2.49137E-01	34263	0.045769	
2.99651E-01	33403	0.044621	X
3.60407E-01	33292	0.044472	X
4.33482E-01	33040	0.044136	X
5.21374E-01	32425	0.043314	X
6.27087E-01	32713	0.043699	X
7.54234E-01	32534	0.043460	X
9.07160E-01	32342	0.043203	X
1.09109E+00	32784	0.043794	X
1.31232E+00	32688	0.043666	X
1.57840E+00	32942	0.044005	X
1.89844E+00	33629	0.044923	X
2.28336E+00	34248	0.045749	X
2.74633E+00	35305	0.047161	X
3.30317E+00	37126	0.049594	X
3.97291E+00	39623	0.052929	X
4.77845E+00	42668	0.056997	X
5.74732E+00	46936	0.062698	X
6.91263E+00	53603	0.071604	X
8.31422E+00	63036	0.084205	X
1.00000E+01	0	0.0	X

Fig. 6.3.1

6.3-2



## CHAPTER 6

### 6.4 Using the TESTSR Card Output with the HPLT Option of PEGS

As described in Section 5.3.10, the TESTSR control data output can be used along with the HPLT option of PEGS in order to produce a line printer plot comparing the sampled and theoretical distributions. The deck setup corresponding to the sample problem described above is as follows:

```
ELEM
  &INP &END
AL          DUMMY NAME
AL
HPLT
  &INP EI=    10.000,ISUB= 2,&END
  TEST DATA FOR ROUTINE=COMPT G, #SAMPLES=748600, NBINS=20
  IQI=0, RNLO,RNHI=0.35996425 1.00000286, IRNFLG= 0
  34263 33403 33292 33040 32425 32713 32534 32342 32784
  32688 32942 33629 34248 35305 37126 39623 42668 46936
  53603 63036
```

Note: The data above has been condensed (columnwise) in order to fit on this page. The actual output from TESTSR, corresponding to the last seven data cards above, is in the correct format for use with the HPLT option of PEGS, however.

The line printer plot comparing the sampled and theoretical distributions is shown in Fig. 6.4-1. Three types of data are plotted here; namely, the differential cross section points (D), the range-integrated points (R), and the sampled Monte Carlo points (M). In this particular example, we have limited the D-points to two in order to shorten the plot (the default is IPNTS=10). The range of integration is determined by the D-values to the right of each R.

To check the sampled data against the theoretical data, it suffices to compare M and R as a function of energy. In this example there are twenty such pairs because we chose NBINS=20 in the TESTSR example above. The M and R results do, in fact, agree with one another over the entire energy range plotted, and one can conclude that the routine being checked (i.e., COMPT) correctly samples the secondary energy in the range specified (i.e., 10 MeV down to the kinematic Compton limit) for the material selected (i.e., aluminum).

```

HPLT FUNCTIONS:MCNTE,DSIG,RSIG,TSIG,CDP,CDFINVERSE,PDF=COMPT G      ,COMPON,COMPEN,COMPTN,ALOG ,EXP ,AREC
BTOT,TTOT=      3.54640E-01      3.54640E-01
HPLT:RAW EGS DATA FOR ROUTINE COMPT G      ,EI,ELO,ERI=      10.000      0.249      10.000,NBINS,NTIMES=      20      748600,DATA=
34263      33403      33292      33080      32425      32713      32534      32302      32784      32688
32942      33629      34248      35305      37126      39623      42668      46936      53603      63036
KEY TO PLOT,H=MCNTECARLO DATA,F=THEORETICAL INTEGRALS OVER BINS,D=DIFFERENTIAL CROSS-SECTION
ENERGY      VALUE
2.49138E-01      8.79209E-02 I
2.49138E-01      8.79470E-02 I
2.49138E-01      8.87198E-02 I
2.99653E-01      8.72247E-02 I
2.99653E-01      8.57141E-02 I
2.99653E-01      8.65970E-02 I
2.99653E-01      8.72247E-02 I
3.60410E-01      8.60142E-02 I
3.60410E-01      8.54293E-02 I
3.60410E-01      8.55131E-02 I
3.60410E-01      8.60142E-02 I
4.33486E-01      8.50506E-02 I
4.33486E-01      8.47826E-02 I
4.33486E-01      8.46609E-02 I
4.33486E-01      8.50506E-02 I
5.21378E-01      8.43063E-02 I
5.21378E-01      8.32045E-02 I
5.21378E-01      8.40182E-02 I
5.21378E-01      8.43063E-02 I
6.27091E-01      8.37638E-02 I
6.27091E-01      8.39435E-02 I
6.27091E-01      8.35730E-02 I
6.27091E-01      8.37638E-02 I
7.54238E-01      8.34152E-02 I
7.54238E-01      8.34842E-02 I
7.54238E-01      8.33226E-02 I
7.54238E-01      8.34152E-02 I
9.07165E-01      8.32651E-02 I
9.07165E-01      8.29915E-02 I
9.07165E-01      8.32793E-02 I
9.07165E-01      8.32651E-02 I
1.09110E+00      8.33316E-02 I
1.05110E+00      8.41257E-02 I
1.09110E+00      8.34680E-02 I
1.09110E+00      8.33316E-02 I
1.31233E+00      8.36509E-02 I
1.31233E+00      8.38794E-02 I
1.31233E+00      8.39373E-02 I
1.31233E+00      8.36509E-02 I
1.57841E+00      8.42828E-02 I
1.57841E+00      8.45311E-02 I
1.57841E+00      8.47623E-02 I
1.57841E+00      8.42828E-02 I
1.89845E+00      8.53195E-02 I
1.89845E+00      8.62941E-02 I
1.89845E+00      8.60566E-02 I
1.89845E+00      8.53195E-02 I
2.28337E+00      8.68989E-02 I
2.28337E+00      8.78825E-02 I
2.28337E+00      8.79880E-02 I
2.28337E+00      8.68989E-02 I
2.74634E+00      8.92228E-02 I
2.74634E+00      9.05948E-02 I
2.74634E+00      9.08020E-02 I
2.74634E+00      8.92228E-02 I
3.30318E+00      9.25849E-02 I
3.30318E+00      9.52675E-02 I
3.30318E+00      9.45529E-02 I
3.30318E+00      9.25849E-02 I
3.97292E+00      9.74098E-02 I
3.97292E+00      1.01675E-01 I
3.97292E+00      1.00655E-01 I
3.97292E+00      9.74098E-02 I
4.77846E+00      1.04311E-01 I
4.77846E+00      1.05489E-01 I
4.77846E+00      1.08948E-01 I
4.77846E+00      1.04311E-01 I
5.74732E+00      1.14172E-01 I
5.74732E+00      1.20441E-01 I
5.74732E+00      1.20800E-01 I
5.74732E+00      1.14172E-01 I
6.91264E+00      1.28267E-01 I
6.91264E+00      1.37549E-01 I
6.91264E+00      1.37749E-01 I
6.91264E+00      1.28267E-01 I
8.31422E+00      1.48435E-01 I
8.31422E+00      1.61754E-01 I
8.31422E+00      1.62018E-01 I
8.31422E+00      1.48435E-01 I
1.00000E+01      1.77330E-01 I

```

Fig. 6.4.1

6.4-2

APPENDIX UC

The following User Codes have been referred to in Chapter 3:

```
%I4
%E
"*****"
"***** UCCONEFF *****"
"*****"
"***MAIN PROGRAM***"
"*****"

"1.  USER-OVER-RIDE-OF-EGS-MACROS.....NONE"

COMIN/MEDIA,MISC,RANDOM/;
COMMON/PLDATA/PCOORD(3,100),PNORM(3,100);
COMMON/ETALLY/ESCINT;
REAL*8 ESCINT;
INTEGER MEDARR(24,2)/$S'PB',22*' ', $S'POLYSTYRENE',13*' '/;

"2.  PRE-HATCH-CALL-INITIALIZATION COMES NEXT"
NMED=2;      "NUMBER OF MEDIA USED"
DO J=1,NMED <DO I=1,24 <MEDIA(I,J)=MEDARR(I,J);>>
IREG=4;
"SET MEDIUM INDEX FOR EACH REGION"
MED(1)=0;      "VACUUM"
MED(2)=1;      "LEAD"
MED(3)=2;      "POLYSTYRENE (PLASTIC SCINTILLATOR)"
MED(4)=0;      "VACUUM"
"DUNIT UNCHANGED---WORKING IN CM-UNITS BY DEFAULT"

"3.  HATCH-CALL COMES NEXT"
CALL HATCH;

"4.  HOWFAR-INITIALIZATION COMES NEXT"
"DEFINITION OF PLANES"
IPLAN=3;      "NUMBER OF PLANES"
TPB=1.0;      "LEAD PLATE THICKNESS (CM)"
TPS=0.5;      "FIXED THICKNESS OF PLASTIC SCINTILLATOR (CM)"
DO I=1,3 <DO J=1,IPLAN <PCOORD(I,J)=0.0; "SET ALL TO ZERO">>
"NOW, PUT IN THE EXCEPTIONS"
PCOORD(3,2)=TPB; PCOORD(3,3)=PCOORD(3,2)+TPS;
DO I=1,3 <DO J=1,IPLAN <PNORM(I,J)=0.0;"START WITH ZERO">>
"NOW, PUT IN EXCEPTIONS IN ORDER TO PROPERLY DEFINE"
"THE UNIT NORMAL VECTORS (ALONG Z-DIRECTION)"
DO J=1,3 <PNORM(3,J)=1.0;>
OUTPUT; ('1');
```

APPENDIX UC

```

"5.  INITIALIZATION FOR AUSGAB COMES NEXT"
NCOUNT=0;    "INCIDENT PARTICLE COUNTER INITIALIZATION"
NSCINT=0;     "CONVERSION COUNTER INITIALIZATION"

"6.  DETERMINATION OF INCIDENT PARTICLE PARAMETERS"
"    (PLUS OTHER THINGS)"
IQI=0;       "INCIDENT PHOTON"
EI=177.0;    "INCIDENT (TOTAL) ENERGY (MEV)"
XI=0.0; YI=0.0; ZI=0.0;  "BEAM ENTERS AT PLANE 1"
UI=0.0; VI=0.0; WI=1.0;  "BEAM NORMAL TO SURFACE ALONG Z-AXIS"
IRI=2;      "REGION 2 IS THE ENTRANCE REGION"
WTI=1.0;    "WEIGHT FACTOR OF UNITY"

ICODE=-1;    "THIS MARKS THE INCIDENT PARTICLES IN THE AUSGAB"
ITYPE=IQI;
TYMOUT=10.0; "THE NUMBER OF SECONDS NEEDED FOR CLEAN-UP"
IXX=123456789; "RANDOM NUMBER SEED"
NCASES=1000000; "NO. OF INCIDENT CASES"
ELEVEL=0.060; "DISCRIMINATION LEVEL (MEV) IN PLASTIC SCINT."

"7.  SHOWER-CALL---NEXT"
DO I=1,NCASES <
"CHECK FIRST TO SEE IF ENOUGH TIME LEFT"
CALL LEFT1A(TYMNOW); "SLAC FACILITY-DEPENDENT ROUTINE"
IF(TYMNOW.LT.TYMOUT) <EXIT;>
ESCINT=0.DO; "INITIALIZE TOTAL ENERGY DEPOSITED"
"          IN PLASTIC SCINTILLATOR"
CALL SHOWER(IQI,EI,XI,YI,ZI,UI,VI,WI,IRI,WTI);
NCOUNT=NCOUNT+1;
"COUNT THOSE CASES WHERE MORE THAN ELEVEL ENERGY IS DEPOSITED"
"IN THE PLASTIC SCINTILLATOR AND ACCUMULATE HISTOGRAM"
IF(ESCINT.GT.ELEVEL) <NSCINT=NSCINT+1;>
"NOTE:  THE HISTOGRAMMING PART OF THIS CODE HAS BEEN EXCLUDED"
"          FROM THIS LISTING FOR THE SAKE OF BREVITY"
"END OF SHOWER GENERATION LOOP">

"8.  OUTPUT OF RESULTS"
OUTPUT NCOUNT,NCASES;
('1',I10,' CASES OUT OF ',I10,' REQUESTED COMPLETED',//);
"CALCULATE THE CONVERSION EFFICIENCY AND WRITE OUT RESULTS"
CONEFF=FLOAT(NSCINT)/NCOUNT;"FRACTION OF PHOTONS THAT CONVERT"
OUTPUT EI,TPB,NSCINT,NCOUNT,CONEFF;
('1CONVERSION EFFICIENCY RESULTS:',//,' PHOTON ENERGY=',G15.7,
' MEV',/, ' LEAD THICKNESS=',G15.7, ' CM',//,' NSCINT=',I12,
/, ' NCOUNT=',I12,//,' CONVERSION EFFICIENCY=',G15.7);

STOP;
END; "END OF MAIN PROGRAM"

```

APPENDIX UC

```
%E
SUBROUTINE HOWFAR;
COMIN/STACK,EPCONT/;
IF(IR(NP).EQ.1.OR.IR(NP).EQ.4) <IDISC=1; "DISCARD PARTICLE">
ELSEIF(IR(NP).EQ.2) <CALL PLANE2(2,3,1,1,1,-1);>
ELSEIF(IR(NP).EQ.3) <CALL PLANE2(3,4,1,2,2,-1);>
ELSE <
  OUTPUT IR(NP);(' STOPPED IN HOWFAR WITH IR(NP)=' ,I12);STOP;>
RETURN; END; "END OF SUBROUTINE HOWFAR"
```

```
%E
SUBROUTINE AUSGAB(IARG);
COMIN/STACK,EPCONT/;
COMMON/ETALLY/ESCINT;
REAL*8 ESCINT;
"SUM ENERGY WHENEVER IN PLASTIC SCINTILLATOR (REGION 3)"
IF(IR(NP).EQ.3) <ESCINT=ESCINT+EDEP;>
RETURN; END; "END OF SUBROUTINE AUSGAB"
```

```
%E
SUBROUTINE CHGTR(TVALP,IRNEWP);
COMIN/EPCONT/;
IF(TVALP.LE.USTEP) <USTEP=TVALP; IRNEW=IRNEWP;>
RETURN; END; "END OF SUBROUTINE CHGTR"
```

```
%E
SUBROUTINE PLANE1(NPLAN,ISIDE,IHIT,TVAL);
COMIN/STACK/;
COMMON/PLDATA/PCOORD(3,100),PNORM(3,100);
"NPLAN=ID NUMBER OF PLANE"
"ISIDE= 1 IF REGION IS BETWEEN ORIGIN AND OUTWARD NORMAL"
"      =-1 IF REGION IS NOT BETWEEN ORIGIN AND OUTWARD NORMAL"
"IHIT=1  MEANS PARTICLE TRAJECTORY WILL HIT PLANE"
"      =2  MEANS PARTICLE TRAJECTORY IS PARALLEL TO PLANE"
"      =0  MEANS PARTICLE TRAJECTORY IS AWAY FROM PLANE"
"TVAL= DISTANCE TO PLANE IF IHIT=1"
IHIT=1; "ASSUME A HIT UNLESS OTHERWISE"
UDOTA=PNORM(1,NPLAN)*U(NP)+PNORM(2,NPLAN)*V(NP)
      +PNORM(3,NPLAN)*W(NP);
IF(UDOTA.EQ.0.0) <IHIT=2; RETURN;> "PARTICLE TRAVELING"
"                                     PARALLEL TO SURFACE OF PLANE."
UDOTAP=UDOTA*ISIDE;
IF(UDOTAP.LT.0.0) <IHIT=0;>
ELSE <
TNUM=PNORM(1,NPLAN)*(PCOORD(1,NPLAN)-X(NP))
      +PNORM(2,NPLAN)*(PCOORD(2,NPLAN)-Y(NP))
      +PNORM(3,NPLAN)*(PCOORD(3,NPLAN)-Z(NP));
TVAL=TNUM/UDOTA;>
RETURN; END; "END OF SUBROUTINE PLANE1"
```

APPENDIX UC

```

%E
SUBROUTINE PLANE2(NPL1,NRG1,ISIDE1,NPL2,NRG2,ISIDE2);
CALL PLANE1(NPL1,ISIDE1,IHIT,TVAL);
IF(IHIT.EQ.1) <"HITS FIRST PLANE"
  CALL CHGTR(TVAL,NRG1); "CHANGE REGION IF NECESSARY">
ELSEIF(IHIT.EQ.0) <"HEADING AWAY FROM FIRST PLANE"
"
  AND MAY INTERSECT SECOND PLANE"
  CALL PLANE1(NPL2,ISIDE2,IHIT,TVAL);
  IF(IHIT.EQ.1) <CALL CHGTR(TVAL,NRG2); >>
ELSEIF(IHIT.NE.2) <OUTPUT NPL1,NRG1,NPL2,NRG2,IHIT;
  (' STOPPED IN SUBROUTINE PLANE2 WITH NPL1,NRG1,NPL2,NRG2=' ,
  4I6,/, ' AND WITH IHIT=' ,I6); STOP;>
ELSE <"TRAVELING PARALLEL TO PLANES IN ORIGINAL REGION">
RETURN; END; "END OF SUBROUTINE PLANE2"

"*****"
"***** END OF UCCONEFF *****"
"*****"

%I4
%E
"*****"
"***** UCSPARK *****"
"*****"
"***MAIN PROGRAM***"
"*****"

"1. USER-OVER-RIDE-OF-EGS-MACROS"
%'$EVALUATE#USING SIN(#); '=' #1=SIN(#2); 'I.E., REVERT TO EGS1"
%'$SET INTERVAL#,SINC; '='; ' "METHOD OF TAKING SIN"

COMIN/MEDIA,MISC,RANDOM,BOUNDS/;
COMMON/PDATA/PCOORD(3,100),PNORM(3,100);
COMMON/CHAMBR/EMASS2,BFIELD,YTILDA,ZPLUS,ZMINUS,XPLUS,XMINUS;
COMMON/NVALS/N25,N10,N5,NP25,NP10,NP5;
INTEGER MEDARR(24)/$S'PB',22*' '/;

"2. PRE-HATCH-CALL-INITIALIZATION COMES NEXT"
NMED=1; "NUMBER OF MEDIA USED"
DO I=1,24 <MEDIA(I,1)=MEDARR(I);>
MED(1)=0; "VACUUM"
MED(2)=1; "LEAD"
MED(3)=0; "VACUUM"
MED(4)=0; "VACUUM"
DO I=1,$MXREG <ECUT(I)=4.5; PCUT(I)=4.5;> "CUTOFFS CHANGED"
"DUNIT UNCHANGED---WORKING IN CM-UNITS BY DEFAULT"

```

APPENDIX UC

"3. HATCH-CALL COMES NEXT"  
CALL HATCH;

"4. HOWFAR-INITIALIZATION COMES NEXT"  
"DEFINITION OF PLANES"  
IPLAN=3; "NUMBER OF PLANES"  
RADL=0.51; "RADIATION LENGTH OF LEAD (CM)"  
TRL=1.0; "LEAD PLATE THICKNESS (R.L.)"  
TCM=TRL\*RADL; "LEAD PLATE THICKNESS (CM)"  
DIST=4.5;"SEPARATION BETWEEN LEAD PLATE AND SPARK CHAMBER(CM)"  
SPARKX=13.0\*2.54/2.0; "HALF-WIDTH OF SPARK CHAMBER (CM)"  
SPARKZ=12.0/2.0; "HALF-HEIGHT OF SPARK CHAMBER GAP (CM)"  
DO I=1,3 <DO J=1,IPLAN <PCOORD(I,J)=0.0;"ZERO TO START WITH">>  
"NOW, PUT IN THE EXCEPTIONS"  
PCOORD(2,2)=TCM;  
PCOORD(2,3)=PCOORD(2,2)+DIST;  
DO I=1,3 <DO J=1,IPLAN <PNORM(I,J)=0.0; "START WITH ZERO">>  
"NOW, PUT IN EXCEPTIONS IN ORDER TO PROPERLY DEFINE"  
"UNIT NORMAL VECTORS"  
DO J=1,3 <PNORM(2,J)=1.0;>

"5. INITIALIZATION FOR AUSGAB COMES NEXT"  
"SET VARIABLES FOR COMMON/NVALS/ TO ZERO"  
N25=0; N10=0; N5=0;  
NP25=0; NP10=0; NP5=0;  
NCOUNT=0;  
BFIELD=1.665; "MAGNETIC FIELD STRENGTH IN KG"  
BFIELD=BFIELD\*0.3; "CHANGE FOR COMPUTATIONAL EFFICIENCY LATER"  
YTILDA=PCOORD(2,3)+2.54; "LOCATION OF SCANNING CRITERIA PLANE"  
"CHANGE PCOORD(2,3) TO LOCATION OF SCANNING CRITERIA PLANE"  
"WHEN BFIELD IS ZERO"  
IF(BFIELD.EQ.0.0) <PCOORD(2,3)=YTILDA;>  
ZPLUS=SPARKZ; "UPPER EXTENT OF CHAMBER"  
ZMINUS=-SPARKZ; "LOWER EXTENT OF CHAMBER"  
XPLUS=SPARKX; "RIGHT EXTENT OF CHAMBER"  
XMINUS=-SPARKX; "LEFT EXTENT OF CHAMBER"  
EMASS2=EMASS\*EMASS;"NEEDED LATER FOR COMPUTATIONAL EFFICIENCY"

"6. DETERMINATION OF INCIDENT PARTICLE PROPERTIES"  
IQI=-1; "INCIDENT ELECTRON"  
EI=1000.0; "TOTAL ENERGY (MEV)"  
XI=0.0; YI=0.0; ZI=0.0; "BEAM ENTERS AT PLANE 1"  
UI=0.0; VI=1.0; WI=0.0; "BEAM ENTERS NORMAL TO SURFACE"  
IRI=2; "REGION 2 IS THE ENTRANCE REGION"  
WTI=1.0; "WEIGHT FACTOR OF UNITY"  
ICODE=-1; "THIS MARKS THE INCIDENT PARTICLES IN THE AUSGAB"  
TYMOUT=10.0; "THE NUMBER OF SECONDS NEEDED FOR CLEAN-UP"  
IXX=123456789; "RANDOM NUMBER SEED"  
NCASES=1000000; "NO. OF INCIDENT CASES"

APPENDIX UC

```

"7. SHOWER-CALL---NEXT"
DO I=1,NCASES <
"CHECK FIRST TO SEE IF ENOUGH TIME LEFT"
CALL LEFT1A(TYMNOW); "SLAC FACILITY-DEPENDENT ROUTINE"
IF(TYMNOW.LT.TYMOUT) <EXIT;>
CALL SHOWER(IQI,EI,XI,YI,ZI,UI,VI,WI,IRI,WTI);
NCOUNT=NCOUNT+1;
"END OF SHOWER GENERATION LOOP">

"8. OUTPUT OF RESULTS"
OUTPUT NCOUNT,NCASES;
  ('1',I10,' CASES OUT OF ',I10,' REQUESTED COMPLETED',//);
XN25=FLOAT(N25)/NCOUNT;
XN10=FLOAT(N10)/NCOUNT;
XN5=FLOAT(N5)/NCOUNT;
XNP25=FLOAT(NP25)/NCOUNT;
XNP10=FLOAT(NP10)/NCOUNT;
XNP5=FLOAT(NP5)/NCOUNT;

OUTPUT; ('RESULTS SORTED BY ENERGY:',///);
OUTPUT N25,XN25; (' NO. OF CHARGED PARTICLES GE 25 MEV=',I10,
  '=',G15.7,' PER INCIDENT ELECTRON');
OUTPUT N10,XN10; (' NO. OF CHARGED PARTICLES GE 10 MEV=',I10,
  '=',G15.7,' PER INCIDENT ELECTRON');
OUTPUT N5,XN5; (' NO. OF CHARGED PARTICLES GE 5 MEV=',I10,
  '=',G15.7,' PER INCIDENT ELECTRON');
OUTPUT; ('RESULTS SORTED BY MOMENTUM:',///);
OUTPUT NP25,XNP25; (' NO. OF CHARGED PARTICLES GE 25 MEV/C=',
  I10,'=',G15.7,' PER INCIDENT ELECTRON');
OUTPUT NP10,XNP10; (' NO. OF CHARGED PARTICLES GE 10 MEV/C=',
  I10,'=',G15.7,' PER INCIDENT ELECTRON');
OUTPUT NP5,XNP5; (' NO. OF CHARGED PARTICLES GE 5 MEV/C=',I10,
  '=',G15.7,' PER INCIDENT ELECTRON');
STOP; END; "END OF MAIN PROGRAM"

"*****"
"***** USE SUBROUTINE HOWFAR FROM UCCONEFF*****"
"*****"

%E
SUBROUTINE AUSGAB(IARG);
COMIN/STACK,EPCONT/;
COMMON/NVALS/N25,N10,N5,NP25,NP10,NP5;
COMMON/CHAMBR/EMASS2,BFIELD,YTILDA,ZPLUS,ZMINUS,XPLUS,XMINUS;

"ONLY SORT CHARGED PARTICLES THAT HAVE BEEN DISCARDED BY USER"
"AND HAVE REACHED REGION 4"
IF(IQ(NP).EQ.0.OR.IR(NP).NE.4.OR.IARG.NE.3) <RETURN;>

```



APPENDIX UC

```

"NOW WE START ACCEPTANCE CHECK"
"FIRST, THROW OUT PARTICLES WHOSE COORDINATES"
"ARE OUTSIDE CHAMBER"
IF(ABS(X(NP)).GT.XPLUS.OR.ABS(Z(NP)).GT.ZPLUS) <RETURN;>
PSQ=E(NP)*E(NP)-EMASS2;
P=SQRT(PSQ); "MOMENTUM IN MEV/C"
IF(BFIELD.EQ.0.0) <GO TO :ZEROFIELD:; "SKIP THE RCURV CALC.">
POVERB=P/BFIELD; "FOR CALCULATIONAL EFFICIENCY"
"RADIUS OF CURVATURE IS CALCULATED NEXT"
RCURV=IQ(NP)*POVERB*SQRT(U(NP)*U(NP)+V(NP)*V(NP));
YO=Y(NP)-RCURV*U(NP); "Y-COORD OF CENTER OF CIRCLE"
YTDIFF=YTILDA-YO; "Y-DISTANCE BETWEEN CENTER OF CIRCLE"
"
" AND SCAN-PLANE"
IF(ABS(RCURV).LT.ABS(YTDIFF)) <RETURN;> "DID NOT REACH PLANE"
YTDIF2=YTDIFF*YTDIFF; "FOR CALCULATIONAL EFFICIENCY"
XO=X(NP)+RCURV*V(NP); "X-COORD OF CENTER OF CIRCLE"
XTILDA=XO-IQ(NP)*SQRT(RCURV*RCURV-YTDIF2); "X-VALUE"
"
" AT INTERSECTION"
"IF PARTICLE GOES OUT CHAMBER Laterally, THEN REJECT"
IF(XTILDA.LT.XMINUS.OR.XTILDA.GT.XPLUS) <RETURN;>
"IF PARTICLE STILL Laterally IN CHAMBER,"
"THEN CHECK ON Z-POSITION"
XDIFX=X(NP)-XO;
XTDIFX=XTILDA-XO;
YDIFX=Y(NP)-YO;
ADOTB=(XDIFX*XTDIFX + YDIFX*YTDIFX)/SQRT((XDIFX*XDIFX
+YDIFX*YDIFX)*(XTDIFX*XTDIFX + YTDIF2));
ZTILDA=Z(NP)+POVERB*W(NP)*ARCOS(ADOTB); "Z-VALUE"
"
" AT INTERSECTION"

"IF PARTICLE GOES OUT CHAMBER VERTICALLY, THEN REJECT"
IF(ZTILDA.LT.ZMINUS.OR.ZTILDA.GT.ZPLUS) <RETURN;>
"IF WE GET TO HERE, THE SCANNING CRITERIA IS SATISFIED"
"THAT IS, IT GOES ONE INCH INTO CHAMBER IN BEAM DIRECTION AND"
"SHOULD BE SCORED"
:ZEROFIELD: "A JUMP TO THIS POINT MEANS THAT BFIELD WAS ZERO"
IF(E(NP).GE.25.0) <N25=N25+1;>
IF(E(NP).GE.10.0) <N10=N10+1;>
IF(E(NP).GE.5.0) <N5=N5+1;>
IF(P.GE.25.0) <NP25=NP25+1;>
IF(P.GE.10.0) <NP10=NP10+1;>
IF(P.GE.5.0) <NP5=NP5+1;>
RETURN; END; "END OF SUBROUTINE AUSGAB"

"*****"
"***** END OF UCSPARK *****"
"*****"

```

APPENDIX UC

```

%I4
%E
"*****"
"***** UCH2O&AL *****"
"*****"
"***MAIN PROGRAM***"
"*****"

"1. USER-OVER-RIDE-OF-EGS-MACROS"

%'$MXREG'='150' "MACROS TO RE-SET MAXIMUM NUMBER OR REGIONS"

COMIN/MEDIA,MISC,RANDOM,USEFUL/;
COMMON/PASS/NR,NZ;
COMMON/PLDATA/PCOORD(3,100),PNORM(3,100);
COMMON/STOPIT/NWRITE,NCOUNT;
COMMON/CYDATA/CYRAD2(75);
COMIN/ETALLY/;
REAL CYRAD(75);
REAL*8 EKIN,EI,TOTKE;
REAL*8 EREG($MXREG);
REAL WMASS(100);
REAL PI/3.1415926/;
INTEGER*2 ITYPE,ICODE;

INTEGER MEDARR(24,1)/$S'WATER',19*' '/;

"2. PRE-HATCH-CALL-INITIALIZATION COMES NEXT"

NMED=1; "NUMBER OF MEDIA USED"
DO J=1,NMED <
DO I=1,24 <MEDIA(I,J)=MEDARR(I,J);>>

INPUT IPLAN; (I5); "INPUT THE NUMBER OF PLANES"
"
" DEFINING THE REGIONS"
INPUT IRADII; (I5); "INPUT THE NUMBER OF RADII THAT DEFINE THE"
"
" CYLINDRICAL REGIONS---NOTE: THE FINAL"
"
" CYLINDER IS RADIALLY INFINITE"

NZ=IPLAN; "NO. OF SLABS"
NR=IRADII+1; "NO. OF CYLINDER SHELLS"
IREG=NZ*NR+1; "NUMBER OF REGIONS DEFINED"

```

APPENDIX UC

```

"SET MEDIUM INDEX FOR EACH REGION"
MED(1)=0;          "FIRST REGION IS VACUUM"
DO I=2, IREG <MED(I)=1; "SET ALL OTHERS TO WATER OR ALUMINUM">

"3. HATCH-CALL COMES NEXT"
CALL HATCH;

"4. HOWFAR-INITIALIZATION COMES NEXT"
"DEFINITION OF PLANES"
DO J=1, IPLAN <
  PCOORD(1,J)=0.0;  PCOORD(2,J)=0.0;
  PNORM(1,J)=0.0;  PNORM(2,J)=0.0;  PNORM(3,J)=1.0;
>

"READ-IN THE PCOORD-VALUES"
INPUT (PCOORD(3,I), I=1, IPLAN); (E15.5);

OUTPUT; ('1PCOORD AND PNORM VALUES FOR EACH J-PLANE (I=1,3):',
        //);
DO J=1, IPLAN <
OUTPUT J, ((PCOORD(I,J), I=1, 3), (PNORM(I,J), I=1, 3));
(I5, 6G15.7); >

"DEFINITION OF CYLINDRICAL RADII AND RADII-SQUARED"
"READ-IN THE CYLINDER RADII"
INPUT (CYRAD(I), I=1, IRADII); (E15.3);

OUTPUT; ('1CYLINDER RADII:', //);

DO I=1, IRADII <"SEE DATA INITIALIZATION FOR CYRAD-VALUES"
  CYRAD2(I)=CYRAD(I)*CYRAD(I);
  OUTPUT I, CYRAD(I); (' CYRAD(', I2, ')=' , G15.7);
>

OUTPUT; ('1');

```

APPENDIX UC

"5. INITIALIZATION FOR AUSGAB COMES NEXT"

```
CALL ECONSV(0,IREG,TOTKE);" INITIALIZE ESUM ARRAY FOR ENERGY"
" CONSERVATION CALCULATION."
" IREG=NUMBER OF REGIONS"
" TOTKE=TOTAL KE (DUMMY HERE)"
```

```
NCOUNT=0; "INITIALIZE PARTICLE HISTORY COUNTER"
```

"6. DETERMINATION OF INCIDENT PARTICLE PROPERTIES"

```
IQI=-1; "INCIDENT ELECTRON"
```

```
EI=1000.0; "TOTAL ENERGY (MEV)"
EKIN=EI-PRM; "KINETIC ENERGY (MEV)"
ESING=EI; "SINGLE PRECISION ENERGY VARIABLE"
XI=0.0; YI=0.0; ZI=0.0; "BEAM ENTERS AT VACUUM WINDOW SURFACE"
UI=0.0; VI=0.0; WI=1.0; "BEAM ENTERS NORMAL TO SURFACE"
IRI=2; "ENTRANCE REGION DEFINITION"
WTI=1.0; "WEIGHT FACTOR OF UNITY"
```

```
ICODE=-1; "THIS MARKS THE INCIDENT PARTICLES IN THE AUSGAB"
ITYPE=IQI;
```

```
TYMOUT=10.0; "THE NUMBER OF SECONDS NEEDED FOR CLEAN-UP"
IXX=123456789; "RANDOM NUMBER SEED"
IXXST=IXX;
```

```
NCASES=1000000; "NO. OF INCIDENT CASES"
```

```
NWRITE=1; "NWRITE IS THE NUMBER OF INCIDENT CASES"
" TO RECORD ON PAPER"
```

"7. SHOWER-CALL---NEXT"

```
DO I=1,NCASES <
```

```
"CHECK FIRST TO SEE IF ENOUGH TIME LEFT"
```

```
CALL LEFTIA(TYMNOW);
IF(TYMNOW.LT.TYMOUT) <EXIT;>
```

```
IF(NCOUNT.LT.NWRITE) <
WRITE(6,:FMTA:) ESING,XI,YI,ZI,UI,VI,WI,ITYPE,ICODE;
:FMTA: FORMAT(7F15.6,2I5);>
```

APPENDIX UC

```

CALL SHOWER(IQI, EI, XI, YI, ZI, UI, VI, WI, IRI, WTI);
NCOUNT=NCOUNT+1;
IXXEND=IXX;
"END OF SHOWER GENERATION LOOP">

"8. OUTPUT OF RESULTS"

WRITE(6, :FMT2:) NCOUNT, NCASES, IXXST, IXXEND;
  :FMT2: FORMAT('1', I10, ' CASES OUT OF ', I10,
    ' REQUESTED COMPLETED', //, ' IXX START=', I12, /,
    ' IXX END=', I12, //);

TOTKE=EKIN*NCOUNT; "TOTAL KINETIC ENERGY INVOLVED IN RUN"

"DETERMINE AND WRITE-OUT THE LONGITUDINAL DE/DV"
"FOR EACH RADIAL BIN"

DO J=1, IREG <
  EREG(J)=0.D0;
  DO I=1, 3 <
    DO K=1, 5 <
      EREG(J)=EREG(J)+ESUM(I, J, K);
    >>
  EREG(J)=EREG(J)/NCOUNT; "NORMALIZE DATA TO INCIDENT PARTICLES"

"END OF J-LOOP">

"WRITE-OUT THE LONGITUDINAL HISTOGRAMS FOR EACH RADIAL BIN"

NR1=NR-1; "SKIP THE INFINITE RADIAL BIN"

DO JR=1, NR1 <

  IF(JR.EQ.1) <
    AREA=PI*CYRAD2(JR);
    CYRLOW=0.0;
  >
  ELSE <
    AREA=PI*(CYRAD2(JR)-CYRAD2(JR-1));
    CYRLOW=CYRAD(JR-1);
  >

  OUTPUT CYRLOW, CYRAD(JR);
  ('1LONGITUDINAL HISTOGRAM OUTPUT:', ///, ' RADIUS=',
    G15.7, ' TO', G15.7, ' CM', ///);

NZ1=NZ-1; "SKIP THE INFINITE DEPTH BIN"

```

APPENDIX UC

```

DO JZ=1,NZ1 <

VOL=AREA*(PCOORD(3,JZ+1)-PCOORD(3,JZ));
DEBYDV=EREG(1+JZ+(JR-1)*NZ)/VOL;

OUTPUT PCOORD(3,JZ),PCOORD(3,JZ+1),DEBYDV;
(' DEPTH=',G15.7,' TO ',G15.7,' CM',5X,'DE/DV=',G15.7,
 ' MEV/CU.CM/INCIDENT ELECTRON');

"END OF JZ-LOOP">
"END OF JR-LOOP">

"CALL SUBROUTINE ECONSV TO WRITE-OUT THE ENERGY DEPOSITION"
"TOTALS---TO CHECK ENERGY CONSERVATION FOR ONE THING"

CALL ECONSV(1,IREG,TOTKE);

STOP;
END;
%E
SUBROUTINE AUSGAB(IARG);
COMIN/DEBUG,EPCONT,STACK/;
COMMON/STOPIT/NWRITE,NCOUNT;
COMIN/ETALLY/;
INTEGER*2 ITYPE,ICODE;

"KEEP TRACK OF ENERGY DEPOSITION---FOR CONSERVATION PURPOSES"
ESUM(IQ(NP)+2,IR(NP),IARG+1)=ESUM(IQ(NP)+2,IR(NP),IARG+1)
+ EDEP;

RETURN; END;

%E
SUBROUTINE HOWFAR;
COMIN/DEBUG,EPCONT,STACK/;
COMMON/PASS/NR,NZ;

IRL=IR(NP); "SET LOCAL VARIABLE"

IF(IRL.EQ.1)<IDISC=1;RETURN;"DISCARD BACKSCATTERED PARTICLES">

JR1=(IRL-2)/NZ;
JZ=IRL-1-JR1*NZ;

```

APPENDIX UC

```

IF(JZ.EQ.NZ) <"WE ARE IN THE END REGIONS"
  CALL PLANE1(JZ,-1,IHIT,TVAL);
  IF(IHIT.EQ.1) <CALL CHGTR(TVAL,IRL-1);>
>

ELSE <
IF(JZ.EQ.1) <IRBACK=1;> ELSE <IRBACK=IRL-1;>

CALL PLANE2(JZ+1,IRL+1,1,JZ,IRBACK,-1);
>

IF(JR1.EQ.0) <
  CALL CYLNR(1,1,IHIT,TVAL);
  IF(IHIT.EQ.1) <CALL CHGTR(TVAL,IRL+NZ);>
>

ELSE <
  CALL CYLNR(JR1,0,IHIT,TVAL);
  IF(IHIT.EQ.1) <CALL CHGTR(TVAL,IRL-NZ);>
  ELSEIF(JR1+1.NE.NR) <
    CALL CYLNR(JR1+1,1,IHIT,TVAL);
    IF(IHIT.EQ.1) <CALL CHGTR(TVAL,IRL+NZ);>
  >
>
RETURN;
END;

%E
SUBROUTINE CYLNR(ICYL,INFL,IHIT,TCYL);
COMIN/DEBUG,STACK/;
COMMON/CYDATA/CYRAD2(75);

"PROGRAM TO BE CALLED BY SUBROUTINE HOWFAR IN EGS CODE SYSTEM"

"WHETHER INSIDE OR OUTSIDE A RIGHT CIRCULAR CYLINDER, THIS"
"PROGRAM DETERMINES WHETHER A PARTICLE INTERSECTS THE"
"CYLINDER SURFACE AND, IF IT DOES, IT DETERMINES THE DISTANCE"
"TO THE SURFACE FROM THE PARTICLES COORDINATE LOCATION."

" ICYL=NUMBER OF CYLINDER"
" INFL=1 MEANS PARTICLE IS INSIDE CYLINDER"
" =0 MEANS PARTICLE IS OUTSIDE CYLINDER"
" IHIT=1 MEANS PARTICLE INTERSECTS SURFACE"
" =0 MEANS PARTICLE MISSES SURFACE"
" TCYL=DISTANCE TO SURFACE IF INTERSECTED"

```

APPENDIX UC

```

"NOTE: DATA IN THE FORM OF THE CYLINDER RADIUS SQUARED IS"
"      REQUIRED AND IS TRANSMITTED VIA COMMON/CYDATA/"
"      THIS MAY BE DEFINED IN MAIN (FOR EXAMPLE)."
```

IHIT=1; "ASSUME A HIT UNLESS OTHERWISE"

"CALCULATE THE QUADRATIC PARAMETERS A,B,C"

```

A=U(NP)*U(NP)+V(NP)*V(NP);
B=X(NP)*U(NP)+Y(NP)*V(NP);
C=X(NP)*X(NP)+Y(NP)*Y(NP)-CYRAD2(ICYL);
```

IF(A.EQ.0.0)<IHIT=0;RETURN; "QUADRATIC IS INDETERMINATE">

"NOTE---1.0E-4 HAS BEEN CHANGED TO 1.0E-3 IN NEXT STATEMENT"

```

AC=A*C;B2=B*B;RTARG=B2-AC;
IF(ABS(C).LT.1.0E-3)<"NEAR THE SURFACE"
  IF(INFL.NE.0)<IF(B.LT.0.0)<TCYL=-2.*B/A;> ELSE <TCYL=0.0;>>
  ELSE <IF(B.LT.0.0) <TCYL=0.0;> ELSE <IHIT=0;>>
RETURN;>
```

IF(RTARG.LT.0.0)<IHIT=0;RETURN; "IMAGINARY SOLUTION">

ROOT=SQRT(RTARG);

"CALCULATE THE ROOT(S) AND CHOOSE THE SMALLEST POSITIVE ONE"

```

IF(B.GT.0.0) <TCYL=(-B-ROOT)/A;> ELSE <TCYL=-C/(B-ROOT);>
IF(TCYL.GE.0.0)<RETURN;>
IF(B.LT.0.0) <TCYL=(-B+ROOT)/A;> ELSE <TCYL=-C/(B+ROOT);>
IF(TCYL.GE.0.0)<RETURN;>
IHIT=0;
RETURN;
END;
```

%E

SUBROUTINE ECONSV(NTREE,NREG,TOTKE);

"SUBROUTINE FOR KEEPING TRACK OF ENERGY CONSERVATION---"

"TO BE USED WITH EGS USER CODES. WHEN NTREE=0,"

"THE PROGRAM IS ENTERED IN ORDER TO INITIALIZE THE"

"ESUM ARRAY TO ZERO. OTHERWISE, IT IS ENTERED FOR"

"TOTALING AND OUTPUTTING THE RESULTS. THE ESUM ARRAY"

"IS NEEDED IN SUBROUTINE AUSGAB, WHERE EDEP (ENERGY"

"DEPOSITION) IS ADDED TO THE ELEMENT OF THE"

"ARRAY CORRESPONDING TO THE VALUE OF IQ, IR, AND IARG."



APPENDIX UC

```

COMIN/ETALLY/; "INSERT THIS STATEMENT IN ALL SUBPROGRAMS"
"          THAT USE ESUM"
REAL*8 ROWSUM(3,$MXREG),COLSUM(3,5),SUMSUM(3),GSUM,TOTKE;

"CHECK WHETHER NREG IS GE $MXREG.  IF IT IS, STOP AND OUTPUT."
IF(NREG.GT.$MXREG) <
  MDUMMY=$MXREG;
  OUTPUT NREG,MDUMMY;
  (///,' ***** STOPPED IN SUBROUTINE ECONSV BECAUSE NREG= ',I5,
  ' IS LARGER THAN $MXREG= ',I5,' *****');
  STOP;>

IF(NTREE.EQ.0) < "INITIALIZE ESUM TO ZERO AND RETURN"
DO I=1,3 <DO J=1,NREG <DO K=1,5 <ESUM(I,J,K)=0.D0;>>>
RETURN;>

"REACH THIS POINT WHEN FINAL TALLY IS TO BE MADE."

"FIRST, INITIALIZE SUMS"

GSUM=0.D0;

DO IQ=1,3 <
SUMSUM(IQ)=0.D0;
DO IR=1,NREG <ROWSUM(IQ,IR)=0.D0;>
DO ICODE=1,5 <COLSUM(IQ,ICODE)=0.D0;>
"END OF IQ-LOOP">

"NORMALIZE DATA TO TOTKE"

DO IQ=1,3 <
DO IR=1,NREG <
DO ICODE=1,5 <
ESUM(IQ,IR,ICODE)=ESUM(IQ,IR,ICODE)/TOTKE;
>>>

"SUM-UP COLUMNS AND ROWS"

DO IQ=1,3 <
DO IR=1,NREG <
DO ICODE=1,5 <
ROWSUM(IQ,IR)=ROWSUM(IQ,IR)+ESUM(IQ,IR,ICODE);
>>

```

APPENDIX UC

```

DO ICODE=1,5 <
DO IR=1,NREG <
COLSUM(IQ,ICODE)=COLSUM(IQ,ICODE)+ESUM(IQ,IR,ICODE);
>>
"END OF IQ-LOOP">

"NOW GET TOTAL FOR IQ AND GRAND TOTAL"

DO IQ=1,3 <
DO IR=1,NREG <
DO ICODE=1,5 <
SUMSUM(IQ)=SUMSUM(IQ)+ESUM(IQ,IR,ICODE);
GSUM=GSUM+ESUM(IQ,IR,ICODE);
>>>

"NOW WRITE-OUT THE RESULTS OF THE ENERGY DEPOSITION SUMMARY"

DO IQ=1,3 <
IQNOW=IQ-2;
OUTPUT IQNOW;
('1ENERGY DEPOSITION SUMMARY FOR PARTICLES WITH IQ=',I2,///,
55X,'IARG',/,19X,'0',15X,'1',13X,'2',14X,'3',14X,'4',16X,
'ROW SUM',/,3X,'REGION',/);

DO IR=1,NREG <
OUTPUT IR,(ESUM(IQ,IR,ICODE),ICODE=1,5),ROWSUM(IQ,IR);
(I7,5X,5G15.7,5X,G15.7);
"END OF IR-LOOP">

OUTPUT (COLSUM(IQ,ICODE),ICODE=1,5),SUMSUM(IQ);
(/,3X,'COL SUM',2X,5G15.7,5X,G15.7);

"END OF IQ-LOOP">

OUTPUT GSUM; (/////,' TOTAL FRACTION=',G15.7,
' NOTE: THIS NUMBER SHOULD BE VERY CLOSE TO UNITY');

RETURN;
END; "END OF SUBROUTINE ECONSV"

"*****"
"* NOTE: SUBROUTINES CHGTR, PLANE1, AND PLANE2 ARE *"
"* LISTED IN UCCONEFF. *"
"*****"

"*****"
"***** END OF UCH20&AL *****"
"*****"

```

## REFERENCES

- R. G. Alsmiller, Jr. and H. S. Moran, "Electron-Photon Cascade Calculations and Neutron Yields from Electrons in Thick Targets," Oak Ridge National Laboratory Report Number ORNL-TM-1502 (1966).
- R. G. Alsmiller, Jr. and H. S. Moran, "The Electron-Photon Cascade Induced in Lead by Photons in the Energy Range 15 to 100 MeV," Oak Ridge National Laboratory Report Number ORNL-4192 (1968).
- R. G. Alsmiller, Jr., "High-Energy ( $< 18$  GeV) Muon Transport Calculations and Comparison with Experiment," Nucl. Instr. Meth. 71, 121 (1969a).
- R. G. Alsmiller, Jr. and H. S. Moran, "Calculation of the Energy Deposited in Thick Targets by High-Energy (1 GeV) Electron-Photon Cascades and Comparison with Experiment," Nucl. Sci. Eng. 38, 131 (1969b).
- R. G. Alsmiller, Jr. and J. Barish, "Energy Deposition by 45-GeV Photons in H, Be, Al, Cu, and Ta," Oak Ridge National Laboratory Report Number ORNL-4933 (1974a).
- R. G. Alsmiller, Jr., J. Barish, and S. R. Dodge, "Energy Deposition by High-Energy Electrons (50 to 200 MeV) in Water," Nucl. Instr. Meth. 121, 161 (1974b).
- T. W. Armstrong and R. G. Alsmiller, Jr., "An Approximate Density-Effect Correction for Ionization Loss of Charged Particles," Nucl. Instr. Meth. 82, 289 (1970).
- M. J. Berger and S. M. Seltzer, "Tables of Energy Losses and Range of Electrons and Positrons," National Aeronautics and Space Administration Report Number NASA-SP-3012 (1964); National Academy of Sciences ---National Research Council Publication Number 1133 (1964, Second Printing 1967).

- M. J. Berger and S. M. Seltzer, "Bremsstrahlung and Photoneutrons from Thick Tungsten and Tantalum Targets," Phys. Rev. C2, 621 (1970).
- M. J. Berger, private communication with W. R. Nelson, July, 1976.
- M. J. Berger, private communication with W. R. Nelson, January, 1978.
- H. A. Bethe, "Theory of Passage of Swift Corpuscular Rays Through Matter," Ann. Physik 5, 325 (1930); "Scattering of Electrons," Z. für Physik 76, 293 (1932).
- H. A. Bethe and J. Ashkin, "Passage of Radiation Through Matter," in Experimental Nucleus Physics, Vol. I, Part II, E. Segre, Editor (Wiley and Sons, New York, 1953).
- H. A. Bethe, "Moliere's Theory of Multiple Scattering," Phys. Rev. 89, 1256 (1953).
- H. J. Bhabha, "Scattering of Positrons by Electrons with Exchange on Dirac's Theory of the Positron," Proc. Roy. Soc. (London) A154, 195 (1936).
- F. Bloch, "Stopping Power of Atoms with Several Electrons," Z. für Physik 81, 363 (1933).
- H. Burfeindt, "Monte-Carlo Rechnung für 3 GeV-Schauer in Blei," Deutsches Elektronen-Synchrotron Report Number DESY-67/24 (1967).
- J. C. Butcher and H. Messel, "Electron Number Distribution in Electron-Photon Showers" Phys. Rev. 112, 2096 (1958).
- J. C. Butcher and H. Messel, "Electron Number Distribution in Electron-Photon Showers in Air and Aluminum Absorbers," Nucl. Phys. 20, 15 (1960).
- J. W. Butler, "Machine Sampling from Given Probability Distributions," from Symposium on Monte Carlo Methods, H. A. Meyer (Ed.) (John Wiley & Sons, Inc., New York, 1956).

- L. L. Carter and E. D. Cashwell, Particle-Transport Simulation with the Monte Carlo Method, TID-26607 (National Technical Information Service, U. S. Department of Commerce, Springfield, Virginia, 1975).
- A. Clark, private communication with R. L. Ford and W. R. Nelson, August, 1977.
- G. Clement, "Differential Path Length of the Photons Produced by an Electron of Very High Energy in a Thick Target," *Comptes Rendus* 257, 2971 (1963); translated for the Stanford Linear Accelerator Center, SLAC-TRANS-141 (1972).
- H. M. Colbert, "SANDYL: A Computer Program for Calculating Combined Photon-Electron Transport in Complex Systems," Sandia Laboratories, Livermore, Report Number SCL-DR-720109 (1973).
- A. J. Cook and L. J. Shustek, "A User's Guide to MORTRAN2," Stanford Linear Accelerator Center Computation Research Group Report Number CGTM No. 165 (1975).
- C. J. Crannell, H. Crannell, R. R. Whitney, and H. D. Zeman, "Electron-Induced Cascade Showers in Water and Aluminum," *Phys. Rev.* 184, 426 (1969).
- P. Darriulat, E. Gygi, M. Holder, K. T. McDonald, H. G. Pugh, F. Schneider, and K. Tittel, "Conversion Efficiency of Lead for 30-200 MeV Photons," *Nucl. Instr. Meth.* 129, 105 (1975).
- H. Davies, H. A. Bethe, and L. C. Maximon, "Theory of Bremsstrahlung and Pair Production. II. Integral Cross Section for Pair Production," *Phys. Rev.* 93, 788 (1954).
- D. J. Drickey, J. R. Kilner, and D. Benaksas, "Charged Component of 1-GeV Electron Showers in Lead," *Phys. Rev.* 171, 310 (1968).

- R. D. Evans, *The Atomic Nucleus* (McGraw-Hill Book Co., New York, 1955).
- E. L. Feinberg and I. Pomerancuk, "High Energy Inelastic Diffraction Phenomena," *Nuovo Cimento Supp.* 3, 652 (1956).
- R. L. Ford, B. L. Beron, R. L. Carrington, R. Hofstadter, E. B. Hughes, G. I. Kirkbridge, L. H. O'Neill, and J. W. Simpson, "Performance of Large, Modularized NaI(Tl) Detectors," High Energy Physics Laboratory Report Number HEPL-789 (September 1976); presented at the IEEE 1976 Nuclear Science Symposium and Scintillation and Semiconductor Symposium, New Orleans, LA., October 20-22, 1976.
- P. H. Fowler, D. H. Perkins, and K. Pinkau, "Observation of the Suppression Effect on Bremsstrahlung," *Phil. Mag.* 4, 1030 (1959).
- M. L. Goldberger, "The Interaction of High Energy Neutrons and Heavy Nuclei," *Phys. Rev.* 74, 1269 (1948).
- S. Goudsmit and J. L. Saunderson, "Multiple Scattering of Electrons," *Phys. Rev.* 57, 24 (1940a).
- S. Goudsmit and J. L. Saunderson, "Multiple Scattering of Electrons. II," *Phys. Rev.* 58, 36 (1940b).
- P. R. Halmos, Measure Theory (D. Van Nostrand Co., Princeton, New Jersey, 1950).
- J. M. Hammersley and D. C. Handscomb, Monte Carlo Methods (John Wiley & Sons, Inc., New York, 1964).
- A. O. Hanson, L. H. Lanzl, E. M. Lyman, and M. B. Scott, "Measurement of Multiple Scattering of 15.7 MeV Electrons," *Phys. Rev.* 84, 634 (1951).

- W. Heitler, The Quantum Theory of Radiation (Clarendon Press, Oxford, 1954).
- J. M. Jauch and F. Rohrlich, The Theory of Photons and Electrons (Addison-Wesley, Reading, MA., 1955).
- H. Kahn, "Applications of Monte Carlo," USAEC Report Number AECU-3259, The Rand Corporation, 1954.
- K. R. Kase and W. R. Nelson, Concepts of Radiation Dosimetry (Pergamon Press, Inc., New York, 1978).
- J. F. C. Kingman and S. J. Taylor, Introduction to Measure and Probability (Cambridge University Press, 1966).
- O. Klein and Y. Nishina, "Über die Streuung von Strahlung durch freie Elektronen nach der Neuen Relativistischen Quantum Dynamik von Dirac," Z. für Physik 52, 853 (1929).
- H. W. Koch and J. W. Motz, "Bremsstrahlung Cross-Section Formulas and Related Data," Rev. Mod. Phy. 31, 920 (1959).
- L. B. Levy, R. G. Waggener, W. D. McDavid, and W. H. Payne, "Experimental and Calculated Bremsstrahlung Spectra from a 25-MeV Linear Accelerator and a 19-MeV Betatron," Med. Phy. 1, 62 (1974).
- M. Loeve, Probability Theory (Van Nostrand Reinhold Co., New York, 1950).
- C. A. Logg, A. M. Boyarski, A. J. Cook, and R. L. A. Cottrell, "DPAK and HPAK --- A Versatile Display and Histogramming Package," Stanford Linear Accelerator Center Report Number SLAC-196 (1976).

- H. Messel, A. D. Smirnov, A. A. Varfolomeev, D. F. Crawford and J. C. Butcher, "Radial and Angular Distributions of Electrons in Electron-Photon Showers in Lead and in Emulsion Absorbers," Nucl. Phys. 39, 1 (1962).
- H. Messel and D. F. Crawford, Electron-Photon Shower Distribution Function (Pergamon Press, Oxford, 1970).
- A. B. Migdal, "Bremsstrahlung and Pair Production in Condensed Media at High Energies," Phys. Rev. 103, 1811 (1956).
- G. Z. Moliere, "Theorie der Streuung schneller geladener Teilchen I. Einzelstreuung am abgeschirmten Coulomb-Feld," Z. Naturforsch 2a, 133 (1947).
- G. Z. Moliere, "Theorie der Streuung schneller geladener Teilchen II. Mehrfach- und Vielfachstreuung," Z. Naturforsch 3a, 78 (1948).
- C. Møller, "Passage of Hard Beta Rays Through Matter," Ann. Physik 14, 531 (1932).
- J. W. Motz, H. A. Olsen, and H. W. Koch, "Pair Production by Photons," Rev. Mod. Phy. 41, 581 (1969).
- H. H. Nagel and C. Schlier, "Berechnung von Elektron-Photon-Kaskaden in Blei für eine Primärenergie von 200 MeV," Z. Physik 174, 464 (1963).
- H. H. Nagel, "Die Berechnung von Elektron-Photon-Kaskaden in Blei mit Hilfe der Monte-Carlo Methode," Inaugural-Dissertation zur Erlangung des Doktorgrades der Hohen Mathematisch-Naturwissenschaftlichen Fakultät der Rheinischen Friedrich-Wilhelms-Universität zu Bonn, 1964.



- H. H. Nagel, "Elektron-Photon-Kaskaden in Blei: Monte-Carlo Rechnungen für Primärelektronenenergien zwischen 100 und 1000 MeV," *Z. Physik* 186, 319 (1965); translated for the Stanford Linear Accelerator Center, SLAC-TRANS-28 (1965).
- H. H. Nagel, private communication, August, 1966.
- D. F. Nicoli, "The Application of Monte Carlo Cascade Shower Generation in Lead," submitted in Partial Fulfillment of the Requirement for the Degree of Bachelor of Science at The Massachusetts Institute of Technology, June, 1966.
- A. A. O'Dell, Jr., C. W. Sandifer, R. B. Knowlen, and W. D. George, "Measurement of Absolute Thick-Target Bremsstrahlung Spectra," *Nucl. Instr. Meth.* 61, 340 (1968).
- E. Parzen, Modern Probability Theory and Its Applications (John Wiley & Sons, Inc., New York, 1960).
- F. Rohrlich and B. C. Carlson, "Positron-Electron Differences in Energy Loss and Multiple Scattering," *Phys. Rev.* 93, 38 (1954).
- B. Rossi, High-Energy Particles (Prentice-Hall, Inc., Englewood Cliffs, New Jersey, 1952).
- W. T. Scott, "The Theory of Small-Angle Multiple Scattering of Fast Charged Particles," *Rev. Mod. Phy.* 35, 231 (1963).
- S. M. Seltzer, private communication, May, 1975.
- Y. A. Shreider (Ed.), The Monte Carlo Method (Pergamon Press, Inc., New York, 1966).

- J. Spanier and E. M. Gelbard, Monte Carlo Principles and Neutron Transport Problems (Addison-Wesley Publishing Co., Inc., Reading, Mass., 1969).
- R. M. Sternheimer, "The Density Effect for the Ionization Loss in Various Materials," Phys. Rev. 88, 851 (1952).
- R. M. Sternheimer, "The Energy Loss of a Fast Charged Particle by Cerenkov Radiation," Phys. Rev. 91, 256 (1953).
- R. M. Sternheimer, "Density Effect for the Ionization Loss in Various Materials, Phys. Rev. 103, 511 (1956).
- R. M. Sternheimer, "Density Effect for the Ionization Loss of Charged Particles," Phys. Rev. 145, 247 (1966).
- R. M. Sternheimer, "Density Effect for the Ionization Loss of Charged Particles. II," Phys. Rev. 164, 349 (1967).
- R. M. Sternheimer, "General Expression for the Density Effect for the Ionization Loss of Charged Particles," Phys. Rev. B3, 3681 (1971).
- E. Storm and H. I. Israel, "Photon Cross Sections from 1 KeV to 100 MeV for Elements Z=1 to Z=100," At. Data and Nucl. Data Tables 7, 565 (1970).
- M. L. Ter-Mikaelyan, "Bremmstrahlung Radiation Spectrum in Medium," Doklady Akad. Nauk S.S.S.R. 94, 1033 (1954a).
- M. L. Ter-Mikaelyan, "Bremsstrahlung Radiation Spectrum in Medium," Zu Eksper. Teor. Fiz. 25, 289, 296 (1954b).
- Y. S. Tsai, "Pair Production and Bremsstrahlung of Charged Leptons," Rev. Mod. Phy. 46, 815 (1974).

- J. E. Turner, "Values of  $I$  and  $I_{adj}$  Suggested by the Subcommittee," in "Studies in Penetration of Charged Particles in Matter," National Academy of Sciences-National Research Council Publication Number 1133 (1964) (Second printing with changes, 1967).
- S. M. Ulam and J. von Neumann, "On Combination of Stochastic and Deterministic Processes," Bull. Amer. Math. Soc. 53, 1120 (1947).
- A. A. Varfolomeev and I. A. Svetlolovov, "Monte Carlo Calculations of Electromagnetic Cascade with Account of the Influence of the Medium on Bremsstrahlung," Soviet Physics JETP 36, 1263 (1959).
- U. Völkel, "Elektron-Photon-Kaskaden in Blei für Primärteilchen der Energie 6 GeV," Deutsches Elektronen-Synchrotron Report Number DESY-65/6 (1965); translated for the Stanford Linear Accelerator Center, SLAC-TRANS-41 (1966).
- R. R. Wilson, "Monte Carlo Study of Shower Production," Phys. Rev. 86, 261 (1952).
- C. T. Zahn, Jr., "A User Manual for the MORTRAN2 Macro-Translator," Stanford Linear Accelerator Laboratory Computation Research Group Report Number CGTM No. 167 (1975).
- C. D. Zerby and H. S. Moran, "Studies of the Longitudinal Development of High-Energy Electron-Photon Cascade Showers in Copper," Oak Ridge National Laboratory Report Number ORNL-3329 (1962a).
- C. D. Zerby and H. S. Moran, "A Monte Carlo Calculation of the Three-Dimensional Development of High-Energy Electron-Photon Cascade Showers," Oak Ridge National Laboratory Report Number ORNL-TM-422 (1962).

C. D. Zerby and H. S. Moran, "Studies of the Longitudinal Development  
of Electron-Photon Cascade Showers," J. Appl. Phys. 34, 2445 (1963).

This document and the material and data contained therein, was developed under sponsorship of the United States Government. Neither the United States nor the Department of Energy, nor the Leland Stanford Junior University, nor their employees, nor their respective contractors, subcontractors, or their employees, makes any warranty, express or implied, or assumes any liability or responsibility for accuracy, completeness or usefulness of any information, apparatus, product or process disclosed, or represents that its use will not infringe privately-owned rights. Mention of any product, its manufacturer, or suppliers shall not, nor is it intended to, imply approval, disapproval, or fitness for any particular use. A royalty-free, nonexclusive right to use and disseminate same for any purpose whatsoever, is expressly reserved to the United States and the University.